Doctoral Thesis

Structural characterization of photosynthetic supercomplexes in plants

Lukáš Nosek

Department of Biophysics

Centre of the Region Haná for Biotechnological and Agricultural Research

Faculty of Science, Palacký University Olomouc, Czech Republic

Olomouc 2016

Bibliographical identification

Name of the author: Lukáš Nosek

Title of the doctoral thesis: Structural characterization of photosynthetic supercomplexes in plants

Degree program field: Biophysics

Duration of Ph.D. study: 2012-2016

Year of defence: 2016

Supervisor: RNDr. Roman Kouřil, Ph.D.

Keywords: CN-PAGE, electron microscopy, Photosystem I, Photosystem II, PSI-NDH supercomplex, Photosystem II megacomplexes, spruce Photosystem II supercomplex

Annotation: This thesis is focused on a structural characterization of various plant photosynthetic supercomplexes and megacomplexes using a combination of CN-PAGE and single particle electron microscopy. In the introductory part of the thesis, current knowledge regarding composition of Photosystem I and Photosystem II is summarized. A special attention is then paid to the ability of Photosystem I and Photosystem II to form larger assemblies with other protein complexes or with each other. An insight into the CN-PAGE and the single particle electron microscopy is also provided. In the experimental part of the thesis, an optimization of conditions for CN-PAGE to isolate protein complexes in form suitable for electron microscopy is described. The optimal conditions were then utilized in research projects, whose results are summarized in three attached papers.

Content

1. Introduction 1
Structure of Photosystems I and II 2
Photosystem I 2
Subunit composition of plant Photosystem I core complex 3
Light-harvesting complex of Photosystem I 5
Photosystem I involved in formation of larger assemblies 7
Photosystem I supercomplexes involved in state transitions 7
Oligomeric forms of Photosystem I 9
PSI-NDH supercomplex 10
Photosystem II 12
Subunit composition of Photosystem II core complex 12
Light-harvesting complex of Photosystem II 14
Structural characterization of the plant PSII-LHCII supercomplex 17
Larger assemblies of Photosystem II 20
Two-dimensional crystals of Photosystem II 20
Megacomplexes of Photosystem II 22
Experimental techniques 23
CN-PAGE 23
Single particle electron microscopy 26
2. Summary 29
3. Experimental approach 31
Methods 31
Plant material 31
Isolation and solubilization of thylakoid and PSII enriched membranes 31
CN-PAGE 32
Gel imaging 32
Electron microscopy and image analysis 32
Optimization of separation method for structural characterization of photosynthetic supercomplexes and megacomplexes 33
Isolation of the PSI-NDH supercomplex 33
Selection of plant material and optimization of solubilization 33
Isolation of PSII megacomplexes from *Arabidopsis thaliana* 40
Optimization of separation conditions for a structural characterization of spruce PSII supercomplex 41
Specimen preparation 43
Single particle Image analysis 46
4. Publications 48
4.1 Structural characterization of a plant photosystem I and NAD(P)H dehydrogenase complex. 48
4.2 Evolutionary loss of light-harvesting proteins Lhcb6 and Lhcb3 in major land plant groups – break-up of current dogma. 58
4.3 Structural variability of plant photosystem II megacomplexes in thylakoid membranes. 66
5. Conclusions 87
6. References 88

Declaration

I hereby declare that this Ph.D. thesis is my original work based on my own experiments. All other sources of information are acknowledged in the section References.

Signature:

Date and Place:

List of Publications

Published:

Kouřil R, Strouhal O, Nosek L, Lenobel R, Chamrád I, Boekema EJ, Šebela M and Ilík P. Structural characterization of a plant photosystem I and NAD(P)H dehydrogenase supercomplex. *Plant Journal* **77**: 568–576, (2014).

Kouřil R, Nosek L, Bartoš J, Boekema EJ and Ilík P. Evolutionary loss of light-harvesting proteins Lhcb6 and Lhcb3 in major land plant groups – break-up of current dogma. *New Phytologist* **210**: 808-814, (2016).

Accepted:

Nosek L, Semchonok D, Boekema EJ, Ilík P and Kouřil R. Structural variability of plant photosystem II megacomplexes in thylakoid membranes. *Plant Journal*, (2016) (doi: 10.1111/tpj.13325).

Acknowledgements

I would like to thank my supervisor Dr. Roman Kouřil for his friendly and patient guidance and help during my entire doctoral studies and prof. Petr Ilík for his inspiring ideas.

Furthermore, I would like to express my thanks to all colleagues from the Department of Biophysics for creating a pleasant and kind environment.

Special thanks belong to Ondřej Strouhal for a very beneficial collaboration at the beginning of my Ph.D. study.

This work was financially supported by the Grant Agency of the Czech Republic (project 13-2809S/P501) and by the Ministry of Education, Youth and Sports of the Czech Republic (projects ED0007/01/01 to Centre of the Region Haná for Biotechnological and Agricultural Research, CZ.1.07/2.3.00/20.0057 and LO1204 - Sustainable development of research in the Centre of the Region Haná).

Abbreviations

CN-PAGE	Clear native polyacrylamide gel electrophoresis
BN-PAGE	Blue native polyacrylamide gel electrophoresis
PSI	Photosystem I
PSII	Photosystem II
LHCI	Light harvesting complex of Photosystem I
LHCII	Light harvesting complex of Photosystem II
α-DDM	n-dodecyl-α-D-maltopyranoside
β-DDM	n-dodecyl-β-D-maltopyranoside
chls	total amount of chlorophylls *a* and *b*
NDH	NAD(P)H:quinone oxidoreductase
PSI-NDH	Photosystem I - NAD(P)H:quinone oxidoreductase supercomplex
CBB	Coomassie brilliant blue dye

1. Introduction

Photosynthesis is a process worth of an extraordinary respect since it remarkably participates on the maintenance of suitable living conditions on the Earth. It is performed mainly by two large supercomplexes known as Photosystem I (PSI) and Photosystem II (PSII), which have been studied for a long time and still, there are many dimensions awaiting their elucidation. It is obvious that especially functional properties of any assembly depend on the structure of individual subunits, which are responsible for its overall performance.

The last few decades clearly showed that photosynthetic complexes can be successfully studied using the X-ray crystallography, which provided most of the structures at atomic resolution available today. However, the method requires a highly concentrated sample, with a maximally homogenous and pure form of a protein in order to crystallize. Any impurities or structural variabilities of the protein are undesirable. Nowadays, this technique is being gradually replaced by the state-of-the-art cryo electron microscopy, which does not demand for crystals. Nevertheless, it still requires homogenous and also concentrated specimen. These requirements are, however, very difficult to fulfil, especially in a case of fragile, transient or rare protein complexes. In this case, single particle electron microscopy of a negatively stained specimen was found to be a very convenient method. Moreover, if it is coupled with a proper separation technique like a clear native polyacrylamide gel electrophoresis (CN-PAGE), it represents a powerful tool for structural characterization of a broad range of proteins, including photosynthetic membrane proteins.

The main aim of this thesis is the structural characterization of photosynthetic supercomplexes and megacomplexes of PSI and PSII using the CN-PAGE and single particle electron microscopy. In the Introduction part, a current knowledge of the structure of main photosynthetic complexes and their larger assemblies in higher plants is summarized. The experimental part of this thesis deals with an optimization of the experimental approach, which was used for isolation of large photosynthetic supercomplexes and megacomplexes. The last part of the thesis summarizes the performed and published research.

Structure of Photosystems I and II

Photosystem I

Photosystem I is a large, pigment-binding supercomplex working as a light-driven plastocyanin:ferredoxin oxidoreductase. It is extraordinarily efficient with quantum yield close to 1 and for this, it is considered as the most effective photovoltaic machine known so far (Nelson, 2009).

Plant PSI is composed from two basic functional moieties: the central core complex and a peripheral light-harvesting complex (LHCI). Central core complex coordinates the components responsible for a light-driven electron transfer and binds chlorophyll *a* molecules, which serve for light-harvesting. LHCI, which forms a crescent-shaped belt at the periphery of PSI, significantly extends its light-harvesting capacity and its main function is the efficient supply of the core complex with excitation energy (Nelson and Ben-Shem, 2005; Nelson and Yocum, 2006; Jensen et al., 2007; Amunts and Nelson, 2008; Busch and Hippler, 2011)

Structure of plant PSI has been extensively studied by the X-ray crystallography method and the resolution and the structural information provided by this method gradually improved during the last years. The first crystal structure of plant PSI was obtained at 4.4 Å resolution (Ben-Shem et al., 2003), when positions of sixteen subunits were determined: twelve core subunits (PsaA - PsaL) and four peripheral light harvesting subunits (Lhca1-4). Although the relatively low resolution did not allow precise identification of important functional features, like interactions among subunits, it provided valuable information about the order of individual Lhca1-4 proteins attached at one side of the PSI core complex. Owing to improved crystallization conditions, the resolution could be later improved to 3.4 Å (Amunts et al., 2007) and further to 3.3 Å (Amunts et al., 2010), both revealing seventeen subunits in total. These improved models provided better insight into interactions among subunits and non-covalently bound cofactors (chlorophylls, carotenoids, Fe-S clusters and phyloquinones). Finally, the most recent plant PSI structure was obtained at 2.8 Å resolution, which refined the current information about how the non-covalently bound cofactors

interact with each other and with the protein subunits within the supercomplex (Mazor et al., 2015) (see Figure. 1).

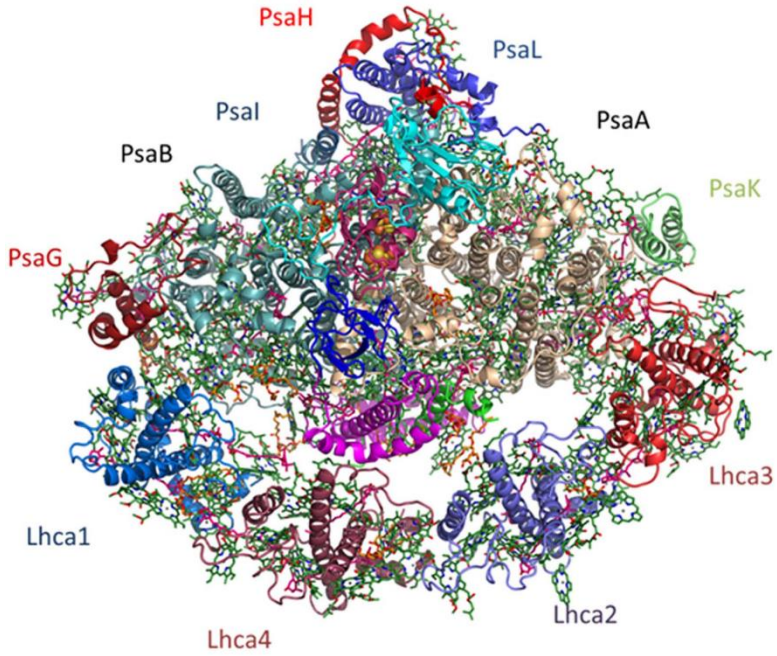

Figure 1. The most recent X-ray structure of the plant PSI-LHCI supercomplex obtained at the 2.8 Å resolution. View from the stromal side. Twelve PsaA-PsaL subunits of PSI including Lhca1-Lhca4 are depicted. PsaF and PsaJ subunits are coloured in magenta and green, respectively. PsaC, PsaD and PsaE subunits are coloured in cyan, pink and blue, respectively. Yellow and orange spheres in the middle of the complex represent Fe-S clusters. Chlorophylls in the core complex are in green, chlorophylls *a* in LHCI in cyan and LHCI chlorophylls *b* in magenta, carotenoids are in blue. Adapted from Mazor et al. (2015).

Subunit composition of plant Photosystem I core complex

The most recent X-ray structural analysis of PSI (Mazor et al., 2015) showed that the core complex is composed of twelve stably bound subunits PsaA-PsaL (coordinating 156 chlorophylls - nine of them are chlorophylls *b*, 32 carotenes and 14 lipids). Moreover, additional peripheral subunits, namely PsaN-PsaP and PsaR, were also revealed to be associated with the PSI core complex. However, PsaN subunit is only weakly bound to the PSI core and it is not considered as its stable part (Amunts et al., 2010). PsaO and PsaP are

subunits, which have not been identified yet in any crystal structure of plant PSI (reviewed in Busch and Hippler, 2011). By contrast, PsaR was identified within the crystal structure of plant PSI (Amunts et al., 2010), however its function is unclear.

PsaA and PsaB represent the largest subunits of PSI, each formed by eleven transmembrane helices with the molecular mass of 84 and 83 kDa, respectively. They form the central heterodimer, which binds P_{700} - the special chlorophyll pair responsible for light driven charge separation and also several primary electron acceptors. PsaC is a small stromal subunit with molecular mass of 9 kDa and together with PsaD (18 kDa) and PsaE (10 kDa) subunits forms a docking site for ferredoxin - a soluble electron transporter (Hayashida et al., 1987; Hoj et al., 1987). PsaF subunit with one transmembrane helix and with molecular mass of 17 kDa binds plastocyanin, the luminal electron donor (Farah et al., 1995) and was shown to be essential for transition of excitation energy from LHCI to PSI core complex (Haldrup et al., 2000). PsaG (11 kDa) and PsaK (9 kDa) are plant specific subunits with two transmembrane helices and play a role in stabilizing of the whole PSI supercomplex (Varotto et al., 2002) and in binding of LHCI to PSI (Ben-Shem et al., 2003). PsaH (11 kDa), PsaL (18 kDa) and PsaO (10 kDa) form a peripheral cluster responsible for interaction of PSI with phosphorylated LHCII, the light-harvesting complexes of PSII (Lunde et al., 2000; Jensen et al., 2004; Zhang and Scheller, 2004) and possibly also PsaI (4 kDa) and PsaP (indistinct mass) subunits may be involved in binding of LHCII to PSI (Zhang and Scheller, 2004). Moreover, PsaL subunit plays a significant role in formation of trimeric PSI assemblies in cyanobacteria (Chitnis and Chitnis, 1993; Jordan et al., 2001) and in plants, this PsaL function is eliminated by a plant-specific PsaH subunit (Ben-Shem et al., 2003). PsaJ (6 kDa) and PsaN (10 kDa) are one transmembrane helix subunits required for formation of the plastocyanin binding domain (Fischer et al., 1999; Haldrup et al., 1999). PsaR is a small, peripheral, one transmembrane helix subunit containing large amount of adenines (Amunts et al., 2010) and there is no biochemical evidence for its role. Therefore, it remains unclear whether it is a stable and functional part of PSI. The subunits of plant PSI and their function are summarized in Table 1.

Table 1. Subunit composition of a plant PSI core complex with subunits functions and bound cofactors.

Subunit name	Mass (kDa)	Gene location	Function
PsaA	84	chloroplast	Light harvesting, charge separation, electron transport, coordination of P_{700}, A_0, A_1 and F_X, binding of 80 chlorophylls, Lhca binding
PsaB	83	chloroplast	
PsaC	9	chloroplast	Coordination of F_A and F_B, ferredoxin binding
PsaD	18	nucleus	ferredoxin binding
PsaE	10	nucleus	ferredoxin binding
PsaF	17	nucleus	plastocyanin binding, Lhca4 binding
PsaG	11	nucleus	PSI stabilization, Lhca1 binding
PsaH	11	nucleus	LHCII binding, prevention of PSI trimerization
PsaI	4	chloroplast	LHCII binding (?)
PsaJ	6	chloroplast	plastocyanin binding, Lhca2 binding
PsaK	9	nucleus	PSI stabilization, Lhca3 binding, LHCII binding
PsaL	18	nucleus	LHCII binding
PsaN	10	nucleus	plastocyanin binding
PsaO	10	nucleus	LHCII binding (?)
PsaP	-	nucleus	LHCII binding (?)
PsaR	-	-	-

Light-harvesting complex of Photosystem I

The main function of LHCI is to provide sufficient amount of energy into the reaction centre of PSI. Plant PSI relies on a nuclear encoded light-harvesting complex composed of six chlorophyll binding proteins Lhca1-6 (Jansson, 1999). The Lhca1-4 proteins are evenly expressed and form two heterodimers assembled into a curved belt at the PsaF/PsaJ side of the PSI reaction centre (Boekema et al., 2001; Ben-Shem et al., 2003; Amunts et al., 2007; Amunts et al., 2010). The composition of heterodimers and their position towards the reaction centre is not random. The first dimer is composed of Lhca1 and Lhca4 proteins and interacts with PSI core complex via PsaG and PsaB subunits (Lhca1) and via PsaF subunit (Lhca4). The other dimer is formed by Lhca2 and Lhca3 proteins. Lhca2 associates with PSI core complex via PsaA and PsaJ and Lhca3 interacts via PsaA and PsaK (Jansson et al., 1996;

Ben-Shem et al., 2003; Amunts et al., 2007; Amunts et al., 2010; Mazor et al., 2015). The individual Lhca proteins in the PSI-LHCI supercomplex are not mutually interchangeable, as it was shown on mutants lacking individual Lhca subunits (Wientjes et al., 2009). That analysis showed that missing Lhca protein leaves an empty space in the supercomplex structure. This indicates that binding of individual Lhca proteins to the PSI core complex is highly specific, only with the exception of Lhca4 subunit, which can be substituted with Lhca5 subunit. The Lhca1-4 subunits also contain so-called far-red chlorophylls responsible for far red absorption and fluorescence emission (Morosinotto et al., 2003), which is a characteristic feature of the PSI (Gobets and van Grondelle, 2001).

The Lhca5-6 proteins represent subunits, which are expressed at a very low level (Klimmek et al., 2006). It means that these proteins bind to PSI in a substoichiometric amount with respect to other Lhca1-4 proteins. The exact role of Lhca5 and Lhca6 was unclear, until the mutants lacking these subunits were constructed. Analysis of plants lacking these subunits indicated their direct involvement in formation and stabilization of the PSI-NAD(P)H dehydrogenase (PSI-NDH) supercomplex (Peng et al., 2009). This analysis showed that mutants without Lhca5 and Lhca6 subunits have impaired formation of the PSI-NDH supercomplex. The general properties of Lhca1-6 proteins are summarized in Table 2.

Table 2. Subunits of plant Photosystem I light-harvesting complex with bound cofactors.

Subunit name	Mass (kDa)	Bound cofactors
Lhca1	22	13 chlorophylls, 3 carotenoids
Lhca2	23	13 chlorophylls, 2 carotenoids
Lhca3	25	13 chlorophylls, 3 carotenoids
Lhca4	22	13 chlorophylls, 2 carotenoids
Lhca5	24	13 chlorophylls, 2 carotenoids
Lhca6	25	-

Photosystem I involved in formation of larger assemblies

Plant PSI predominantly exists in the monomeric form in the thylakoid membrane (Kouril et al., 2005a). Nevertheless, this supercomplex also tends to form larger assemblies with other protein complexes like Cytb6f complex (Iwai et al., 2010), LHCII (Kouril et al., 2005b), and NDH complex (Kouril et al., 2014). Moreover, PSI can associate even with each other and form oligomers as have been shown in several electron microscopy studies (Boekema et al., 2001; Kouril et al., 2005a). Thus, the following paragraphs will briefly describe those larger PSI associations: supercomplexes involved in so-called state transitions, PSI oligomers and PSI-NDH supercomplex.

Photosystem I supercomplexes involved in state transitions

State transitions is a mechanism, by which plants balance the distribution of excitation energy between PSII and PSI upon changing light conditions (reviewed e.g. in Allen, 1992; Wollman, 2001).

Upon light conditions, when PSII is preferentially excited, over-reduction of plastoquinone and the cytochrome b_6f complex occurs. This over-reduction serves as a signal for plant kinases STN7 and STN8, which phosphorylate light-harvesting complex of PSII (LHCII) and some proteins of the PSII core complex (Bennett et al., 1980; Bellafiore et al., 2005; Bonardi et al., 2005). Once phosphorylated, LHCII dissociates from PSII and associates with PSI to form PSI-LHCI-LHCII supercomplex (state 2). Effect of this transition is in lowering of excitation pressure to PSII and in increased excitation of PSI. The whole process is reversible. When the pool of plastoquinone becomes oxidized, LHCII is dephosphorylated and migrates back to PSII (state 1) (Forsberg and Allen, 2001). In the state transitions, PsaH subunit plays a significant role. LHCII cannot transfer the excitation energy to PSI and the state transitions are impaired if the PsaH subunit is missing (Lunde et al., 2000).

Despite there was ample functional evidence for state transitions, the structure of the PSI-LHCI-LHCII supercomplex was obscured for a long time. Its structure was for the first time demonstrated in *Arabidopsis thaliana* by Kouřil et al. (2005), which was long time after discovery of state transitions (Bonavent.C and Myers, 1969; Murata, 1969; Bennett, 1977).

This time delay was caused by the difficulty to purify the supercomplex with a sufficient yield due to its fragility and instability. It was shown that LHCII trimer together with PSI-LHCI supercomplex form a pear-shaped structure and that LHCII is to PSI attached at the PsaH side (Fig. 2). Origin of the LHCII trimer migrating towards PSI was also investigated and still remains the matter of debate. For instance, it was proposed that it may originate in the M trimer dissociating from the PSII supercomplex (Kouril et al., 2005b). Nevertheless, taking into consideration that M trimer specific subunit Lhcb3 (Caffarri et al., 2009) is not present in stromal thylakoids (Bassi et al., 1988), the M trimer in most probably not involved in state transitions. Further, it was also proposed that LHCII trimer, which associate with PSI during state transitions, may originate also in a specific subset of LHCII weakly bound to PSII supercomplex (Galka et al., 2012) or in the pool of free LHCII (Wientjes et al., 2013). Structure of PSI-LHCI-LHCII supercomplex is illustrated in Figure 2.

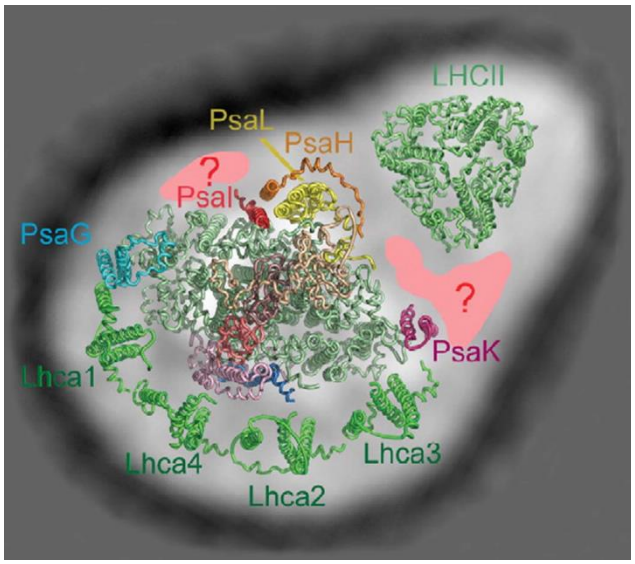

Figure 2. Structure of the plant PSI-LHCI-LHCII supercomplex. Supercomplex is formed by PSI with attached LHCI and trimeric LHCII. The question marked areas represent the unassigned densities probably occupied by some additional subunits. Stromal side view. Adapted from Jensen et al. (2007).

Oligomeric forms of Photosystem I

Electron microscopy analysis of mildly solubilized, chromatographically or electrophoretically purified thylakoid membranes also showed that PSI tends to form larger oligomeric forms like dimers, trimers and even tetramers.

The first structure of PSI oligomers was reported in the thermophilic cyanobacterium *Synechococcus* (Boekema et al., 1987). Nevertheless, there was a question whether these PSI trimers represent native arrangements or an artificial association between solubilized PSI complexes. No details regarding the interactions between individual PSI supercomplexes could be concluded due to the limited resolution of trimers. Thus, as the individual PSI supercomplexes in trimers were rotationally symmetrical, this was taken as the main evidence of their nativity. Later, the formation of PSI trimers in *Synechococcus* was confirmed using the X-ray analysis (Jordan et al., 2001). This study also revealed that the trimerization domain is formed of PsaL, as the individual PSI interact via these subunits.

A search for similar PSI associations in plants was also performed (Boekema et al., 2001). In that study, PSI dimers, trimers and tetramers were discovered in pea thylakoid membranes mildly solubilized by α-dodecyl maltoside. However, as the electron microscopy analysis showed, all found PSI oligomers represented artificial assemblies probably created as the artefact of solubilization. The individual PSI supercomplexes in the PSI oligomers had mirror symmetry and different handedness, which certainly does not reflect the situation in the native membrane. Comparable research was repeated later with digitonin as the detergent and similar dimeric, trimeric and tetrameric PSI structures were discovered (Kouril et al., 2005a). Regrettably, results of this electron microscopic analysis agreed with the former findings, i.e. that the found plant PSI oligomers likely represent artificial associations. Based on these results, it was concluded that native plant PSI exists in monomeric form. The trimerization of plant PSI is moreover hindered by the PsaH subunit (Ben-Shem et al., 2003), which shields the PsaL subunits responsible for PSI trimerization in cyanobacteria (Chitnis and Chitnis, 1993). Presence of PsaH in plant PSI is important as it enables association of plant PSI with LHCII during state transitions (Lunde et al., 2000). Examples of plant PSI oligomers are shown in Figure 3.

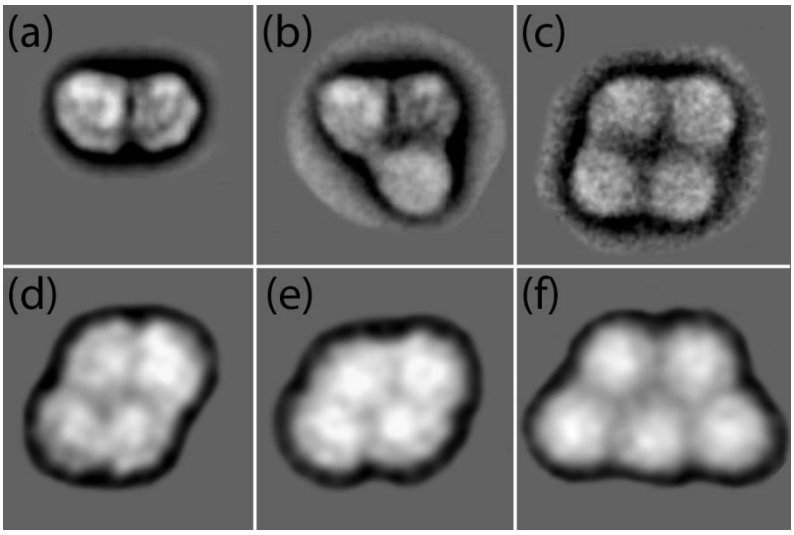

Figure 3. Plant PSI oligomers. (a-c) Artificial plant PSI oligomers as published by Boekema et al., (2001); a: PSI dimer composed of two up and down oriented monomers; b: PSI trimer, where two monomers have the same orientation as in dimer, next monomer is associated at different position; c: PSI tetramer formed as dimer of dimers. (d-f) Plant PSI oligomers discovered during optimization of native separation technique (Experimental approach chapter, unpublished data); d, e: PSI tetramers; f: PSI pentamer.

PSI-NDH supercomplex

The PSI-NDH supercomplex represents the assembly of PSI with NAD(P)H dehydrogenase and its native structure was revealed recently with a significant contribution of our group (chapter 4.1).

NDH complex is localized in stromal thylakoids and its existence was firstly suggested after tobacco and liverwort *Marchantia polymorpha* chloroplast genome sequencing (Ohyama et al., 1986; Shinozaki et al., 1986). It is involved in one of the pathways of cyclic electron flow (CET) around PSI (known as NDH-dependent pathway), which is essential for preventing of stroma over-reduction and also contributes to balancing of ATP and NADPH production (Shikanai, 2007). Thus, association of NDH with PSI seems to be beneficial for execution of these functions.

The plant NDH complex is composed of more than 20 subunits. It can be divided into five subcomplexes: A and B subcomplexes, EDB (electron donor binding), membrane and lumen subcomplexes (Peng et al., 2011; Shikanai, 2016) and shares a homology with

mitochondrial respiratory complex I (Efremov et al., 2010). Membrane subcomplex contains NdhA-NdhG subunits, subcomplex A contains NdhH-NdhO subunits, subcomplex B contains NDF1, NDF2, NDF4, NDF6 and NDH18 subunits and lumen subcomplex is composed of PPL2, CYP20-2, FKBP16-2 and PQL subunits. Nevertheless, exact function of all these subunits is still not fully clarified. EDB subcomplex represents recently discovered moiety of NDH and consists of NdhT, NdhU and NdhS subunits (Yamamoto et al., 2011). These subunits are suggested to form a ferredoxin binding site. Due to the fact that NDH binds ferredoxin, the chloroplast NDH may be reconsidered to be an ferredoxin dependent plastoquinone reductase, instead of generally accepted NAD(P)H dehydrogenase.

Existence of the PSI-NDH supercomplex was firstly evidenced in 2008 (Peng et al., 2008). Authors electrophoretically separated mildly solubilized *Arabidopsis thaliana* thylakoid membranes and discovered a high molecular weight band, which was after subjection to biochemical analysis attributed to association of PSI with NDH. Later, it was shown that association with Lhca5 and Lhca6 minor antenna is required for the efficient operation of the PSI-NDH supercomplex using the mutants lacking these Lhca subunits (Peng et al., 2009). The NDH complex is also stabilized by interaction with PSI especially under stress conditions (Peng and Shikanai, 2011). A structural model of PSI-NDH supercomplex with two copies of PSI attached to one copy of NDH was also proposed (Peng et al., 2011). Nevertheless, no structural evidence was available. There is also a recent indication that NDH-dependent CET might play a role in the regulation of photosynthetic redox state at low light condition (Yamori et al., 2015).

In our work (chapter 4.1), we provided the first structural characterization of the PSI-NDH supercomplex. We used mildly solubilized barley thylakoid membranes separated by native electrophoresis and band corresponding to PSI-NDH was structurally characterized by electron microscopy and image analysis. Our results correspond with previous propositions, as we revealed one NDH complex interacting with two copies of PSI. Also a minor form with only one PSI copy was discovered, but this was attributed to dissociation of the complete supercomplex during sample preparation. Fitting of crystal structures of PSI and NDH (or its analogue – respiratory complex I, respectively (Baradaran et al., 2013)) into the electron

microscopy projection map of PSI-NDH supercomplex indicated subunits involved in mutual interaction between PSI and NDH. This model proposes that while all Lhca1-4 subunits to some extent participate in the interaction, only NdhA-G subunits of the membrane NDH subcomplex are involved in the interaction. The model also shows some unassigned densities in the PSI-NDH supercomplex, which likely correspond to attached Lhca5 or Lhca6 antennas.

In the PSI-NDH supercomplex, the ferredoxin reduced at the acceptor side of PSI passes to NDH, where it reduces plastoquinone. Reduced plastoquinone then transfers electrons back to PSI via cytochrome b_6f complex and the cyclic pathway is completed. Ferredoxin can be alternatively reduced by NAD(P)H through the reverse reaction of FNR (ferredoxin:NAD(P)H oxidoreductase), which can associate with NDH (Hu et al., 2013). For more structural and functional details, see chapter 4.1.

Photosystem II

Photosystem II is a large, multisubunit pigment-protein supercomplex embedded in grana regions of thylakoid membranes and it works as a light-driven water:plastoquinone oxidoreductase with high quantum yield around 0.85 (Nelson and Ben-Shem, 2004). In plants, it consists of two functional moieties: the PSII core complex, which is usually present as a dimer (C_2) and a peripheral light harvesting complex (LHCII), formed by monomers or trimers of specific light harvesting proteins.

Subunit composition of Photosystem II core complex

The most recent cryo electron microscopy structural analysis of the plant PSII supercomplex (Wei et al., 2016) showed a detailed architecture of the PSII core complex. It consists of four large intrinsic subunits (PsbA (D1), PsbB (CP47), PsbC (CP43), PsbD (D2)), twelve small subunits (PsbE-F, PsbH, PsbI-M, PsbTc, PsbW, PsbX, PsbZ) and four extrinsic, lumen exposed subunits (PsbO-Q, PsbTn).

The central part of plant PSII core complex is formed by large D1, D2, CP43 and CP47 subunits. D1 and D2 subunits form central heterodimer, which constitutes the photochemical reaction centre P_{680} and where light driven charge separation takes place. Both D1 and D2 are formed by five helices of molecular mass 39 kDa and bind six chlorophyll *a* molecules and two pheophytins. CP43 and CP47 are six helix subunits with mass of 43 and 47 kDa. They fulfil the function of inner antenna, which means that they participate in light harvesting and coordinate 14 and 16 chlorophyll *a* molecules, respectively. These subunits also play an important role in energy transfer from outer light harvesting complex into the reaction centre. Moreover, it was shown that D1 together with CP43 are involved in coordinating of manganese cluster in oxygen evolving complex (Wei et al., 2016).

The group of twelve small subunits can be divided into stromal exposed ones (PsbE, PsbF, PsbH, PsbJ and PsbL) and lumen exposed ones (PsbI, PsbK, PsbM, PsbTc, PsbW, PsbX and PsbZ). All those subunits do not bind any pigment molecule and are present as one helical proteins only, with the exception of double helix PsbZ subunit. They pursue several functions, i.e. enhance dimerization of core complexes (PsbL, PsbM, PsbTc), stabilize the core complex (PsbE, PsbF, PsbJ, PsbK and PsbX), mediate association of outer light harvesting complex (PsbH, PsbW and PsbZ) and bind cytochrome b_{559} (PsbE, PsbF) (Shi and Schroder, 2004; Wei et al., 2016).

PsbO, PsbP, PsbQ represent extrinsic, lumen exposed subunits with molecular masses of 33, 20 and 17 kDa constituting a heterotrimeric assembly known as oxygen evolving complex. This complex coordinates a $Mn_4CaO_5^-$ cluster, which is responsible for water oxidation. Electrons released from oxidized water molecule are forwarded to electron transport chain and molecular oxygen is released to the environment (Umena et al., 2011; Wei et al., 2016). Function of PsbTn (5 kDa) is not clarified (Shi and Schroder, 2004). The basic properties of plant PSII subunits are summarized in Table 3.

Table 3. Subunit composition of plant Photosystem II core complex with subunits functions and bound cofactors.

Subunit name	Mass (kDa)	Gene location	Function
D1	39	chloroplast	Charge separation, electron transport, chlorophyll *a*, pheophytin and electron transport chain cofactors coordination
D2	39	chloroplast	
CP43	43	chloroplast	Light harvesting, chlorophyll *a* binding
CP47	47	chloroplast	
PsbE	9	chloroplast	Core complex stabilization or dimerization
PsbF	4	chloroplast	Core complex stabilization or dimerization
PsbH	8	chloroplast	Association of core complex with LHCII
PsbI	4	chloroplast	Core complex stabilization or dimerization
PsbJ	4	chloroplast	Core complex stabilization or dimerization
PsbK	4	chloroplast	Core complex stabilization or dimerization
PsbL	4	chloroplast	Core complex stabilization or dimerization
PsbM	4	chloroplast	Core complex stabilization or dimerization
PsbTc	4	chloroplast	Core complex stabilization or dimerization
PsbW	6	chloroplast	Association of core complex with LHCII
PsbX	4	chloroplast	Core complex stabilization or dimerization
PsbZ	7	chloroplast	Association of core complex with LHCII
PsbO	33	nucleus	Oxygen evolving complex
PsbP	20	nucleus	Oxygen evolving complex
PsbQ	17	nucleus	Oxygen evolving complex
PsbTn	5	nucleus	-

Light-harvesting complex of Photosystem II

Light harvesting complex of PSII (LHCII) is formed by different types of antenna proteins, which specifically associate at the periphery of the PSII core dimer. It fulfils several important tasks: it is responsible for a light harvesting and transfer of excitation energy to the reaction centre and it plays a crucial role in photoprotection of PSII against excessive light and photooxidative damage (Niyogi, 2000; Ruban et al., 2012; Ruban, 2016).

In plants, LHCII is composed of eight nuclear encoded pigment protein complexes named Lhcb1 – Lhcb8 (Ballottari et al., 2012). They are formed by three transmembrane helices and coordinate chlorophylls *a*, chlorophylls *b* and carotenoids in different ratios. Based on their occurrence, they can be generally divided into three subclasses.

First subclass is formed by Lhcb1 – Lhcb3 proteins, which usually occur in the ratio of about 8:3:1 (Jansson, 1994) and represents so-called major antenna proteins. These proteins associate into homotrimers (composed of Lhcb1 or Lhcb2) or into heterotrimers (composed of Lhcb1, Lhcb2 and Lhcb3) and share in their structure a typical "WYGPDR" trimerization motif (Jansson, 1999). Detailed information about the architecture of the LHCII trimer is available from X-ray structure (Liu et al., 2004; Standfuss et al., 2005). Trimers associate with dimeric PSII core complex into larger assemblies via monomeric antenna. According to the character of the binding to the PSII core complex, the LHCII trimers were designated as "S" and "M" (Strongly and Moderately bound LHCII, respectively) (Dekker and Boekema, 2005; Kouril et al., 2012). Occasionally the core complex can associate also with "L" trimers (Loosely bound) (Boekema et al., 1999a). Single particle electron microscopy analysis of various land plant species indicates that the largest stable form of the PSII-LHCII supercomplex has a form of the $C_2S_2M_2$ supercomplex. The Lhcb3 is present exclusively in the M trimer (Dainese and Bassi, 1991) and there are some indications that Lhcb2 is more likely present in the S trimer (Caffarri et al., 2009). Lhcb1 is evenly distributed among both the trimers (Caffarri et al., 2009). Moreover, it is interesting that there are up to eight LHCII trimers per one dimeric core complex (Peter and Thornber, 1991; van Oort et al., 2010). By considering the fact that dimeric PSII core complex can bind up to six trimers (Boekema et al., 1999a), this implies that there is a pool of free LHCII in thylakoid membrane, which may play a role e.g. in additional light harvesting (van Oort et al., 2010) and state transitions (Wientjes et al., 2013).

The second group is formed by Lhcb4 (CP29), Lhcb5 (CP26) and Lhcb6 (CP24) proteins and represents so-called minor antennas. These proteins are in the PSII supercomplex present in monomeric form and they interconnect the core complex with the major trimeric LHCII (Caffarri et al., 2009). Lhcb4-6 also pursue several other functions, as it was studied on

plants lacking these subunits: Lhcb6 is essential for the M trimer binding (Caffarri et al. 2009), as only C_2S_2 supercomplexes were found in mutant lacking this subunit (Kovacs et al., 2006). Moreover, it was also shown that Lhcb6 plays a role in PSII photoprotection, as the plants lacking Lhcb6 had a significantly reduced capacity for non-photochemical quenching (de Bianchi et al., 2008). Lhcb6 was also found to be unique for land plants (Alboresi et al., 2008) and might play a role in adaptation to aerial environment. Lhcb5 is involved in supercomplex stabilization, as the amount of supercomplexes was significantly reduced in the mutant lacking Lhcb5 (Yakushevska et al., 2003; Caffarri et al., 2009). In our work (chapter 4.3) we also propose that Lhcb5 is involved in formation or stabilization of PSII megacomplexes. Moreover, it was shown that Lhcb5 may substitute Lhcb1 and Lhcb2 subunits in trimers in plants lacking these two subunits (Ruban et al., 2003). Lhcb4 was found to be essential for function and structural organization of PSII supercomplexes, as no large supercomplexes could be found in the mutant plants (Yakushevska et al., 2003; de Bianchi et al., 2011). Lack of this subunit also affects binding of S trimer and negatively influences non-photochemical quenching capacity (de Bianchi et al., 2011). A crystal structure of the Lhcb4 was solved recently (Pan et al., 2011). Minor antenna proteins also associate with major antennas into larger functional units, as it was shown on a pentameric complex composed of Lhcb4, Lhcb6 and the M trimer (Betterle et al., 2009). This unit disconnects from PSII upon illumination and re-associates with PSII during dark recovery, which was shown to be important for establishment of non-photochemical quenching.

Moreover, as we have recently demonstrated (chapter 4.2), Lhcb6 and Lhcb3 antennas are surprisingly not present in *Pinaceae* and *Gnetales*, subgroups of higher plants. Lhcb6 was considered to be plant specific subunit, which has, together with Lhcb3, evolved during transition of plants from water to land habitat. Their lack in *Pinaceae* and *Gnetales* modifies the PSII supercomplex in such a way that it resembles PSII from evolutionary older organisms and breaks the current dogma that these two subunits are essential for all land plants (for structural details and functional implications, see chapter 4.2).

The last group of plant LHCII is represented by Lhcb7 and Lhcb8, the most recently discovered subunits. Lhcb7 is structurally similar to Lhcb5 and origin of Lhcb8 is in

reclassification of Lhcb4.3, one of isoforms of CP29 (Klimmek et al., 2006). Both of them are rarely expressed, i.e. they are present in substoichiometric amount and their function remains unclear (Ballottari et al., 2012).

LHC-like proteins represent a special example of LHC proteins, from whom PsbS is worth of special interest. This is a four helix, pigment-less subunit, which plays a key role in process of non-photochemical quenching (Li et al., 2000). Recent data indicate that it associates with LHCII trimers and PSII core proteins (Gerotto et al., 2015; Correa-Galvis et al., 2016), nevertheless it is probably not a specific part of the PSII-LHCII supercomplex (Caffarri et al., 2009). It also participates on PSII-LHCII structural reorganization upon high light condition (Betterle et al., 2009; Kereiche et al., 2010; Ruban et al., 2012) and impairs formation of PSII semi crystalline arrays (Kereiche et al., 2010). The basic properties of plant PSII light harvesting proteins are summarized in Table 4.

Table 4. Subunits of plant LHCII with bound cofactors (if known exactly).

Subunit name	Mass (kDa)	Bound cofactors
Lhcb1	28	8 chl *a*, 6 chl *b*, 4 carotenoids
Lhcb2	29	
Lhcb3	29	
Lhcb4 (CP29)	31	9 chl *a*, 3 chl *b*, 1 chl *a*/*b*, 3 carotenoids
Lhcb5 (CP26)	30	8 chl *a*, 4 chl *b*, 1 chl *a*/*b*, 3 carotenoids
Lhcb6 (CP24)	28	-
Lhcb7	40	-
Lhcb8	30	-

Structural characterization of the plant PSII-LHCII supercomplex

In the last decades, a lot of effort has been put into solving a high resolution structure of the plant PSII-LHCII supercomplex. Attempts to solve a high resolution structure of a plant PSII-LHCII supercomplex using X-ray crystallography most likely failed due to the impossibility to purify the supercomplex in a homogeneous and stable form. Therefore, most

of the X-ray crystallography work has been performed on cyanobacterial PSII core complexes due to their greater stability (Zouni et al., 2001; Guskov et al., 2009; Umena et al., 2011). Due to the above-mentioned limitation, our knowledge about the architecture of the plant PSII-LHCII supercomplex comes from single particle electron microscopy studies combined with image analysis.

The first structural characterization of plant PSII with associated LHCII was obtained using mildly solubilized spinach PSII enriched membranes (Boekema et al., 1995). As the outcome, the C_2S_2 supercomplex at 25 Å resolution was obtained. Revealed structure provided the first details about organization of LHCII around PSII core complex. However, as the isolating procedures and instrumental facilities gradually improved, it was possible to achieve higher resolution of larger PSII-LHCII supercomplexes, as it is evidenced by spinach C_2S_2M and $C_2S_2M_2$ supercomplexes obtained at 16 Å resolution (Boekema et al., 1999b; Boekema et al., 1999a). A next significant step forward was achieved in 2009, when a $C_2S_2M_2$ supercomplex at 12 Å resolution was obtained from mildly solubilized *Arabidopsis thaliana* thylakoid membranes (Caffarri et al., 2009). Obtaining of PSII supercomplex structure at such high resolution enabled sufficiently precise fitting of X-ray structures of individual PSII moieties (core complex and trimeric and monomeric LHCII) into the electron microscopy projection map. The structural model further allowed characterization of mutual interactions among PSII subunits and energy transfer routes (Kouril et al., 2012). Structure of such PSII supercomplex is presented in Figure 4.

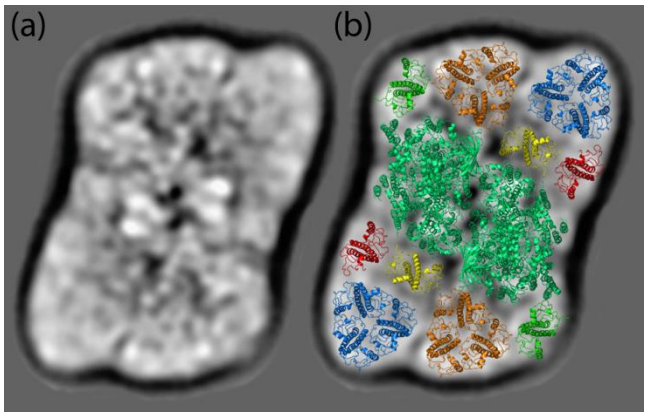

Figure 4. Structure of *Arabidopsis thaliana* $C_2S_2M_2$ supercomplex. (a) electron microscopy map of supercomplex obtained at 12 Å resolution. (b) fitting of X-ray structures into the supercomplex as proposed by Caffarri et al., (2009). Pale green: core complex; blue: M trimer; orange: S trimer; red: Lhcb6; green: Lhcb5; yellow: Lhcb4. Adapted from Caffarri et al. (2009).

Recently, a breakthrough was achieved, when the 3D structure of the C_2S_2 supercomplex was obtained using cryo electron microscopy at 3.2 Å resolution (Wei et al., 2016). This study improved the current knowledge about the organization of the whole supercomplex, as precise localization of PsbO-Q subunits constituting the oxygen evolving complex was presented. A detailed insight into energy transfer pathways between antennas and core complex was also brought, as the exact positions of individual Lhcb proteins were located. The structure of this PSII C_2S_2 supercomplex is presented in the Figure 5.

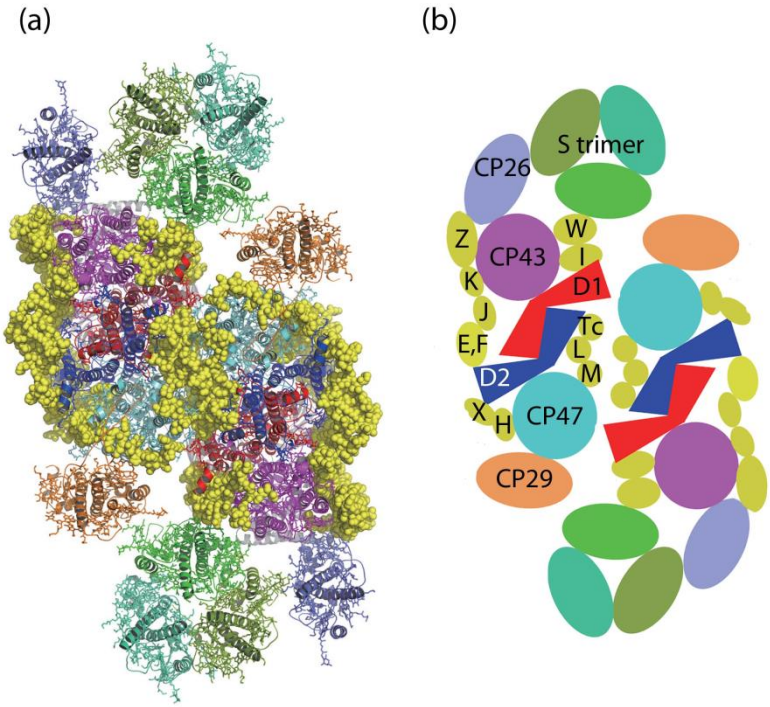

Figure 5. Cryo electron microscopy structure of spinach C_2S_2 supercomplex obtained at 2.8 Å resolution. (a) crystal structure of C_2S_2 supercomplex, (b) schematic subunit depiction. Adapted from Wei et al. (2016).

Larger assemblies of Photosystem II

Photosystem II also tends to form larger assemblies in the grana membrane, which are, in contrast to PSI, formed exclusively between each other. Thus, the following paragraphs will briefly summarize current knowledge about formation of such associations, namely two-dimensional crystals and PSII megacomplexes.

Two-dimensional crystals of Photosystem II

The first evidence of regular arrangements of PSII supercomplexes into semi-crystalline arrays was given several decades ago by freeze fracture analysis of thylakoid membranes (Garber and Steponkus, 1976; Simpson, 1978). Nevertheless, due to the limited resolving possibilities, no structural details could be concluded. The first reasonable results were obtained several years later after electron microscopy investigation of mildly solubilized spinach thylakoid membranes by α-dodecyl maltoside (Boekema et al., 2000). In

these membranes, regular arrangements of PSII supercomplexes into long rows were observed. After a detailed analysis, several types of crystal lattices were discovered. They were composed of either C_2S_2M or C_2S_2 supercomplexes. Later, another type of crystal lattice was found in *Arabidopsis thaliana*, which was formed by $C_2S_2M_2$ supercomplex (Yakushevska et al., 2001a). It was also shown that occurrence and lattice properties of the PSII semi-crystalline arrays are dependent on growth conditions. In plants grown under high light conditions, the amount of semi-crystalline arrays was significantly reduced compared to normal and low light (Kouril et al., 2013). Moreover, there was a relative increase in semi-crystalline arrays formed by C_2S_2 supercomplexes in high light variant compared to crystals formed by $C_2S_2M_2$ in the other light variants, probably as the consequence of light induced disassembly of larger complexes. The formation of semi-crystalline arrays is also initiated by the adaptation of plants to low temperature (Garber and Steponkus, 1976) or by different conditions (e.g. high sugar concentration in the storage medium) used to store the isolated thylakoid membranes or chloroplasts (Semenova, 1995).

The function of the PSII semi-crystalline arrays is still a matter of debates and several possibilities were proposed. It was suggested that these ordered arrays may serve to enhance diffusion of plastoquinone to cytochrome b_6f complex in the crowded membrane (Kirchhoff et al., 2007) and regular arrangements of PSII may also participate on grana formation via mutual interactions of LHCII in the adjacent membrane layers (Yakushevska et al., 2001a; Daum et al., 2010; Kirchhoff et al., 2013; Tietz et al., 2015). It was also shown that formation of the semi-crystalline arrays is dependent on PsbS (Kereiche et al., 2010). In plants with normal or decreased level of PsbS, the formation of semi-crystalline arrays was unaffected, while no arrays were detected in the plants overproducing the PsbS. Thus, it was suggested that formation of these semi-crystalline arrays is also related to non-photochemical quenching, since PsbS is involved in regulation of non-photochemical quenching process (Niyogi et al., 2005).

Megacomplexes of Photosystem II

PSII megacomplexes represent a lateral and specific association of two PSII-LHCII supercomplexes. They were, for the first time, detected in chromatographically purified spinach thylakoid membranes mildly solubilized by α-dodecyl maltoside. The analysis of electron micrographs of that sample revealed three different in parallel arranged PSII megacomplexes (Boekema et al., 1999b; Boekema et al., 1999a) and later, another type of the PSII megacomplex was discovered in *Arabidopsis thaliana* (Yakushevska et al., 2001b). Later, the PSII megacomplexes were detected also in other studies (e.g. Caffarri et al., 2009; Jarvi et al., 2011), but they were not subjected to any structural characterization. The origin and a biological relevance of PSII megacomplexes were obscured since they were considered as building blocks or just fragments of two-dimensional crystals.

In our work (chapter 4.3), we performed a thorough structural analysis of PSII megacomplexes from mildly solubilized *Arabidopsis thaliana* thylakoid membranes. Our results indicate similar arrangements of PSII as published previously (Boekema et al., 1999b; Boekema et al., 1999a; Yakushevska et al., 2001b), when we detected PSII megacomplexes arranged in parallel. However, we also detected several novel types of megacomplexes formed by two PSII supercomplexes interacting in a non-parallel manner. Importantly, we also brought evidence of native origin of both parallel and non-parallel megacomplexes as they were successfully detected at the level of native grana membranes. We also proposed their function in a tuning of utilization of absorbed light energy, however, this has to be elucidated in more detail in further studies.

Experimental techniques

Electron microscopy represents a powerful tool for structural characterization of protein complexes, as it was demonstrated on several PSI and PSII supercomplexes and megacomplexes described in the previous chapter. To facilitate the electron microscopy analysis of protein complexes, a proper separation method is also desirable to purify the complex in a high quantity, purity and a native form. Nowadays, there are generally two native separation methods widely used. The first method represents an ultracentrifugation in sucrose gradient. This technique has been successfully used several times for a separation of large PSII-LHCII supercomplexes (e.g. Caffarri et al., 2009; Wei et al., 2016). However, this technique is vastly time consuming (a run usually takes about 16 h) and demanding for a very expensive equipment. On the other hand, native electrophoresis, which represents the second separation technique, brings several benefits compared to ultracentrifugation. It remarkably shortens the time needed for separation (it takes about 2 h) and uses relatively inexpensive equipment. The following paragraph will briefly introduce the issue of native polyacrylamide gel electrophoresis, namely the so-called clear native polyacrylamide gel electrophoresis (CN-PAGE), a separation technique successfully utilized in all our studies (chapters 4.1, 4.2, 4.3). It is followed by an insight into the basic principles of transmission electron microscopy and image analysis.

CN-PAGE

Clear-native polyacrylamide gel electrophoresis represents a special type of electrophoresis nowadays conveniently used for separation of large and fragile protein complexes in native state.

It was used for the first time in early nineties for separation of labile mitochondrial complexes and it is principally based on an older technique known as blue-native PAGE (BN-PAGE) (Schagger et al., 1994). Nevertheless, the original setup of CN-PAGE had limited resolving possibilities and till these days, it had to undergo several improvement steps.

Originally, the only difference between CN-PAGE and BN-PAGE lied in the complete absence of anionic dye Coomassie brilliant blue (CBB) in the case of CN-PAGE (Schagger et

al., 1994). Since the principle of BN-PAGE is based on the ability of this dye to adsorb to the protein complexes which sets them negative charge necessary for their movement in the electric field (Schagger and Vonjagow, 1991), a usage of CN-PAGE was limited due to the CBB absence to separation of complexes with certain isoelectric point (pI) only. All native electrophoretic applications apply exclusively neutral pH, which means that only acidic proteins with pI lower than the pH of electrophoretic system could be separated (because only those proteins have negative charge). The other "disadvantage" of original CN-PAGE setup was in a significantly prolonged separation and weak resolution of separated protein complexes (Schagger et al., 1994; Wittig and Schagger, 2005). On the other hand, the separation in absence of CBB provided several very important advantages. This dye significantly hampered estimation of catalytic activity of separated protein complexes and interfered with detection of fluorescently labelled proteins, which was conveniently overcome in the case of CN-PAGE. Moreover, there were some indications that CBB might disturb very weak protein-protein interactions and thus, CN-PAGE was considered to be the mildest electrophoretic technique (Wittig and Schagger, 2005).

Therefore, there was an effort to combine advantages of both electrophoretic techniques. This resulted in the high resolution CN-PAGE, an improved method combining the resolving efficiency of BN-PAGE with an exceptional mildness of CN-PAGE (Wittig et al., 2007). This was achieved by a mild, anionic detergent sodium deoxycholate present in a cathode buffer. This detergent incorporates into detergent micelles of solubilized protein complexes and sets them a negative charge, which is essential for their effective separation in the electric field. Moreover, to our best knowledge there is no evidence regarding any negative impact of this detergent on protein-protein interaction.

The separation of protein complexes by native electrophoresis is usually performed using linear gradient polyacrylamide resolving gel. Obviously, gradient gel is used, when a mixture of proteins with broad range of molecular masses is separated. This is typically the case of photosynthetic membrane-bound complexes, which can have a form of large megacomplexes as well as small complexes. When the size of gel pores in the gradient gel meats with the size of a separated protein complex, the complex significantly decreases its

speed of movement in the gel and focuses in a sharp band. Thus, usage of the gradient gel is a beneficial way, how to separate individual proteins of different size from each other. The proper gradient constitution has to be also considered prior every experiment to achieve sufficient separation of complexes of interest. It is practically impossible to clearly resolve all individual protein complexes from a heterogeneous mixture and the gel density should be always adequate to molecular mass of complex of interest. The rule of thumb is: the larger complexes are to be resolved, the less concentrated gel has to be used (and vice versa). Consequently, a proper separation of larger complexes is at the expense of the smaller ones.

Prior the separation of protein complexes by native electrophoresis, biological membranes have to be solubilized in order to extract the protein complexes from the lipid layer. For this purpose, detergents efficiently relieving lipid-lipid and lipid-protein interactions and maintaining even the weakest protein-protein interactions should be used. Nowadays, there are plenty of detergents suitable for extraction of protein complexes from biological membranes (Crepin et al., 2016). Nevertheless, as our long-term experience showed, dodecyl-maltosides (DDM) are the most suitable ones. Dodecyl-maltosides belong to the group of alkyl-glucosides, non-ionic detergents, which combine in their molecules a long hydrophobic alkyl chain with a large hydrophilic head group. In the case of DDM, the alkyl chain is formed by a non-branched twelve-carbon chain and the head group is composed of a maltose molecule. Based on the position of alkyl chain on the maltose head, α- and β- anomers can be distinguished. In the case of α-DDM, the side chain is connected to the head in the axial position, while β-DDM is connected in equatorial position (Seddon et al., 2004). Even though both these detergents share their basic chemical characteristics, their physical properties differ significantly. The best example of different physical properties is the different solubilizing power of both detergents, as evidenced e.g. by Pagliano et al., (2012) and Barera et al., (2012) and also by our results (see Experimental approach chapter). To achieve the optimal yield and resolution of complex of interest, proper detergent (α- or β-DDM in our case) and its concentration have to be determined. For this purpose, a constant amount of membranes is usually treated with different detergents at increasing concentration. This is so-called detergent concentration line, which provides an outline of sample response. Using this approach, the suitable detergent and its concentration can be

determined to obtain specific complexes. As the results presented in the Experimental approach chapter imply, both DDM's are useful in dependence on solubilized plant material and stability of studied protein complex.

Single particle electron microscopy

Single particle electron microscopy is a powerful technique used for both 2D and 3D structural characterization of protein complexes. It is highly suitable for protein assemblies, whose physical properties make difficult their structural characterization by other structural method like X-ray crystallography. Certainly, single particle electron microscopy provides several advantages compared to X-ray crystallography: there is no need to grow crystals, the biological sample does not need to be purified into homogeneity and high protein concentration and it is highly suitable for a study of large and often transient and unstable supercomplexes and megacomplexes. It combines transmission electron microscopy and image analysis (reviewed e.g. in Boekema et al., 2009).

Transmission electron microscopy is an advanced technique, employing its high magnification capacity for visualization of small details, even within individual molecules. In principle, it is, to some extent, similar to a commonly known optical microscopy. However, it uses electrons instead of visible light. The limitation of optical microscopy lies right in the use of visible light (about 380-760 nm), since wavelength of photons is one of the resolution (and magnification) limiting factors. Wavelength of electron is dependent on voltage used for electron acceleration inside the electron microscope column and it can be up to 2.5 pm (if 200 kV acceleration voltage is used). This means that electron microscope may offer several orders of magnitude higher resolution than optical microscope. On the other hand, there are also several instrumental factors like aberration of lenses, which limit the final resolution of electron microscope.

The general setup of transmission electron microscopy is the following: a path of electrons, which are emitted from an electron gun, is controlled and aligned by a set of lenses to form coherent and maximally monochromatic electron beam. These electrons then interact with a specimen, what affects their directions (i.e. the electrons are scattered by

interaction with the specimen). The scattered electrons, which carry now information about the specimen, further pass through the objective lens and through a set of projector lenses, where magnification occurs. Then they interact with a detector, which transforms the carried information into an image.

In the electron microscopy, contrast of the image is one of the crucial factors, which has a great impact of the final results. A general origin of the contrast is in scattering of electrons on the specimen level and the scattering is directly proportional to the atomic number of elements, which form the specimen. Since the biological specimens are formed mostly of biomacromolecules composed of light elements (C, H, O, N), the scattering and resulting contrast is insufficient. A more sufficient contrast can be obtained by a negative staining (Brenner and Horne, 1959). In the negative staining, the biomacromolecules are embedded in heavy metal salt, whose heavy atoms strongly interact with electrons. The heavy metal salt surrounds the space around biomacromolecules and fills their cavities, but the hydrophobic protein interior remains untouched. This causes that the biomacromolecules project out from the background with a good contrast. Nevertheless, negative staining brings an inconvenience, as the complexes in the specimen may become deformed during the staining procedure. This undesirable deformation of complexes is avoided in cryo electron microscopy (Adrian et al., 1984), which represents an alternative for negative staining technique. In this technique, a liquid specimen containing biomacromolecules is rapidly frozen on the electron microscopy grid. Using this method, the biomacromolecules are embedded in a thin layer of amorphous ice and better reflect the genuine cellular aqueous situation of studied complexes. Since the contrast is caused preferentially by the difference between densities of ice and biomacromolecules, the contrast is much weaker compared to the negative staining. Due to this fact, it is uneasy to distinguish between complexes of interest and contaminants or breakdown products. Thus, the cryo electron microscopy is rather suitable for large and symmetric macromolecules, while negative staining is more suitable for smaller and structurally variable macromolecules. In cryo electron microscopy, the complexes are also present in all possible orientations as they are freely distributed in the ice. On the other hand, the complexes are in

negatively stained specimen adhered on the support carbon film and their spatial layout is limited.

The biological samples are also highly sensitive to radiation damage and thus, the intensity of incident electron beam has to be minimized. This results in a low signal-to-noise ratio in the micrograph. To cope with this, image analysis is employed.

Image analysis consists of three basic steps: alignment, classification and averaging. During the alignment step, all the individual projections of complexes (or any inspected particles) obtained by imaging of the specimen are arranged into the same direction. Classification, the second step, efficiently sorts out all different proteins in a heterogeneous dataset into individual classes. This step is able to distinguish even between very fine variances, if performed properly. However, this step is greatly time-consuming and demanding for high computing capacity. The last step, averaging, simply averages individual projections belonging to one class raised from the classification and significantly increases the signal-to-noise ratio. The higher amount of particles is summed, the higher resolution, contrast and structural information is achieved. Nowadays, the image analysis can be performed using various number of specialized software tools, such as XMIPP (Sorzano et al., 2004), RELION (Scheres, 2012), Spider (Frank et al., 1996), EMAN (Ludtke et al., 1999) or IMAGIC (vanHeel et al., 1996).

The final projection map of a protein complex can be fitted with the X-ray structures of its individual subunits (if accessible). This fitting significantly helps to understand the overall structure and organization of studied complex, interactions between subunits and it is also helpful for understanding of complex function.

2. Summary

This thesis is aimed on the structural characterization of various plant photosynthetic complexes using a combination of CN-PAGE and single particle electron microscopy. Single particle electron microscopy is a powerful structural technique and provides ample structural information about a studied complex. In order to facilitate the structural characterization, optimization of a specimen preparation for electron microscopy is a very important step. The optimization is a complex process and comprises of several steps, as described in details in the chapter 3. Experimental approach. First of all, a proper plant material has to be selected. Then, conditions of a protein separation using CN-PAGE, including selection of a proper detergent and its concentration, are optimized. Final step involves extraction of separated protein complexes from the CN-PAGE gel and a preparation of specimen for electron microscopy. Once the workflow is optimized, it can be successfully applied in a structural study. The aim of my thesis was a structural characterization of three large protein assemblies involved in photosynthesis like the PSI-NDH supercomplex from barley, the PSII-LHCII supercomplex from Norway spruce and the PSII megacomplex from *Arabidopsis thaliana*.

The first paper (chapter 4.1) deals with the structural characterization of the PSI-NDH supercomplex isolated from barley (*Hordeum vulgare*). The structural analysis revealed that one NDH complex binds up to two PSI supercomplexes, which are to NDH bound at asymmetric positions. Moreover, positions of rare Lhca5 and Lhca6 antennas stabilizing the whole supercomplex were indicated. As we discovered both supercomplexes with one and two PSI bound to NDH, it implies that gradual formation and dissociation of the PSI-NDH supercomplex may function as a tuning of cyclic electron flow around PSI.

The second paper (chapter 4.2) describes the structural characterization of the PSII supercomplex isolated from Norway spruce (*Picea abies*). Spruce belongs to the group of gymnospermous plants (family *Pinaceae*) and we provided the first structural analysis of PSII supercomplex isolated from this plant group. Moreover, using an extensive genomic analysis we also discovered that the group of land plants including families *Pinaceae* and also

Gnetales lack genes for Lhcb3 and Lhcb6 subunits, which has a noticeable impact on the structural organization of PSII supercomplexes. These two subunits have evolved during transition of plants from water to land and were considered to be characteristic for all land plants. Their absence in these plant groups breaks the current evolutionary dogma and modifies PSII supercomplex in such a way that it resembles PSII from evolutionary older organism, alga *Chlamydomonas reinhardtii*.

The third paper (chapter 4.3) structurally characterizes PSII megacomplexes isolated from *Arabidopsis thaliana*. These megacomplexes are formed of two PSII supercomplexes, which mutually interact in parallel and in non-parallel. The structural characterization of megacomplexes interacting in non-parallel was performed for the first time. The presence of both groups of megacomplexes was also detected on the level of native grana thylakoid membrane, which is an evidence of their nativity and thus a physiological significance.

3. Experimental approach

Methods

Plant material

Arabidopsis thaliana plants were grown for 8 weeks in soil in a growth chamber at 21°C with a photoperiod of 8h light and 16h dark at 100 µmol of photons.m^{-2}.s^{-1} of photosynthetically active radiation.

Barley (*Hordeum vulgare*) plants were grown for 8 days in perlite in a growth chamber at 25°C with a photoperiod of 16h light and 8h dark at 100 µmol of photons.m^{-2}.s^{-1} of photosynthetically active radiation.

Spruce (*Picea abies*) plants were grown for 18 days in perlite in a growth chamber at 21°C with a photoperiod of 16h light and 8h dark at 100 µmol of photons.m^{-2}.s^{-1} of photosynthetically active radiation.

Isolation and solubilization of thylakoid and PSII enriched membranes

Thylakoid membranes from *Arabidopsis thaliana* and barley were isolated according to (Dau et al., 1995)and PSII enriched membranes from spruce were isolated according to (Caffarri et al., 2009).

In all the cases, a constant amount of membranes (corresponding to 10 µg of chlorophylls) was treated with a certain amount of detergent. The detergent amount is defined as the mass ratio of detergent to chlorophylls (DDM/chl). Prior the electrophoretic separation, the mixture of membranes with detergent was supplemented with sample buffer to the final volume of 30 µl (20% glycerol, 50 mM HEPES, 400 mM sucrose, 15 mM NaCl, 5 mM $MgCl_2$, pH 7.2) and centrifuged (10 minutes, 20000g) to remove nonsolubilized material.

CN-PAGE

In all our experiments, CN-PAGE (Wittig et al., 2007) as the separation technique was used. Because we aimed on complexes of high molecular weight, we modified the gel concentration in order to resolve the large complexes at the expense of the smaller ones. We used 4-8% gradient resolving gel with 4% stacking gel. The electrophoretic separation was performed using the Bio-Rad Mini-PROTEAN Tetra Cell system.

Gel imaging

After electrophoresis, the gels were scanned using a gel scanner Amersham Imager 600RGB. To visualise all the bands in the gel, an ordinary image upon white light illumination in transmission mode was acquired. To distinguish between PSI and PSII complexes, a fluorescent image was acquired. The fluorescence quantum yield of PSI is very low at room temperature compared to the high quantum yield of fluorescence of PSII, which unambiguously discriminates both types of photosystems. Excitation was performed at 460 nm, detection of fluorescence was performed using a band-pass filter (690-720 nm).

Electron microscopy and image analysis

Electron microscopy was performed using several electron microscopy configurations: 1) using Philips CM120 electron microscope equipped with a LaB6 filament operating at 120 kV. Images were recorded with a Gatan 4000 SP 4K slow-scan CCD camera at 130000x magnification with a pixel size of 0.23 nm at the specimen level after binning the images to 2048 x 2048 pixels, 2) Tecnai G2 20 Twin electron microscope equipped with a LaB6 cathode, operated at 200 kV. Images were recorded with an UltraScan 4000UHS CCD camera at 130000x magnification with a pixel size of 0.224 nm at the specimen level after binning the images to 2048 x 2048 pixels.

Image analysis was performed using GRIP (GRoningen Image Processing), XMIPP (Sorzano et al., 2004) and RELION (Scheres, 2012) software including multireference and nonreference alignments, multivariate statistical analysis and classification.

Optimization of separation method for structural characterization of photosynthetic supercomplexes and megacomplexes

Plant PSI and PSII are large, multisubunit photosynthetic pigment-protein supercomplexes performing light-driven reactions. Extensive information regarding their structure is available (in detail reviewed e.g. in Busch and Hippler, 2011; Shen, 2015). Moreover, both PSI and PSII supercomplexes tend to form larger associations with other protein complexes and also with each other (summarized in chapter 1). Although these large associations perform physiologically important functions, information regarding their structural organization is still rather limited. Thus, we focused our attention to reveal structures of some of them.

Isolation of the PSI-NDH supercomplex

Selection of plant material and optimization of solubilization

Although there was ample functional and biochemical evidences for the existence of the PSI-NDH supercomplex (Peng et al., 2008; Peng et al., 2009; Peng and Shikanai, 2011), the information regarding its structural organization was missing.

The PSI-NDH supercomplex was originally isolated from *Arabidopsis thaliana* thylakoid membranes solubilized by β-DDM using BN-PAGE (Peng et al., 2008). Thus, we decided to structurally characterize the PSI-NDH supercomplex from the same plant material. Moreover, as we expected that this supercomplex might be too fragile, we tested, in addition to β-DDM, a detergent α-DDM as well for its milder solubilizing action. To optimize yield of the PSI-NDH supercomplex using CN-PAGE separation, we treated thylakoid membranes with gradually increased amounts of individual detergents (Figures 6 and 7).

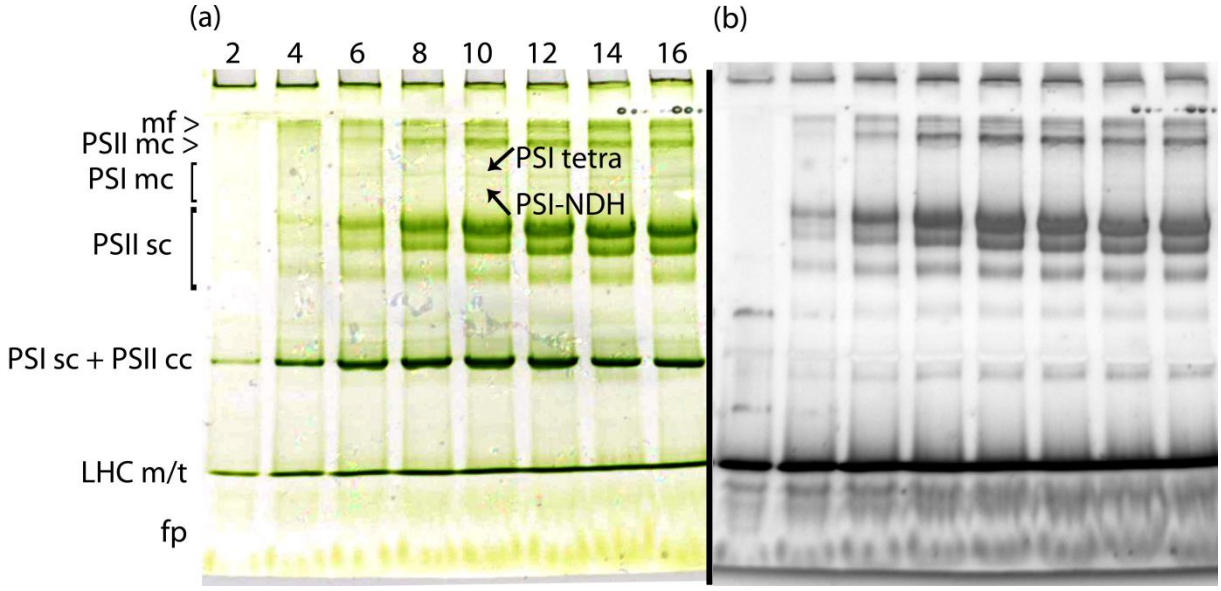

Figure 6. Electrophoretic separation of *Arabidopsis thaliana* thylakoid membranes solubilized by increasing amount of α-DDM. (a) colour image of the gel, (b) room temperature fluorescence of supercomplexes from the same gel. 2-16: DDM/chl ratio; mf: membrane fragments; PSII mc: megacomplexes of PSII; PSI mc: megacomplexes of PSI; PSI tetra: tetramers of PSI; PSII sc: supercomplexes of PSII; PSI sc: supercomplex of PSI; PSII cc: core complex of PSII; LHCm/t: LHC monomers and trimers; fp: free pigments. Designation of individual bands is substantiated in the text.

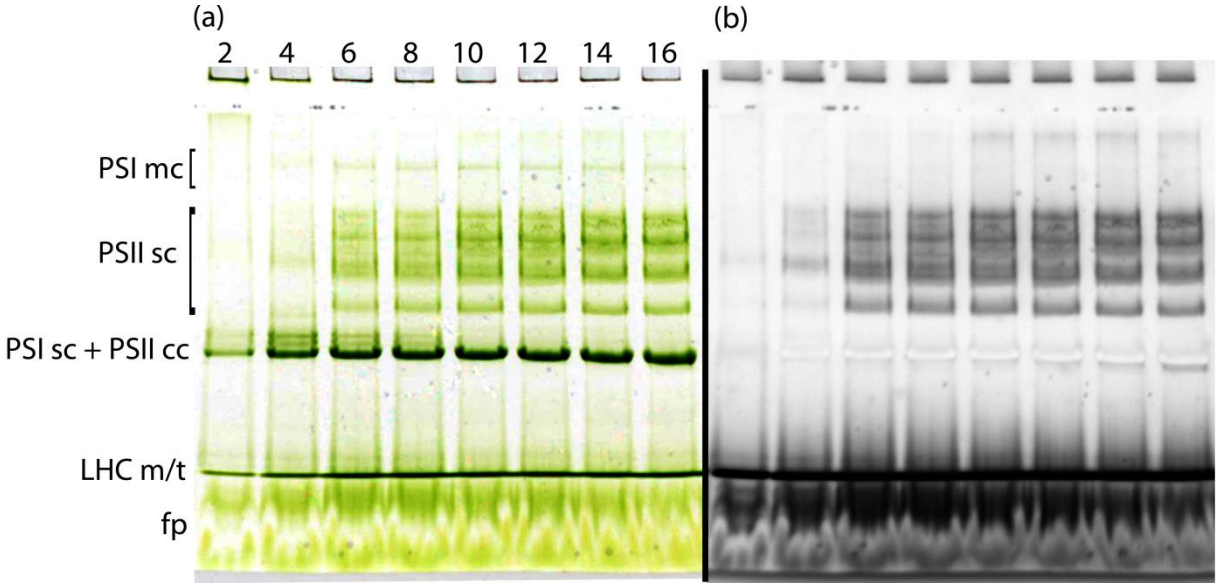

Figure 7. Electrophoretic separation of *Arabidopsis thaliana* thylakoid membranes solubilized by increasing amount of β-DDM. (a) colour image of the gel, (b) room temperature fluorescence of supercomplexes from the same gel. 2-16: DDM/chl ratio; PSI mc: megacomplexes of PSI; PSII sc: supercomplexes of PSII; PSI sc: supercomplex of PSI; PSII cc: core complex of PSII; LHCm/t: LHC monomers and trimers; fp: free pigments. Designation of individual bands is substantiated in the text.

As we aimed preferentially on the PSI-NDH supercomplex, we expected comparable results as originally published by Peng et al., (2008). In that study, a combination of BN-PAGE separation with a western-blotting analysis revealed two high molecular weight bands containing PSI and NDH subunits just above bands with PSII supercomplexes. Thus, in our case, it was necessary to unambiguously distinguish between the PSI-containing bands and the PSII-containing bands in both the CN-PAGE gels (in Figures 6 and 7). This was achieved by the fluorescence imaging of both the gels (details are in the part Methods). Using this method, bands containing the PSI supercomplex can be identified due to a lack of room temperature fluorescence. Thus, the fluorescence imaging unambiguously revealed the position of the PSI supercomplex. Further, it became clear that the group of bands above the PSI supercomplex contain PSII, as they were highly fluorescent. By comparing of our results with other papers dealing with the electrophoretic separation of pigment-protein complexes from thylakoid membranes (Jarvi et al., 2011; Kouril et al., 2016; Pavlovic et al., 2016), we took the liberty to assign the group of PSII-containing bands in the middle of both gels

(Figures 6 and 7) as the PSII supercomplexes. Just above the PSII supercomplexes, the fluorescence imaging of both the gels (Figures 6 and 7) revealed the presence of faint high molecular weight PSI-containing bands most likely corresponding to the bands detected by Peng et al., (2008). In the sample solubilized by α-DDM (Figure 6), two high molecular weight PSI-containing bands were observed. In the case of the sample solubilized with β-DDM, only one high molecular weight PSI-containing band was detected (Figure 7). Nevertheless, densities of all these high molecular weight PSI-containing bands seemed to be insufficient for structural characterization of the PSI-NDH supercomplex. Therefore, we decided to test another plant species in order to determine whether it is possible to obtain these high molecular weight PSI-containing bands with a higher yield. For this purpose, barley plants (*Hordeum vulgare*) were tested. Thylakoid membranes from barley were subjected to the same solubilizing conditions as thylakoid membranes from *Arabidopsis thaliana* (i.e. membranes were solubilized by both α- or β-DDM) and results of their electrophoretic separation are shown in the Figures 8 and 9.

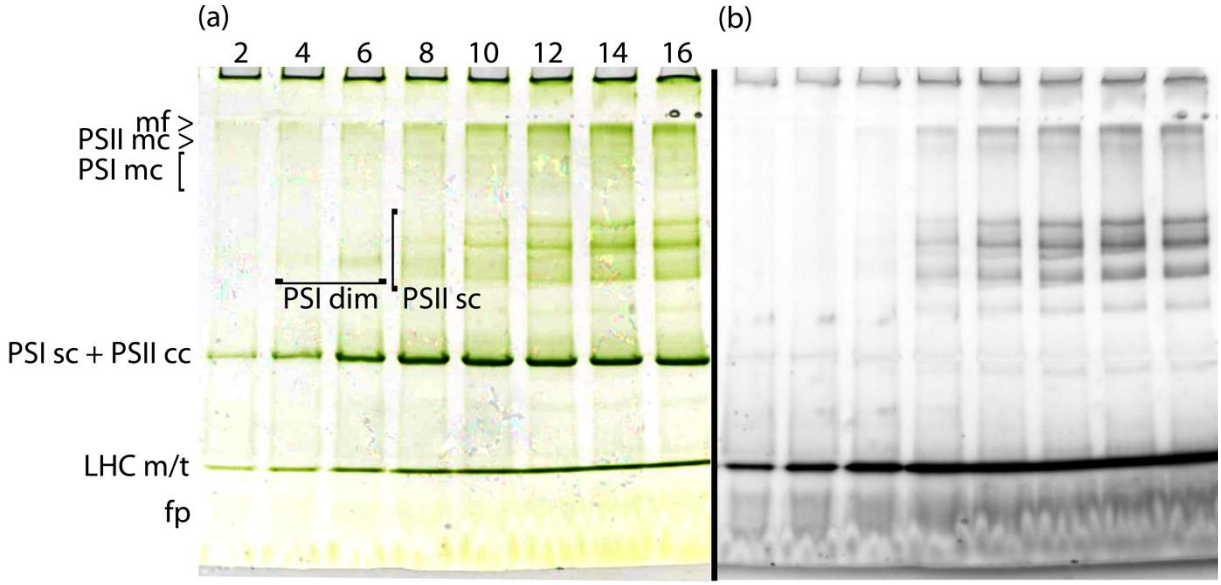

Figure 8. Electrophoretic separation of barley thylakoid membranes solubilized by increasing amount of α-DDM. (a) colour image of the gel, (b) room temperature fluorescence of supercomplexes from the same gel. 2-16: DDM/chl ratio; mf: membrane fragments; PSII mc: megacomplexes of PSII; PSI mc: megacomplexes of PSI; PSI dim: dimers of PSI; PSII sc: supercomplexes of PSII; PSI sc: supercomplex of PSI; PSII cc: core complex of PSII; LHCm/t: LHC monomers and trimers; fp: free pigments. Designation of individual bands is substantiated in the text.

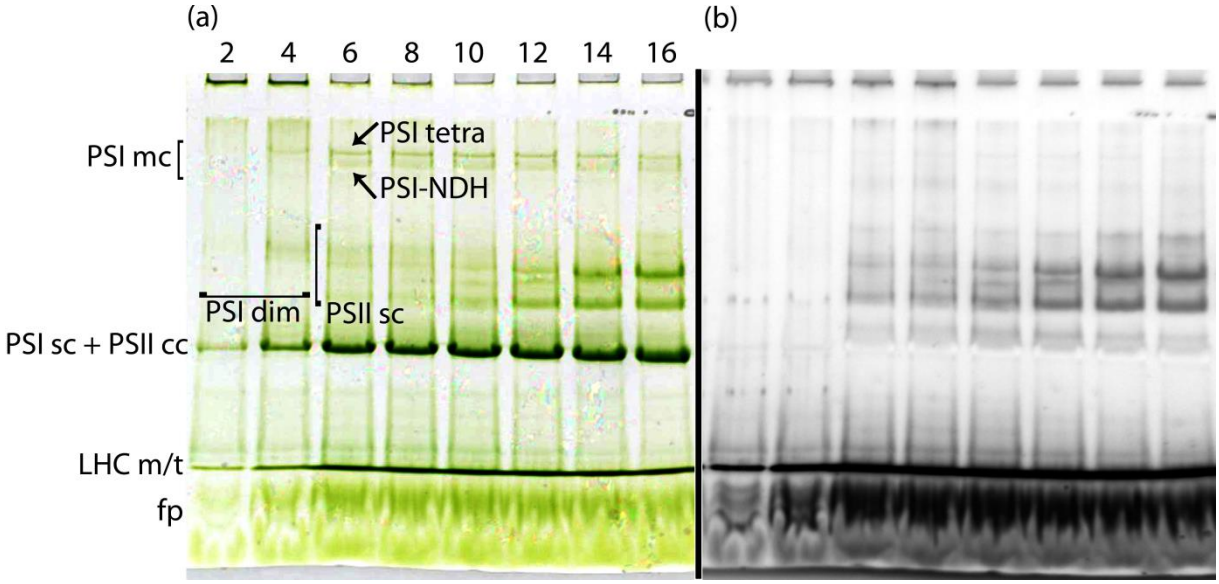

Figure 9. Electrophoretic separation of barley thylakoid membranes solubilized by increasing amount of β-DDM. (a) colour image of the gel, (b) room temperature fluorescence of supercomplexes from the same gel. 2-16: DDM/chl ratio; PSI mc: megacomplexes of PSI; PSI tetra: tetramers of PSI; PSI dim: dimers of PSI; PSII sc: supercomplexes of PSII; PSI sc: supercomplex of PSI; PSII cc: core complex of PSII; LHCm/t: LHC monomers and trimers; fp: free pigments. Designation of individual bands is substantiated in the text.

In the terms of high molecular weight PSI-containing bands, the electrophoretic separation of barley thylakoid membranes provided opposite results compared to membranes isolated from *Arabidopsis thaliana*: whereas barley sample solubilized by β-DDM contained two such bands (Figure 9), barely one band could be detected in barley sample solubilized by α-DDM (Figure 8). However, for the reason that the two high molecular weight PSI-containing bands in the barley sample solubilized by β-DDM (Figure 9) were much denser then the corresponding bands in the *Arabidopsis thaliana* sample (Figure 7), the thylakoid membranes isolated from barley and solubilized by β-DDM were selected for the structural characterization of the PSI-NDH supercomplex.

When the proper plant material providing sufficiently dense high molecular weight PSI-containing bands was selected, suitable amount of detergent (DDM/chl ratio) had to be chosen. After considering the impact of detergent on the densities of bands in the detergent concentration line (Figure 9, values 2-16), the ratio eight was selected as the most proper. At

this ratio, densities of both high molecular weight PSI-containing bands seemed to be equally dense.

After brief electron microscopy screening of both the high molecular weight PSI-containing bands, we discovered that PSI-NDH supercomplex is present in the lower one. Structural characterization of the PSI-NDH supercomplex is described in the chapter 4.1.

On the other hand, electron microscopy inspection of the upper band revealed that the band did not contain PSI-NDH supercomplex, as it was indicated in the paper by Peng et al. (2008). Instead, the band was composed of tetrameric PSI megacomplexes. Figure 10 represents preliminary structural characterization of such tetrameric PSI supercomplexes (unpublished data). However, as it was published already (Kouril et al., 2005a), native plant PSI is present in monomeric form and these PSI tetramers likely represent artificial aggregates.

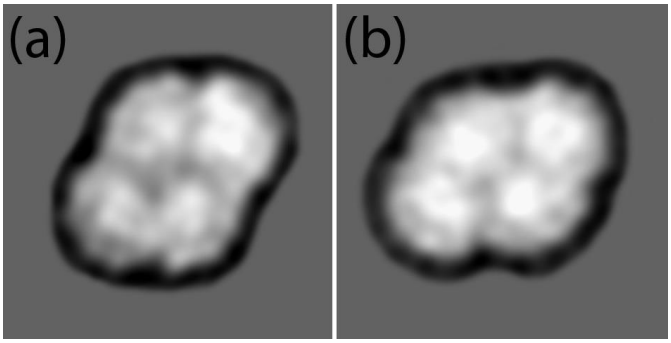

Figure 10. Tetrameric PSI supercomplexes. (a, b) structures represent two types of tetrameric PSI associations discovered in a CN-PAGE gel (Fig. 9).

Moreover, at low detergent concentrations, faint PSI-containing bands appeared in the middle of both CN-PAGE gels with barley sample (Figures 8 and 9). To reveal their composition, complexes from these bands were subjected to electron microscopic analysis. Unfortunately, no reasonable results indicating bands composition were obtained due to very low protein concentration in these bands. However, by considering of the relative

molecular weight of complexes present in mentioned bands and that fluorescence imaging clearly showed the presence of PSI, these bands were preliminarily assigned as dimers of PSI.

It is also worth of interest that the complexes from thylakoid membranes solubilized by α-DDM showed higher level of intactness compared to β-DDM solubilized ones. This is evidenced mainly by higher densities of bands with larger PSII supercomplexes in the samples solubilized by α-DDM (Figures 7 and 9) compared to samples solubilized by β-DDM (Figures 6 and 8). This is in agreement with previously published papers (Barera et al., 2012; Pagliano et al., 2012), which were also dealing with separation of photosynthetic complexes solubilized by α- and β-DDM. These papers show that α-DDM preserves the complexes more intact due to its milder solubilizing properties. The milder solubilizing action of α-DDM is also clearly evident from less dense bands with LHC and free pigments and from higher amount of non-solubilized material stuck in the wells in both samples solubilized by α-DDM.

Despite the original work, dealing with the isolation of the PSI-NDH supercomplex, used *Arabidopsis thaliana* thylakoid membranes (Peng et al., 2008), we found that barley thylakoid membranes are a better option as the PSI-NDH supercomplex was yielded in higher quantity in the barley sample. This implies that optimization of separation technique is an important step preceding structural analysis.

Isolation of PSII megacomplexes from *Arabidopsis thaliana*

In the CN-PAGE gels with *Arabidopsis thaliana* and barley thylakoid membranes solubilized by α-DDM (Figures 6 and 8), two high molecular weight bands appeared just on the top of resolving gels. The fluorescence imaging of the gels showed that both the bands contain PSII. To exclude the possibility that these PSII-containing bands represent fragments of insufficiently solubilized membranes, a brief electron microscopy inspection of complexes present in these bands was performed. The analysis showed that the uppermost band was composed of unspecific aggregates and membrane fragments (data not shown), which were likely formed as a solubilizing artefact or due to insufficient solubilization. On the other hand, the lower band contained a large amount of different megacomplexes, from whose PSII megacomplexes formed of two $C_2S_2M_2$ supercomplexes were vastly prevailing. As these

high molecular weight PSII megacomplex bands were not present in gels with samples solubilized with β-DDM (Figures 7 and 9), it highlights the milder solubilizing action of α-DDM. Details of structural characterization of PSII megacomplexes with proof of their intactness are summarized in the chapter 4.3.

Optimization of separation conditions for a structural characterization of spruce PSII supercomplex

It is known that land plants are generally divided into two major groups: gymnospermous and angiospermous plants. The photosynthetic apparatus of angiospermous plants is well explored, as it is evidenced by dozens of studies performed on *Arabidopsis thaliana*, pea, barley and many other representatives of this group (e.g. Boekema et al., 2001; Caffarri et al., 2009; Jarvi et al., 2011). On the other hand, structural information regarding photosynthetic complexes from gymnospermous plants was completely missing. Thus, we decided to perform structural characterization of the PSII supercomplex in Norway spruce (*Picea abies*), which represents the most abundant and economically the most significant member of gymnosperms. As we aimed on the structural characterization of the PSII supercomplex, we selected PSII enriched membranes isolated from young spruce seedlings. PSII enriched membranes were selected in order to increase the yield of the PSII supercomplexes. Optimization of solubilization conditions was performed in the similar way as in the case of *Arabidopsis thaliana* and barley. Results of electrophoretic separation of spruce PSII enriched membranes solubilized by α- or β-DDM are shown in Figure 11.

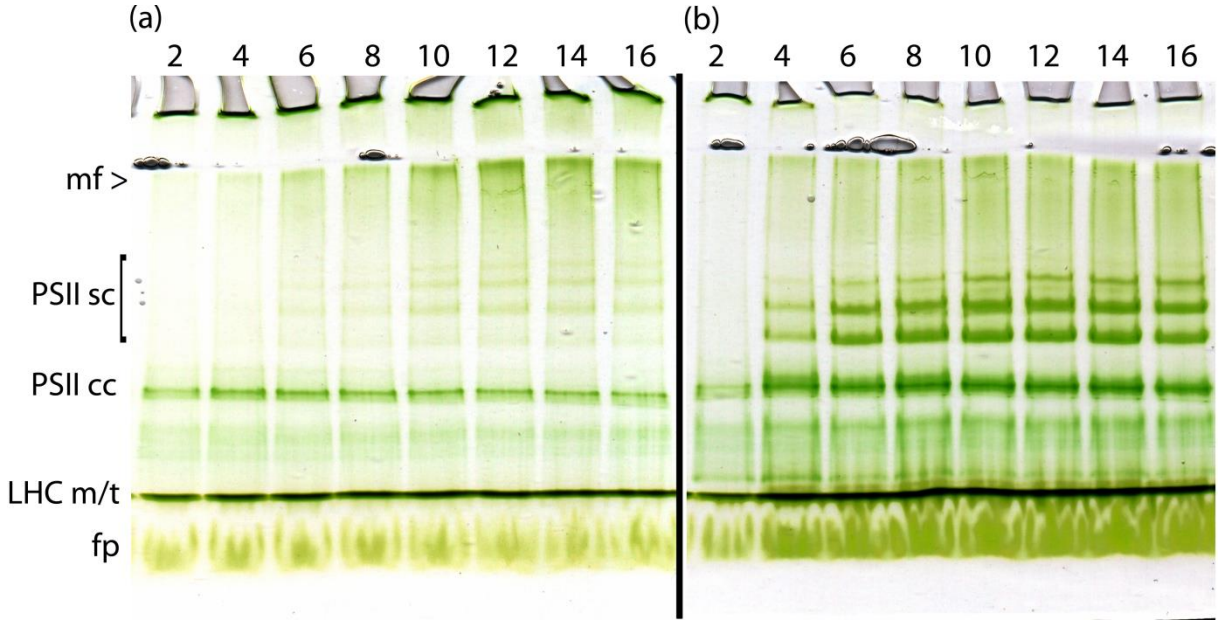

Figure 11. Electrophoretic separation of spruce PSII enriched membranes solubilized by increasing amount of α- or β-DDM. (a) colour image of gel with sample solubilized by α-DDM (b) colour image of gel with sample solubilized by β-DDM. 2-16: DDM/chl ratio; mf: membrane fragments; PSII sc: supercomplexes of PSII; PSII cc: core complex of PSII; LHCm/t: LHCII monomers and trimers; fp: free pigments.

All the bands present in CN-PAGE gel (Figure 11) were composed of different forms of PSII and their assignment was performed in analogy with previous experiments (Figures 6-9). Figure 11 shows that solubilization of membranes by β-DDM provides more dense bands. Thus, for the structural characterization of the PSII supercomplex, solubilization was performed at β-DDM/chl ratio 12. At this ratio, the uppermost PSII supercomplex band subjected to structural analysis seemed to be the densest. The results of structural analysis showed that the architecture of spruce PSII is changed as a consequence of missing Lhcb6 subunit. Thus, a genomic analysis in order to investigate gymnospermous plants' light harvesting proteins was performed. Results imply that spruce is evolutionary deflected from other land plants, as it is lacking Lhcb6 and also Lhcb3 proteins. Details regarding structural characterization of PSII supercomplexes and genomic analysis are summarized in the chapter 4.2.

It is also interesting that the solubilization with β-DDM provided much denser bands with PSII supercomplexes, than solubilization with α-DDM (Figure 11). This is in contrary with membranes from *Arabidopsis thaliana* and barley (Figures 6-9) and refers to possible different lipid composition of spruce thylakoid membranes. Results presented on Figure 11 also clearly show that there were no PSII megacomplexes detected in the CN-PAGE gels with spruce sample. This can be caused by the missing minor antenna Lhcb6 in the spruce PSII (summarized in the chapter 4.2), as it is involved in the PSII megacomplexes formation (summarized in the chapter 4.3).

Specimen preparation

Once the bands with complexes of interest were obtained in sufficient density, a way how to get the complexes out of the gel on the electron microscopy support grid had to be found. There are several methods available.

At first, a method enabling direct transfer of separated protein complexes from a native gel on the grid was recently described (Knispel et al., 2012). Using this method, the grid is placed directly onto a gel band and protein complexes spontaneously adhere on the grid surface. Nevertheless, we did not obtain any satisfying results using this method. We can speculate that protein complex properties (a size and shape) can make the method less suitable for photosynthetic membrane proteins.

The other option is a pipetting of solution containing the protein complexes on the grid – thus the complexes had to be extracted from the gel into solution. Generally, there were two possibilities how to extract protein complexes from the gel into solution: electro elution and spontaneous elution. Electro elution represents a technique allowing fast and quantitative extraction of protein complexes from the gel. During this procedure, the eluted complexes ale electrically forced from a gel and retained on a hydrophobic membrane, where they concentrate. Nevertheless, as the photosynthetic complexes are largely hydrophobic, they frequently irreversibly aggregate on the hydrophobic membrane. Thus, their structural characterization is strongly hampered and this extraction technique seems to be useless for purposes of structural characterization of hydrophobic photosynthetic

complexes. Moreover, the electro elution requires specific and costly equipment. On the other hand, spontaneous elution of protein complexes represents an easy method without any demands for special equipment. It is based on a free diffusion of protein complexes from a cut gel stripe into an elution buffer. When a spontaneous elution is performed, a band (or bands) containing the complexes is excised from the gel. Then the gel stripe is chopped into smaller pieces to enhance the diffusion by increasing its surface and immersed into elution buffer in a micro tube. Volume of the elution buffer should be adjusted to the apparent concentration (density) of complexes in the gel stripe and should be as low as possible. On the other hand, the pieces of the gel have to be always fully immersed in the buffer. As it is described in the methodical part of the chapter 4.1, 30 µl of elution buffer was usually sufficient per one cut gel stripe.

Based on our experience, the spontaneous elution should be performed in dark and cold conditions to minimize a risk of a disintegration of protein complexes. It is usually finished within two hours. A longer time had no significant effect on a higher concentration of protein complexes in the eluate. The density of a gel band subjected to elution was found to be the most critical aspect necessary for reaching sufficient protein concentration in the eluate.

Figure 12 illustrates how the different gel band densities influence the amount of protein complexes present in the specimen.

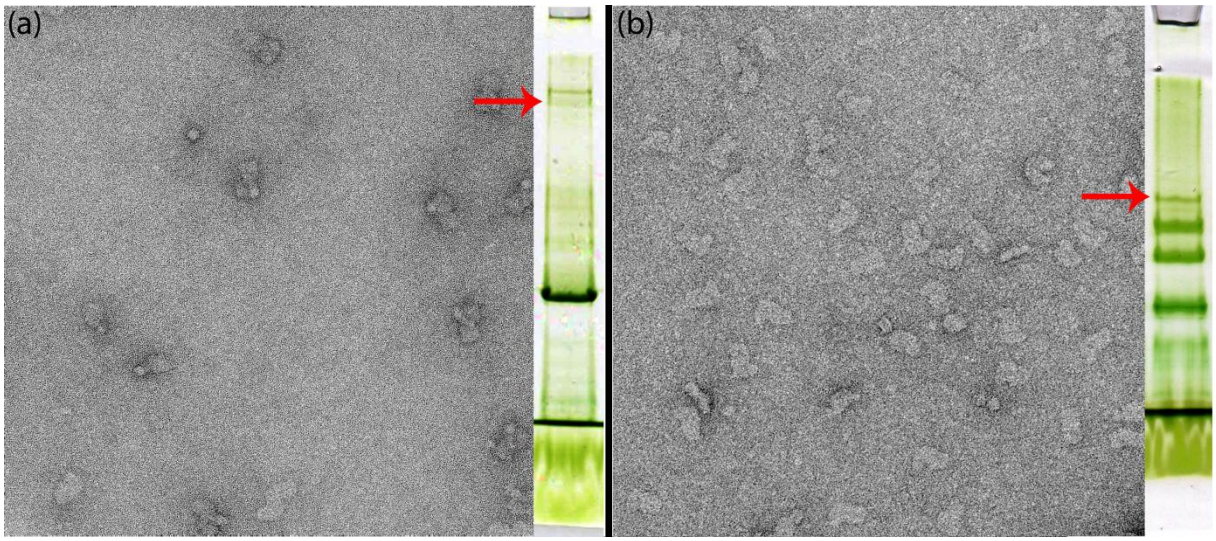

Figure 12. Impact of band density on the amount of protein complexes present in the specimen. (a) left: electron micrograph with the PSI-NDH supercomplexes, right: electrophoretic separation of barley thylakoid membranes as presented in Fig. 9 with marked band used for specimen preparation, (b) left: electron micrograph with the spruce PSII supercomplexes, right: electrophoretic separation of spruce PSII enriched membranes as presented in Fig. 10 with marked band used for specimen preparation. Both excised bands were subjected to the same eluting conditions as described in chapter 4.1.

When the concentration of eluted proteins is too low, the solution can be further concentrated using special centrifugal columns, which are specifically meant for concentrating of protein solutions. These columns contain a hydrophobic membrane with a defined pore size, which retains large protein molecules and releases small solvent and buffer molecules during centrifugation. However, as in the case of electro elution, the photosynthetic complexes largely aggregate on the membrane. This fact emphasizes the importance of optimization of separation conditions to gain dense bands as much as possible.

When the complexes were extracted from the gel into the solution, the specimen was prepared by pipetting the eluate on the glow-discharged carbon coated copper grid and negatively stained with 2% uranyl acetate.

Single particle Image analysis

Single particle image analysis is a step following the specimen imaging. It aligns projections of the protein complexes present in electron micrographs and sorts them out according to their size and shape. As the specimen is usually prepared from one gel band, a homogenous sample of complexes is expected. The CN-PAGE used in our experiments was optimized for separation of large complexes and usually provides very good resolving ability. On the other hand, the specimen can be also very heterogeneous, as complexes of similar molecular weight are difficult to be well separated from each other If this is the case, the imperfectly resolved complexes can be additionally "separated" during image analysis. As an example, Figure 13 represents a result of such image analysis, i.e. its classification part, performed on a data set of PSII megacomplexes from *Arabidopsis thaliana.*

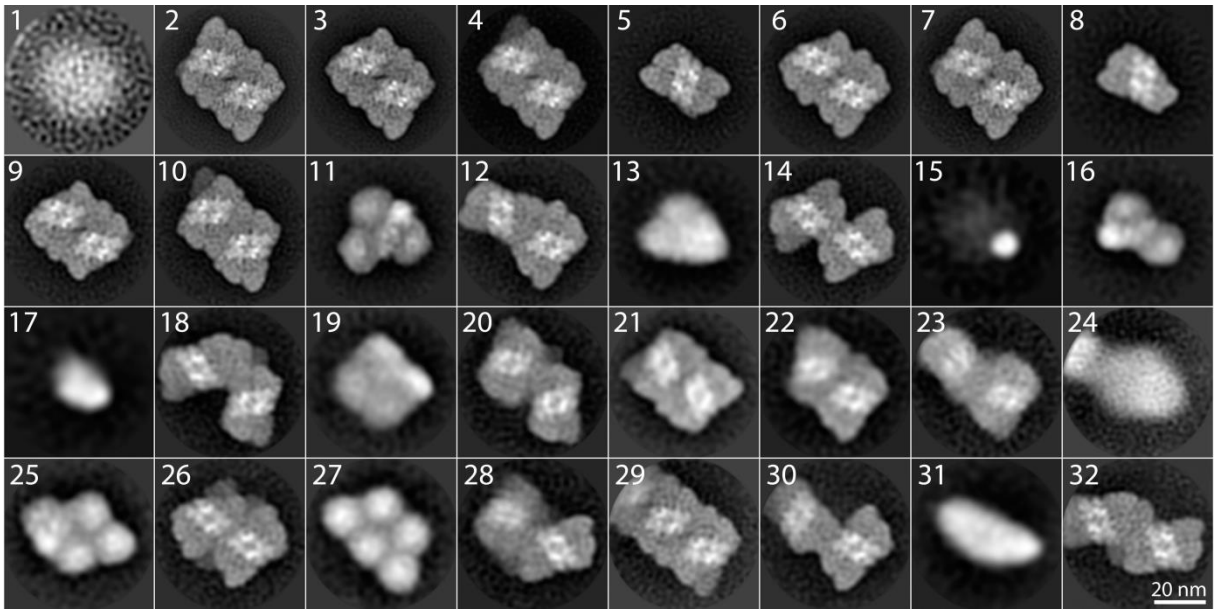

Figure 13. Classification of megacomplexes from specimen obtained from the uppermost *Arabidopsis thaliana* band (Fig. 6). The numbered boxes represent individual classes of different megacomplexes. The classes 2-4, 6, 7, 9, 10, 12, 14, 18, 20-23, 26, 28-30 and 32 represent PSII megacomplexes; classes 5 and 8 represent PSII supercomplexes; classes 11, 16 and 25 represent PSI-NDH supercomplexes; class 27 represents oligomers of PSI and classes 1, 13, 15, 17, 19, 24 and 31 represent impurities or unspecific proteins.

The results presented in Figure 13 show that one band contained large amount of different megacomplexes, which could not be resolved during electrophoretic separation because of their similar molecular weight. The results presented in Figure 13 also imply that theoretically, the separation of solubilized complexes has not indispensably preceded their structural characterization as the image analysis can efficiently sort out different complexes. Nevertheless, it is important to realize that image analysis is greatly time-consuming and the time necessary for its execution significantly rises with increasing number of individual particles. Further, if the separation is not performed, it is necessary to acquire a large amount of micrographs to work with sufficiently large dataset. Thus, as the structural characterization is usually aimed to one complex, it is very convenient to work with a homogenous specimen. Therefore, the optimization of the purification step in order to gain maximally homogenous specimen should be always performed.

4. Publications

4.1 Structural characterization of a plant photosystem I and NAD(P)H dehydrogenase complex.

Reprint of: Kouřil R, Strouhal O, Nosek L, Lenobel R, Chamrád I, Boekema EJ, Šebela M and Ilík P. *Plant Journal* **77**: 568–576, (2014)

the plant journal

SEB Society for Experimental Biology

The Plant Journal (2014) **77,** 568–576 doi: 10.1111/tpj.12402

Structural characterization of a plant photosystem I and NAD(P)H dehydrogenase supercomplex

Roman Kouřil[1,*,†], Ondřej Strouhal[1,†], Lukáš Nosek[1], René Lenobel[2], Ivo Chamrád[2], Egbert J. Boekema[3], Marek Šebela[2] and Petr Ilík[1]

[1]*Department of Biophysics, Centre of the Region Haná for Biotechnological and Agricultural Research, Faculty of Science, Palacký University, Šlechtitelů 11, 783 71 Olomouc, Czech Republic,*

[2]*Department of Protein Biochemistry and Proteomics, Centre of the Region Haná for Biotechnological and Agricultural Research, Faculty of Science, Palacký University, Šlechtitelů 11, 783 71 Olomouc, Czech Republic, and*

[3]*Electron Microscopy Group, Groningen Biomolecular Sciences and Biotechnology Institute, University of Groningen, Nijenborgh 7, 9747 AG Groningen, The Netherlands*

Received 3 October 2013; revised 21 November 2013; accepted 2 December 2013; published online 8 December 2013.
*For correspondence (e-mail roman.kouril@upol.cz).
†Both authors contributed equally to this work.

SUMMARY

Cyclic electron transport (CET) around photosystem I (PSI) plays an important role in balancing the ATP/NADPH ratio and the photoprotection of plants. The NAD(P)H dehydrogenase complex (NDH) has a key function in one of the CET pathways. Current knowledge indicates that, in order to fulfill its role in CET, the NDH complex needs to be associated with PSI; however, until now there has been no direct structural information about such a supercomplex. Here we present structural data obtained for a plant PSI–NDH supercomplex. Electron microscopy analysis revealed that in this supercomplex two copies of PSI are attached to one NDH complex. A constructed pseudo-atomic model indicates asymmetric binding of two PSI complexes to NDH and suggests that the low-abundant Lhca5 and Lhca6 subunits mediate the binding of one of the PSI complexes to NDH. On the basis of our structural data, we propose a model of electron transport in the PSI–NDH supercomplex in which the association of PSI to NDH seems to be important for efficient trapping of reduced ferredoxin by NDH.

Keywords: clear native electrophoresis, *Hordeum vulgare*, single particle electron microscopy, PSI–NDH supercomplex, cyclic electron transport.

INTRODUCTION

In oxygenic photosynthesis, light reactions are driven by photosystem I (PSI) and photosystem II (PSII), two multisubunit protein complexes embedded in the thylakoid membrane. The photosystems cooperatively transfer electrons released from water molecules via plastoquinone (PQ), cytochrome (cyt) b_6/f complex and plastocyanin to ferredoxin (Fd). Electron transport is coupled with the translocation of protons across the thylakoid membrane, which contributes to the generation of a transmembrane ΔpH gradient utilized by ATP synthase to produce ATP. The fate of electrons transported to Fd depends on whether PSI operates in linear (LET) or cyclic (CET) electron transport. In LET, Fd reduces $NADP^+$ via ferredoxin-$NADP^+$ oxidoreductase (FNR) to NADPH, which is utilized in various biosynthetic pathways. In CET, electrons are driven back to the PQ pool and cyt b_6/f complex and this contributes to the formation of a transmembrane ΔpH gradient and thus ATP synthesis without the net production of NADPH. Since it has been reported that LET by itself cannot meet the ATP demands of a plant even under optimal environmental conditions, CET has been generally recognized as an important electron transfer pathway in photosynthetic organisms (see Kramer *et al.*, 2004; Munekage *et al.*, 2004; Shikanai, 2007). Moreover, a temporary change in the relative contribution of LET and CET to overall electron transport can balance the changing ATP/NADPH demands of a plant under varying environmental conditions (for a review see Kramer *et al.*, 2004).

There are currently two main CET pathways that are considered to operate around PSI. One of them depends on the PROTON GRADIENT REGULATION5 (PGR5) and PGR5-LIKE1 (PGRL1) complex (Munekage *et al.*, 2002; DalCorso *et al.*, 2008). The PGRL1 complex could be the elusive Fd–PQ reductase (FQR), as has been recently proposed by

Hertle *et al.* (2013). The other pathway depends on NAD(P)H dehydrogenase (NDH; Burrows *et al.*, 1998; Kofer *et al.*, 1998; Shikanai *et al.*, 1998). The PGR-dependent pathway has been proposed to play an essential role in the balancing of the ATP/NADPH ratio and in plant photoprotection (via energy-dependent non-photochemical quenching, q_E) under naturally fluctuating environmental conditions (see Munekage *et al.*, 2002, 2004; Kramer *et al.*, 2004). While this function of the PGR-dependent pathway is generally accepted, the role of the NDH-dependent pathway is still a matter of debate. Studies based on mutants with impaired NDH function indicate that the NDH pathway is not essential for photosynthesis under normal conditions (e.g. Munekage *et al.*, 2004). Nevertheless, its importance becomes more evident under stress conditions, when this pathway seems to participate in protection against oxidative stress by preventing over-reduction of the chloroplast stroma (for a review see Shikanai, 2007). Indeed, when transgenic tobacco plants with a disrupted NDH function were exposed to stresses preferentially inhibiting CO_2 fixation (e.g. Horváth *et al.*, 2000; Li *et al.*, 2004), i.e. when these plants were experiencing conditions leading to stroma over-reduction, their photosynthetic rate or q_E induction were reduced in comparison to the wild type (WT). Also a recent study with high cyclic electron flow (*hcef*) Arabidopsis mutants, which have constitutively impaired function of the Calvin–Benson cycle, has shown that under such conditions the NDH pathway enhanced q_E and augmented production of ATP (Livingston *et al.*, 2010). Generally, it seems that plants stressed by the factors leading to the over-reduction of chloroplast stroma utilize NDH-dependent CET for both maintenance and photoprotection of the photosynthetic function.

The discovery of the chloroplast NDH complex was based on the identification of 11 plastid genes, *ndhA–ndhK*, which are homologs of genes encoding subunits of mitochondrial complex I (Matsubayashi *et al.*, 1987). Later it was shown that chloroplast NDH is even more similar to bacterial respiratory complex I (NDH-1), except for three bacterial subunits (NuoE–G) whose homologs are missing in the chloroplast NDH. These subunits form the NADH-binding domain in NDH-1 (Friedrich and Scheide, 2000) and therefore their absence indicates that the electron-binding domain in the NDH complex of photosynthetic organisms is probably different. The identity of the electron donor-binding domain in chloroplast NDH has been unknown until recently, when three specific subunits (CRR31, CRRJ and CRRL) were suggested to form the Fd-binding site (Yamamoto *et al.*, 2011). This finding has prompted the reconsideration of the generally accepted idea that NAD(P)H is a direct electron donor to the chloroplast NDH complex. Except for the difference in the electron-binding domain, the photosynthetic NDH complexes have been found to contain other specific subunits which are missing in bacterial NDH-1 (see Battchikova *et al.*, 2011; Ifuku *et al.*, 2011; Peng *et al.*, 2011, for recent reviews). Currently, high-resolution structural data are available only for bacterial NDH-1 (Baradaran *et al.*, 2013). The crystal structures of its counterparts in either cyanobacteria or higher plants are still missing, but electron microscopy (EM) studies of cyanobacterial NDH-1 complexes revealed that it has an L-shaped structure similar to bacterial NDH-1 (Arteni *et al.*, 2006).

The original idea that chloroplast NDH forms a supercomplex with PSI in the thylakoid membrane was formulated on the basis of data obtained using blue-native polyacrylamide gel electrophoresis (BN-PAGE) and the subsequent biochemical characterization (Aro *et al.*, 2005; Peng *et al.*, 2008). Detailed studies of the PSI–NDH supercomplex in various Arabidopsis mutants by Shikanai's group revealed that two minor light-harvesting antenna proteins, Lhca5 and Lhca6, are required for the formation of the supercomplex and for the efficient operation of the NDH pathway (Peng *et al.*, 2009) and that two copies of PSI can be associated with the NDH complex (Peng and Shikanai, 2011). Nevertheless, detailed information about the spatial interaction and stoichiometry of the components of the PSI–NDH supercomplex has not been available so far.

In the study presented here we provide the first structural evidence of the formation of the PSI–NDH supercomplex. We isolated PSI–NDH supercomplexes using high-resolution clear-native (CN)-PAGE under mild conditions and used single-particle EM for their structural characterization. Image analysis revealed the presence of two forms of the PSI–NDH supercomplex. The larger one consists of one NDH complex associated with two copies of the PSI complex, whereas in the smaller one only one PSI is bound to NDH. A comparison of the projection maps of electron densities of the NDH–PSI supercomplex with known atomic X-ray structures of the bacterial NDH-1 complex (Baradaran *et al.*, 2013) and PSI complex (Amunts *et al.*, 2010) enabled us to construct a pseudo-atomic model, which provides a structural insight into the interactions within the supercomplex and allows us to discuss their implications for the function of NDH-dependent CET.

RESULTS AND DISCUSSION

We aimed at a high-yield separation of PSI–NDH supercomplexes from thylakoid membranes in an intact and pure form as we were subsequently going to analyze them using mass spectrometry (MS) and single-particle EM. We decided to perform this separation using high-resolution native PAGE. Generally, native PAGE performed in gels with a gradient density starting at 4% acrylamide enables separation of large protein supercomplexes with a molecular mass even exceeding 1 MDa in the form of well distinguished and focused bands. In our separation, we preferred CN-PAGE to the more often used BN-PAGE

because it generally works under milder conditions (Wittig and Schägger, 2005).

As the chloroplast NDH complex in plants grown under normal conditions was estimated to be only about 1–2% of PSI on a molar basis (Peng *et al.*, 2008), it was crucial to carefully adjust the separation and isolation conditions to yield a sufficient amount of the PSI–NDH supercomplex for the subsequent analysis. In order to prepare a sample enriched in intact PSI–NDH supercomplexes from thylakoid membranes, we treated the membranes with a low concentration of *n*-dodecyl-β-D-maltoside (DDM). Under these conditions, the solubilization of membrane protein complexes from large grana was incomplete and the solubilized protein fraction was enriched in protein complexes from stroma thylakoids including the PSI–NDH supercomplex (Peng *et al.*, 2008, 2009). The subsequent separation of this protein fraction by CN-PAGE showed several green bands containing PSI (Figure 1). Most of the PSII–LHCII complexes remained unsolubilized or they were retained on the top of the polyacrylamide gel.

We analyzed the separated green bands by MS and identified PSI in five green bands (bands 1–5; Figure 1). Based on the MS analysis of the bands and the comparison of our separation with similar separations using CN-PAGE, BN-PAGE (e.g. Järvi *et al.*, 2011) or Deriphat-PAGE (e.g. Lípová *et al.*, 2010), we attributed the lightest PSI-containing band (band 5) to PSI monomer, which co-migrates with the dimeric PSII core. Heavier PSI-containing bands, above band 5 in Figure 1, represent the PSI/PSII supercomplex

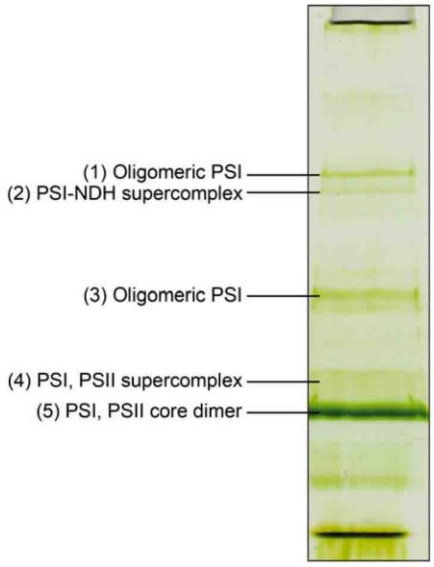

Figure 1. Separation of pigment-protein complexes by clear native-PAGE. Thylakoid membranes isolated from barley leaves were solubilized by *n*-dodecyl-β-D-maltoside (DDM; 6 μl of 10% (w/v) β-DDM per 100 μg of chlorophyll). PSI, photosystem I; PSII, photosystem II; NDH, NAD(P)H dehydrogenase.

(band 4) or PSI oligomers (bands 3 and 1). In band 2 we detected a large number of NDH subunits together with PSI subunits, thus we attributed this band to the PSI–NDH supercomplex (Table 1).

Band 2 was excised and the supercomplexes were extracted from the gel by spontaneous elution and directly used for structural analysis using single-particle EM. Inspection of electron micrographs revealed the presence of two forms of PSI–NDH particle, which differed in size (Figure 2a). Image analysis of about 11 000 single-particle projections indicated that the larger particle consists of two PSI complexes attached to the sides of one NDH complex, which can be clearly recognized in the central part of the projection map due to the typically curved shape of the membrane arm and the very strong density of the hydrophilic arm (Figure 2b). The smaller particle contains only one copy of the PSI complex and one copy of NDH (Figure 2c). The assignment of the NDH complex indicates that the projection maps obtained for both the smaller and larger PSI–NDH supercomplexes represent views from the stromal side of the thylakoid membrane. Due to the fact that the PSI–NDH supercomplexes were separated by CN-PAGE as a single band (i.e. they have the same molecular mass), the smaller particles have to be considered as artificial breakdown products. Since there are hardly any free PSI complexes in the electron micrographs (Figure 2a), it is likely that the dissociation of one PSI from the supercomplex does not take place during the final preparation of the EM specimen but most probably one PSI remains in the gel during the elution of the PSI–NDH supercomplexes. Interestingly, the image analysis revealed only one form of the smaller supercomplex, where the single PSI complex is bound to the outer part of the curved membrane arm of the NDH complex (Figure 2c). This implies that the binding of PSI at this site is stronger than the binding of PSI to the inner part of the curved membrane arm of the NDH.

We constructed a pseudo-atomic model of the PSI–NDH supercomplex by fitting the EM projection map with the known X-ray structures of the plant PSI complex (Amunts *et al.*, 2010) and the entire bacterial NDH-1 complex from *Thermus thermophilus* (Baradaran *et al.*, 2013). The latter was used as an approximation of the 'core part' of the chloroplast NDH complex due to a high homology between 11 chloroplast NDH (NdhA–K) and bacterial NDH-1 (Nqo4–14) subunits (see Peng *et al.*, 2011; for the nomenclature of these subunits). The validation of the model was based on the comparison of the EM projection map with the two-dimensional projection map of the PSI–NDH supercomplex generated from the pseudo-atomic model composed of the truncated X-ray structures (Figure 2e).

The pseudo-atomic model shows that the EM projection map of the chloroplast NDH complex is well fitted with the membrane subunits of NDH-1. Nevertheless, compared

Table 1 A summary of the identified photosystem I (PSI)–NAD(P)H dehydrogenase (NDH) complex subunits isolated from barley

	Protein	UniProt accession code or AGI code	Organism	Mowse score	Peptide counts	Spectral counts	Sequence coverage (%)
PSI complex	PsaA	sp|A1E9J1	*H. vulgare*	789/355	22/11	83/31	21.3/12.7
	PsaB	ATCG00340	*A. thaliana*	493/449	10/14	51/39	13.4/14.7
	PsaD	tr|F2EJP2	*H. vulgare*	393/326	13/10	53/47	47.3/41
	PsaE	tr|M0YUC4	*H. vulgare*	181/117	6/3	20/16	42.9/32.7
	PsaF	tr|F2E4W0/tr|M0Y678	*H. vulgare*	220/563	5/13	21/57	14.5/29.9
	PsaG	tr|M0YYL3/tr|F2DE22	*H. vulgare*	84/91	2/3	6/8	23.2/11.9
	PsaH	tr|M0WPH0	*H. vulgare*	147/180	4/6	25/24	23.1/29.6
	PsaK	tr|M0YAU7	*H. vulgare*	175/75	5/2	17/9	34.4/13
	PsaL	sp|P23993	*H. vulgare*	262/168	8/5	24/13	30.6/15.8
	Lhca1	tr|M0V8T9	*H. vulgare*	342/138	10/5	38/19	30.4/17
	Lhca2	tr|M0XHH9	*H. vulgare*	240/138	4/3	15/13	12.9/9.4
	Lhca3	tr|F2D9M7	*H. vulgare*	341/89	8/2	31/8	23.8/8.9
	Lhca4	tr|M0W877/tr|F2CRC1	*H. vulgare*	312/111	8/2	34/9	27.9/8.6
	Lhca5	tr|M0UPG7/tr|M0UPG6	*H. vulgare*	182/123	4/5	12/9	16.3/25.9
	Lhca6	tr|M0V4V6	*H. vulgare*	114/127	4/3	16/10	11.4/8.1
NDH membrane subcomplex	NdhA	sp|P92432/ATCG01100	*H. vulgare/A. thaliana*	214/141	4/4	14/10	9.7/11.7
	NdhC	sp|A1E9J6	*H. vulgare*	–/47	–/1	–/4	–/9.2
	NdhD	sp|O03060	*H. vulgare*	168/160	4/6	12/11	6.4/8
NDH subcomplex A	NdhH	sp|O98691	*H. vulgare*	416/290	11/13	54/21	24.2/27.2
	NdhI	ATCG01090	*A. thaliana*	106/–	3/–	13/–	15.1/–
	NdhJ	tr|M0VEF6	*H. vulgare*	105/132	3/3	13/15	17.9/19.1
	NdhK	sp|Q85XC3	*H. vulgare*	228/213	6/7	25/22	17.3/16.9
	NdhL	tr|F2CUR7	*H. vulgare*	69/–	3/–	7/–	9.9/–
	NdhM	tr|M0VHJ2	*H. vulgare*	239/85	7/3	22/9	37.2/20.9
	NdhN	tr|M0XNR3	*H. vulgare*	397/99	12/2	46/8	61/14
	NdhO	tr|M0USN8	*H. vulgare*	163/169	4/5	17/9	25.2/21.3
NDH subcomplex B	NDF1	tr|F2D3G1	*H. vulgare*	605/401	14/14	60/34	21.1/26
	NDF2	tr|F2D932	*H. vulgare*	720/308	18/8	70/32	36/22.7
	NDF6	tr|F2CPQ4	*H. vulgare*	238/81	7/3	16/6	32.6/22.5
	NDH18	tr|F2DWH9	*H. vulgare*	–/81	–/3	–/5	–/15.3
	PQL	tr|M0XTT4	*H. vulgare*	79/49	3/2	9/5	15.2/11.6
Lumen subcomplex	PPL2	tr|M0XDE0	*H. vulgare*	231/185	6/6	31/15	15.3/21
	CYP20-2	tr|F2CTD7	*H. vulgare*	134/112	6/4	13/9	18.1/15.6
	FKBP16-2	tr|F2DIC1	*H. vulgare*	182/57	6/2	19/7	23.8/7
	PQL	tr|F2CTW7	*H. vulgare*	147/127	3/4	22/10	16.2/17.6
NDH electron donor-binding	NdhU	tr|F2DY44/tr|F2D6X3	*H. vulgare*	168/102	4/4	15/9	18.4/18

Basic protein identification statistics is related to trypsin/chymotrypsin digestion. Individual proteins are named according to Peng *et al.* (2011) and Ifuku *et al.* (2011).

with the generated projection map, in the EM projection map we observed a stronger density variation in the membrane arm of the NDH. Our MS analysis (Table 1) suggests that this difference can be attributed to the presence of additional subunits, specific to the chloroplast NDH complex (see Ifuku *et al.*, 2011; Peng *et al.*, 2011). An unassigned strong density of the hydrophilic arm (blue asterisk, Figure 2d) may also represent subunits specific to the chloroplast NDH complex. We might speculate that the additional density comes from the recently discovered CRR31, CRRJ and CRRL subunits, which form the Fd-binding domain in the chloroplast NDH (Yamamoto *et al.*, 2011). One of these subunits, CRRL (NdhU), was indeed identified in the PSI–NDH supercomplex by the MS analysis (Table 1).

Fitting of the PSI complexes was facilitated by resolved strong densities of the PSI core complex at the periphery of the supercomplex, which indicates that the PSI complexes interact with the membrane domain of the NDH through their light-harvesting antenna proteins. Inspection of the pseudo-atomic model shows that the PSI complex at the outer part of the curved membrane domain binds to NdhD and NdhF subunits through Lhca2/4 proteins. Involvement of the NdhD and NdhF subunits in association with PSI and NDH is in agreement with earlier biochemical data (Peng *et al.*, 2009). The other PSI complex, which is attached to the inner part of the curved membrane domain, interacts with NdhB/D/F subunits mainly through Lhca2/4, where Lhca4 is also in the vicinity of NdhE and NdhG. The pseudo-atomic model indicates that Lhca1 is facing the area of strong density corresponding to the hydrophilic arm, which overlaps the tip of the NDH membrane arm.

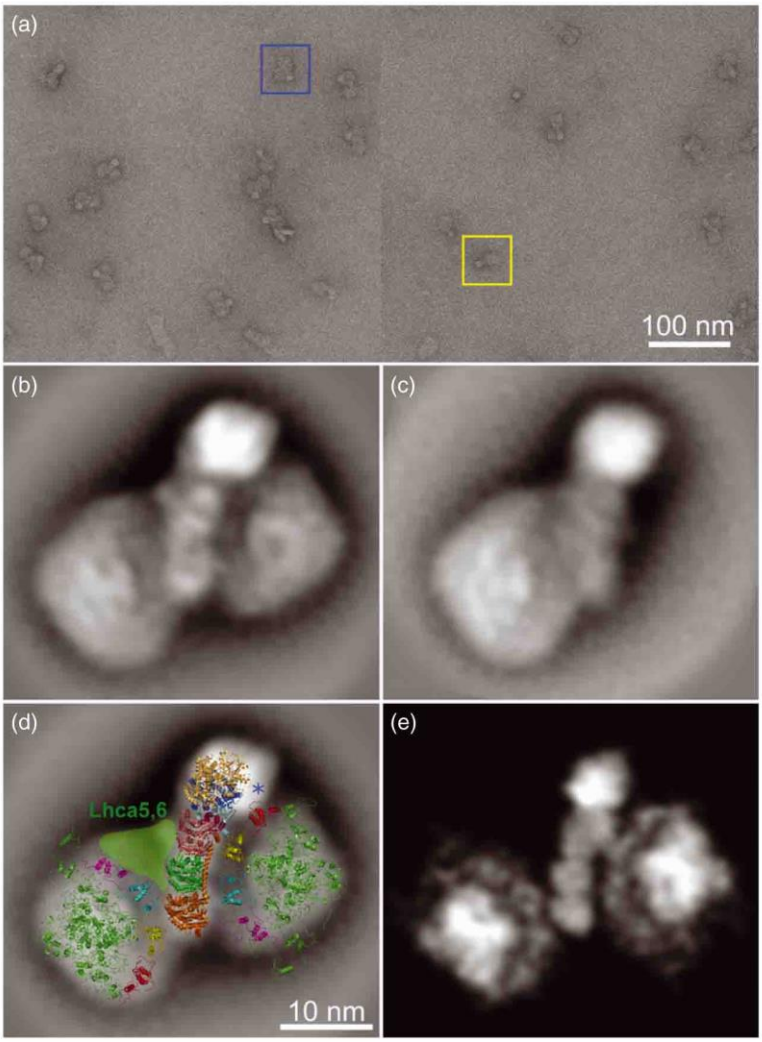

Figure 2. Structural characterization of the photosystem I (PSI)–NAD(P)H dehydrogenase (NDH) supercomplex by single-particle electron microscopy.
(a) Examples of two raw electron micrographs of a negatively stained specimen with two forms of the PSI–NDH supercomplex. A more abundant larger form is highlighted in the blue box, a smaller form in the yellow box.
(b) Averaged projection map of the larger PSI–NDH supercomplex (sum of 4608 particles) consisting of the NDH complex and two copies of the PSI complex.
(c) Averaged projection map of the smaller PSI–NDH supercomplex (sum of 1031 particles) containing single copies of both NDH and PSI complex.
(d) Structural assignment of the larger PSI–NDH supercomplex based on fitting with the X-ray structures of the PSI complex (Amunts *et al.*, 2010) and the respiratory complex I (Baradaran *et al.*, 2013; the Protein Data Bank accession numbers 3LW5 and 4HEA, respectively). The PSI complex is shown in green with highlighted Lhca proteins (Lhca1 in red, Lhca4 in yellow, Lhca2 in cyan, Lhca3 in magenta). Subunits of the membrane part of the respiratory complex are shown in orange (NdhF), green (NdhD), salmon (NdhB), warm pink (NdhE), pale cyan (NdhG) and blue (NdhA and NdhC). The hydrophilic arm is in light-orange. Nqo1–3 subunits, which are missing in the chloroplast NDH complex, were omitted in the model. The blue asterisk indicates an unassigned density area of the hydrophilic arm.
(e) Projection map of the PSI–NDH supercomplex generated from the proposed pseudo-atomic model at 20 Å resolution.

The fact that PSI binds to NDH in two different ways is quite unusual. To facilitate their binding, PSI complexes possibly need 'help' from additional proteins. There is an unassigned protein density between the Lhca2/3 of the left PSI complex and the NdhD/B subunits (Figure 2d). The area is large enough to accommodate additional light-harvesting proteins or another Ndh subunit, specific to the chloroplast NDH complex. We propose that the unassigned area contains minor light-harvesting proteins, Lhca5 and/or Lhca6, which were found to play a critical role in supercomplex formation (Peng *et al.*, 2009). This is supported by our MS analysis, which identified both Lhca5 and Lhca6 in the PSI–NDH supercomplex (Table 1). The proposed location of the Lhca5/6 proteins is in agreement with the cross-linking studies, which indicate that Lhca5 associates with PSI complex at the Lhca2/3 site (Lucinski *et al.*, 2006). Nevertheless, a complete absence of association of PSI to NDH complex was observed in the Arabidopsis *lhca5–lhca6* double mutant (Peng and Shikanai, 2011). In the light of this finding, one would expect that Lhca5 and Lhca6 proteins mediate binding of PSI complexes to both sides of the NDH complex. The same conclusion can also be drawn from a former study of individual Arabidopsis *lhca5* and *lhca6* single mutants, where only a smaller form of the PSI–NDH supercomplex (one PSI complex/NDH) was detected (Peng *et al.*, 2009). However, our data imply that, at least in barley, both Lhca5 and Lhca6 participate in binding of only one of the PSI complexes and support its strong association with the NDH complex (Figure 2b–d). The binding of the other PSI complex to NDH is weak, which is evidenced by the fact that it can dissociate from the intact PSI–NDH supercomplex during its elution from the gel (see discussion above). Based on our current data obtained for barley we can only speculate whether the

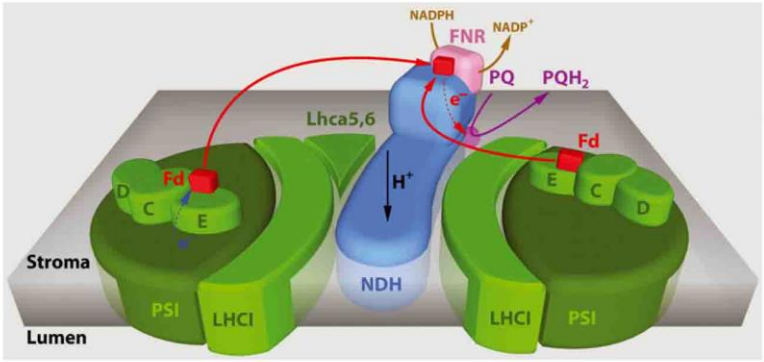

Figure 3. Structure–functional model of the photosystem I (PSI)–NAD(P)H dehydrogenase (NDH) supercomplex in the thylakoid membrane.
Ferredoxin (Fd) binds to the hydrophilic arm of the NDH complex (continuous red arrows) upon its reduction at the acceptor side of the PSI complex (dotted blue arrow). Then Fd reduces the plastoquinone (PQ) molecule, which is bound at the back side of the membrane arm of the NDH complex (continuous violet arrow), via intermediate NDH electron carriers (dotted red arrow). Then the cyclic pathway is completed by a transfer of the electron from the PQ molecule back to the PSI complex via the cyt b_6/f complex and plastocyanine. Alternatively, Fd can be reduced by NAD(P)H through the reverse reaction of FNR, which is attached to the NDH complex. In this way, the alternative reduction of Fd can alleviate the stromal over-reduction. The NDH complex may also function as a proton pump. LHCI, light-harvesting complex I.

smaller PSI–NDH supercomplex formed in Arabidopsis *lhca5* and *lhca6* single mutants represents the complex with the strongly or the weakly bound PSI. Nevertheless, a complete absence of PSI–NDH supercomplexes in the Arabidopsis *lhca5–lhca6* double mutant indicates that (i) the strongly bound PSI requires these minor antenna proteins for its stable association with the NDH complex and (ii) the interaction between the strongly bound PSI and NDH is required for the association of the weakly bound PSI to the NDH complex. However, further structural analysis of individual Arabidopsis mutants is needed to fully clarify this issue.

The question is, what benefit is brought by the organization of NDH and PSI in such a peculiarly shaped supercomplex? Firstly, the binding of two PSI complexes along the membrane arm of the NDH maximizes the interaction interface between these complexes, which clarifies the stabilization of the NDH complex observed when NDH is part of the supercomplex (Peng and Shikanai, 2011). Secondly, the formation of the supercomplex guarantees short distances between the hydrophilic arm of the NDH, which most probably accommodates the Fd-binding domain, and two PSI–Fd-binding sites (approximately 11 and 22 nm). Further, the 2:1 stoichiometry between PSI and NDH in the supercomplex can locally increase the population of reduced Fd. Taken together, these facts suggest that supercomplex formation can make the trapping of the reduced Fd by the NDH complex more efficient. This interpretation coincides with the recent results of Yamamoto *et al.* (2011), who showed the importance of Fd in the function of the chloroplast NDH complex. These authors showed that the NDH complex accepts electrons from Fd rather than from NAD(P)H and thus they proposed that the chloroplast NDH complex may function in a similar way to the PGRL1 complex, i.e. as the FQR (Hertle *et al.*, 2013). From this point of view, NDH-dependent CET might be much more similar to PGR-dependent CET than previously assumed.

Despite this similarity, we have to bear in mind that in the case of NDH-dependent CET, NAD(P)H is widely accepted as the main electron donor and therefore we can ask what the exact role of Fd in this pathway is. We hypothesize that within the PSI–NDH supercomplex, Fd can be reduced at the expense of NAD(P)H via the reverse reaction of FNR bound to NDH complex. Indeed, there is experimental evidence that the reverse reaction of FNR can operate *in vitro* (Munekage *et al.*, 2002; Shikanai, 2007; Hu *et al.*, 2013) and that FNR associates with NDH complex (Quiles *et al.*, 2000; Hu *et al.*, 2013). The oxidation of NAD(P)H via this alternative pathway can alleviate stroma over-reduction, which is one of the proposed physiological roles of NDH-dependent CET.

Based on our structural results and the discussion above we suggest a structure–functional model of the PSI–NDH supercomplex (Figure 3). In this model, electron transfer between PSI complexes and the NDH complex is mediated by Fd, which binds to the Fd-binding domain in the hydrophilic arm of the NDH. Alternatively, Fd can be reduced by NAD(P)H via the reverse reaction of FNR. The Fd then reduces a PQ molecule via intermediate NDH electron carriers. Considering the structural homology of the chloroplast NDH with bacterial (Baradaran *et al.*, 2013) and cyanobacterial NDH-1 (Hu *et al.*, 2013), we propose that the PQ molecule also binds at the lower back side of the membrane arm, which is freely accessible due to the architecture of the PSI–NDH supercomplex. The proposed model has to be verified by experiments focusing on a detailed functioning of the PSI–NDH supercomplex.

CONCLUSION

The first evidence of the existence of the PSI–NDH supercomplex was based on extensive biochemical studies (Peng *et al.*, 2008, 2009) and the absence of structural data can be ascribed mainly to the low abundance of the NDH complex in the thylakoid membrane. The fact that the NDH content is generally as low as 1–2% of the total PSI content (Peng *et al.*, 2008) makes any structural analysis of the supercomplex rather challenging. An optimized mild separation of solubilized thylakoid membrane using CN-PAGE, followed by MS of separated bands, allowed us to isolate an intact PSI–NDH supercomplex with a yield sufficient for single-particle structural analysis. The structural analysis shows asymmetric binding of two PSI complexes to an NDH complex and indicates the position of the Lhca5 and Lhca6 antenna proteins of PSI, which are present in the thylakoid at enigmatically low substoichiometric levels (Ganeteg *et al.*, 2004). These antenna proteins are probably needed for the attachment of one of the two PSI complexes to the low-abundant NDH.

The formation of the PSI–NDH supercomplex is another factor supporting the hypothesis that the key reactions in photosynthesis and in the mitochondrial respiratory chain require a high level of organization. Besides the increase in the stability of individual components, supercomplex formation has important functional implications, which result from possibly enhanced electron transfer rates and substrate channeling (Dudkina *et al.*, 2010). It has been reported that in *Chlamydomonas reinhardtii* CET depends on the formation of a PSI–LHCI–LHCII–FNR–cytb_6/*f*–PGRL1 supercomplex (Iwai *et al.*, 2010). Here, we provide a structural evidence for PSI–NDH supercomplex formation in higher plants. As the formation of the PSI–NDH supercomplex was found to be necessary for the efficient operation of the NDH complex (Peng *et al.*, 2009), it is essential for proper function of the NDH-dependent pathway of CET. The formation and dissociation of supercomplexes can function as a switch between LET and CET. Different triggers have been proposed to induce the formation of supercomplexes participating in CET, including a low ATP content (Joliot and Joliot, 2002), a high NADPH concentration (Joliot and Johnson, 2011) or protein phosphorylation (Iwai *et al.*, 2010). Nevertheless, further studies are necessary to understand the exact mechanism governing the reversible formation of these supercomplexes.

EXPERIMENTAL PROCEDURES

Plant material and sample preparation

Barley (*Hordeum vulgare* L. cv. Akcent) seedlings were grown in a growth chamber with a 16-h/8-h light/dark photoperiod at 25°C. During the light period, the seedlings were illuminated with a white fluorescent lamp at an intensity of about 100 μmol photons m^{-2} sec^{-1} (400–700 nm). Thylakoid membranes were isolated as described in Dau *et al.* (1995) and a quantity of thylakoids corresponding to 100 μg of chlorophyll was solubilized by the addition of 6 μl of 10% (w/v) DDM. The mixture was supplemented with solubilizing buffer (50 mM HEPES, 400 mM sucrose, 15 mM NaCl, 5 mM $MgCl_2$, pH 7.2) containing 10% (v/v) glycerol to a final volume of 50 μl. After solubilization, membrane fragments were removed by centrifugation (22 000 ***g***, 4°C, 10 min). Then CN-PAGE was performed with a 4–8% gradient resolving gel and 4% stacking gel (Wittig *et al.*, 2007). The separation started at a constant current of 7 mA for 15 min and continued at a constant current of 15 mA for an additional 2 h. The chlorophyll content was determined by extraction and assay in 80% acetone (Lichtenthaler and Buschmann, 2001).

Sample preparation and liquid chromatography (LC)-MS/MS-based analysis of the PSI–NDH supercomplex

The PSI–NDH supercomplex separated by CN-PAGE was excised from the gel slab and in-gel digested either with trypsin or chymotrypsin as described elsewhere (Shevchenko *et al.*, 2006). The resultant peptides were desalted on C18 microcolumns (Rappsilber *et al.*, 2007) and analyzed using a nanoLC-electrospray ionization-ultrahigh resolution-quantitative time-of-flight LC-MS system (Proxeon, Denmark, www.proxeon.com; Bruker Daltonik, Germany, www.bruker.com). Protein identification was achieved by searching the acquired data against a custom protein database with the Mascot search algorithm (Perkins *et al.*, 1999). For detailed information on the digestion procedure, peptide desalting, LC-MS/MS analysis and data processing see the Supporting Information (Methods S1–S3, Tables S1 and S2, Data S1 and S2).

Electron microscopy and image processing

The gel stripe containing PSI–NDH supercomplexes was excised from the CN-PAGE gel, chopped up and placed in an Eppendorf tube with 50 μl of buffer (50 mM HEPES, 15 mM NaCl, 5 mM $MgCl_2$, pH 7.2) for 2 h at 4°C to achieve spontaneous elution of the supercomplexes. The solution was then directly used for EM specimen preparation by negative staining with 2% uranyl acetate on a glow-discharged carbon-coated copper grid. Electron microscopy was performed on a Philips CM120 electron microscope (www.fei.com) equipped with a LaB_6 filament operating at 120 kV. Images were recorded with a Gatan 4000 SP (www.gatan.com) 4K slow-scan charge-coupled device camera at 130 000× magnification with a pixel size of 0.23 nm at the specimen level after binning the images to 2048 × 2048 pixels. GRACE software was used for semi-automated data acquisition (Oostergetel *et al.*, 1998). Single-particle analysis was performed using GRIP software including multi-reference and non-reference alignments, multivariate statistical analysis and classification. A pseudo-atomic model of the PSI–NDH supercomplex was created using PyMOL (DeLano, 2002). Truncated versions and a two-dimensional projection map of the generated model for the PSI–NDH supercomplex at 20Å resolution were generated using routines from the EMAN package (Ludtke *et al.*, 1999). A schematic model of the PSI–NDH supercomplex was created using a free version of GOOGLE SKETCHUP software.

ACKNOWLEDGEMENTS

This work was supported by the Ministry of Education, Youth and Sports of the Czech Republic (ED0007/01/01 to Centre of the Region Haná for Biotechnological and Agricultural Research and CZ.1.07/2.3.00/20.0057), the Grant Agency of the Czech Republic (project 13-28093S/P501 to RK) and by a Marie Curie Career Integration Grant call FP7-PEOPLE-2012-CIG (322139 to RK). We thank Dr Iva Ilíková for editing the manuscript.

SUPPORTING INFORMATION

Additional Supporting Information may be found in the online version of this article.

Table S1. Complete list of identified proteins for trypsin digestion.

Table S2. Complete list of identified proteins for chymotrypsin digestion.

Data S1. Complete list of identified proteins for trypsin digestion.

Data S2. Complete list of identified proteins for chymotrypsin digestion.

Methods S1. Protein digestion and peptide desalting.

Methods S2. Liquid chromatography-MS/MS analysis.

Methods S3. Protein data analysis.

REFERENCES

Amunts, A., Toporik, H., Borovikova, A. and Nelson, N. (2010) Structure determination and improved model of plant photosystem I. *J. Biol. Chem.* **285**, 3478–3486.

Aro, E.M., Suorsa, M., Rokka, A., Allahverdiyeva, Y., Paakkarinen, V., Saleem, A., Battchikova, N. and Rintamäki, E. (2005) Dynamics of photosystem II: a proteomic approach to thylakoid protein complexes. *J. Exp. Bot.* **56**, 347–356.

Arteni, A.A., Zhang, P., Battchikova, N., Ogawa, T., Aro, E.M. and Boekema, E.J. (2006) Structural characterization of NDH-1 complexes of *Thermosynechococcus elongatus* by single particle electron microscopy. *Biochim. Biophys. Acta*, **1757**, 1469–1475.

Baradaran, R., Berrisford, J.M., Minhas, G.S. and Sazanov, L.A. (2013) Crystal structure of the entire respiratory complex I. *Nature*, **494**, 443–448.

Battchikova, N., Eisenhut, M. and Aro, E.M. (2011) Cyanobacterial NDH-1 complexes: novel insights and remaining puzzles. *Biochim. Biophys. Acta*, **1807**, 935–944.

Burrows, P.A., Sazanov, L.A., Svab, Z., Maliga, P. and Nixon, P.J. (1998) Identification of a functional respiratory complex in chloroplasts through analysis of tobacco mutants containing disrupted plastid *ndh* genes. *EMBO J.* **17**, 868–876.

DalCorso, G., Pesaresi, P., Masiero, S., Aseeva, E., Schünemann, D., Finazzi, G., Joliot, P., Barbato, R. and Leister, D. (2008) A complex containing PGRL1 and PGR5 is involved in the switch between linear and cyclic electron flow in *Arabidopsis*. *Cell*, **132**, 273–285.

Dau, H., Andrews, J., Roelofs, T., Latimer, M., Liang, W., Yachandra, V., Sauer, K. and Klein, M. (1995) Structural consequences of ammonia binding to the manganese center of the photosynthetic oxygen-evolving complex: an X-ray absorption spectroscopy study of isotropic and oriented photosystem II particles. *Biochemistry*, **34**, 5274–5287.

DeLano, W.L. (2002) *The PyMOL Molecular Graphics System*. San Carlos, CA: DeLano Scientific.

Dudkina, N.V., Kouřil, R., Peters, K., Braun, H.P. and Boekema, E.J. (2010) Structure and function of mitochondrial supercomplexes. *Biochim. Biophys. Acta*, **1797**, 664–670.

Friedrich, T. and Scheide, D. (2000) The respiratory complex I of bacteria, archaea and eukarya and its module common with membrane-bound multisubunit hydrogenase. *FEBS Lett.* **479**, 1–5.

Ganeteg, U., Klimmek, F. and Jansson, S. (2004) Lhca5 – an LHC-type protein associated with photosystem I. *Plant Mol. Biol.* **54**, 641–651.

Hertle, A., Blunder, T., Wunder, T., Pesaresi, P., Pribil, M., Armbruster, U. and Leister, D. (2013) PGRL1 is the elusive ferredoxin-plastoquinone reductase in photosynthetic cyclic electron flow. *Mol. Cell*, **49**, 511–523.

Horváth, E.M., Peter, S.O., Joët, T., Rumeau, D., Cournac, L., Horváth, G.V., Kavanagh, T.A., Schäfer, C., Peltier, G. and Medgyesy, P. (2000) Targeted inactivation of the plastid *ndhB* gene in tobacco results in an enhanced sensitivity of photosynthesis to moderate stromal closure. *Plant Physiol.* **123**, 1337–1349.

Hu, P., Lv, J., Fu, P. and Hualing, M. (2013) Enzymatic characterization of an active NDH complex from *Thermosynechococcus elongates*. *FEBS Lett.* **587**, 2340–2345.

Ifuku, K., Endo, T., Shikanai, T. and Aro, E.M. (2011) Structure of the chloroplast NADH dehydrogenase-like complex: nomenclature for nuclear-encoded subunits. *Plant Cell Physiol.* **52**, 1560–1568.

Iwai, M., Takizawa, K., Tokutsu, R., Okamura, A., Takahashi, Y. and Minagawa, J. (2010) Isolation of the elusive supercomplex that drives cyclic electron flow in photosynthesis. *Nature*, **464**, 1210–1213.

Järvi, S., Suorsa, M., Paakkarinen, V. and Aro, E.M. (2011) Optimized native gel systems for separation of thylakoid protein complexes: novel super- and mega-complexes. *Biochem. J.* **439**, 207–214.

Joliot, P. and Johnson, G.N. (2011) Regulation of cyclic and linear electron flow in higher plants. *Proc. Natl Acad. Sci. USA*, **108**, 13317–13322.

Joliot, P. and Joliot, A. (2002) Cyclic electron transfer in plant leaf. *Proc. Natl Acad. Sci. USA*, **99**, 10209–10214.

Kofer, W., Koop, H.U., Wanne, G. and Steinmüller, K. (1998) Mutagenesis of the genes encoding subunits A, C, H, I, J and K of the plastid NAD(P)H-plastoquinone-oxidoreductase in tobacco by polyethylene glycol-mediated plastome transformation. *Mol. Gen. Genet.* **258**, 166–173.

Kramer, D.M., Avenson, T.J. and Edwards, G.E. (2004) Dynamics flexibility in the light reactions of photosynthesis governed by both electron and proton transfer reactions. *Trends Plant Sci.* **9**, 349–357.

Li, X.G., Duan, W., Meng, Q.W., Zou, Q. and Zhao, S.J. (2004) The function of chloroplastic NAD(P)H dehydrogenase in tobacco during chilling stress under low irradiance. *Plant Cell Physiol.* **45**, 103–108.

Lichtenthaler, H. and Buschmann, C. (2001) Chlorophylls and carotenoids: measurement and characterization by UV-VIS spectroscopy. *Curr. Protoc. Food Anal. Chem.* F4.3.1–F4.3.8.

Lípová, L., Krchňák, P., Komenda, J. and Ilík, P. (2010) Heat-induced disassembly and degradation of chlorophyll-containing protein complexes *in vivo*. *Biochim. Biophys. Acta*, **1797**, 63–70.

Livingston, A.K., Cruz, J.A., Kohzuma, K., Dhingra, A. and Kramer, D.M. (2010) An *Arabidopsis* mutant with high cyclic electron flow around photosystem I (*hcef*) involving the NADPH dehydrogenase complex. *Plant Cell*, **22**, 221–233.

Lucinski, R., Volkmar, H.R., Jansson, S. and Klimmek, F. (2006) Lhca5 interaction with plant photosystem I. *FEBS Lett.* **580**, 6485–6488.

Ludtke, S.J., Baldwin, P.R. and Chiu, W. (1999) EMAN: semiautomated software for high-resolution single-particle reconstructions. *J. Struct. Biol.* **128**, 82–97.

Matsubayashi, T., Wakasugi, T., Shinozaki, K. *et al.* (1987) Six chloroplast genes (*ndhA-F*) homologous to human mitochondrial genes encoding components of the respiratory chain NADH dehydrogenase are actively expressed: determination of the splice sites in *ndhA* and *ndhB* pre-mRNAs. *Mol. Gen. Genet.* **210**, 385–393.

Munekage, Y., Hojo, M., Meurer, J., Endo, T., Tasaka, M. and Shikanai, T. (2002) PGR5 is involved in cyclic electron flow around photosystem I and is essential for photoprotection in *Arabidopsis*. *Cell*, **110**, 361–371.

Munekage, Y., Hashimoto, M., Miyake, C., Tomizawa, K.I., Endo, T., Tasaka, M. and Shikanai, T. (2004) Cyclic electron flow around photosystem I is essential for photosynthesis. *Nature*, **429**, 579–582.

Oostergetel, G.T., Keegstra, W. and Brisson, A. (1998) Automation of specimen selection and data acquisition for protein electron crystallography. *Ultramicroscopy*, **74**, 47–59.

Peng, L. and Shikanai, T. (2011) Supercomplex formation with photosystem I is required for the stabilization of the chloroplast NADH dehydrogenase-like complex in *Arabidopsis*. *Plant Physiol.* **155**, 1629–1639.

Peng, L., Shimizu, H. and Shikanai, T. (2008) The chloroplast NAD(P)H dehydrogenase complex interacts with photosystem I in *Arabidopsis*. *J. Biol. Chem.* **283**, 34873–34879.

Peng, L., Fukao, Y., Fujiwara, M., Takami, T. and Shikanai, T. (2009) Eficient operation of NAD(P)H dehydrogenase requires supercomplex formation with photosystem I via minor LHCI in *Arabidopsis*. *Plant Cell*, **21**, 3623–3640.

Peng, L., Yamamoto, H. and Shikanai, T. (2011) Structure and biogenesis of the chloroplast NAD(P)H dehadrogenase complex. *Biochim. Biophys. Acta*, **1807**, 945–953.

Perkins, D.N., Pappin, D.J., Creasy, D.M. and Cottrell, J.S. (1999) Probability-based protein identification by searching sequence databases using mass spectrometry data. *Electrophoresis*, **20**, 3551–3567.

Quiles, M.J., García, A. and Cuello, J. (2000) Separation by blue-native PAGE and identification of the whole NAD(P)H dehydrogenase complex from barley stroma thylakoids. *Plant Physiol. Biochem.* **38**, 225–232.

Rappsilber, J., Mann, M. and Ishihama, Y. (2007) Protocol for micro-purification, enrichment, pre-fractionation and storage of peptides for proteomics using StageTips. *Nat. Protoc.* **2**, 1896–1906.

Shevchenko, A., Tomas, H., Havlis, J., Olsen, J. and Mann, M. (2006) In-gel digestion for mass spectrometric characterization of proteins and proteomes. *Nat. Protoc.* **1**, 2856–2860.

Shikanai, T. (2007) Cyclic electron transport around photosystem I: genetic approaches. *Annu. Rev. Plant Biol.* **58**, 199–217.

Shikanai, T., Endo, T., Hashimoto, T., Yamada, Y., Asada, K. and Yokota, A. (1998) Directed disruption of the tobacco *ndhB* gene impairs cyclic electron flow around photosystem I. *Proc. Natl Acad. Sci. USA*, **95**, 9705–9709.

Wittig, I. and Schägger, H. (2005) Advantages and limitations of clear-native PAGE. *Proteomics*, **5**, 4338–4346.

Wittig, I., Karas, M. and Schägger, H. (2007) High resolution clear native electrophoresis for In-gel functional assays and fluorescence studies of membrane protein complexes. *Mol. Cell. Proteomics*, **6**, 1215–1225.

Yamamoto, H., Peng, L., Fukao, Y. and Shikanai, T. (2011) An Src homology 3 domain-like fold protein forms a ferredoxin binding site for the chloroplast NADH dehydrogenase-lie complex in *Arabidopsis*. *Plant Cell*, **23**, 1480–1493.

4.2 Evolutionary loss of light-harvesting proteins Lhcb6 and Lhcb3 in major land plant groups – break-up of current dogma.

Reprint of: Kouřil R, Nosek L, Bartoš J, Boekema EJ and Ilík P. *New Phytologist* **210**: 808-814, (2016).

Research

New Phytologist

Rapid report

Evolutionary loss of light-harvesting proteins Lhcb6 and Lhcb3 in major land plant groups – break-up of current dogma

Author for correspondence:
Roman Kouřil
Tel: +420 585634837
Email: roman.kouril@upol.cz

Received: *7 January 2016*
Accepted: *25 February 2016*

Roman Kouřil[1], Lukáš Nosek[1], Jan Bartoš[2], Egbert J. Boekema[3] and Petr Ilík[1]

[1]Department of Biophysics, Centre of the Region Haná for Biotechnological and Agricultural Research, Faculty of Science, Palacký University, Šlechtitelů 27, 783 71 Olomouc, Czech Republic; [2]Centre of the Region Haná for Biotechnological and Agricultural Research, Institute of Experimental Botany, Šlechtitelů 31, 783 71 Olomouc, Czech Republic; [3]Electron Microscopy Group, Groningen Biomolecular Sciences and Biotechnology Institute, University of Groningen, Nijenborgh 7, 9747 AG Groningen, the Netherlands

New Phytologist (2016) **210:** 808–814
doi: 10.1111/nph.13947

Key words: conifers, electron microscopy, evolution, land plants, Lhcb proteins, photosystem II (PSII), supercomplex.

Summary

- Photosynthesis in plants and algae relies on the coordinated function of photosystems (PS) I and II. Their efficiency is augmented by finely-tuned light-harvesting proteins (Lhcs) connected to them. The most recent Lhcs (in evolutionary terms), Lhcb6 and Lhcb3, evolved during the transition of plants from water to land and have so far been considered to be an essential characteristic of land plants.
- We used single particle electron microscopy and sequence analysis to study architecture and composition of PSII supercomplex from Norway spruce and related species.
- We have found that there are major land plant families that lack functional *lhcb6* and *lhcb3* genes, which notably changes the organization of PSII supercomplexes. The Lhcb6 and Lhcb3 proteins have been lost in the gymnosperm genera *Picea* and *Pinus* (family Pinaceae) and *Gnetum* (Gnetales). We also revealed that the absence of these proteins in Norway spruce modifies the PSII supercomplex in such a way that it resembles its counterpart in the alga *Chlamydomonas reinhardtii*, an evolutionarily older organism.
- Our results break a deep-rooted concept of Lhcb6 and Lhcb3 proteins being the essential characteristic of land plants, and beg the question of what the evolutionary benefit of their loss could be.

Introduction

A key reaction of oxygenic photosynthesis, the photooxidation of water to molecular oxygen, is carried out by photosystem II (PSII), a multi-subunit pigment-protein supercomplex. It consists of a highly conserved core and light harvesting antenna (Kouřil *et al.*, 2012). The latter is much more prone to evolutionary changes (Büchel, 2015). The huge variability of the antenna system was crucial during the evolutionary adaptation of photosynthetic organisms to different conditions (Jansson, 2006). The colonization of land by plants required the presence of an efficient and dynamic mechanism to control safe utilization of absorbed light under variable environmental conditions.

Electron microscopy studies revealed that in land plants, the largest stable PSII supercomplex consists of a PSII core dimer (C_2) bound by four trimeric light-harvesting proteins (LHCIIs), encoded by the *lhcb1–3* genes (*lhcbm* for evolutionarily older species). Two trimers (S_2) are bound strongly to the dimeric PSII core, while the other two are bound only moderately (M_2). The LHCIIs are specifically connected to PSII core via monomeric antenna proteins Lhcb4–6 (Caffarri *et al.*, 2009). This PSII supercomplex, denoted as $C_2S_2M_2$, has been observed in liverworts (Harrer, 2003), the oldest land plants, as well as in angiosperms (Caffarri *et al.*, 2009; Kouřil *et al.*, 2012) (see later Fig. 2b), which belong to the most recent land plants. These findings led to a formulation of the current concept that the $C_2S_2M_2$ PSII supercomplex has been conserved throughout the evolution of land plants. In green algae, their ancestors, the structure of the PSII supercomplex is somewhat different (Tokutsu *et al.*, 2012; Drop *et al.*, 2014) – the M trimers have a different orientation and two additional LHCII trimers (N_2) are attached to form the $C_2S_2M_2N_2$ structure (see later Fig. 2c). Since green algae lack Lhcb6 proteins

that mediate the attachment of the M trimers, the N trimers may substitute their role by stabilizing the $C_2S_2M_2N_2$ supercomplex (Tokutsu *et al.*, 2012; Drop *et al.*, 2014).

The Lhcb6 protein was found to be unique to land plants (Alboresi *et al.*, 2008). Another monomeric antenna protein, Lhcb3, which is a part of the M trimer (Dainese & Bassi, 1991), is also exclusive to land plants. Current knowledge strongly implies that land plants benefit from the presence of both these proteins. The interaction between Lhcb6 and Lhcb3 is important for the stable attachment of M to C_2S_2 (Kovács *et al.*, 2006; Caffarri *et al.*, 2009; Kouřil *et al.*, 2013). The proteins therefore enable a flexible enlargement of the PSII antenna size, leading to an optimal macro-organization of PSII supercomplexes and to more efficient connectivity between PSII cores (Kovács *et al.*, 2006; Caffarri *et al.*, 2009). These factors are important in achieving maximum efficiency of PSII photochemistry as well as for effective photoprotective dissipation of absorbed light energy (so-called nonphotochemical quenching) (Kovács *et al.*, 2006). Thus, the appearance of both Lhcb6 and Lhcb3 is considered as a milestone in the evolution of the PSII supercomplex, allowing the transition of photosynthesizing organisms from the relatively stable water habitat to land (Koziol *et al.*, 2007; Alboresi *et al.*, 2008; de Bianchi *et al.*, 2008; Büchel, 2015). However, here we show that there are representatives of gymnosperms that lack functional *lhcb6* and *lhcb3* genes. Thus, our work breaks the current concept that Lhcb6 and Lhcb3 proteins in the light-harvesting antenna of PSII are an essential characteristic of all land plants.

Materials and Methods

Plant material and sample preparation

Norway spruce (*Picea abies* (L.) Karst.) (Semenoles, Liptovský Hrádok, Slovakia) seedlings were grown in a growth chamber with 16 h : 8 h, light : dark photoperiod at 21°C. Plants were illuminated with white light at 100 μmol photons $m^{-2}\,s^{-1}$ (400–700 nm). PSII-enriched membranes were isolated from 18-d-old spruce seedlings according to Caffarri *et al.* (2009). Chlorophyll content in the final suspension was determined spectrophotometrically in 80% acetone according to Lichtenthaler & Buschmann (2001). For the electrophoretic separation of PSII supercomplexes, PSII membranes containing 10 μg of chlorophyll were solubilized with *n*-dodecyl-*β*-D-maltoside (β-DDM) at chlorophyll : β-DDM mass ratio of 12, supplemented with sample buffer (50 mM HEPES (4-(2-hydroxyethyl)-1-piperazineethanesulfonic acid) pH 7.2, 400 mM sucrose, 15 mM sodium chloride (NaCl), 10% glycerol) to a final volume of 30 μl. Nonsolubilized membranes were removed by centrifugation (20 000 ***g***, 10 min, 4°C) and samples were directly loaded onto the gel. The clear native polyacrylamide gel electrophoresis (CN-PAGE) separation procedure described by Wittig *et al.* (2007) was used with 4–8% gradient separation gel and 4% stacking gel. The separation started at a constant current of 4 mA for 15 min and continued at a constant current of 7 mA until the front reached the bottom of the gel.

Electron microscopy and image processing

PSII supercomplexes were eluted from excised CN-PAGE gel bands according to Kouřil *et al.* (2014); the solution with eluted supercomplexes was then directly used for electron microscopy specimen preparation by negative staining with 2% uranyl acetate on glow-discharged carbon-coated copper grids. Electron microscopy was performed on a Tecnai G2 20 Twin electron microscope (FEI, Eindhoven, the Netherlands) equipped with a LaB_6 cathode, operated at 200 kV. Images were recorded with an UltraScan 4000 UHS CCD camera (Gatan, Pleasanton, CA, USA) at ×13 000 magnification with a pixel size of 0.224 nm at the specimen level after binning the images to 2048 × 2048 pixels. GRACE software (Oostergetel *et al.*, 1998) was used for semi-automated acquisition of 4200 images, from which *c.* 80 000 particle projections were selected. Single particle analysis was performed using GRIP software (Groningen, the Netherlands) including multireference and nonreference alignments, multivariate statistical analysis and classification.

The projection map with best resolution (14 Å) was obtained for the C_2S_2M supercomplex (Fig. 1d) and therefore this map was used for the construction of a pseudo-atomic model of the PSII

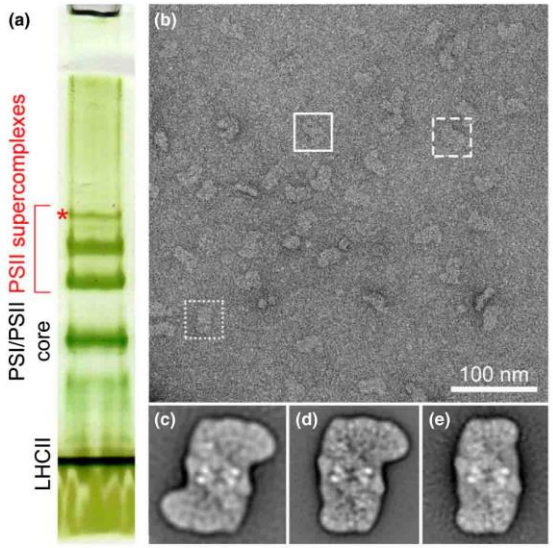

Fig. 1 Separation and structural characterization of photosystem II (PSII) supercomplexes. (a) Separation of PSII supercomplexes from Norway spruce (*Picea abies*) by clear native polyacrylamide electrophoresis. PSII-enriched membranes from spruce seedlings were solubilized in *n*-dodecyl-*β*-D-maltoside. The red star indicates the band with the largest form of PSII supercomplex, which was analyzed by electron microscopy. (b) Example of raw electron micrograph of a negatively-stained specimen; three different forms of the PSII supercomplexes are indicated: $C_2S_2M_2$ (solid line), C_2S_2M (dashed line) and C_2S_2 (dotted line). (c–e) Averaged projection maps of supercomplexes (c) $C_2S_2M_2$ (sum of 1048 particles), (d) C_2S_2M (sum of 10 000 particles) and (e) C_2S_2 (sum of 4608 particles) revealed by single particle electron microscopy.

supercomplex and for the estimation of the mutual position of the M and S trimers. The constructed model was also used for the fitting of the spruce $C_2S_2M_2$ supercomplex (Fig. 2a). The resolution was measured using Fourier-ring correlation and the 3σ criterion (Vanheel, 1987).

Identification of Lhcb homologs

Amino acid sequences of Lhcb1–6 proteins identified in *Arabidopsis thaliana* (Lhcb1 isoforms: Lhcb1.1, AT1G29920.1; Lhcb1.2, AT1G29910.1; Lhcb1.3, AT1G29930.1; Lhcb1.4, AT2G34430.1; Lhcb1.5, AT2G34420.1; Lhcb2 isoforms: Lhcb2.1, AT2G05100.1; Lhcb2.2, AT2G05070.1; Lhcb2.3, AT3G27690.1; Lhcb3, AT5G54270.1; Lhcb4 isoforms: Lhcb4.1, AT5G01530.1; Lhcb4.2, AT3G08940.2; Lhcb4.3, AT2G40100.1; Lhcb5, AT4G10340.1; Lhcb6, AT1G15820.1) were downloaded from the TAIR.10 database (Lamesch *et al.*, 2012; https://www.arabidopsis.org/) and used for homology search against the *Picea abies* genome and transcriptomes of the species listed later, using the TBLASTN algorithm. The spruce genome (Nystedt *et al.*, 2013) was downloaded from the Congenie database (http://congenie.org/). Transcriptomes of Norway spruce and closely related *Picea* and *Pinus* species (*Picea abies*, *Picea glauca*, *Picea sitchensis*, *Pinus bankdiana*, *Pinus contorta*, *Pinus pinaster*, *Pinus sylvestris* and *Pinus tadea*) were downloaded from the PlantGDB database (Duvick *et al.*, 2008; http://www.plantgdb.org/). Transcriptomes of other Gymnosperm species (*Cycas rumphii*, *Ginkgo biloba*, *Podocarpus macrophyllus*, *Cryptomeria japonica*, *Seqouia sempervirens*, *Sciadopitys verticillata*, *Taxus baccata*, *Gnetum gnemon*) and representatives of ferns (*Ceratopteris richardii*), lycophytes (*Selaginella moellendorffii*), mosses (*Physcomitrella patens*), liverworts (*Marchantia polymorpha*) and algae (*Chlamydomonas reinhardtii*) were downloaded from either the PlantGDB or Dendrome databases (http://dendrome.ucdavis.edu/) (Supporting Information Table S1). In addition, raw data from transcriptome/RNA sequencing using Roche 454 technology were downloaded from the Sequence Read Archive (SRA; http://www.ncbi.nlm.nih.gov/sra), when available. If possible, at least one million reads were retrieved for each species. The number of sequences and cumulative length of all databases used for homology search are listed in Table S1. Each database was analyzed separately. First, scaffold/transcript with best BLAST hit was retrieved for each *A. thaliana* Lhcb protein using TBLASTN with default parameters, but e-value = 1e-10. Subsequently, a particular scaffold/transcript was compared with the full set of *A. thaliana* proteins (TAIR.10) using the BLASTX algorithm with default parameters, but e-value = 1e-10. Best hits for all Lhcb proteins in each database as well as best hits of particular scaffolds/transcripts in TAIR.10 are listed in Table S2. Scaffolds/transcripts matching reciprocally with a single *A. thaliana* Lhcb protein were considered as representatives of a particular gene in the analyzed species. The same strategy and dataset (transcriptomes and raw 454 data) were used to reveal the presence of transcripts for homologues of *A. thaliana* PGR5 (AT2G05620.1; retrieved from TAIR.10) and *C. reinhardtii* Lhcsr proteins (Lhcsr1, Cre08.g365900.t1.2; Lhcsr2, Cre08.g367500.t1.1; Lhcsr3, Cre08.g367400.t1.1; retrieved from PHYTOZOME v.11; Goodstein *et al.*, 2012; https://phytozome.jgi.doe.gov). In the case Lhcsr-like transcripts, a particular scaffold/transcript was compared with the complete *C. reinhardtii* proteome v.5.5 (Merchant *et al.*, 2007; downloaded from PHYTOZOME v.11) using the BLASTX algorithm with default parameters, but e-value = 1e-10.

Results and Discussion

Here we present for the first time the structure of the PSII supercomplex in a representative of gymnosperms, Norway spruce (*P. abies*). Mildly solubilized PSII-enriched thylakoid membranes were electrophoresed using CN-PAGE, which resulted in the separation of PSII supercomplexes into three bands (Fig. 1a). The largest PSII supercomplexes, present in the band with the shortest migration distance, were analyzed by single particle electron microscopy and image processing. Inspection of raw electron micrographs indicated the presence of several forms of the PSII supercomplex, which differed in the size of their antenna (Fig. 1b). Image analysis of *c.* 80 000 single particle projections revealed structures $C_2S_2M_2$, C_2S_2M and C_2S_2 (Fig. 1b–e). The largest, that is the most intact, supercomplex ($C_2S_2M_2$) was further analyzed in detail. The smaller supercomplexes represent degradation products of $C_2S_2M_2$ supercomplexes, which disintegrate during the preparation of the samples for electron microscopy analysis.

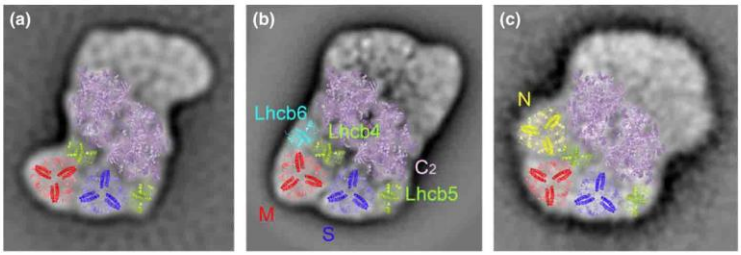

Fig. 2 Structural assignment of protein subunits of the photosystem II (PSII) supercomplex. (a) PSII supercomplexes from Norway spruce (*Picea abies*) and its counterparts from (b) *Arabidopsis thaliana* and (c) *Chlamydomonas reinhardtii*. Averaged projection maps are shown for the $C_2S_2M_2$ supercomplexes from Norway spruce and *A. thaliana*, and $C_2S_2M_2N_2$ from *C. reinhardtii* (adapted from Drop *et al.*, 2014). High-resolution structures were fitted to the projection maps; the PSII core complex (C_2, light violet) (Guskov *et al.*, 2009), trimeric (the S, M and N trimer in blue, red and yellow, respectively) and monomeric (Lhcb4 and Lhcb5 in green, Lhcb6 in cyan) Lhcb proteins (Liu *et al.*, 2004).

We constructed a pseudo-atomic model of the $C_2S_2M_2$ supercomplex from spruce by fitting the electron microscopy projection map with known PSII and Lhcb X-ray structures and compared it with the models of the $C_2S_2M_2$ supercomplex from *A. thaliana*, a representative of angiosperms, and with $C_2S_2M_2N_2$ from *C. reinhardtii* (Fig. 2). It is clear that the position occupied by the minor antenna protein Lhcb6 in *A. thaliana* remains unoccupied in the spruce PSII supercomplex. Due to the absence of Lhcb6, the M trimer associates to the PSII core complex in a different orientation, which has never been observed in land plants before. The rotation of the M trimer by *c.* 52° enables its tighter association with the S trimer, decreasing their mutual distance by *c.* 7 Å (for details see the Materials and Methods section). Interestingly, the same orientation of the M and S trimers was recently observed in an evolutionarily older organism, the green alga *C. reinhardtii*, which also lacks the Lhcb6 protein (Fig. 2c) (Tokutsu *et al.*, 2012; Drop *et al.*, 2014).

The reason for the observed absence of the Lhcb6 protein in separated PSII supercomplexes from spruce could either be the downregulation of its transcription or translation or the absence of the *lhcb6* gene. To distinguish between these possibilities, we have performed *in silico* analysis of the *P. abies* genome (Nystedt *et al.*, 2013) and transcriptome using the Lhcb6 protein sequence from *A. thaliana*. Basic local alignment search tool (BLAST) was used to retrieve best reciprocal BLAST hits for Lhcb1–6. The analysis clearly reveals the absence of a genomic sequence corresponding to *lhcb6* as well as of its transcript in *P. abies*. As in land plants the appearance of Lhcb6 coincides with Lhcb3 (see earlier), we performed the same analysis for *lhcb3* and obtained the same results. Moreover, we have also observed the loss of the *lhcb6* and *lhcb3* gene products in the transcriptomes of other *Picea* and *Pinus* species, which implies that this loss affects the whole pine family (Pinaceae) (Table 1). The absence of transcripts for Lhcb6 and Lhcb3 proteins was also observed in *G. gnemon* (Table 1), a representative of Gnetales (Fig. 3). Importantly, we have found the *lhcb6* and *lhcb3* transcripts in transcriptomes of representatives of all other groups of gymnosperms (cupressophytes, cycads, Ginkgoales) and of evolutionarily older land plant groups (mosses, liverworts, lycophytes, ferns) (Table 1; Fig. 3).

Although the absence of the Lhcb6 protein in the structure of PSII supercomplex from spruce is clearly visible, the absence of the Lhcb3 protein in the PSII structure is not so evident (Fig. 2). The Lhcb3 protein in the M trimer seems to be replaced by another Lhcb protein, as was observed in the PSII supercomplex isolated from *A. thaliana* mutant lacking Lhcb3 (Damkjær *et al.*, 2009). In spruce, however, the nature of the Lhcb3-replacing protein could be unique as it enables a stable binding of the M trimer to the PSII core complex at the absence of Lhcb6 protein (Fig. 2a) (see the

Table 1 The presence of homologs of *Arabidopsis thaliana lhcb1–6* genes identified by the best reciprocal basic local alignment search tool (BLAST) hit in transcriptomes of selected organisms

Organism	*lhcb1*	*lhcb2*	*lhcb3*	*lhcb4*	*lhcb5*	*lhcb6*	Group
Chlamydomonas reinhardtii		(+)		+	+		Algae
Marchantia polymorpha		(+)	+	+	+	+	Liverworts
Physcomitrella patens		(+)	+	+	+	+	Mosses
Selaginella moellendorffii		(+)	+	+	+	+	Lycophytes
Ceratopteris richardii	+	+	+	+	+	+	Ferns
Cycas rumphii	+	+	+	+	+	+	Cycads
Ginkgo biloba	+	+	+	+	+	+	Gingkoales
Podocarpus macrophillus	+	+	+	+	+	+	Cupressophytes
Cryptomeria japonica	+	+	+	+	+	+	Cupressophytes
Sequoia sempervirens	+	+	+	+	+	+	Cupressophytes
Sciadopitys verticillata	+	+	+	+	+	+	Cupressophytes
Taxus baccata	+	+	+	+	+	+	Cupressophytes
Picea abies (genome)	+	+		+	+		Pinaceae
Picea abies (transcriptome)	+	+		+	+		Pinaceae
Picea glauca	+	+		+	+		Pinaceae
Picea sitchensis	+	+		+	+		Pinaceae
Pinus banksiana	+	+		+	+		Pinaceae
Pinus contorta	+	+		+	+		Pinaceae
Pinus pinaster	+	+		+	+		Pinaceae
Pinus sylvestris	+	+		+	+		Pinaceae
Pinus taeda	+	+		+	+		Pinaceae
Gnetum gnemon	+	+		+	+		Gnetales
Arabidopsis thaliana	+	+	+	+	+	+	Angiosperms

Note: In the case of *P. abies*, the analysis was also performed within its genome. Homologs of *lhcb6* and *lhcb3* are clearly missing in the genome of *P. abies* (see Supporting Information Table S1) and in the transcriptomes of *Picea*, *Pinus* and *Gnetum* species (see Table S2). Color coding corresponds to different plants groups: bryophyte (orange), lycophytes (light blue), ferns (violet), gymnosperms (light green), gymnosperms lacking the lhcb3 and lhcb6 genes (dark green), angiosperms (gray). Homologs of *A. thaliana lhcb2* but not *lhcb1* were revealed for representatives of algae, liverworts, mosses and lycophytes by best reciprocal BLAST hit. However, in *C. reinhardtii* and *P. patens* LHCII trimeric proteins are encoded by *lhcbm* genes (*C. reinhardtii*), and *lhcbm* and *lhcb3* (*P. patens*) genes, respectively (Ballottari *et al.*, 2012). Generally, Lhcbm proteins could not be specifically associated with individual Lhcb proteins in *A. thaliana*. Thus, the identified *lhcb2* homologs (+) are most probably representatives of *lhcbm* genes.

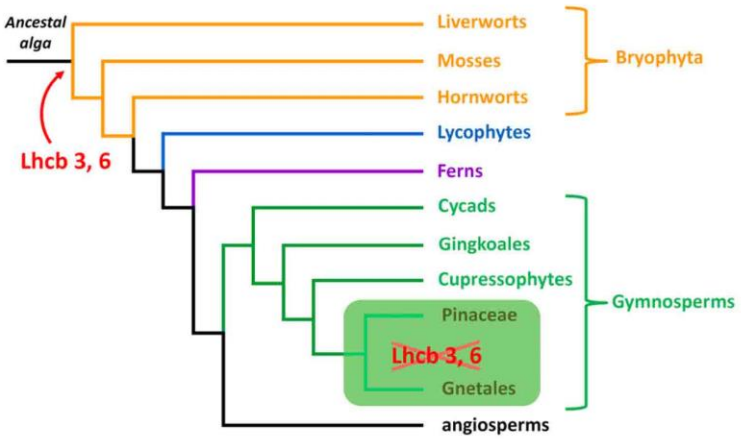

Fig. 3 Phylogenetic tree of land plant groups with indicated appearance and loss of Lhcb3 and Lhcb6 proteins. The tree was made according to Clarke *et al.* (2011).

Introduction section). The origin of the substitute of the Lhcb3 in spruce remains an intriguing question.

The sequence analysis, together with the structural changes in the PSII supercomplex in spruce, indicates that the evolution of Pinaceae and Gnetales is associated with significant modification of the light-harvesting antenna system of PSII. According to current phylogeny of plants, these groups are, despite their morphological differences, considered to be sister groups and represent a crown group of gymnosperms (Fig. 3) (see Bowe *et al.*, 2000; Chaw *et al.*, 2000; Clarke *et al.*, 2011; Wang & Ran, 2014, and references cited therein). In the light of this phylogenetic tree it is reasonable to assume that the loss of the genes for Lhcb6 and Lhcb3 proteins has occurred in a common ancestor of these groups, although individual losses of the genes in each group cannot be excluded.

During evolution, every important mutation/genetic change that is transferred to following generations offers some evolutionary advantage. The question arises what could be the cause(s) for the loss of Lhcb6 and Lhcb3 and what benefit would it provide? An important finding which offers the answer comes from the analysis of PSII supercomplex of angiosperms acclimated to high light conditions. Kouřil *et al.* (2013) have observed that long-term acclimation of *A. thaliana* to excess light leads to a selective downregulation of the Lhcb6 and Lhcb3 proteins, which further leads to a transition of the most abundant PSII supercomplex $C_2S_2M_2$ to C_2S_2. This indicates that long-term high light conditions in the past might be the environmental factor that affected the evolution of the common ancestor of Pinaceae and Gnetales. These gymnosperm families evolved most probably in the Triassic (Miller, 1999; Clarke *et al.*, 2011; He *et al.*, 2012), that is, after the greatest extinction event in Earth history (Great Dying). This catastrophe probably opened the canopy for a very long time period (until middle Triassic) (Retallack *et al.*, 1996; McElwain & Punyasena, 2007), exposing those surviving plants to high light.

It is also important to mention that in contrast to all other land plant groups, Pinaceae and Gnetales have also lost an entire set of plastid genes for NAD(P)H dehydrogenase (NDH) (Braukmann *et al.*, 2009). The NDH enzyme participates in one of two main pathways of cyclic electron flow (CEF) around PSI. On the contrary to the proton gradient regulation 5 protein (PGR5) dependent pathway (Munekage *et al.*, 2002), which was found to be essential for photosynthesis (Munekage *et al.*, 2004) and which seems to be operational in Pinaceae and Gnetales families (based on the presence of PGR5 in their transcriptomes, Table S2), the NDH-dependent electron pathway is not functional in these plant groups. The NDH pathway is used by photosynthetic machinery of stressed plants when the chloroplast stroma becomes over-reduced (for review see Shikanai, 2007). This pathway is very important for plants grown at low light, but for high light grown plants it does not have significant physiological function (Yamori *et al.*, 2015). This finding again supports our hypothesis that the common ancestor of Pinaceae and Gnetales evolved in high light conditions. It is also of note that extant species of Pinaceae and Gnetales are high-light tolerant, even though some of the evolutionarily more recent ones (e.g. *Gnetum* species, *Pinus krempfii*) prefer shade conditions (Brodribb & Feild, 2008; Feild & Balun, 2008).

The absence of the Lhcb6 protein in Pinaceae and Gnetales also evokes a question related to the nonphotochemical quenching (NPQ) of excess light energy, as Lhcb6 is known to play an important role in NPQ of land plants. Based on a dramatic decrease in NPQ observed in *A. thaliana* mutant lacking Lhcb6, it has been suggested that the Lhcb6, with associated M trimer, provides an interaction site for PsbS (Kovács *et al.*, 2006), a protein indispensable for fast and full activation of NPQ (Li *et al.*, 2000). Thus, it can be assumed that in Pinaceae and Gnetales, the mode of action of PsbS is different (due to the lack of Lhcb6) and/or that an additional protein is involved in the NPQ process. The structural similarities between the PSII supercomplexes from green alga *C. reinhardtii* and Norway spruce (Fig. 2) raise a question whether they also share similar NPQ features. In all photosynthetic organisms evolutionarily older than vascular plants (except of red algae), the NPQ depends on stress-related light harvesting complex (Lhcsr) (Koziol *et al.*, 2007; Peers *et al.*, 2009). Therefore, we performed additional

analysis of transcriptomes, which revealed *lhcsr*-like transcripts in some species of Pinaceae family (*P. glauca*, *P. sitchensis*, *P. abies* and *P. pinaster*) (Table S2). Thus, both the lack of the Lhcb6 protein and a possible presence of the Lhcsr protein indicate that Pinaceae can have a different mechanism of NPQ, which requires further in-depth investigation.

In conclusion, our results show that Pinaceae and Gnetales are exceptional land plant groups that deserve particular attention in plant physiology. The absence of Lhcb6 and Lhcb3 proteins revealed in this work changes the organization of antenna complexes in PSII supercomplex, which indicate that these plants use a different strategy to cope with changing light conditions.

Acknowledgements

This work was supported by the Grant Agency of the Czech Republic (project 13-28093S/P501 to R.K.), by a Marie Curie Career Integration Grant call FP7-PEOPLE-2012-CIG (322193 to R.K.) and by grant LO1204 (Sustainable development of research in the Centre of the Region Haná) from the National Program of Sustainability I from the Ministry of Education, Youth and Sports, Czech Republic. The authors thank Dr Iva Ilíková for editing and Dr Andrew A. Pascal for critical reading of the manuscript.

Author contributions

R.K., L.N., J.B. and P.I. planned and designed the research. R.K., L.N., and E.J.B. performed experiments. R.K., L.N., J.B., E.J.B. and P.I. analyzed the data. R.K., L.N., J.B. and P.I. wrote the manuscript and all authors revised and approved it.

References

Alboresi A, Caffarri S, Nogue F, Bassi R, Morosinotto T. 2008. *In silico* and biochemical analysis of *Physcomitrella patens* photosynthetic antenna: identification of subunits which evolved upon land adaptation. *PLoS ONE* **3**: e2033.

Ballottari M, Girardon J, Dall'osto L, Bassi R. 2012. Evolution and functional properties of photosystem II light harvesting complexes in eukaryotes. *Biochimica et Biophysica Acta – Bioenergetics* **1817**: 143–157.

de Bianchi S, Dall'Osto L, Tognon G, Morosinotto T, Bassi R. 2008. Minor antenna proteins CP24 and CP26 affect the interactions between photosystem II subunits and the electron transport rate in grana membranes of Arabidopsis. *Plant Cell* **20**: 1012–1028.

Bowe LM, Coat G, De Pamphilis CW. 2000. Phylogeny of seed plants based on all three genomic compartments: extant gymnosperms are monophyletic and Gnetales' closest relatives are conifers. *Proceedings of the National Academy of Sciences, USA* **97**: 4092–4097.

Braukmann TWA, Kuzmina M, Stefanovic S. 2009. Loss of all plastid *ndh* genes in Gnetales and conifers: extent and evolutionary significance for the seed plant phylogeny. *Current Genetics* **55**: 323–337.

Brodribb TJ, Feild TS. 2008. Evolutionary significance of a flat-leaved *Pinus* in Vietnamese rainforest. *New Phytologist* **178**: 201–209.

Büchel C. 2015. Evolution and function of light harvesting proteins. *Journal of Plant Physiology* **172**: 62–75.

Caffarri S, Kouřil R, Kereiche S, Boekema EJ, Croce R. 2009. Functional architecture of higher plant photosystem II supercomplexes. *EMBO Journal* **28**: 3052–3063.

Chaw SM, Parkinson CL, Cheng Y, Vincent TM, Palmer JD. 2000. Seed plant phylogeny inferred from all three plant genomes: monophyly of extant gymnosperms and origin of Gnetales from conifers. *Proceedings of the National Academy of Sciences, USA* **97**: 4086–4091.

Clarke JT, Warnock RCM, Donoghue PCJ. 2011. Establishing a time-scale for plant evolution. *New Phytologist* **192**: 266–301.

Dainese P, Bassi R. 1991. Subunit stoichiometry of the chloroplast photosystem-II antenna system and aggregation state of the component chlorophyll-*a*/*b* binding proteins. *Journal of Biological Chemistry* **266**: 8136–8142.

Damkjær JT, Kereiche S, Johnson MP, Kovacs L, Kiss AZ, Boekema EJ, Ruban AV, Horton P, Jansson S. 2009. The photosystem II light-harvesting protein Lhcb3 affects the macrostructure of photosystem II and the rate state transitions in *Arabidopsis*. *Plant Cell* **21**: 3245–3256.

Drop B, Webber-Birungi M, Yadav SK, Filipowicz-Szymanska A, Fusetti F, Boekema EJ, Croce R. 2014. Light-harvesting complex II (LHCII) and its supramolecular organization in *Chlamydomonas reinhardtii*. *Biochimica et Biophysica Acta – Bioenergetics* **1837**: 63–72.

Duvick J, Fu A, Muppirala U, Sabharwal M, Wilkerson MD, Lawrence CJ, Lushbough C, Brendel V. 2008. PlantGDB: a resource for comparative plant genomics. *Nucleic Acids Research* **36**: 959–965.

Feild TS, Balun L. 2008. Xylem hydraulic and photosynthetic function of *Gnetum* (Gnetales) species from Papua New Guinea. *New Phytologist* **177**: 665–675.

Goodstein DM, Shu S, Howson R, Neupane R, Hayes RD, Fazo J, Mitros T, Dirks W, Hellsten U, Putnam N *et al.* 2012. Phytozome: a comparative platform for green plant genomics. *Nucleic Acids Research* **40**: 1178–1186.

Guskov A, Kern J, Gabdulkhakov A, Broser M, Zouni A, Saenger W. 2009. Cyanobacterial photosystem II at 2.9-Å resolution and the role of quinones, lipids, channels and chloride. *Nature Structural & Molecular Biology* **16**: 334–342.

Harrer R. 2003. Association between light-harvesting complexes and photosystem II from *Marchantia polymorpha* L. determined by two- and three-dimensional electron microscopy. *Photosynthesis Research* **75**: 249–258.

He T, Pausas JG, Belcher CM, Schwilk DW, Lamont BB. 2012. Fire-adapted traits of *Pinus* arose in the fiery Cretaceous. *New Phytologist* **194**: 751–759.

Jansson S. 2006. A protein family saga: from photoprotection to light-harvesting (and back?). In: Demmig-Adams B, Adams WW III, Mattoo AK, eds. *Photoprotection, photoinhibition, gene regulation, and environment. Advances in photosynthesis and respiration.* Dordrecht, the Netherlands: Springer, 145–153.

Kouřil R, Dekker JP, Boekema EJ. 2012. Supramolecular organization of photosystem II in green plants. *Biochimica et Biophysica Acta – Bioenergetics* **1817**: 2–12.

Kouřil R, Strouhal O, Nosek L, Lenobel R, Chamrád I, Boekema EJ, Šebela M, Ilík P. 2014. Structural characterization of a plant photosystem I and NAD(P)H dehydrogenase supercomplex. *Plant Journal* **77**: 568–576.

Kouřil R, Wientjes E, Bultema JB, Croce R, Boekema EJ. 2013. High-light vs. low-light: effect of light acclimation on photosystem II composition and organization in *Arabidopsis thaliana*. *Biochimica et Biophysica Acta – Bioenergetics* **1827**: 411–419.

Kovács L, Damkjær J, Kereïche S, Ilioaia C, Ruban AV, Boekema EJ, Jansson S, Horton P. 2006. Lack of the light-harvesting complex CP24 affects the structure and function of the grana membranes of higher plant chloroplasts. *Plant Cell* **18**: 3106–3120.

Koziol AG, Borza T, Ishida K, Keeling P, Lee RW, Durnford DG. 2007. Tracing the evolution of the light-harvesting antennae in chlorophyll *a*/*b*-containing organisms. *Plant Physiology* **143**: 1802–1816.

Lamesch P, Berardini TZ, Li D, Swarbreck D, Wilks C, Sasidharan R, Muller R, Dreher K, Alexander DL, Garcia-Hernandez G *et al.* 2012. The Arabidopsis information resource (TAIR): improved gene annotation and new tools. *Nucleic Acids Research* **40**: 1202–1210.

Li XP, Björkman O, Shih C, Grossman AR, Rosenquist M, Jansson S, Niyogi KK. 2000. A pigment-binding protein essential for regulation of photosynthetic light harvesting. *Nature* **403**: 391–395.

Lichtenthaler H, Buschmann C. 2001. Chlorophylls and carotenoids: measurement and characterization by UV-VIS spectroscopy. In: Wrolstad RE, Acree TE, An H, Decker EA, Penner MH, Reid DS, Schwartz SJ, Shoemaker CF, Sporns P, eds. *Current protocols in food analytical chemistry.* New York, NY, USA: John Wiley & Sons, F4.3.1–F4.3.8.

Liu Z, Yan H, Wang K, Kuang T, Zhang J, Gui L, An X, Chang W. 2004. Crystal structure of spinach major light-harvesting complex at 2.72 Å resolution. *Nature* **428**: 287–292.
McElwain JC, Punyasena SW. 2007. Mass extinction events and the plant fossil record. *Trends in Ecology & Evolution* **22**: 548–557.
Merchant SS, Prochnik SE, Vallon O, Harris EH, Karpowicz SJ, Witman GB, Terry A, Salamov A, Fritz-Laylin LK, Maréchal-Drouard L *et al.* 2007. The *Chlamydomonas* genome reveals the evolution of key animal and plant functions. *Science* **318**: 245–250.
Miller CN. 1999. Implications of fossil conifers for the phylogenetic relationships of living families. *Botanical Review* **65**: 239–277.
Munekage Y, Hashimoto M, Miyake C, Tomizawa KI, Endo T, Tasaka M, Shikanai T. 2004. Cyclic electron flow around photosystem I is essential for photosynthesis. *Nature* **429**: 579–582.
Munekage Y, Hojo M, Meurer J, Endo T, Tasaka M, Shikanai T. 2002. *PGR5* is involved in cyclic electron flow around photosystem I and is essential for photoprotection in Arabidopsis. *Cell* **110**: 361–371.
Nystedt B, Street NR, Wetterbom A, Zuccolo A, Lin YC, Scofield DG, Vezzi F, Delhomme N, Giacomello S, Alexeyenko A *et al.* 2013. The Norway spruce genome sequence and conifer genome evolution. *Nature* **497**: 579–584.
Oostergetel GT, Keegstra W, Brisson A. 1998. Automation of specimen selection and data acquisition for protein electron crystallography. *Ultramicroscopy* **74**: 47–59.
Peers G, Truong TB, Ostendorf E, Busch A, Elrad D, Grossman AR, Hippler M, Niyogi KK. 2009. An ancient light-harvesting protein is critical for the regulation of algal photosynthesis. *Nature* **462**: 518–521.
Retallack GJ, Veevers JJ, Morante R. 1996. Global coal gap between Permian–Triassic extinction and Middle Triassic recovery of peatforming plants. *Geological Society of America Bulletin* **108**: 195–207.
Shikanai T. 2007. Cyclic electron transport around photosystem I: genetic approaches. *Annual Review of Plant Biology* **58**: 199–217.
Tokutsu R, Kato N, Bui KH, Ishikawa T, Minagawa J. 2012. Revisiting the supramolecular organization of Photosystem II in *Chlamydomonas reinhardtii*. *Journal of Biological Chemistry* **287**: 31574–31581.
Vanheel M. 1987. Angular reconstitution – *a posteriori* assignment of projection directions for 3-D reconstruction. *Ultramicroscopy* **21**: 111–123.
Wang XQ, Ran JH. 2014. Evolution and biogeography of gymnosperms. *Molecular Phylogenetics and Evolution* **75**: 24–40.
Wittig I, Karas M, Schägger H. 2007. High resolution clear native electrophoresis for In-gel functional assays and fluorescence studies of membrane protein complexes. *Molecular & Cellular Proteomics* **6**: 1215–1225.
Yamori W, Shikanai T, Makino A. 2015. Photosystem I cyclic electron flow via chloroplast NADH dehydrogenase-like complex performs a physiological role for photosynthesis at low light. *Scientific Reports* **5**: 13908.

Supporting Information

Additional supporting information may be found in the online version of this article.

Table S1 Number of sequences, cumulative length and source of databases used for the identification of Lhcb transcripts in analyzed species using basic local alignment search tool (BLAST)

Table S2 Best hits for *Arabidopsis thaliana* Lhcb proteins and PGR5 and *Chlamydomonas reinhardtii* Lhcsr proteins in transcriptomes of selected species, particular scaffolds/transcripts in TAIR.10 or *C. reinhardtii* proteome and between scaffolds/transcript and proteins

Please note: Wiley Blackwell are not responsible for the content or functionality of any supporting information supplied by the authors. Any queries (other than missing material) should be directed to the *New Phytologist* Central Office.

4.3 Structural variability of plant photosystem II megacomplexes in thylakoid membranes.

Nosek L, Semchonok D, Boekema EJ, Ilík P and Kouřil R., manuscript accepted in *Plant Journal*, (2016) (doi: 10.1111/tpj.13325)

Structural variability of plant photosystem II megacomplexes in thylakoid membranes

Lukáš Nosek[1], Dmitry Semchonok[2], Egbert J. Boekema[2], Petr Ilík[1] and Roman Kouřil[1,*]

[1]Centre of the Region Haná for Biotechnological and Agricultural Research, Department of Biophysics, Faculty of Science, Palacký University, Šlechtitelů 27, 783 71 Olomouc, Czech Republic

[2]Electron microscopy group, Groningen Biomolecular Sciences and Biotechnology Institute, University of Groningen, Nijenborgh 7, 9747 AG Groningen, The Netherlands

* Corresponding author: Roman Kouřil, Centre of the Region Haná for Biotechnological and Agricultural Research, Department of Biophysics, Faculty of Science, Palacký University, Šlechtitelů 27, 783 71 Olomouc, Czech Republic, Tel.: +420 585634837, e-mail: roman.kouril@upol.cz

A running title: Plant Photosystem II megacomplexes

Keywords: clear native polyacrylamide electrophoresis, *Arabidopsis thaliana*, photosystem II, megacomplex, single particle electron microscopy, grana membrane

Summary

Plant photosystem II (PSII) is organized into large supercomplexes with variable amount of membrane-bound light-harvesting proteins (LHCII). The largest stable form of the PSII supercomplex involves four LHCII trimers, which are specifically connected to the PSII core dimer via monomeric antenna proteins. The PSII supercomplexes can further interact in thylakoid membrane, forming PSII megacomplexes. So far, only megacomplexes consisting of two PSII supercomplexes associated in parallel have been observed. Here we show that the forms of PSII megacomplexes can be much more variable. We performed single particle electron microscopy (EM) analysis of PSII megacomplexes isolated from *Arabidopsis thaliana* using clear-native polyacrylamide gel electrophoresis. Extensive image analysis of a large data set revealed that besides the known PSII megacomplexes, there are distinct groups of megacomplexes with non-parallel association of supercomplexes. In some of them, we have found additional LHCII trimers, which appear to stabilize the non-parallel assemblies. We also performed EM analysis of the PSII supercomplexes on the level of whole grana membranes and successfully identified several types of megacomplexes, including those with non-parallel supercomplexes, which strongly supports their natural origin. Our data demonstrate a remarkable ability of plant PSII to form various larger assemblies, which may control photochemical utilization of absorbed light energy in plants in changing environment.

Significance statement

Plant photosystems II (PSII) form multi-subunit pigment-protein supercomplexes, which can associate into larger PSII megacomplexes. Extensive structural analysis of isolated PSII megacomplexes revealed their remarkable structural variability. Besides the known PSII megacomplexes, which consist of the supercomplexes connected in parallel, we have found unique non-parallel supercomplex associations. Importantly, we have demonstrated that these structures are native, as they have been identified also on the level of thylakoid membranes, and thus can have physiological significance.

Introduction

Photosystem II (PSII) is one of the key protein complexes involved in the light reactions of photosynthesis. It is embedded in thylakoid membranes of cyanobacteria, algae and higher plants, where it utilizes captured light energy for splitting of water molecules. In cooperation with other protein complexes such as photosystem I (PSI) and cytochrome b_6f complex, it participates in the production of energetically rich molecules of ATP and NADPH, which drive reactions of CO_2 assimilation.

Plant PSII consists of a dimeric core complex (C_2) and a variable number of light-harvesting proteins (Lhcb1-6), which form light-harvesting complex II (LHCII). The major part of the plant LHCII is represented by LHCII trimers, which consist of three Lhcb proteins (Lhcb1-3) and which are associated to C_2 via monomeric antenna proteins Lhcb4 (also called CP29), Lhcb5 (CP26), and Lhcb6 (CP24). According to the strength of their binding to C_2, the LHCII trimers were designated as "S" and "M" (strongly and moderately bound LHCII, respectively) (Dekker and Boekema, 2005; Kouřil et al., 2012). Occasionally, C_2 can associate also with the "L" (loosely bound) trimers (Boekema et al., 1999a). Single particle electron microscopy (EM) analysis of PSII in various land plant species indicates that the $C_2S_2M_2$ supercomplex is the largest stable form of PSII supercomplex. In this supercomplex, the C_2 associates with four LHCII trimers; two of them are strongly bound (S trimers) at the side of Lhcb5 and two are moderately bound (M trimers) via Lhcb4 and Lhcb6 (Boekema et al., 1995; Caffarri et al., 2009). A recent finding has revealed that the composition and architecture of the $C_2S_2M_2$ supercomplex is not conserved through all land plant species. There are two land plant groups, the pine family (Pinaceae) and Gnetales, which lack Lhcb3 (a constituent of the M trimer) and Lhcb6 proteins. Apart from so far unspecified physiological consequences, the absence of these proteins results in a structural modification of the $C_2S_2M_2$ supercomplex. This modified supercomplex is unique among land plants (Kouřil et al., 2016) and resembles its counterpart in green alga *Chlamydomonas reinhardtii* (Tokutsu et al., 2012; Drop et al., 2014).

Despite the progress in the specification of the positions of Lhcb proteins in PSII supercomplexes, there are still some Lhcb proteins with unclear localization. Biochemical

analysis indicates that in the thylakoid membrane, up to eight LHCII trimers can be present per C_2 (Peter and Thornber, 1991; van Oort et al., 2010; Kouřil et al., 2013). However, the binding capacity of C_2 is limited to six LHCII trimers (including the L trimers). The remaining LHCIIs have so far been considered to be "free" in the thylakoid membrane.

Besides a demand for the improvement of structural information about the PSII supercomplexes, the investigation of their organization in thylakoid membranes is also highly relevant. Considering that the excitation energy transfer between pigment-protein complexes strongly depends on their mutual distances, the interactions and connectivity between adjacent PSII complexes in the thylakoid membrane are very important for the regulation and optimization of their photochemical yield (e.g. van Oort et al., 2010; Amarnath et al., 2016). Most of the EM studies suggest that the organization of PSII supercomplexes in the thylakoid membrane is random (Dekker and Boekema, 2005; Kouřil et al., 2012). However, in some cases, a preference for parallel association of PSII supercomplexes into megacomplexes was observed both on the level of isolated protein complexes (see Dekker and Boekema, 2005) and isolated grana membranes (Kirchhoff et al. 2008). The mutual interaction between two parallel PSII supercomplexes involves C_2, the M trimers and the minor antenna proteins Lhcb5 and Lhcb6. The S trimers and the Lhcb4 protein were also shown to be able to mediate the interaction between supercomplexes, however, only in the case of smaller C_2S_2 supercomplexes (Boekema et al., 1999a; Boekema et al., 1999b; Yakushevska et al., 2001a). The megacomplexes can further associate into various semi-crystalline arrays, which have been often observed in grana thylakoid membranes (Boekema et al., 1999a; Boekema et al., 1999b; Boekema et al., 2000; Yakushevska et al., 2001a; Yakushevska et al., 2001b; Kirchhoff et al., 2007; Daum et al., 2010; Kouřil et al., 2013). A mechanism controlling the formation of the megacomplexes and semi-crystalline arrays as well as their functional relevance is still not fully understood. However, there is increasing evidence that these structures, in analogy to respiratory megacomplexes in mitochondria (see e.g. Dudkina et al., 2010 for review), are important for the regulation and optimization of photosynthetic processes and small protein traffic (for reviews see e.g. Kouřil et al., 2012; Kirchhoff, 2013; Tietz et al., 2015) and may also contribute to grana formation (Daum et al., 2010).

In this work, we have revealed a remarkable ability of PSII supercomplexes from *Arabidopsis thaliana* to form variable types of megacomplexes. Apart from the known parallel association of two PSII supercomplexes, we have also found variable associations between two non-parallel PSII supercomplexes. In some megacomplexes, novel binding positions for additional LHCII trimers (including the LHCII trimers so far considered to be "free") were revealed at the sides of the S and M trimers. Importantly, we have found some of these megacomplexes also on the level of grana membranes, which evidences their natural origin. We propose that a dynamic formation of different types of PSII megacomplexes can optimize photochemical utilization of absorbed light energy under variable environmental conditions.

Results

Separation of PSII megacomplexes using CN-PAGE

PSII supercomplexes and megacomplexes can be separated from gently solubilized thylakoid membranes by ultracentrifugation using sucrose gradient (Caffarri et al., 2009) or by clear/blue-native polyacryamide gel electrophoresis (CN/BN-PAGE) (e.g. Järvi et al., 2011). The advantage of the latter method is that it provides well focused protein zones. In order to preserve integrity and to maximize the yield of PSII megacomplexes, a mild detergent such as n-dodecyl-α-D-maltopyranoside is often used. We solubilized thylakoid membranes from *Arabidopsis thaliana* leaves using this detergent and modified the gradient of the resolving gel in order to achieve optimal resolution of pigment-protein complexes of the highest molecular weight. Figure 1a shows that a combination of these approaches ensured a clear separation of PSII- and PSI-containing supercomplexes and PSII megacomplexes at the expense of the small protein complexes/proteins such as trimeric or monomeric LHCII (see the band at the bottom part of the gel).

To clarify the band assignment, we measured chlorophyll fluorescence from the whole gel at room temperature using a gel imager (Figure 1a). As the quantum yield of PSII fluorescence at room temperature is much higher than the quantum yield of PSI

fluorescence, this measurement enabled us to identify both types of photosystems. Using this approach, PSI supercomplexes (PSI core with LHCI) were identified in a relatively dense band with undetectable fluorescence (see Fig. 1a). In native electrophoresis of pigment-protein complexes from thylakoid membranes (BN-PAGE, CN-PAGE), PSII core dimer migrates close to the PSI supercomplex because it has similar molecular weight (e.g. Lípová et al., 2010; Järvi et al., 2011). In our gel, PSII core dimer is represented by a very faint green band, which can be observed just below the PSI supercomplex band and which has high chlorophyll fluorescence yield. The fluorescence imaging of the gel further revealed that the green bands above the PSI supercomplex band are highly fluorescent, i.e. that they contain PSII. Based on the analogy with many papers dealing with native electrophoresis of chlorophyll-containing proteins from thylakoids (e.g. Järvi et al., 2011; Albanese et al., 2016), we designated the group of the bands above the PSI supercomplex band as PSII supercomplexes and PSII megacomplexes.

It is clearly visible that the amount of isolated PSII megacomplexes is much smaller compared to the amount of supercomplexes. A lower yield of PSII megacomplexes can be caused either by their lower stability during the isolation procedure (both solubilisation and separation by CN-PAGE) or by their lower abundance in the thylakoid membrane. In order to characterize the structure and the composition of the separated megacomplexes, we excised the corresponding green band from the gel, extracted the pigment-protein megacomplexes by spontaneous elution and performed their detailed structural characterization by single particle EM and image analysis.

PSII megacomplexes with specifically associated supercomplexes

Figure 1b shows an electron micrograph of a negatively stained specimen, where several PSII megacomplexes of different shape can be distinguished. Image processing of large amount of projections (about 50 000) selected from almost 12 000 micrographs revealed the presence of thirteen different types of megacomplexes. Each megacomplex consisted of two PSII supercomplexes. Based on the mutual position of individual PSII

supercomplexes, the PSII megacomplexes could be divided into two groups. While in the first group, representing a major part of megacomplexes (about 80 % of the data set), the PSII supercomplexes associate in parallel (Figure 2a-f), the second group (about 20 % of the data set) represents PSII supercomplexes interacting in a non-parallel manner (Figure 2g-m). In order to reveal the architecture of individual megacomplexes in detail, the EM projection maps were fitted with the pseudo-atomic X-ray model of the PSII supercomplex (Caffarri et al., 2009). It is obvious that most of the megacomplexes are formed by two copies of the complete $C_2S_2M_2$ supercomplex (Figure 3), with an exception of one megacomplex that lacks one M trimer (Figure 3l). Interestingly, the detailed image analysis revealed the presence of additional LHCII trimers in some of the megacomplexes (Figure 3e, f, g, k). These LHCII trimers are not regular constituents of PSII supercomplexes and so far have been assumed to be "free" in the thylakoid membrane. Our results indicate that these trimers can interact with PSII supercomplexes at so far uncharacterized binding sites.

Electron microscopy of grana membranes

In order to investigate the physiological relevance of the PSII megacomplexes separated using CN-PAGE, we searched for the megacomplexes also on the level of isolated grana membranes. Figure 4a shows an example of electron micrograph of the grana membrane with resolved densities of PSII complexes. Projections of individual PSII complexes were selected and processed by image analysis. If there are any specific interactions between some of these neighbouring PSII complexes in the grana membrane, they should be revealed as distinct classes after the image processing. Indeed, image analysis revealed five specific classes with resolved densities of pairs of PSII core complexes (Figure 4b-f). Based on their mutual distance and orientation, we were able to relate these pairs to the corresponding class averages of PSII megacomplexes separated using CN-PAGE (Figure 4g-k). Using this approach, the PSII megacomplexes with both parallel and non-parallel association of PSII supercomplexes were identified in the granal thylakoid membrane,the parallel associations being about two times more abundant than the non-parallel ones. This

result provides evidence that the PSII megacomplexes separated using CN-PAGE represent native PSII structures appearing in thylakoid membranes.

Discussion

Structural studies of plant PSII revealed its remarkable ability to form variable types of PSII supercomplexes, consisting of PSII core and Lhcb proteins. Moreover, the proximity of PSII supercomplexes in the grana membrane enables the formation of larger assemblies, i.e. PSII megacomplexes or even structures of higher order (see Dekker and Boekema, 2005; Kouřil et al., 2012 for reviews). Assembly/disassembly of PSII supercomplexes or megacomplexes modulates the antenna size of PSII, which was found to have an influence on the overall photochemical yield (e.g. Amarnath et al., 2016). These changes of higher PSII organization can represent one of the responses of plants to dynamic changes of environmental conditions such as light intensity (Ballottari et al., 2007; Kouřil et al., 2013). A recent theoretical study indicates that the excitation can move diffusively through the antenna proteins within a radius of about 50 nm until it reaches the reaction center (Amarnath et al., 2016). As the dimensions of the PSII supercomplex $C_2S_2M_2$ are 20 nm x 33 nm, the excitation can thus be shared within the whole megacomplex formed by two supercomplexes.

Our structural analysis of PSII megacomplexes separated using CN-PAGE revealed that a majority of them is formed by the parallel association of two PSII supercomplexes (Figure 2a-f, 3a-f). The reason for their abundance can be their higher structural stability when compared to the megacomplexes formed by the non-parallel association of PSII supercomplexes. Alternatively, it could reflect a fact that the megacomplexes with PSII supercomplexes associated in parallel originate from solubilized semi-crystalline arrays, which appear occasionally in grana membranes (Boekema et al., 1999a; Boekema et al., 1999b; Boekema et al., 2000; Yakushevska et al., 2001a; Yakushevska et al., 2001b; Kirchhoff et al., 2007; Daum et al., 2010; Kouřil et al., 2013).

In the most abundant megacomplexes, PSII supercomplexes interact in parallel via core complexes, M trimers, Lhcb5 and Lhcb6 proteins (Figure 3a-c). Obviously, the involvement of all these components in the interaction increases the overall stability of megacomplexes, resulting in their relatively high abundance. However, it seems that just the interaction between the Lhcb5 and the core complex is strong enough for the formation of the "parallel" PSII megacomplex (Figure 3d). Moreover, novel types of PSII megacomplexes which consists of the parallel supercomplexes and additional LHCII trimers were revealed (Figure 3e, f). The additional LHCII trimers seem to be indispensable for the stability of these megacomplexes as no analogous PSII megacomplexes lacking these additional trimers were detected.

In addition to the parallel association of the PSII supercomplexes into megacomplexes, the PSII megacomplexes with non-parallel orientation of supercomplexes were detected for the first time (Figure 3g-m). The supercomplex interactions within these megacomplexes are, as in the previous case, mediated by core complexes, S and M trimers, Lhcb5 and Lhcb6 proteins and additional LHCII trimers, although not all components are always involved in the megacomplex formation. Due to the asymmetric structure, these megacomplexes lack the possibility to form an arrangement similar to two-dimensional crystals.

Another interesting question that can be at least partially answered by our structural study is which subunits are, in general, essential for the formation of PSII megacomplex. Their identification will help to understand a regulatory mechanism controlling the formation and dissociation of these megacomplexes. We propose that the contribution of the Lhcb5 in the PSII megacomplex formation is the most significant, as it participates to some extent in the formation of all types of PSII megacomplexes, even in those where the Lhcb6 and the M trimer are not involved (Figure 3d-f).

In the grana membrane, the majority of PSII supercomplexes seems to be randomly organized (Figure 4) (see also Kouřil et al., 2013). However, the observed variability in the architecture of the PSII megacomplexes separated using CN-PAGE indicates that what originally looked like complete randomness can at least partially be explained by the

abundance of specific megacomplex forms. Image analysis of PSII supercomplexes within the grana membrane revealed specific associations of PSII supercomplexes (both the parallel and non-parallel interaction), which nicely corresponded with the structures of PSII megacomplexes isolated using CN-PAGE (Figure 4). In the light of these results, we realize that the positions of interacting PSII supercomplexes that we observed previously in the cryo-tomogram of the grana membranes (Kouřil et al., 2011) do not have to be random, but can indeed be specific.

Taken together, the two sets of characterized PSII megacomplexes (with parallel and non-parallel arrangement of PSII supercomplexes) indicate that there are more LHCII trimers bound in specific positions to PSII than has been considered previously (Dekker and Boekema, 2005). This fact reduces the pool of "free" LHCII trimers and supports the idea of a more defined packing of all PSII related components in the grana membrane. The packing of PSII supercomplexes with "free" LHCII trimers can be important for the regulation of effective PSII antenna size. A dynamic formation/disintegration of the PSII megacomplexes can efficiently manage the utilization of absorbed light energy by PSII supercomplexes, as it enables to change the contact between PSII reaction centers and adjacent antenna proteins. Nevertheless, a physiological significance and potential benefit of the formation of PSII megacomplexes under varying environmental conditions remains to be elucidated.

Experimental procedures

Plant material and sample preparation

Arabidopsis thaliana plants were grown in a growth chamber at 21°C with a photoperiod 8h light/16h dark at irradiance of 100 µmol of photons m^{-2} s^{-1} of photosynthetically active radiation (400 – 700 nm). Thylakoid membranes were isolated from 8-weeks-old plants using the protocol described by (Dau et al., 1995). The chlorophyll content in final thylakoid membrane suspension was determined by a pigment extraction into 80% acetone (Lichtenthaler, 1987). Thylakoid membranes with 10 µg of chlorophylls were solubilized with n-dodecyl-α-D-maltopyranoside using the detergent:chlorophyll mass

ratio of 20 and supplemented with sample buffer (50 mM HEPES pH 7.2, 400 mM sucrose, 5 mM $MgCl_2$, 15 mM NaCl, 10% glycerol) to the final volume of 30 µl. Non-solubilized membranes were removed by a short centrifugation (22 000g, 4°C). After the centrifugation, the supernatant was immediately loaded onto a polyacrylamide gel with 4-8% gradient resolving gel and 4% stacking gel (Wittig et al., 2007). The electrophoretic separation was conducted in a Bio-rad Mini protean tetra cell system, started at the constant current of 4 mA for 15 minutes and then continued at the constant current of 7 mA until the front reached the bottom of the resolving gel. The CN-PAGE gel was analyzed using a gel scanner Amersham Imager 600RGB (GE HealthCare Life Sciences, Japan). To visualize all the bands, the gel was scanned in transmission mode using white light illumination. The black and white image of the same gel was acquired in fluorescent mode to identify PSI- and PSII-containing bands. The excitation wavelength was 460 nm and the fluorescence signal was detected through a bandpass filter (690-720 nm). Subsequent elution of protein complexes from the gel and preparation of specimen for EM analysis was performed according to the procedure described by (Kouril et al., 2014).

Grana membranes were obtained by a solubilization of thylakoid membranes using digitonin (0.5 mg of chlorophylls per ml, 0.5% digitonin in a buffer (20 mM HEPES pH 7.5, 5 mM $MgCl_2$). Incubation (20 min at 4 °C while slowly stirred) was followed by a centrifugation in an Eppendorf table centrifuge (5 min, 12 000g, 4°C). The pellet with the non-solubilized grana thylakoid membranes was used for EM analysis.

Electron microscopy and image processing

Electron microscopy was performed on a Tecnai G2 20 Twin electron microscope (FEI, Eindhoven, The Netherlands) equipped with a LaB_6 cathode, operated at 200 kV. Images were recorded with an UltraScan 4000 UHS CCD camera (Gatan, Pleasanton, CA, USA) either at 130,000x magnification (in case of isolated PSII megacomplexes) or at 80,000x magnification (in case of grana membranes) with a pixel size of 0.224 nm and 0.375 nm, respectively, at the specimen level after binning the images to 2048x2048 pixels. GRACE

software (Oostergetel et al., 1998) was used for a semi-automated acquisition of about 12000 images, from which a data set of about 50 000 single particle projections of PSII megacomplexes separated by CN-PAGE was obtained. Single particle image analysis (see e.g. Boekema et al., 2009) was performed using GRIP and Relion software (Scheres, 2012). Image analysis revealed that about 75% of the projections from the data set could be assigned to one of the distinct classes. The remaining 25% of the data set represented projections of PSI-NDH supercomplex (Kouřil et al., 2014), which co-migrated with the PSII megacomplexes during CN-PAGE separation, and projections of other unassigned particles. In the case of grana membranes, about 800 images were recorded and about 20 000 projections of PSII particles were manually selected. Image analysis using the Relion software revealed that about 35 % of the projections from the data set could be resolved into five specific classes, for which we were able to reliably determine the mutual orientation of the PSII core complexes. The remaining 65 % of the projections represented classes where the orientation could not be determined, either due to a low signal to noise ratio (i.e. a small number of particles) or due to non-specific interactions between the adjacent PSII complexes.

Acknowledgements

This work was supported by the Grant Agency of the Czech Republic (project 13-28093S/P501 to RK), by a Marie Curie Career Integration Grant call FP7-PEOPLE-2012-CIG (322193 to RK) and by grant LO1204 (Sustainable development of research in the Centre of the Region Haná) from the National Program of Sustainability I from the Ministry of Education, Youth and Sports, Czech Republic. Work at University of Groningen was supported by NOW Chemical Sciences. We thank Dr. Iva Ilíková for editing the manuscript.

References

Albanese, P., Manfredi, M., Meneghesso, A., Marengo, E., Saracco, G., Barber, J., Morosinotto, T. and Pagliano, C. (2016) Dynamic reorganization of photosystem II supercomplexes in response to variations in light intensities. *Biochim. Biophys. Acta*, (in press).

Amarnath, K., Bennet, D.I.G., Schneider, A.R. and Fleming, G.R. (2016) Multiscale model of light harvesting by photosystem II in plants. *Proc. Natl. Acad. Sci. USA*, **113**, 1156-1161.

Ballottari, M., Dall´Osto, L., Morosinotto, T. and Bassi, R. (2007) Contrasting behavior of higher plant photosystem I and II antenna systems during acclimation. *J. Biol. Chem.* **282**, 8947–8958.

Boekema, E.J., Folea, M. and Kouřil, R. (2009) Single particle electron microscopy. *Photosynth. Res.* **102**, 189-196.

Boekema, E.J., Hankamer, B., Bald, D., Kruip, J., Nield, J., Boonstra, A.F., Barber, J. and Rögner, M. (1995) Supramolecular structure of the photosystem II complex from green plants and cyanobacteria. *Proc. Natl. Acad. Sci. USA,* **92**, 175–179.

Boekema, E.J., van Roon, H., Calkoen, F., Bassi, R. and Dekker, J.P. (1999a) Multiple types of association of photosystem II and its light-harvesting antenna in partially solubilized photosystem II membranes. *Biochemistry*, **38**, 2233-2239.

Boekema, E.J., van Roon, H., van Breemen, J.F.L. and Dekker, J.P. (1999b) Supramolecular organization of photosystem II and its light-harvesting antenna in partially solubilized photosystem II membranes. *Eur. J. Biochem.* **266**, 444-452.

Boekema, E.J., van Breemen, J.F.L., van Roon, H. and Dekker, J.P. (2000) Arrangement of photosystem II supercomplexes in crystalline macrodomains within the thylakoid membrane of green plant chloroplasts. *J. Mol. Biol.* **301**, 1123-1133.

Caffarri, S., Kouřil, R., Kereiche, S., Boekema, E.J. and Croce, R. (2009) Functional architecture of higher plant photosystem II supercomplexes. *EMBO J.* **28**, 3052-3063.

Dau, H., Andrews, J., Roelofs, T., Latimer, M., Liang, W., Yachandra, V., Sauer, K. and Klein, M. (1995) Structural consequences of ammonia binding to the manganese center of the photosynthetic oxygen-evolving complex: an X-ray absorption spectroscopy study of isotropic and oriented photosystem II particles. *Biochemistry*, **34**, 5274–5287.

Daum, B., Nicastro, D., Austin, J., McIntosh, J. and Kühlbrandt, W. (2010) Arrangement of Photosystem II and ATP Synthase in chloroplast membranes of Spinach and Pea. *Plant Cell*, **22**, 1299–1312.

Dekker, J.P. and Boekema, E.J. (2005) Supramolecular organization of thylakoid membrane proteins in green plants. *Biochim. Biophys. Acta*, **1706**, 12-39.

Drop, B., Webber-Birungi, M., Yadav, S.K., Filipowicz-Szymanska, A., Fusetti, F., Boekema, E.J. and Croce, R. (2014) Light-harvesting complex II (LHCII) and its supramolecular organization in *Chlamydomonas reinhardtii*. *Biochim. Biophys. Acta*, **1837**, 63-72.

Dudkina, N.V., Kouřil, R., Peters, K., Braun, H.P. and Boekema, E.J. (2010) Structure and function of mitochondrial supercomplexes. *Biochim. Biophys. Acta*, **1797**, 664–670.

Järvi S., Suorsa M., Paakkarinen V., Aro E. M. (2011) Optimized native gel systems for separation of thylakoid protein complexes: novel super- and mega-complexes. *Biochem. J.* **439**, 207-214.

Kirchhoff, H., Haase, W., Wegner, S., Danielsson, R., Ackermann, R. and Albertsson, P.A. (2007) Low-light-induced formation of semicrystalline photosystem II arrays in higher plant chloroplast. *Biochemistry*, **46**, 11169-11176.

Kirchhoff, H. (2013) Architectural switches in plant thylakoid membranes. *Photosynth. Res.* **116**, 481-487.

Kouřil, R., Oostergetel, G.T. and Boekema, E.J. (2011) Fine structure of granal thylakoid membrane organization using cryo electron tomography. *Biochim. Biophys. Acta*, **1807**, 368-374.

Kouřil, R., Dekker, J.P. and Boekema, E.J. (2012) Supramolecular organization of photosystem II in green plants. *Biochim. Biophys. Acta,* **1817**, 2-12.

Kouřil, R., Wientjes, E., Bultema, J.B., Croce, R. and Boekema, E.J. (2013) High-light vs. low-light: effect of light acclimation on photosystem II composition and organization in *Arabidopsis thaliana*. *Biochim. Biophys. Acta,* **1827**, 411-419.

Kouřil, R., Strouhal, O., Nosek, L., Lenobel, R., Chamrád, I., Boekema, E.J., Šebela, M. and Ilík, P. (2014) Structural characterization of a plant photosystem I and NAD(P)H dehydrogenase supercomplex. *Plant J.* **77**, 568-576.

Kouřil, R., Nosek, L., Bartoš, J., Boekema, E.J. and Ilík, P. (2016) Evolutionary loss of light-harvesting proteins Lhcb6 and Lhcb3 in major land plant groups - break-up of current dogma. *New Phytol*. **210**, 808-814.

Lichtenthaler, H.K. (1987) Chlorophylls and carotenoids. Pigments of photosynthetic biomembranes. In: *Methods in Enzymology* (Colowick, S.P. and Kaplan, N.O., eds). San Diego/New York: Academic Press, pp. 350–382.

Lípová, L., Krchňák, P., Komenda, J. and Ilík, P. (2010) Heat-induced disassembly and degradation of chlorophyll-containing protein complexes in vivo. *Biochim. Biophys. Acta*, **1797**, 63-70.

van Oort, B., Alberts, M., de Bianchi, S., Dall´Osto, L., Bassi, R., Trinkunas, G., Croce, R. and van Amerongen, H. (2010) Effect of antenna-depletion in photosystem II on excitation energy transfer in *Arabidopsis thaliana*. *Biophys. J.* **98**, 922–931.

Oostergetel, G.T., Keegstra, W. and Brisson, A. (1998) Automation of specimen selection and data acquisition for protein electron crystallography. *Ultramicroscopy*, **74**, 47–59.

Peter, G.F. and Thornber, J.P. (1991) Biochemical composition and organization of higher plant photosystem II light harvesting pigment-proteins. *J. Biol. Chem.* **266**, 16745-16754.

Scheres, S.H. (2012) RELION: implementation of a Bayesian approach to cryo-EM structure determination. *J. Struct. Biol.* **180**, 519-530.

Tietz, S., Puthiyaveetil, S., Enlow, H.M., Yarbrough, R., Wood, M., Semchonok, D.A., Lowry, T., Li, Z., Jahns, P., Boekema, E.J., Lenhert, S., Niyogi, K.K. and Kirchhoff, H. (2015) Functional implications of photosystem II crystal formation in photosynthetic membranes. *J. Biol. Chem.* **290**, 14091-14106.

Tokutsu, R., Kato, N., Bui, K.H., Ishikawa, T. and Minagawa, J. (2012) Revisiting the supramolecular organization of Photosystem II in *Chlamydomonas reinhardtii*. *J. Biol. Chem.* **287**, 31574–31581.

Wittig, I., Karas, M. and Schagger, H. (2007) High resolution clear native electrophoresis for in-gel functional assays and fluorescence studies of membrane protein complexes. *Mol. Cell. Proteomics*, **6**, 1215–1225.

Yakushevska, A.E., Jensen, P.E., Keegstra, W., van Roon, H., Scheller, H.S., Boekema, E.J. and Dekker, J.P. (2001a) Supermolecular organization of photosystem II and its

associated light-harvesting antenna in *Arabidopsis thaliana*. *Eur. J. Biochem.* **268**, 6020-6028.

Yakushevska, A.E., Ruban, A.V., Jensen, P.E., van Roon, H., Niyogi, K.K., Horton, P., Dekker, J.P. and Boekema, E.J. (2001b) Supermolecular organization of photosystem II and its associated light-harvesting antenna in the wild- type and *npq4* mutant of *Arabidopsis thaliana*. In *Proceedings: 12th International Congress on Photosynthesis*. CSIRO Publishing, Melbourne, Australia, pp. S5–006.

Figures

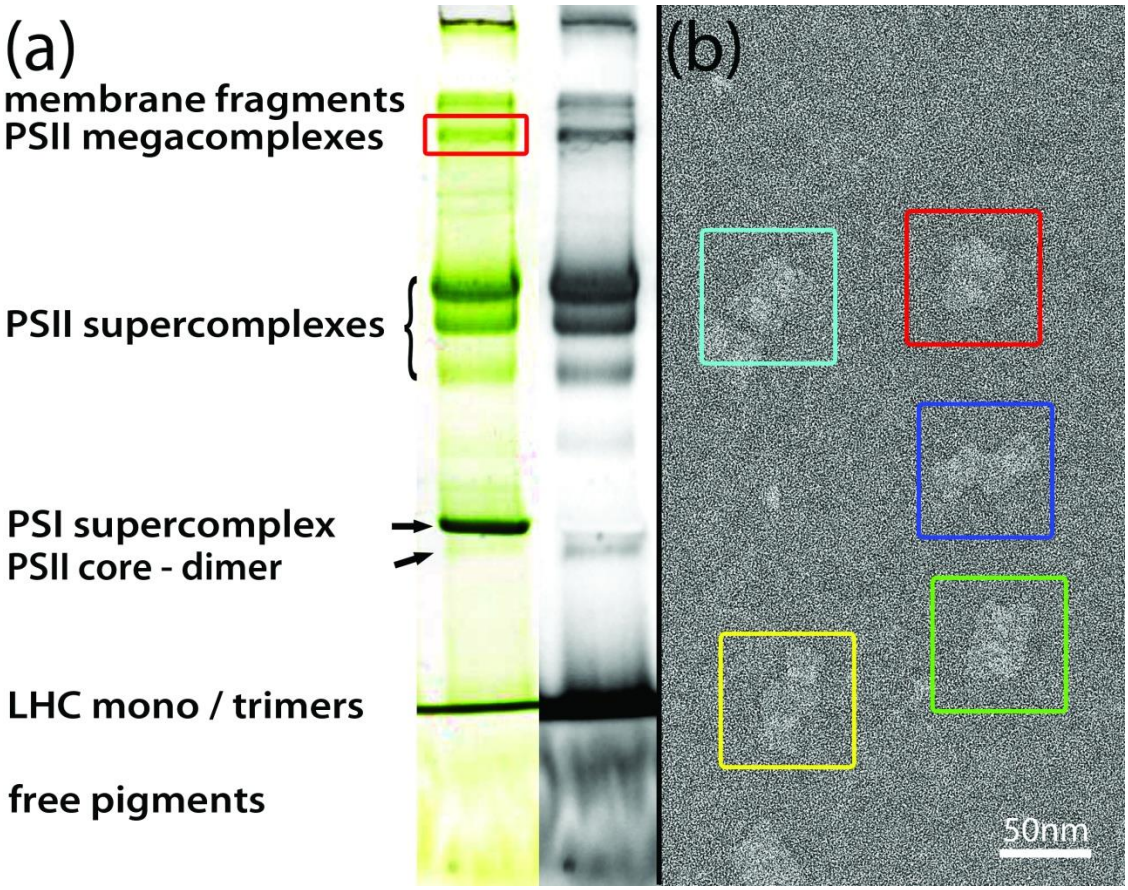

Figure 1. Separation and imaging of *Arabidopsis thaliana* pigment-protein complexes. (a) CN-PAGE separation of pigment-protein complexes from thylakoid membranes solubilized by n-dodecyl-α-D-maltopyranoside. The red frame indicates the band with megacomplexes subjected to elution and subsequent single particle electron microscopy analysis. The black and white image represents the chlorophyll fluorescence emission detected from the same gel. The fluorescence signal was detected through a bandpass filter (690-720 nm); the excitation wavelength was 460 nm. (b) A part of an electron micrograph of a negatively stained specimen with PSII megacomplexes. The colour frames highlight different forms of PSII megacomplexes.

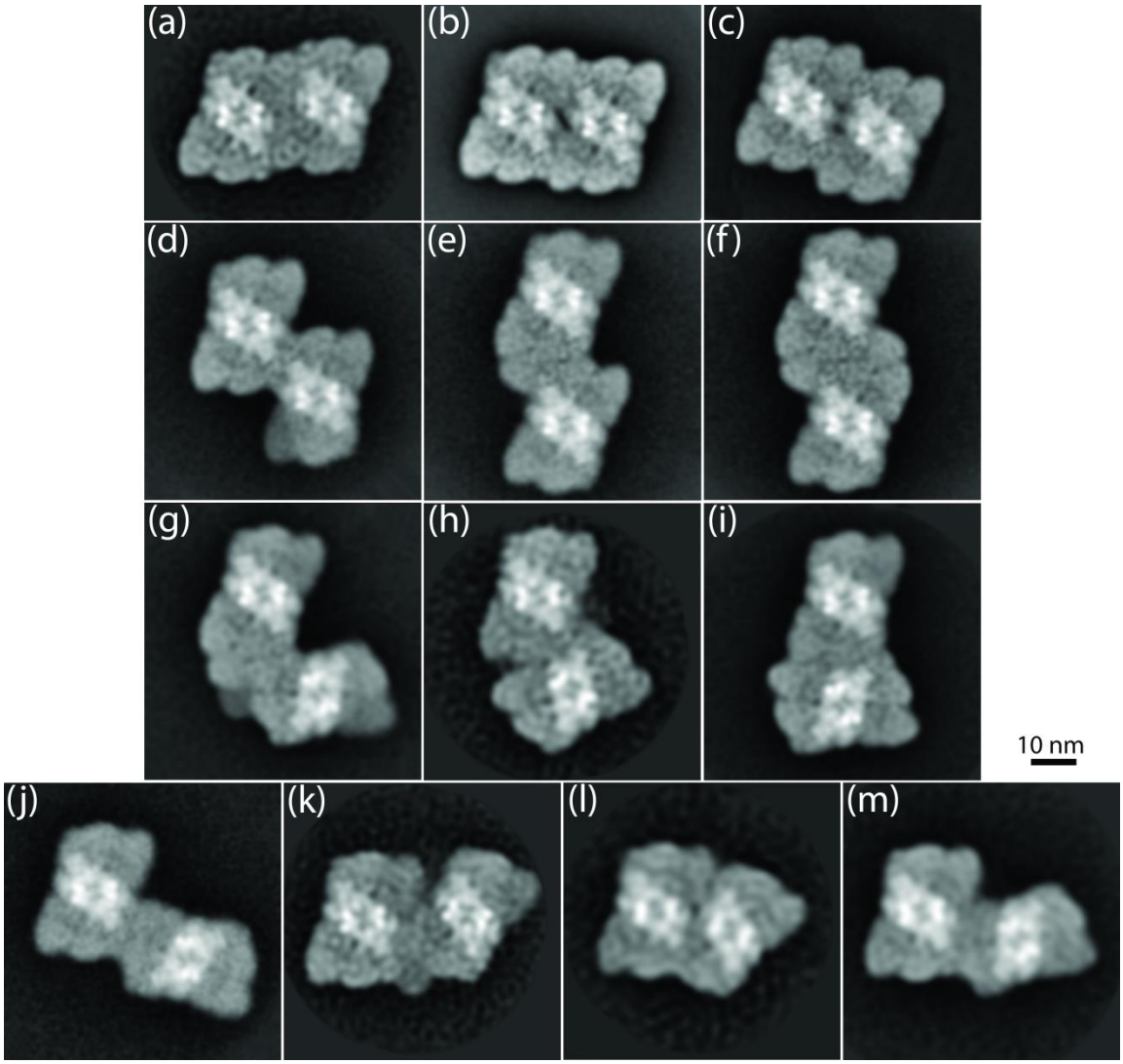

Figure 2. Structural characterization of PSII megacomplexes. (a-f) represent the megacomplexes with parallel orientation of PSII supercomplexes, whereas images (g-m) represent the megacomplexes formed by two supercomplexes associated in non-parallel manner. Total sum of particles which contributed to the final images: a: 1637 (4%); b: 8411 (22%); c: 16928 (45%); d: 2105 (6%); e: 378 (1%); f: 779 (2%); g: 1640 (4%); h: 418 (1%); i: 2789 (7%); j: 506 (1%); k: 582 (2%); l: 488 (1%); m: 1082 (3%). Percentage indicates a relative abundance of the particular form of PSII megacomplex.

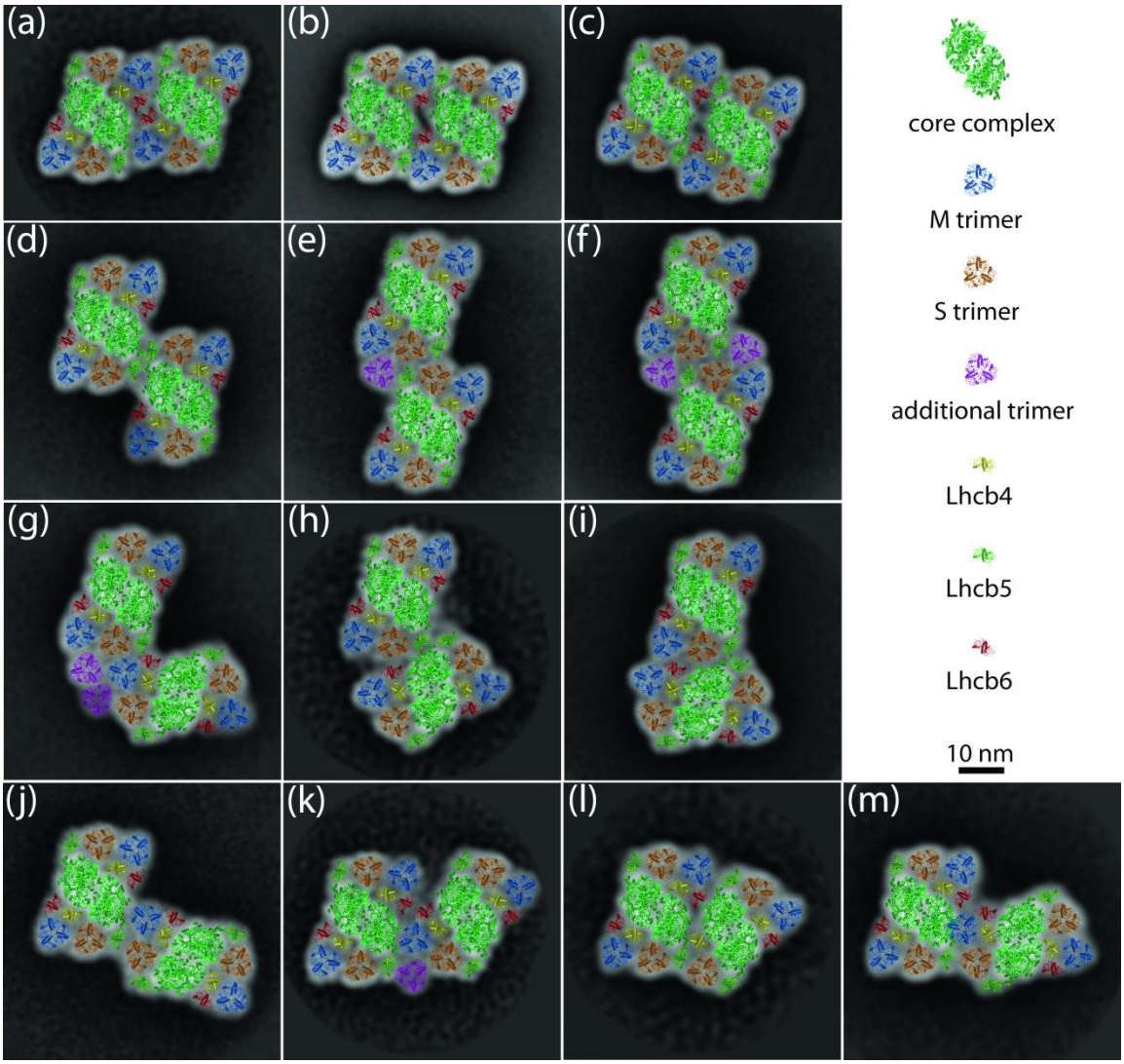

Figure 3. Structural models of the PSII megacomplexes shown in Figure 2. (a-m) PSII megacomplexes fitted with the proposed PSII crystalline structure as published by (Caffarri et al., 2009). Individual PSII subunits are color-coded in the following manner: pale green: core complex; blue: M trimer; orange: S trimer; magenta: additional LHCII trimers; yellow: Lhcb4; green: Lhcb5; red: Lhcb6.

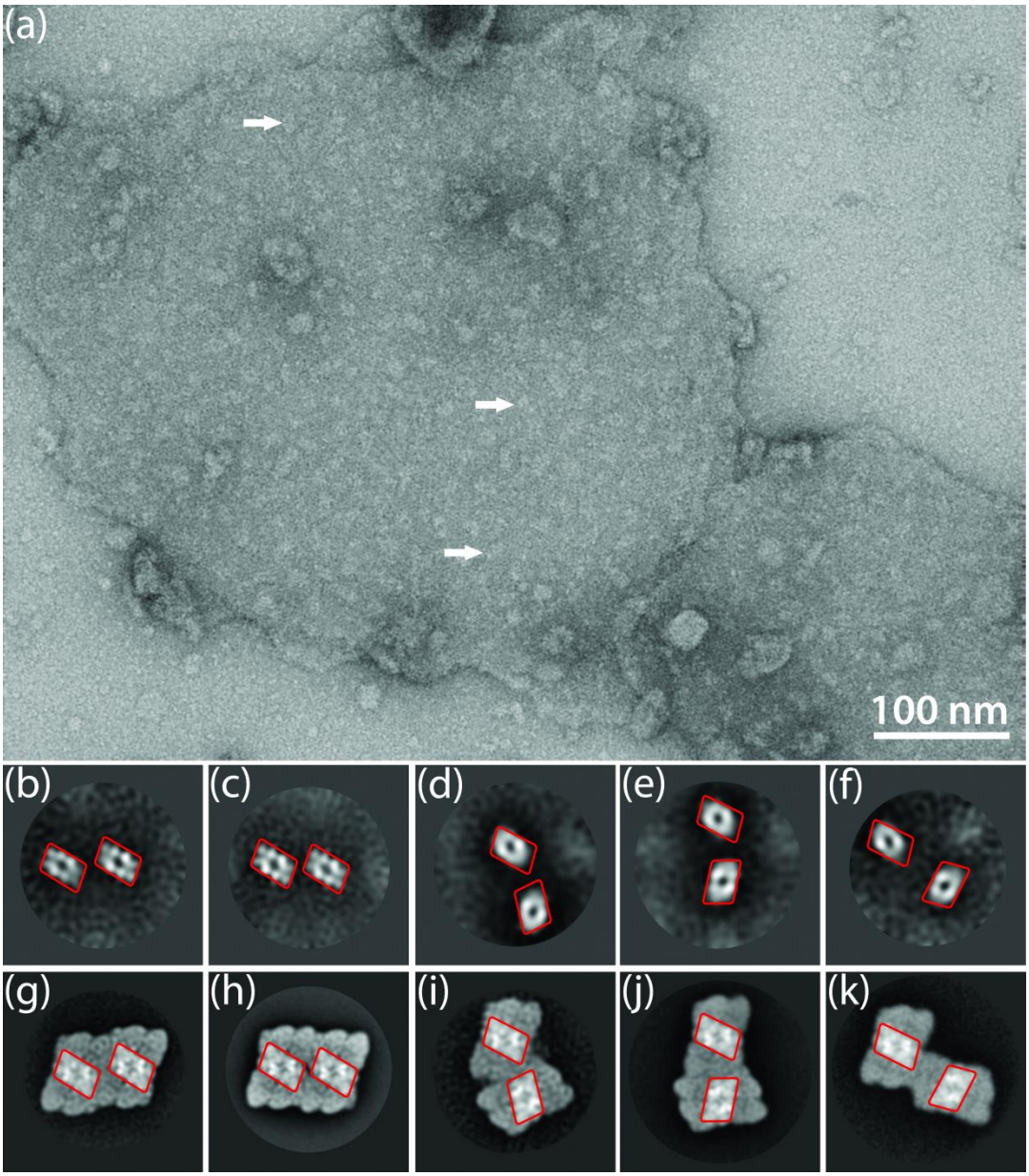

Figure 4. PSII megacomplexes found within an intact thylakoid membrane. (a) represents an example of electron micrograph of negatively stained thylakoid membrane isolated from *Arabidopsis thaliana* with densities corresponding to PSII core complex indicated by white arrows. (b-f) represent PSII megacomplexes found within the thylakoid membrane (the number of summed projections was 1838, 2620, 940, 682, and 825, respectively); (g-k) represent their analogues found in the sample separated by CN-PAGE. (g-k) correspond to megacomplexes (a), (b), (h), (i) and (j), respectively from Figure 2. The red frames surround core complexes of individual PSII supercomplexes and highlight that the megacomplexes found in the thylakoid membrane match with those obtained using CN-PAGE.

5. Conclusions

This thesis is focused on structural characterization of plant photosynthetic supercomplexes and megacomplexes by a combination of CN-PAGE and single particle electron microscopy. Combination of these two techniques represents a powerful method for structural studies of various complexes and using this approach, the structural characterizations of the PSI-NDH supercomplex isolated from barley, PSII megacomplexes isolated from *Arabidopsis thaliana* and PSII supercomplex isolated from Norway spruce were performed. These structural studies were published in two co-author and one first-author publications, which are attached to this thesis. The main conclusions are the following:

- PSI-NDH supercomplex represents an association between PSI and NDH and we provided the very first structural evidence of its formation (chapter 4.1). We propose that the gradual formation and dissociation of the PSI-NDH supercomplex is involved in tuning of cyclic electron flow around PSI.
- The structure of spruce PSII supercomplex represents the first structure of a photosynthetic complex isolated from gymnospermous plants (chapter 4.2). Moreover, we discovered that spruce (and also other members of *Pinaceae* and *Gnetales* families) are evolutionary deflected from other land plants, which has the impact in structure of their PSII supercomplexes.
- PSII megacomplexes represent a lateral association between two PSII supercomplexes (chapter 4.3). We provided an evidence of their native origin, as they were also discovered in the level of native membrane. This is also an evidence of their physiological significance, which remains an object of further research.

6. References

Adrian, M., Dubochet, J., Lepault, J., and McDowall, A.W. (1984). CRYO-ELECTRON MICROSCOPY OF VIRUSES. Nature **308,** 32-36.

Alboresi, A., Caffarri, S., Nogue, F., Bassi, R., and Morosinotto, T. (2008). In Silico and Biochemical Analysis of Physcomitrella patens Photosynthetic Antenna: Identification of Subunits which Evolved upon Land Adaptation. Plos One **3**.

Allen, J.F. (1992). PROTEIN-PHOSPHORYLATION IN REGULATION OF PHOTOSYNTHESIS. Biochimica Et Biophysica Acta **1098,** 275-335.

Amunts, A., and Nelson, N. (2008). Functional organization of a plant photosystem I: Evolution of a highly efficient photochemical machine. Plant Physiology and Biochemistry **46,** 228-237.

Amunts, A., Drory, O., and Nelson, N. (2007). The structure of a plant photosystem I supercomplex at 3.4 angstrom resolution. Nature **447,** 58-63.

Amunts, A., Toporik, H., Borovikova, A., and Nelson, N. (2010). Structure Determination and Improved Model of Plant Photosystem I. Journal of Biological Chemistry **285,** 3478-3486.

Ballottari, M., Girardon, J., Dall'Osto, L., and Bassi, R. (2012). Evolution and functional properties of Photosystem II light harvesting complexes in eukaryotes. Biochimica Et Biophysica Acta-Bioenergetics **1817,** 143-157.

Baradaran, R., Berrisford, J.M., Minhas, G.S., and Sazanov, L.A. (2013). Crystal structure of the entire respiratory complex I. Nature **494,** 443-448.

Barera, S., Pagliano, C., Pape, T., Saracco, G., and Barber, J. (2012). Characterization of PSII-LHCII supercomplexes isolated from pea thylakoid membrane by one-step treatment with alpha- and beta-dodecyl-D-maltoside. Philosophical Transactions of the Royal Society B-Biological Sciences **367,** 3389-3399.

Bassi, R., Rigoni, F., Barbato, R., and Giacometti, G.M. (1988). LIGHT-HARVESTING CHLOROPHYLL-A/B-PROTEINS (LHCII) POPULATIONS IN PHOSPHORYLATED MEMBRANES. Biochimica Et Biophysica Acta **936,** 29-38.

Bellafiore, S., Barneche, F., Peltier, G., and Rochaix, J.D. (2005). State transitions and light adaptation require chloroplast thylakoid protein kinase STN7. Nature **433,** 892-895.

Ben-Shem, A., Frolow, F., and Nelson, N. (2003). Crystal structure of plant photosystem I. Nature **426,** 630-635.

Bennett, J. (1977). PHOSPHORYLATION OF CHLOROPLAST MEMBRANE POLYPEPTIDES. Nature **269,** 344-346.

Bennett, J., Steinback, K.E., and Arntzen, C.J. (1980). CHLOROPLAST PHOSPHOPROTEINS - REGULATION OF EXCITATION-ENERGY TRANSFER BY PHOSPHORYLATION OF THYLAKOID MEMBRANE POLYPEPTIDES. Proceedings of the National Academy of Sciences of the United States of America-Biological Sciences **77,** 5253-5257.

Betterle, N., Ballottari, M., Zorzan, S., de Bianchi, S., Cazzaniga, S., Dall'Osto, L., Morosinotto, T., and Bassi, R. (2009). Light-induced Dissociation of an Antenna Hetero-oligomer Is Needed for Non-photochemical Quenching Induction. Journal of Biological Chemistry **284,** 15255-15266.

Boekema, E.J., Folea, M., and Kouril, R. (2009). Single particle electron microscopy. Photosynthesis Research **102,** 189-196.

Boekema, E.J., van Roon, H., van Breemen, J.F.L., and Dekker, J.P. (1999a). Supramolecular organization of photosystem II and its light-harvesting antenna in partially solubilized photosystem II membranes. European Journal of Biochemistry **266,** 444-452.

Boekema, E.J., van Breemen, J.F.L., van Roon, H., and Dekker, J.P. (2000). Arrangement of photosystem II supercomplexes in crystalline macrodomains within the thylakoid membrane of green plant chloroplasts. Journal of Molecular Biology **301,** 1123-1133.

Boekema, E.J., van Roon, H., Calkoen, F., Bassi, R., and Dekker, J.P. (1999b). Multiple types of association of photosystem II and its light-harvesting antenna in partially solubilized photosystem II membranes. Biochemistry **38,** 2233-2239.

Boekema, E.J., Dekker, J.P., Vanheel, M.G., Rogner, M., Saenger, W., Witt, I., and Witt, H.T. (1987). EVIDENCE FOR A TRIMERIC ORGANIZATION OF THE PHOTOSYSTEM-I COMPLEX FROM THE THERMOPHILIC CYANOBACTERIUM SYNECHOCOCCUS SP. Febs Letters **217,** 283-286.

Boekema, E.J., Jensen, P.E., Schlodder, E., van Breemen, J.F.L., van Roon, H., Scheller, H.V., and Dekker, J.P. (2001). Green plant photosystem I binds light-harvesting complex I on one side of the complex. Biochemistry **40,** 1029-1036.

Boekema, E.J., Hankamer, B., Bald, D., Kruip, J., Nield, J., Boonstra, A.F., Barber, J., and Rogner, M. (1995). SUPRAMOLECULAR STRUCTURE OF THE PHOTOSYSTEM-II COMPLEX FROM GREEN PLANTS AND CYANOBACTERIA. Proceedings of the National Academy of Sciences of the United States of America **92,** 175-179.

Bonardi, V., Pesaresi, P., Becker, T., Schleiff, E., Wagner, R., Pfannschmidt, T., Jahns, P., and Leister, D. (2005). Photosystem II core phosphorylation and photosynthetic acclimation require two different protein kinases. Nature **437,** 1179-1182.

Bonavent.C, and Myers, J. (1969). FLUORESCENCE AND OXYGEN EVOLUTION FROM CHLORELLA PYRENOIDOSA. Biochimica Et Biophysica Acta **189,** 366-+.

Brenner, S., and Horne, R.W. (1959). A NEGATIVE STAINING METHOD FOR HIGH RESOLUTION ELECTRON MICROSCOPY OF VIRUSES. Biochimica Et Biophysica Acta **34,** 103-110.

Busch, A., and Hippler, M. (2011). The structure and function of eukaryotic photosystem I. Biochimica Et Biophysica Acta-Bioenergetics **1807,** 864-877.

Caffarri, S., Kouril, R., Kereiche, S., Boekema, E.J., and Croce, R. (2009). Functional architecture of higher plant photosystem II supercomplexes. Embo Journal **28,** 3052-3063.

Chitnis, V.P., and Chitnis, P.R. (1993). PSAL SUBUNIT IS REQUIRED FOR THE FORMATION OF PHOTOSYSTEM-I TRIMERS IN THE CYANOBACTERIUM SYNECHOCYSTIS SP PCC-6803. Febs Letters **336,** 330-334.

Correa-Galvis, V., Poschmann, G., Melzer, M., Stuhler, K., and Jahns, P. (2016). PsbS interactions involved in the activation of energy dissipation in Arabidopsis. Nature Plants **2**.

Crepin, A., Santabarbara, S., and Caffarri, S. (2016). Biochemical and Spectroscopic Characterization of Highly Stable Photosystem II Supercomplexes from Arabidopsis. (J Biol Chem), pp. 19157-19171.

Dainese, P., and Bassi, R. (1991). SUBUNIT STOICHIOMETRY OF THE CHLOROPLAST PHOTOSYSTEM-II ANTENNA SYSTEM AND AGGREGATION STATE OF THE COMPONENT CHLOROPHYLL-A/B BINDING-PROTEINS. Journal of Biological Chemistry **266,** 8136-8142.

Dau, H., Andrews, J.C., Roelofs, T.A., Latimer, M.J., Liang, W.C., Yachandra, V.K., Sauer, K., and Klein, M.P. (1995). STRUCTURAL CONSEQUENCES OF AMMONIA BINDING TO THE MANGANESE CENTER OF THE PHOTOSYNTHETIC OXYGEN-EVOLVING COMPLEX - AN X-RAY-ABSORPTION SPECTROSCOPY STUDY OF ISOTROPIC AND ORIENTED PHOTOSYSTEM-II PARTICLES. Biochemistry **34,** 5274-5287.

Daum, B., Nicastro, D., Il, J.A., McIntosh, J.R., and Kuhlbrandt, W. (2010). Arrangement of Photosystem II and ATP Synthase in Chloroplast Membranes of Spinach and Pea. Plant Cell **22,** 1299-1312.

de Bianchi, S., Dall'Osto, L., Tognon, G., Morosinotto, T., and Bassi, R. (2008). Minor antenna proteins CP24 and CP26 affect the interactions between photosystem II Subunits and the electron transport rate in grana membranes of Arabidopsis. Plant Cell **20,** 1012-1028.

de Bianchi, S., Betterle, N., Kouril, R., Cazzaniga, S., Boekema, E., Bassi, R., and Dall'Osto, L. (2011). Arabidopsis Mutants Deleted in the Light-Harvesting Protein Lhcb4 Have a Disrupted Photosystem II Macrostructure and Are Defective in Photoprotection. Plant Cell **23,** 2659-2679.

Dekker, J.P., and Boekema, E.J. (2005). Supramolecular organization of thylakoid membrane proteins in green plants. Biochimica Et Biophysica Acta-Bioenergetics **1706,** 12-39.

Efremov, R.G., Baradaran, R., and Sazanov, L.A. (2010). The architecture of respiratory complex I. Nature **465,** 441-U461.

Farah, J., Rappaport, F., Choquet, Y., Joliot, P., and Rochaix, J.D. (1995). ISOLATION OF A PSAF-DEFICIENT MUTANT OF CHLAMYDOMONAS-REINHARDTII - EFFICIENT INTERACTION OF PLASTOCYANIN WITH THE PHOTOSYSTEM-I REACTION-CENTER IS MEDIATED BY THE PSAF SUBUNIT. Embo Journal **14,** 4976-4984.

Fischer, N., Boudreau, E., Hippler, M., Drepper, F., Haehnel, W., and Rochaix, J.D. (1999). A large fraction of PsaF is nonfunctional in photosystem I complexes lacking the PsaJ subunit. Biochemistry **38,** 5546-5552.

Forsberg, J., and Allen, J.F. (2001). Protein tyrosine phosphorylation in the transition to light state 2 of chloroplast thylakoids. Photosynthesis Research **68,** 71-79.

Frank, J., Radermacher, M., Penczek, P., Zhu, J., Li, Y.H., Ladjadj, M., and Leith, A. (1996). SPIDER and WEB: Processing and visualization of images in 3D electron microscopy and related fields. Journal of Structural Biology **116,** 190-199.

Galka, P., Santabarbara, S., Thi, T.H.K., Degand, H., Morsomme, P., Jennings, R.C., Boekema, E.J., and Caffarri, S. (2012). Functional Analyses of the Plant Photosystem I-Light-Harvesting Complex II Supercomplex Reveal That Light-Harvesting Complex II Loosely Bound to Photosystem II Is a Very Efficient Antenna for Photosystem I in State II. Plant Cell **24,** 2963-2978.

Garber, M.P., and Steponkus, P.L. (1976). ALTERATIONS IN CHLOROPLAST THYLAKOIDS DURING COLD-ACCLIMATION. Plant Physiology **57,** 681-686.

Gerotto, C., Franchin, C., Arrigoni, G., and Morosinotto, T. (2015). In Vivo Identification of Photosystem II Light Harvesting Complexes Interacting with PHOTOSYSTEM II SUBUNIT S. Plant Physiology **168,** 1747-U1105.

Gobets, B., and van Grondelle, R. (2001). Energy transfer and trapping in photosystem I. Biochimica Et Biophysica Acta-Bioenergetics **1507,** 80-99.

Guskov, A., Kern, J., Gabdulkhakov, A., Broser, M., Zouni, A., and Saenger, W. (2009). Cyanobacterial photosystem II at 2.9-angstrom resolution and the role of quinones, lipids, channels and chloride. Nature Structural & Molecular Biology **16,** 334-342.

Haldrup, A., Naver, H., and Scheller, H.V. (1999). The interaction between plastocyanin and photosystem I is inefficient in transgenic Arabidopsis plants lacking the PSI-N subunit of photosystem I. Plant Journal **17,** 689-698.

Haldrup, A., Simpson, D.J., and Scheller, H.V. (2000). Down-regulation of the PSI-F subunit of photosystem I (PSI) in Arabidopsis thaliana - The PSI-F subunit is essential for photoautotrophic growth and contributes to antenna function. Journal of Biological Chemistry **275,** 31211-31218.

Hayashida, N., Matsubayashi, T., Shinozaki, K., Sugiura, M., Inoue, K., and Hiyama, T. (1987). THE GENE FOR THE 9 KD POLYPEPTIDE, A POSSIBLE APOPROTEIN FOR THE IRON-SULFUR CENTER-A AND CENTER-B OF THE PHOTOSYSTEM-I COMPLEX, IN TOBACCO CHLOROPLAST DNA. Current Genetics **12,** 247-250.

Hoj, P.B., Svendsen, I., Scheller, H.V., and Moller, B.L. (1987). IDENTIFICATION OF A CHLOROPLAST-ENCODED 9-KDA POLYPEPTIDE AS A 2 4FE-4S PROTEIN CARRYING CENTER-A AND CENTER-B OF PHOTOSYSTEM-I. Journal of Biological Chemistry **262,** 12676-12684.

Hu, P., Lv, J., Fu, P.C., and Mi, H.L. (2013). Enzymatic characterization of an active NDH complex from Thermosynechococcus elongatus. Febs Letters **587,** 2340-2345.

Iwai, M., Takizawa, K., Tokutsu, R., Okamuro, A., Takahashi, Y., and Minagawa, J. (2010). Isolation of the elusive supercomplex that drives cyclic electron flow in photosynthesis. Nature **464,** 1210-U1134.

Jansson, S. (1994). THE LIGHT-HARVESTING CHLOROPHYLL A/B BINDING-PROTEINS. Biochimica Et Biophysica Acta-Bioenergetics **1184,** 1-19.

Jansson, S. (1999). A guide to the Lhc genes and their relatives in Arabidopsis. Trends in Plant Science **4,** 236-240.

Jansson, S., Andersen, B., and Scheller, H.V. (1996). Nearest-neighbor analysis of higher-plant photosystem I holocomplex. Plant Physiology **112,** 409-420.

Jarvi, S., Suorsa, M., Paakkarinen, V., and Aro, E.M. (2011). Optimized native gel systems for separation of thylakoid protein complexes: novel super- and mega-complexes. Biochemical Journal **439,** 207-214.

Jensen, P.E., Haldrup, A., Zhang, S.P., and Scheller, H.V. (2004). The PSI-O subunit of plant photosystem I is involved in balancing the excitation pressure between the two photosystems. Journal of Biological Chemistry **279,** 24212-24217.

Jensen, P.E., Bassi, R., Boekema, E.J., Dekker, J.P., Jansson, S., Leister, D., Robinson, C., and Scheller, H.V. (2007). Structure, function and regulation of plant photosystem I. Biochimica Et Biophysica Acta-Bioenergetics **1767,** 335-352.

Jordan, P., Fromme, P., Witt, H.T., Klukas, O., Saenger, W., and Krauss, N. (2001). Three-dimensional structure of cyanobacterial photosystem I at 2.5 angstrom resolution. Nature **411,** 909-917.

Kereiche, S., Kiss, A.Z., Kouril, R., Boekema, E.J., and Horton, P. (2010). The PsbS protein controls the macro-organisation of photosystem II complexes in the grana membranes of higher plant chloroplasts. Febs Letters **584,** 759-764.

Kirchhoff, H., Sharpe, R.M., Herbstova, M., Yarbrough, R., and Edwards, G.E. (2013). Differential Mobility of Pigment-Protein Complexes in Granal and Agranal Thylakoid Membranes of C-3 and C-4 Plants. Plant Physiology **161,** 497-507.

Kirchhoff, H., Haase, W., Wegner, S., Danielsson, R., Ackermann, R., and Albertsson, P.-A. (2007). Low-light-induced formation of semicrystalline photosystem II arrays in higher plant chloroplast. Biochemistry **46,** 11169-11176.

Klimmek, F., Sjodin, A., Noutsos, C., Leister, D., and Jansson, S. (2006). Abundantly and rarely expressed Lhc protein genes exhibit distinct regulation patterns in plants. Plant Physiology **140,** 793-804.

Knispel, R.W., Kofler, C., Boicu, M., Baumeister, W., and Nickell, S. (2012). Blotting protein complexes from native gels to electron microscopy grids. Nature Methods **9,** 182-184.

Kouril, R., Dekker, J.P., and Boekema, E.J. (2012). Supramolecular organization of photosystem II in green plants. Biochimica Et Biophysica Acta-Bioenergetics **1817,** 2-12.

Kouril, R., van Oosterwijk, N., Yakushevska, A.E., and Boekema, E.J. (2005a). Photosystem I: a search for green plant trimers. Photochemical & Photobiological Sciences **4,** 1091-1094.

Kouril, R., Wientjes, E., Bultema, J.B., Croce, R., and Boekema, E.J. (2013). High-light vs. low-light: Effect of light acclimation on photosystem II composition and organization in Arabidopsis thaliana. Biochimica Et Biophysica Acta-Bioenergetics **1827,** 411-419.

Kouril, R., Nosek, L., Bartos, J., Boekema, E.J., and Ilik, P. (2016). Evolutionary loss of light-harvesting proteins Lhcb6 and Lhcb3 in major land plant groups - break-up of current dogma. New Phytologist **210,** 808-814.

Kouril, R., Zygadlo, A., Arteni, A.A., de Wit, C.D., Dekker, J.P., Jensen, P.E., Scheller, H.V., and Boekema, E.J. (2005b). Structural characterization of a complex of photosystem I and light-harvesting complex II of Arabidopsis thaliana. Biochemistry **44,** 10935-10940.

Kouril, R., Strouhal, O., Nosek, L., Lenobel, R., Chamrad, I., Boekema, E.J., Sebela, M., and Ilik, P. (2014). Structural characterization of a plant photosystem I and NAD(P)H dehydrogenase supercomplex. Plant Journal **77,** 568-576.

Kovacs, L., Damkjaer, J., Kereiche, S., Ilioaia, C., Ruban, A.V., Boekema, E.J., Jansson, S., and Horton, P. (2006). Lack of the light-harvesting complex CP24 affects the structure and function of the grana membranes of higher plant chloroplasts. Plant Cell **18,** 3106-3120.

Li, X.P., Bjorkman, O., Shih, C., Grossman, A.R., Rosenquist, M., Jansson, S., and Niyogi, K.K. (2000). A pigment-binding protein essential for regulation of photosynthetic light harvesting. Nature **403,** 391-395.

Lichtenthaler, H.K. (1987). CHLOROPHYLLS AND CAROTENOIDS - PIGMENTS OF PHOTOSYNTHETIC BIOMEMBRANES. Methods in Enzymology **148,** 350-382.

Liu, Z.F., Yan, H.C., Wang, K.B., Kuang, T.Y., Zhang, J.P., Gui, L.L., An, X.M., and Chang, W.R. (2004). Crystal structure of spinach major light-harvesting complex at 2.72 angstrom resolution. Nature **428,** 287-292.

Ludtke, S.J., Baldwin, P.R., and Chiu, W. (1999). EMAN: Semiautomated software for high-resolution single-particle reconstructions. Journal of Structural Biology **128,** 82-97.

Lunde, C., Jensen, P.E., Haldrup, A., Knoetzel, J., and Scheller, H.V. (2000). The PSI-H subunit of photosystem I is essential for state transitions in plant photosynthesis. Nature **408,** 613-615.

Mazor, Y., Borovikova, A., and Nelson, N. (2015). The structure of plant photosystem I super-complex at 2.8 angstrom resolution. Elife **4**.

Morosinotto, T., Breton, J., Bassi, R., and Croce, R. (2003). The nature of a chlorophyll ligand in Lhca proteins determines the far red fluorescence emission typical of photosystem I. Journal of Biological Chemistry **278,** 49223-49229.

Murata, N. (1969). CONTROL OF EXCITATION TRANSFER IN PHOTOSYNTHESIS .I. LIGHT-INDUCED CHANGE OF CHLOROPHYLL A FLUORESCENCE IN PORPHYRIDIUM CRUENTUM. Biochimica Et Biophysica Acta **172,** 242-&.

Nelson, N. (2009). Plant Photosystem I - The Most Efficient Nano-Photochemical Machine. Journal of Nanoscience and Nanotechnology **9,** 1709-1713.

Nelson, N., and Ben-Shem, A. (2004). The complex architecture of oxygenic photosynthesis. Nature Reviews Molecular Cell Biology **5,** 971-982.

Nelson, N., and Ben-Shem, A. (2005). The structure of photosystem I and evolution of photosynthesis. Bioessays **27,** 914-922.

Nelson, N., and Yocum, C.F. (2006). Structure and function of photosystems I and II. Annual Review of Plant Biology **57,** 521-565.

Niyogi, K.K. (2000). Safety valves for photosynthesis. Current Opinion in Plant Biology **3,** 455-460.

Niyogi, K.K., Li, X.P., Rosenberg, V., and Jung, H.S. (2005). Is PsbS the site of non-photochemical quenching in photosynthesis? Journal of Experimental Botany **56,** 375-382.

Ohyama, K., Fukuzawa, H., Kohchi, T., Shirai, H., Sano, T., Sano, S., Umesono, K., Shiki, Y., Takeuchi, M., Chang, Z., Aota, S., Inokuchi, H., and Ozeki, H. (1986). CHLOROPLAST GENE ORGANIZATION DEDUCED FROM COMPLETE SEQUENCE OF LIVERWORT MARCHANTIA-POLYMORPHA CHLOROPLAST DNA. Nature **322,** 572-574.

Oostergetel, G.T., Keegstra, W., and Brisson, A. (1998). Automation of specimen selection and data acquisition for protein electron crystallography. Ultramicroscopy **74,** 47-59.

Pagliano, C., Barera, S., Chimirri, F., Saracco, G., and Barber, J. (2012). Comparison of the alpha and beta isomeric forms of the detergent n-dodecyl-D-maltoside for solubilizing photosynthetic complexes from pea thylakoid membranes. Biochimica Et Biophysica Acta-Bioenergetics **1817,** 1506-1515.

Pan, X.W., Li, M., Wan, T., Wang, L.F., Jia, C.J., Hou, Z.Q., Zhao, X.L., Zhang, J.P., and Chang, W.R. (2011). Structural insights into energy regulation of light-harvesting complex CP29 from spinach. Nature Structural & Molecular Biology **18,** 309-U394.

Pavlovic, A., Stolarik, T., Nosek, L., Kouril, R., and Ilik, P. (2016). Light-induced gradual activation of photosystem II in dark-grown Norway spruce seedlings. Biochimica Et Biophysica Acta-Bioenergetics **1857,** 799-809.

Peng, L.W., and Shikanai, T. (2011). Supercomplex Formation with Photosystem I Is Required for the Stabilization of the Chloroplast NADH Dehydrogenase-Like Complex in Arabidopsis. Plant Physiology **155,** 1629-1639.

Peng, L.W., Shimizu, H., and Shikanai, T. (2008). The Chloroplast NAD(P)H Dehydrogenase Complex Interacts with Photosystem I in Arabidopsis. Journal of Biological Chemistry **283,** 34873-34879.

Peng, L.W., Yamamoto, H., and Shikanai, T. (2011). Structure and biogenesis of the chloroplast NAD(P)H dehydrogenase complex. Biochimica Et Biophysica Acta-Bioenergetics **1807,** 945-953.

Peng, L.W., Fukao, Y., Fujiwara, M., Takami, T., and Shikanai, T. (2009). Efficient Operation of NAD(P)H Dehydrogenase Requires Supercomplex Formation with Photosystem I via Minor LHCI in Arabidopsis. Plant Cell **21,** 3623-3640.

Peter, G.F., and Thornber, J.P. (1991). BIOCHEMICAL-COMPOSITION AND ORGANIZATION OF HIGHER-PLANT PHOTOSYSTEM-II LIGHT-HARVESTING PIGMENT-PROTEINS. Journal of Biological Chemistry **266,** 16745-16754.

Ruban, A.V. (2016). Nonphotochemical Chlorophyll Fluorescence Quenching: Mechanism and Effectiveness in Protecting Plants from Photodamage. Plant Physiology **170,** 1903-1916.

Ruban, A.V., Johnson, M.P., and Duffy, C.D.P. (2012). The photoprotective molecular switch in the photosystem II antenna. Biochimica Et Biophysica Acta-Bioenergetics **1817,** 167-181.

Ruban, A.V., Wentworth, M., Yakushevska, A.E., Andersson, J., Lee, P.J., Keegstra, W., Dekker, J.P., Boekema, E.J., Jansson, S., and Horton, P. (2003). Plants lacking the main light-harvesting complex retain photosystem II macro-organization. Nature **421,** 648-652.

Schagger, H., and Vonjagow, G. (1991). BLUE NATIVE ELECTROPHORESIS FOR ISOLATION OF MEMBRANE-PROTEIN COMPLEXES IN ENZYMATICALLY ACTIVE FORM. Analytical Biochemistry **199,** 223-231.

Schagger, H., Cramer, W.A., and Vonjagow, G. (1994). ANALYSIS OF MOLECULAR MASSES AND OLIGOMERIC STATES OF PROTEIN COMPLEXES BY BLUE NATIVE ELECTROPHORESIS AND ISOLATION OF MEMBRANE-PROTEIN COMPLEXES BY 2-DIMENSIONAL NATIVE ELECTROPHORESIS. Analytical Biochemistry **217,** 220-230.

Scheres, S.H.W. (2012). RELION: Implementation of a Bayesian approach to cryo-EM structure determination. Journal of Structural Biology **180,** 519-530.

Seddon, A.M., Curnow, P., and Booth, P.J. (2004). Membrane proteins, lipids and detergents: not just a soap opera. Biochimica Et Biophysica Acta-Biomembranes **1666,** 105-117.

Semenova, G.A. (1995). PARTICLE REGULARITY ON THYLAKOID FRACTURE FACES IS INFLUENCED BY STORAGE-CONDITIONS. Canadian Journal of Botany-Revue Canadienne De Botanique **73,** 1676-1682.

Shen, J.R. (2015). The Structure of Photosystem II and the Mechanism of Water Oxidation in Photosynthesis. Annual Review of Plant Biology, Vol 66 **66,** 23-48.

Shi, L.X., and Schroder, W.P. (2004). The low molecular mass subunits of the photosynthetic supracomplex, photosystem II. Biochimica Et Biophysica Acta-Bioenergetics **1608,** 75-96.

Shikanai, T. (2007). Regulation of photosynthesis via PSI cyclic electron transport. Photosynthesis Research **91,** 246-246.

Shikanai, T. (2016). Chloroplast NDH: A different enzyme with a structure similar to that of respiratory NADH dehydrogenase. Biochimica Et Biophysica Acta-Bioenergetics **1857,** 1015-1022.

Shinozaki, K., Ohme, M., Tanaka, M., Wakasugi, T., Hayashida, N., Matsubayashi, T., Zaita, N., Chunwongse, J., Obokata, J., Yamaguchishinozaki, K., Ohto, C., Torazawa, K., Meng, B.Y., Sugita, M., Deno, H., Kamogashira, T., Yamada, K., Kusuda, J., Takaiwa, F., Kato, A., Tohdoh, N., Shimada, H., and Sugiura, M. (1986). THE COMPLETE NUCLEOTIDE-SEQUENCE OF THE TOBACCO CHLOROPLAST GENOME - ITS GENE ORGANIZATION AND EXPRESSION. Embo Journal **5,** 2043-2049.

Simpson, D.J. (1978). FREEZE-FRACTURE STUDIES ON BARLEY PLASTID MEMBRANES .2. WILD-TYPE CHLOROPLAST. Carlsberg Research Communications **43,** 365-389.

Sorzano, C.O.S., Marabini, R., Velazquez-Muriel, J., Bilbao-Castro, J.R., Scheres, S.H.W., Carazo, J.M., and Pascual-Montano, A. (2004). XMIPP: a new generation of an open-source image processing package for electron microscopy. Journal of Structural Biology **148,** 194-204.

Standfuss, R., van Scheltinga, A.C.T., Lamborghini, M., and Kuhlbrandt, W. (2005). Mechanisms of photoprotection and nonphotochemical quenching in pea light-harvesting complex at 2.5A resolution. Embo Journal **24,** 919-928.

Tietz, S., Puthiyaveetil, S., Enlow, H.M., Yarbrough, R., Wood, M., Semchonok, D.A., Lowry, T., Li, Z., Jahns, P., Boekema, E.J., Lenhert, S., Niyogi, K.K., and Kirchhoff, H. (2015). Functional Implications of Photosystem II Crystal Formation in Photosynthetic Membranes. Journal of Biological Chemistry **290,** 14091-14106.

Umena, Y., Kawakami, K., Shen, J.R., and Kamiya, N. (2011). Crystal structure of oxygen-evolving photosystem II at a resolution of 1.9 angstrom. Nature **473,** 55-U65.

van Oort, B., Alberts, M., de Bianchi, S., Dall'Osto, L., Bassi, R., Trinkunas, G., Croce, R., and van Amerongen, H. (2010). Effect of Antenna-Depletion in Photosystern II on Excitation Energy Transfer in Arabidopsis thaliana. Biophysical Journal **98,** 922-931.

vanHeel, M., Harauz, G., Orlova, E.V., Schmidt, R., and Schatz, M. (1996). A new generation of the IMAGIC image processing system. Journal of Structural Biology **116,** 17-24.

Varotto, C., Pesaresi, P., Jahns, P., Lessnick, A., Tizzano, M., Schiavon, F., Salamini, F., and Leister, D. (2002). Single and double knockouts of the genes for photosystem I subunits G, K, and H of Arabidopsis. Effects on photosystem I composition, photosynthetic electron flow, and state transitions. Plant Physiology **129,** 616-624.

Wei, X.P., Su, X.D., Cao, P., Liu, X.Y., Chang, W.R., Li, M., Zhang, X.Z., and Liu, Z.F. (2016). Structure of spinach photosystem II-LHCII supercomplex at 3.2 angstrom resolution. Nature **534,** 69-+.

Wientjes, E., Oostergetel, G.T., Jansson, S., Boekema, E.J., and Croce, R. (2009). The Role of Lhca Complexes in the Supramolecular Organization of Higher Plant Photosystem I. Journal of Biological Chemistry **284,** 7803-7810.

Wientjes, E., Drop, B., Kouril, R., Boekema, E.J., and Croce, R. (2013). During State 1 to State 2 Transition in Arabidopsis thaliana, the Photosystem II Supercomplex Gets Phosphorylated but Does Not Disassemble. Journal of Biological Chemistry **288,** 32821-32826.

Wittig, I., and Schagger, H. (2005). Advantages and limitations of clear-native PAGE. Proteomics **5,** 4338-4346.

Wittig, I., Karas, M., and Schaegger, H. (2007). High resolution clear native electrophoresis for In-gel functional assays and fluorescence studies of membrane protein complexes. Molecular & Cellular Proteomics **6,** 1215-1225.

Wollman, F.A. (2001). State transitions reveal the dynamics and flexibility of the photosynthetic apparatus. Embo Journal **20,** 3623-3630.

Yakushevska, A.E., Jensen, P.E., Keegstra, W., van Roon, H., Scheller, H.V., Boekema, E.J., and Dekker, J.P. (2001a). Supermolecular organization of photosystem II and its associated light-harvesting antenna in Arabidopsis thaliana. European Journal of Biochemistry **268,** 6020-6028.

Yakushevska, A.E., Keegstra, W., Boekema, E.J., Dekker, J.P., Andersson, J., Jansson, S., Ruban, A.V., and Horton, P. (2003). The structure of photosystem II in Arabidopsis: Localization of the CP26 and CP29 antenna complexes. Biochemistry **42,** 608-613.

Yakushevska, A.E., Ruban, A.V., Jensen, P.E., Keegstra, W., van Roon, H., Niyogi, K.K., Scheller, H.V., Horton, P., Dekker, J.P., and Boekema, E.J. (2001b). Supermolecular organization of photosystem II and its associated light-harvesting antenna in the wild-type and npq4 mutant of Arabidopsis thaliana. Photosynthesis Research **69,** 52-52.

Yamamoto, H., Peng, L.W., Fukao, Y., and Shikanai, T. (2011). An Src Homology 3 Domain-Like Fold Protein Forms a Ferredoxin Binding Site for the Chloroplast NADH Dehydrogenase-Like Complex in Arabidopsis. Plant Cell **23,** 1480-1493.

Yamori, W., Shikanai, T., and Makino, A. (2015). Photosystem I cyclic electron flow via chloroplast NADH dehydrogenase-like complex performs a physiological role for photosynthesis at low light. Scientific Reports **5**.

Zhang, S.P., and Scheller, H.V. (2004). Light-harvesting complex II binds to several small Subunits of photosystem I. Journal of Biological Chemistry **279,** 3180-3187.

Zouni, A., Witt, H.T., Kern, J., Fromme, P., Krauss, N., Saenger, W., and Orth, P. (2001). Crystal structure of photosystem II from Synechococcus elongatus at 3.8 angstrom resolution. Nature **409,** 739-743.

Summary of doctoral thesis

Structural characterization of photosynthetic supercomplexes in plants

Lukáš Nosek

Department of Biophysics

Centre of the Region Haná for Biotechnological and Agricultural Research

Faculty of Science, Palacký University Olomouc, Czech Republic

Olomouc 2016

Dizertační práce byla vypracována během prezenčního doktorského studia programu Fyzika, oboru Biofyzika, na Katedře Biofyziky Přírodovědecké fakulty Univerzity Palackého v Olomouci v období 2012 – 2016.

Uchazeč: Mgr. Lukáš Nosek

Školitel: RNDr. Roman Kouřil, Ph.D.
Univerzita Palackého v Olomouci
Přírodovědecká fakulty, Katedra Biofyziky
Šlechtitelů 27, 771 46 Olomouc

Oponenti: prof. RNDr. Josef Komenda, DSc.
Mikrobiologický ústav AV ČR, v.v.i.
Centrum ALGATECH
Novohradská 237, 379 81 Třeboň

Dr. Stefano Caffarri
Laboratoire de Genetique et Biophysique des Plantes
Universite dAix-Marseille
Faculte des Sciences, 3 place Victor Hugo, Case G
13331 Marseille cedex 3

Obhajoba dizertační práce se koná dne:

S plným textem dizertační práce a oponentskými posudky je možné se seznámit na studijním oddělení Přírodovědecké fakulty Univerzity Palackého v Olomouci

Content

Shrnutí 1
1. Introduction 2
Structure of Photosystems I and II 3
Photosystem I 3
Subunit composition of plant Photosystem I core complex 4
Light-harvesting complex of Photosystem I 6
Photosystem I involved in formation of larger assemblies 8
Photosystem I supercomplexes involved in state transitions 8
Oligomeric forms of Photosystem I 10
PSI-NDH supercomplex 11
Photosystem II 13
Subunit composition of Photosystem II core complex 13
Light-harvesting complex of Photosystem II 15
Structural characterization of the plant PSII-LHCII supercomplex 18
Larger assemblies of Photosystem II 21
Two-dimensional crystals of Photosystem II 21
Megacomplexes of Photosystem II 23
Experimental techniques 24
CN-PAGE 24
Single particle electron microscopy 27
2. Summary 30
3. Experimental approach 32
Methods 32
Plant material 32
Isolation and solubilization of thylakoid and PSII enriched membranes 32
CN-PAGE 33
Gel imaging 33
Electron microscopy and image analysis 33
Optimization of separation method for structural characterization of photosynthetic supercomplexes and megacomplexes 34
Isolation of the PSI-NDH supercomplex 34
Selection of plant material and optimization of solubilization 34
Isolation of PSII megacomplexes from *Arabidopsis thaliana* 41
Optimization of separation conditions for a structural characterization of spruce PSII supercomplex 42
Specimen preparation 44
Single particle Image analysis 47
4. Conclusions 49
5. References 50

List of Publications

Published:

Kouřil R, Strouhal O, Nosek L, Lenobel R, Chamrád I, Boekema EJ, Šebela M and Ilík P. Structural characterization of a plant photosystem I and NAD(P)H dehydrogenase supercomplex. *Plant Journal* **77**: 568–576, (2014).

Kouřil R, Nosek L, Bartoš J, Boekema EJ and Ilík P. Evolutionary loss of light-harvesting proteins Lhcb6 and Lhcb3 in major land plant groups – break-up of current dogma. *New Phytologist* **210**: 808-814, (2016).

Accepted:

Nosek L, Semchonok D, Boekema EJ, Ilík P and Kouřil R. Structural variability of plant photosystem II megacomplexes in thylakoid membranes. *Plant Journal*, (2016) (doi: 10.1111/tpj.13325).

Acknowledgements

I would like to thank my supervisor Dr. Roman Kouřil for his friendly and patient guidance and help during my entire doctoral studies and prof. Petr Ilík for his inspiring ideas.

Furthermore, I would like to express my thanks to all colleagues from the Department of Biophysics for creating a pleasant and kind environment.

Special thanks belong to Ondřej Strouhal for a very beneficial collaboration at the beginning of my Ph.D. study.

This work was financially supported by the Grant Agency of the Czech Republic (project 13-2809S/P501) and by the Ministry of Education, Youth and Sports of the Czech Republic (projects ED0007/01/01 to Centre of the Region Haná for Biotechnological and Agricultural Research, CZ.1.07/2.3.00/20.0057 and LO1204 - Sustainable development of research in the Centre of the Region Haná).

Shrnutí

Ve své dizertační práci jsem se věnoval optimalizaci izolace a strukturní charakterizaci rostlinných fotosyntetických superkomplexů pomocí transmisní elektronové mikroskopie, která ve spojení s obrazovou analýzou poskytuje strukturní informace o studovaném komplexu.

Mezi hlavní studované objekty patřily superkomplexy fotosystému 1 (PSI) a fotosystému 2 (PSII). V obou případech se jedná o velké pigment-proteinové superkomplexy tvořené mnoha podjednotkami, jejichž hlavním úkolem je transformace absorbované světelné energie na energii chemickou. Tyto superkomplexy nejsou v rostlině přítomny volně, ale jsou vázané v thylakoidní membráně chloroplastů. Zmíněné superkomplexy mohou navíc asociovat s dalšími proteinovými komplexy thylakoidní membrány, případně i mezi sebou navzájem a vytvářet tak velké megakomplexy.

Jedním z takových příkladů je tzv. PSI-NDH supercomplex, který představuje asociaci mezi PSI a NDH a jehož existence byla již dříve předpovězena na základě různých biochemických analýz. V disertační práci je detailně popsána jeho strukturní charakterizace pomocí elektronové mikroskopie. Důležitým krokem předcházejícím samotné strukturní charakterizaci byla optimalizace podmínek pro izolaci zmíněného komplexu v dostatečné kvantitě i kvalitě. Optimalizace zahrnovala volbu vhodného rostlinného materiálu, který obsahoval dostatečné množství PSI-NDH superkomplexu a dále také výběr vhodného detergentu, který by účinně a šetrně superkomplex z thylakoidních membrán solubilizoval. Solubilizované thylakoidní membrány z ječmene jarního byly poté separovány pomocí bezbarvé nativní polyakrylamidové gelové elektroforézy (CN-PAGE), optimalizované pro separaci vysokomolekulárních komplexů. Strukturní analýza izolovaného PSI-NDH superkomplexu odhalila prvotní informace o jeho specifické organizaci a schopnosti NDH komplexu vázat dva komplexy PSI.

Během optimalizace izolačních podmínek za účelem zisku dostatečného množství PSI-NDH superkomplexu byly v CN-PAGE detekovány další proteinové pásy s komplexy o velmi vysoké molekulové hmotnosti. Následná strukturní analýza, která je v dizertační práci detailně popsána, ukázala, že zmíněný pás obsahoval několik typů megakomplexů tvořených dvěma PSII superkomplexy. Tyto megakomplexy tvořily dvě skupiny, ve kterých PSII superkomplexy interagovaly buď paralelně, nebo neparalelně. Megakomplexy s paralelně interagujícími fotosystémy byly objeveny již dříve, nicméně strukturní charakterizace megakomplexů s neparalelně interagujícími fotosystémy prezentovaná v dizertační práci byla provedena vůbec poprvé. Detekce PSII megakomplexů na úrovni izolované thylakoidní membrány indikuje jejich fyziologický význam a je předmětem dalšího výzkumu.

Dalším studovaným objektem byl PSII superkomplex izolovaný ze smrku ztepilého. Smrk je zástupce nahosemenných rostlin, čeledi borovicovitých, a struktura prezentovaná v dizertační práci představuje úplně první strukturální studii PSII superkomplexu provedenou na zástupci zmíněné rostlinné skupiny. Strukturní analýza v kombinaci s genetickou analýzou vedla k nečekanému zjištění, že smrk a další zástupci čeledi borovicovitých jsou evolučně odchýleni od zbytku vyšších rostlin, což se projevilo i ve změně struktury PSII superkomplexu oproti ostatním zástupcům vyšších rostlin.

1. Introduction

Photosynthesis is a process worth of an extraordinary respect since it remarkably participates on the maintenance of suitable living conditions on the Earth. It is performed mainly by two large supercomplexes known as Photosystem I (PSI) and Photosystem II (PSII), which have been studied for a long time and still, there are many dimensions awaiting their elucidation. It is obvious that especially functional properties of any assembly depend on the structure of individual subunits, which are responsible for its overall performance.

The last few decades clearly showed that photosynthetic complexes can be successfully studied using the X-ray crystallography, which provided most of the structures at atomic resolution available today. However, the method requires a highly concentrated sample, with a maximally homogenous and pure form of a protein in order to crystallize. Any impurities or structural variabilities of the protein are undesirable. Nowadays, this technique is being gradually replaced by the state-of-the-art cryo electron microscopy, which does not demand for crystals. Nevertheless, it still requires homogenous and also concentrated specimen. These requirements are, however, very difficult to fulfil, especially in a case of fragile, transient or rare protein complexes. In this case, single particle electron microscopy of a negatively stained specimen was found to be a very convenient method. Moreover, if it is coupled with a proper separation technique like a clear native polyacrylamide gel electrophoresis (CN-PAGE), it represents a powerful tool for structural characterization of a broad range of proteins, including photosynthetic membrane proteins.

The main aim of this thesis is the structural characterization of photosynthetic supercomplexes and megacomplexes of PSI and PSII using the CN-PAGE and single particle electron microscopy. In the Introduction part, a current knowledge of the structure of main photosynthetic complexes and their larger assemblies in higher plants is summarized. The experimental part of this thesis deals with an optimization of the experimental approach, which was used for isolation of large photosynthetic supercomplexes and megacomplexes. The last part of the thesis summarizes the performed and published research.

Structure of Photosystems I and II

Photosystem I

Photosystem I is a large, pigment-binding supercomplex working as a light-driven plastocyanin:ferredoxin oxidoreductase. It is extraordinarily efficient with quantum yield close to 1 and for this, it is considered as the most effective photovoltaic machine known so far (Nelson, 2009).

Plant PSI is composed from two basic functional moieties: the central core complex and a peripheral light-harvesting complex (LHCI). Central core complex coordinates the components responsible for a light-driven electron transfer and binds chlorophyll *a* molecules, which serve for light-harvesting. LHCI, which forms a crescent-shaped belt at the periphery of PSI, significantly extends its light-harvesting capacity and its main function is the efficient supply of the core complex with excitation energy (Nelson and Ben-Shem, 2005; Nelson and Yocum, 2006; Jensen et al., 2007; Amunts and Nelson, 2008; Busch and Hippler, 2011)

Structure of plant PSI has been extensively studied by the X-ray crystallography method and the resolution and the structural information provided by this method gradually improved during the last years. The first crystal structure of plant PSI was obtained at 4.4 Å resolution (Ben-Shem et al., 2003), when positions of sixteen subunits were determined: twelve core subunits (PsaA - PsaL) and four peripheral light harvesting subunits (Lhca1-4). Although the relatively low resolution did not allow precise identification of important functional features, like interactions among subunits, it provided valuable information about the order of individual Lhca1-4 proteins attached at one side of the PSI core complex. Owing to improved crystallization conditions, the resolution could be later improved to 3.4 Å (Amunts et al., 2007) and further to 3.3 Å (Amunts et al., 2010), both revealing seventeen subunits in total. These improved models provided better insight into interactions among subunits and non-covalently bound cofactors (chlorophylls, carotenoids, Fe-S clusters and phyloquinones). Finally, the most recent plant PSI structure was obtained at 2.8 Å resolution, which refined the current information about how the non-covalently bound cofactors

interact with each other and with the protein subunits within the supercomplex (Mazor et al., 2015) (see Figure. 1).

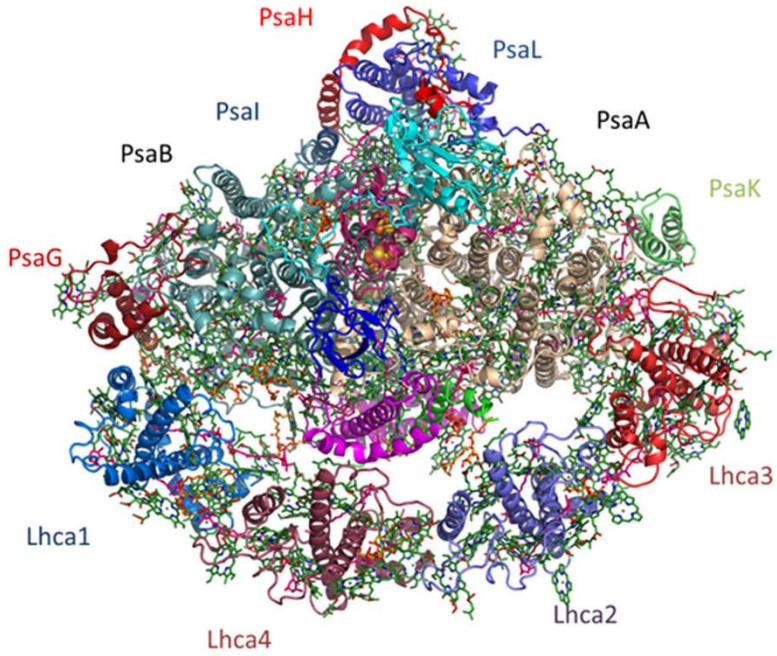

Figure 1. The most recent X-ray structure of the plant PSI-LHCI supercomplex obtained at the 2.8 Å resolution. View from the stromal side. Twelve PsaA-PsaL subunits of PSI including Lhca1-Lhca4 are depicted. PsaF and PsaJ subunits are coloured in magenta and green, respectively. PsaC, PsaD and PsaE subunits are coloured in cyan, pink and blue, respectively. Yellow and orange spheres in the middle of the complex represent Fe-S clusters. Chlorophylls in the core complex are in green, chlorophylls *a* in LHCI in cyan and LHCI chlorophylls *b* in magenta, carotenoids are in blue. Adapted from Mazor et al. (2015).

Subunit composition of plant Photosystem I core complex

The most recent X-ray structural analysis of PSI (Mazor et al., 2015) showed that the core complex is composed of twelve stably bound subunits PsaA-PsaL (coordinating 156 chlorophylls - nine of them are chlorophylls *b*, 32 carotenes and 14 lipids). Moreover, additional peripheral subunits, namely PsaN-PsaP and PsaR, were also revealed to be associated with the PSI core complex. However, PsaN subunit is only weakly bound to the PSI core and it is not considered as its stable part (Amunts et al., 2010). PsaO and PsaP are

subunits, which have not been identified yet in any crystal structure of plant PSI (reviewed in Busch and Hippler, 2011). By contrast, PsaR was identified within the crystal structure of plant PSI (Amunts et al., 2010), however its function is unclear.

PsaA and PsaB represent the largest subunits of PSI, each formed by eleven transmembrane helices with the molecular mass of 84 and 83 kDa, respectively. They form the central heterodimer, which binds P_{700} - the special chlorophyll pair responsible for light driven charge separation and also several primary electron acceptors. PsaC is a small stromal subunit with molecular mass of 9 kDa and together with PsaD (18 kDa) and PsaE (10 kDa) subunits forms a docking site for ferredoxin - a soluble electron transporter (Hayashida et al., 1987; Hoj et al., 1987). PsaF subunit with one transmembrane helix and with molecular mass of 17 kDa binds plastocyanin, the luminal electron donor (Farah et al., 1995) and was shown to be essential for transition of excitation energy from LHCI to PSI core complex (Haldrup et al., 2000). PsaG (11 kDa) and PsaK (9 kDa) are plant specific subunits with two transmembrane helices and play a role in stabilizing of the whole PSI supercomplex (Varotto et al., 2002) and in binding of LHCI to PSI (Ben-Shem et al., 2003). PsaH (11 kDa), PsaL (18 kDa) and PsaO (10 kDa) form a peripheral cluster responsible for interaction of PSI with phosphorylated LHCII, the light-harvesting complexes of PSII (Lunde et al., 2000; Jensen et al., 2004; Zhang and Scheller, 2004) and possibly also PsaI (4 kDa) and PsaP (indistinct mass) subunits may be involved in binding of LHCII to PSI (Zhang and Scheller, 2004). Moreover, PsaL subunit plays a significant role in formation of trimeric PSI assemblies in cyanobacteria (Chitnis and Chitnis, 1993; Jordan et al., 2001) and in plants, this PsaL function is eliminated by a plant-specific PsaH subunit (Ben-Shem et al., 2003). PsaJ (6 kDa) and PsaN (10 kDa) are one transmembrane helix subunits required for formation of the plastocyanin binding domain (Fischer et al., 1999; Haldrup et al., 1999). PsaR is a small, peripheral, one transmembrane helix subunit containing large amount of adenines (Amunts et al., 2010) and there is no biochemical evidence for its role. Therefore, it remains unclear whether it is a stable and functional part of PSI. The subunits of plant PSI and their function are summarized in Table 1.

Table 1. Subunit composition of a plant PSI core complex with subunits functions and bound cofactors.

Subunit name	Mass (kDa)	Gene location	Function
PsaA	84	chloroplast	Light harvesting, charge separation, electron transport, coordination of P_{700}, A_0, A_1 and F_X, binding of 80 chlorophylls, Lhca binding
PsaB	83	chloroplast	
PsaC	9	chloroplast	Coordination of F_A and F_B, ferredoxin binding
PsaD	18	nucleus	ferredoxin binding
PsaE	10	nucleus	ferredoxin binding
PsaF	17	nucleus	plastocyanin binding, Lhca4 binding
PsaG	11	nucleus	PSI stabilization, Lhca1 binding
PsaH	11	nucleus	LHCII binding, prevention of PSI trimerization
PsaI	4	chloroplast	LHCII binding (?)
PsaJ	6	chloroplast	plastocyanin binding, Lhca2 binding
PsaK	9	nucleus	PSI stabilization, Lhca3 binding, LHCII binding
PsaL	18	nucleus	LHCII binding
PsaN	10	nucleus	plastocyanin binding
PsaO	10	nucleus	LHCII binding (?)
PsaP	-	nucleus	LHCII binding (?)
PsaR	-	-	-

Light-harvesting complex of Photosystem I

The main function of LHCI is to provide sufficient amount of energy into the reaction centre of PSI. Plant PSI relies on a nuclear encoded light-harvesting complex composed of six chlorophyll binding proteins Lhca1-6 (Jansson, 1999). The Lhca1-4 proteins are evenly expressed and form two heterodimers assembled into a curved belt at the PsaF/PsaJ side of the PSI reaction centre (Boekema et al., 2001; Ben-Shem et al., 2003; Amunts et al., 2007; Amunts et al., 2010). The composition of heterodimers and their position towards the reaction centre is not random. The first dimer is composed of Lhca1 and Lhca4 proteins and interacts with PSI core complex via PsaG and PsaB subunits (Lhca1) and via PsaF subunit (Lhca4). The other dimer is formed by Lhca2 and Lhca3 proteins. Lhca2 associates with PSI core complex via PsaA and PsaJ and Lhca3 interacts via PsaA and PsaK (Jansson et al., 1996;

Ben-Shem et al., 2003; Amunts et al., 2007; Amunts et al., 2010; Mazor et al., 2015). The individual Lhca proteins in the PSI-LHCI supercomplex are not mutually interchangeable, as it was shown on mutants lacking individual Lhca subunits (Wientjes et al., 2009). That analysis showed that missing Lhca protein leaves an empty space in the supercomplex structure. This indicates that binding of individual Lhca proteins to the PSI core complex is highly specific, only with the exception of Lhca4 subunit, which can be substituted with Lhca5 subunit. The Lhca1-4 subunits also contain so-called far-red chlorophylls responsible for far red absorption and fluorescence emission (Morosinotto et al., 2003), which is a characteristic feature of the PSI (Gobets and van Grondelle, 2001).

The Lhca5-6 proteins represent subunits, which are expressed at a very low level (Klimmek et al., 2006). It means that these proteins bind to PSI in a substoichiometric amount with respect to other Lhca1-4 proteins. The exact role of Lhca5 and Lhca6 was unclear, until the mutants lacking these subunits were constructed. Analysis of plants lacking these subunits indicated their direct involvement in formation and stabilization of the PSI-NAD(P)H dehydrogenase (PSI-NDH) supercomplex (Peng et al., 2009). This analysis showed that mutants without Lhca5 and Lhca6 subunits have impaired formation of the PSI-NDH supercomplex. The general properties of Lhca1-6 proteins are summarized in Table 2.

Table 2. Subunits of plant Photosystem I light-harvesting complex with bound cofactors.

Subunit name	Mass (kDa)	Bound cofactors
Lhca1	22	13 chlorophylls, 3 carotenoids
Lhca2	23	13 chlorophylls, 2 carotenoids
Lhca3	25	13 chlorophylls, 3 carotenoids
Lhca4	22	13 chlorophylls, 2 carotenoids
Lhca5	24	13 chlorophylls, 2 carotenoids
Lhca6	25	-

Photosystem I involved in formation of larger assemblies

Plant PSI predominantly exists in the monomeric form in the thylakoid membrane (Kouril et al., 2005a). Nevertheless, this supercomplex also tends to form larger assemblies with other protein complexes like Cytb6f complex (Iwai et al., 2010), LHCII (Kouril et al., 2005b), and NDH complex (Kouril et al., 2014). Moreover, PSI can associate even with each other and form oligomers as have been shown in several electron microscopy studies (Boekema et al., 2001; Kouril et al., 2005a). Thus, the following paragraphs will briefly describe those larger PSI associations: supercomplexes involved in so-called state transitions, PSI oligomers and PSI-NDH supercomplex.

Photosystem I supercomplexes involved in state transitions

State transitions is a mechanism, by which plants balance the distribution of excitation energy between PSII and PSI upon changing light conditions (reviewed e.g. in Allen, 1992; Wollman, 2001).

Upon light conditions, when PSII is preferentially excited, over-reduction of plastoquinone and the cytochrome b_6f complex occurs. This over-reduction serves as a signal for plant kinases STN7 and STN8, which phosphorylate light-harvesting complex of PSII (LHCII) and some proteins of the PSII core complex (Bennett et al., 1980; Bellafiore et al., 2005; Bonardi et al., 2005). Once phosphorylated, LHCII dissociates from PSII and associates with PSI to form PSI-LHCI-LHCII supercomplex (state 2). Effect of this transition is in lowering of excitation pressure to PSII and in increased excitation of PSI. The whole process is reversible. When the pool of plastoquinone becomes oxidized, LHCII is dephosphorylated and migrates back to PSII (state 1) (Forsberg and Allen, 2001). In the state transitions, PsaH subunit plays a significant role. LHCII cannot transfer the excitation energy to PSI and the state transitions are impaired if the PsaH subunit is missing (Lunde et al., 2000).

Despite there was ample functional evidence for state transitions, the structure of the PSI-LHCI-LHCII supercomplex was obscured for a long time. Its structure was for the first time demonstrated in *Arabidopsis thaliana* by Kouřil et al. (2005), which was long time after discovery of state transitions (Bonavent.C and Myers, 1969; Murata, 1969; Bennett, 1977).

This time delay was caused by the difficulty to purify the supercomplex with a sufficient yield due to its fragility and instability. It was shown that LHCII trimer together with PSI-LHCI supercomplex form a pear-shaped structure and that LHCII is to PSI attached at the PsaH side (Fig. 2). Origin of the LHCII trimer migrating towards PSI was also investigated and still remains the matter of debate. For instance, it was proposed that it may originate in the M trimer dissociating from the PSII supercomplex (Kouril et al., 2005b). Nevertheless, taking into consideration that M trimer specific subunit Lhcb3 (Caffarri et al., 2009) is not present in stromal thylakoids (Bassi et al., 1988), the M trimer in most probably not involved in state transitions. Further, it was also proposed that LHCII trimer, which associate with PSI during state transitions, may originate also in a specific subset of LHCII weakly bound to PSII supercomplex (Galka et al., 2012) or in the pool of free LHCII (Wientjes et al., 2013). Structure of PSI-LHCI-LHCII supercomplex is illustrated in Figure 2.

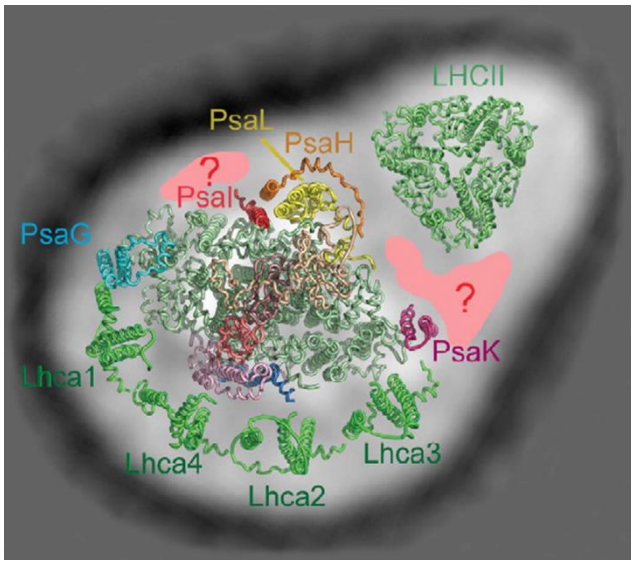

Figure 2. Structure of the plant PSI-LHCI-LHCII supercomplex. Supercomplex is formed by PSI with attached LHCI and trimeric LHCII. The question marked areas represent the unassigned densities probably occupied by some additional subunits. Stromal side view. Adapted from Jensen et al. (2007).

Oligomeric forms of Photosystem I

Electron microscopy analysis of mildly solubilized, chromatographically or electrophoretically purified thylakoid membranes also showed that PSI tends to form larger oligomeric forms like dimers, trimers and even tetramers.

The first structure of PSI oligomers was reported in the thermophilic cyanobacterium *Synechococcus* (Boekema et al., 1987). Nevertheless, there was a question whether these PSI trimers represent native arrangements or an artificial association between solubilized PSI complexes. No details regarding the interactions between individual PSI supercomplexes could be concluded due to the limited resolution of trimers. Thus, as the individual PSI supercomplexes in trimers were rotationally symmetrical, this was taken as the main evidence of their nativity. Later, the formation of PSI trimers in *Synechococcus* was confirmed using the X-ray analysis (Jordan et al., 2001). This study also revealed that the trimerization domain is formed of PsaL, as the individual PSI interact via these subunits.

A search for similar PSI associations in plants was also performed (Boekema et al., 2001). In that study, PSI dimers, trimers and tetramers were discovered in pea thylakoid membranes mildly solubilized by α-dodecyl maltoside. However, as the electron microscopy analysis showed, all found PSI oligomers represented artificial assemblies probably created as the artefact of solubilization. The individual PSI supercomplexes in the PSI oligomers had mirror symmetry and different handedness, which certainly does not reflect the situation in the native membrane. Comparable research was repeated later with digitonin as the detergent and similar dimeric, trimeric and tetrameric PSI structures were discovered (Kouril et al., 2005a). Regrettably, results of this electron microscopic analysis agreed with the former findings, i.e. that the found plant PSI oligomers likely represent artificial associations. Based on these results, it was concluded that native plant PSI exists in monomeric form. The trimerization of plant PSI is moreover hindered by the PsaH subunit (Ben-Shem et al., 2003), which shields the PsaL subunits responsible for PSI trimerization in cyanobacteria (Chitnis and Chitnis, 1993). Presence of PsaH in plant PSI is important as it enables association of plant PSI with LHCII during state transitions (Lunde et al., 2000). Examples of plant PSI oligomers are shown in Figure 3.

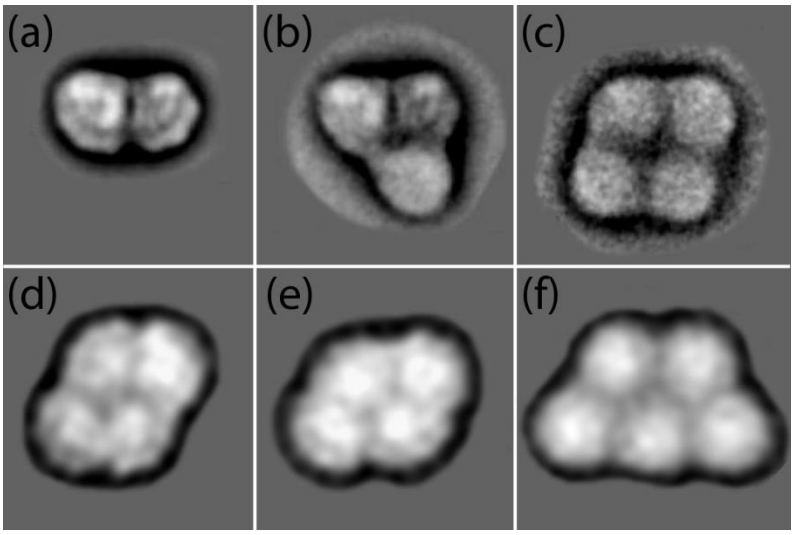

Figure 3. Plant PSI oligomers. (a-c) Artificial plant PSI oligomers as published by Boekema et al., (2001); a: PSI dimer composed of two up and down oriented monomers; b: PSI trimer, where two monomers have the same orientation as in dimer, next monomer is associated at different position; c: PSI tetramer formed as dimer of dimers. (d-f) Plant PSI oligomers discovered during optimization of native separation technique (Experimental approach chapter, unpublished data); d, e: PSI tetramers; f: PSI pentamer.

PSI-NDH supercomplex

The PSI-NDH supercomplex represents the assembly of PSI with NAD(P)H dehydrogenase and its native structure was revealed recently with a significant contribution of our group (chapter 4.1).

NDH complex is localized in stromal thylakoids and its existence was firstly suggested after tobacco and liverwort *Marchantia polymorpha* chloroplast genome sequencing (Ohyama et al., 1986; Shinozaki et al., 1986). It is involved in one of the pathways of cyclic electron flow (CET) around PSI (known as NDH-dependent pathway), which is essential for preventing of stroma over-reduction and also contributes to balancing of ATP and NADPH production (Shikanai, 2007). Thus, association of NDH with PSI seems to be beneficial for execution of these functions.

The plant NDH complex is composed of more than 20 subunits. It can be divided into five subcomplexes: A and B subcomplexes, EDB (electron donor binding), membrane and lumen subcomplexes (Peng et al., 2011; Shikanai, 2016) and shares a homology with

mitochondrial respiratory complex I (Efremov et al., 2010). Membrane subcomplex contains NdhA-NdhG subunits, subcomplex A contains NdhH-NdhO subunits, subcomplex B contains NDF1, NDF2, NDF4, NDF6 and NDH18 subunits and lumen subcomplex is composed of PPL2, CYP20-2, FKBP16-2 and PQL subunits. Nevertheless, exact function of all these subunits is still not fully clarified. EDB subcomplex represents recently discovered moiety of NDH and consists of NdhT, NdhU and NdhS subunits (Yamamoto et al., 2011). These subunits are suggested to form a ferredoxin binding site. Due to the fact that NDH binds ferredoxin, the chloroplast NDH may be reconsidered to be an ferredoxin dependent plastoquinone reductase, instead of generally accepted NAD(P)H dehydrogenase.

Existence of the PSI-NDH supercomplex was firstly evidenced in 2008 (Peng et al., 2008). Authors electrophoretically separated mildly solubilized *Arabidopsis thaliana* thylakoid membranes and discovered a high molecular weight band, which was after subjection to biochemical analysis attributed to association of PSI with NDH. Later, it was shown that association with Lhca5 and Lhca6 minor antenna is required for the efficient operation of the PSI-NDH supercomplex using the mutants lacking these Lhca subunits (Peng et al., 2009). The NDH complex is also stabilized by interaction with PSI especially under stress conditions (Peng and Shikanai, 2011). A structural model of PSI-NDH supercomplex with two copies of PSI attached to one copy of NDH was also proposed (Peng et al., 2011). Nevertheless, no structural evidence was available. There is also a recent indication that NDH-dependent CET might play a role in the regulation of photosynthetic redox state at low light condition (Yamori et al., 2015).

In our work (chapter 4.1), we provided the first structural characterization of the PSI-NDH supercomplex. We used mildly solubilized barley thylakoid membranes separated by native electrophoresis and band corresponding to PSI-NDH was structurally characterized by electron microscopy and image analysis. Our results correspond with previous propositions, as we revealed one NDH complex interacting with two copies of PSI. Also a minor form with only one PSI copy was discovered, but this was attributed to dissociation of the complete supercomplex during sample preparation. Fitting of crystal structures of PSI and NDH (or its analogue – respiratory complex I, respectively (Baradaran et al., 2013)) into the electron

microscopy projection map of PSI-NDH supercomplex indicated subunits involved in mutual interaction between PSI and NDH. This model proposes that while all Lhca1-4 subunits to some extent participate in the interaction, only NdhA-G subunits of the membrane NDH subcomplex are involved in the interaction. The model also shows some unassigned densities in the PSI-NDH supercomplex, which likely correspond to attached Lhca5 or Lhca6 antennas.

In the PSI-NDH supercomplex, the ferredoxin reduced at the acceptor side of PSI passes to NDH, where it reduces plastoquinone. Reduced plastoquinone then transfers electrons back to PSI via cytochrome b_6f complex and the cyclic pathway is completed. Ferredoxin can be alternatively reduced by NAD(P)H through the reverse reaction of FNR (ferredoxin:NAD(P)H oxidoreductase), which can associate with NDH (Hu et al., 2013). For more structural and functional details, see chapter 4.1.

Photosystem II

Photosystem II is a large, multisubunit pigment-protein supercomplex embedded in grana regions of thylakoid membranes and it works as a light-driven water:plastoquinone oxidoreductase with high quantum yield around 0.85 (Nelson and Ben-Shem, 2004). In plants, it consists of two functional moieties: the PSII core complex, which is usually present as a dimer (C_2) and a peripheral light harvesting complex (LHCII), formed by monomers or trimers of specific light harvesting proteins.

Subunit composition of Photosystem II core complex

The most recent cryo electron microscopy structural analysis of the plant PSII supercomplex (Wei et al., 2016) showed a detailed architecture of the PSII core complex. It consists of four large intrinsic subunits (PsbA (D1), PsbB (CP47), PsbC (CP43), PsbD (D2)), twelve small subunits (PsbE-F, PsbH, PsbI-M, PsbTc, PsbW, PsbX, PsbZ) and four extrinsic, lumen exposed subunits (PsbO-Q, PsbTn).

The central part of plant PSII core complex is formed by large D1, D2, CP43 and CP47 subunits. D1 and D2 subunits form central heterodimer, which constitutes the photochemical reaction centre P_{680} and where light driven charge separation takes place. Both D1 and D2 are formed by five helices of molecular mass 39 kDa and bind six chlorophyll *a* molecules and two pheophytins. CP43 and CP47 are six helix subunits with mass of 43 and 47 kDa. They fulfil the function of inner antenna, which means that they participate in light harvesting and coordinate 14 and 16 chlorophyll *a* molecules, respectively. These subunits also play an important role in energy transfer from outer light harvesting complex into the reaction centre. Moreover, it was shown that D1 together with CP43 are involved in coordinating of manganese cluster in oxygen evolving complex (Wei et al., 2016).

The group of twelve small subunits can be divided into stromal exposed ones (PsbE, PsbF, PsbH, PsbJ and PsbL) and lumen exposed ones (PsbI, PsbK, PsbM, PsbTc, PsbW, PsbX and PsbZ). All those subunits do not bind any pigment molecule and are present as one helical proteins only, with the exception of double helix PsbZ subunit. They pursue several functions, i.e. enhance dimerization of core complexes (PsbL, PsbM, PsbTc), stabilize the core complex (PsbE, PsbF, PsbJ, PsbK and PsbX), mediate association of outer light harvesting complex (PsbH, PsbW and PsbZ) and bind cytochrome b_{559} (PsbE, PsbF) (Shi and Schroder, 2004; Wei et al., 2016).

PsbO, PsbP, PsbQ represent extrinsic, lumen exposed subunits with molecular masses of 33, 20 and 17 kDa constituting a heterotrimeric assembly known as oxygen evolving complex. This complex coordinates a $Mn_4CaO_5^-$ cluster, which is responsible for water oxidation. Electrons released from oxidized water molecule are forwarded to electron transport chain and molecular oxygen is released to the environment (Umena et al., 2011; Wei et al., 2016). Function of PsbTn (5 kDa) is not clarified (Shi and Schroder, 2004). The basic properties of plant PSII subunits are summarized in Table 3.

Table 3. Subunit composition of plant Photosystem II core complex with subunits functions and bound cofactors.

Subunit name	Mass (kDa)	Gene location	Function
D1	39	chloroplast	Charge separation, electron transport, chlorophyll *a*, pheophytin and electron transport chain cofactors coordination
D2	39	chloroplast	
CP43	43	chloroplast	Light harvesting, chlorophyll *a* binding
CP47	47	chloroplast	
PsbE	9	chloroplast	Core complex stabilization or dimerization
PsbF	4	chloroplast	Core complex stabilization or dimerization
PsbH	8	chloroplast	Association of core complex with LHCII
PsbI	4	chloroplast	Core complex stabilization or dimerization
PsbJ	4	chloroplast	Core complex stabilization or dimerization
PsbK	4	chloroplast	Core complex stabilization or dimerization
PsbL	4	chloroplast	Core complex stabilization or dimerization
PsbM	4	chloroplast	Core complex stabilization or dimerization
PsbTc	4	chloroplast	Core complex stabilization or dimerization
PsbW	6	chloroplast	Association of core complex with LHCII
PsbX	4	chloroplast	Core complex stabilization or dimerization
PsbZ	7	chloroplast	Association of core complex with LHCII
PsbO	33	nucleus	Oxygen evolving complex
PsbP	20	nucleus	Oxygen evolving complex
PsbQ	17	nucleus	Oxygen evolving complex
PsbTn	5	nucleus	-

Light-harvesting complex of Photosystem II

Light harvesting complex of PSII (LHCII) is formed by different types of antenna proteins, which specifically associate at the periphery of the PSII core dimer. It fulfils several important tasks: it is responsible for a light harvesting and transfer of excitation energy to the reaction centre and it plays a crucial role in photoprotection of PSII against excessive light and photooxidative damage (Niyogi, 2000; Ruban et al., 2012; Ruban, 2016).

In plants, LHCII is composed of eight nuclear encoded pigment protein complexes named Lhcb1 – Lhcb8 (Ballottari et al., 2012). They are formed by three transmembrane helices and coordinate chlorophylls *a*, chlorophylls *b* and carotenoids in different ratios. Based on their occurrence, they can be generally divided into three subclasses.

First subclass is formed by Lhcb1 – Lhcb3 proteins, which usually occur in the ratio of about 8:3:1 (Jansson, 1994) and represents so-called major antenna proteins. These proteins associate into homotrimers (composed of Lhcb1 or Lhcb2) or into heterotrimers (composed of Lhcb1, Lhcb2 and Lhcb3) and share in their structure a typical "WYGPDR" trimerization motif (Jansson, 1999). Detailed information about the architecture of the LHCII trimer is available from X-ray structure (Liu et al., 2004; Standfuss et al., 2005). Trimers associate with dimeric PSII core complex into larger assemblies via monomeric antenna. According to the character of the binding to the PSII core complex, the LHCII trimers were designated as "S" and "M" (Strongly and Moderately bound LHCII, respectively) (Dekker and Boekema, 2005; Kouril et al., 2012). Occasionally the core complex can associate also with "L" trimers (Loosely bound) (Boekema et al., 1999a). Single particle electron microscopy analysis of various land plant species indicates that the largest stable form of the PSII-LHCII supercomplex has a form of the $C_2S_2M_2$ supercomplex. The Lhcb3 is present exclusively in the M trimer (Dainese and Bassi, 1991) and there are some indications that Lhcb2 is more likely present in the S trimer (Caffarri et al., 2009). Lhcb1 is evenly distributed among both the trimers (Caffarri et al., 2009). Moreover, it is interesting that there are up to eight LHCII trimers per one dimeric core complex (Peter and Thornber, 1991; van Oort et al., 2010). By considering the fact that dimeric PSII core complex can bind up to six trimers (Boekema et al., 1999a), this implies that there is a pool of free LHCII in thylakoid membrane, which may play a role e.g. in additional light harvesting (van Oort et al., 2010) and state transitions (Wientjes et al., 2013).

The second group is formed by Lhcb4 (CP29), Lhcb5 (CP26) and Lhcb6 (CP24) proteins and represents so-called minor antennas. These proteins are in the PSII supercomplex present in monomeric form and they interconnect the core complex with the major trimeric LHCII (Caffarri et al., 2009). Lhcb4-6 also pursue several other functions, as it was studied on

plants lacking these subunits: Lhcb6 is essential for the M trimer binding (Caffarri et al. 2009), as only C_2S_2 supercomplexes were found in mutant lacking this subunit (Kovacs et al., 2006). Moreover, it was also shown that Lhcb6 plays a role in PSII photoprotection, as the plants lacking Lhcb6 had a significantly reduced capacity for non-photochemical quenching (de Bianchi et al., 2008). Lhcb6 was also found to be unique for land plants (Alboresi et al., 2008) and might play a role in adaptation to aerial environment. Lhcb5 is involved in supercomplex stabilization, as the amount of supercomplexes was significantly reduced in the mutant lacking Lhcb5 (Yakushevska et al., 2003; Caffarri et al., 2009). In our work (chapter 4.3) we also propose that Lhcb5 is involved in formation or stabilization of PSII megacomplexes. Moreover, it was shown that Lhcb5 may substitute Lhcb1 and Lhcb2 subunits in trimers in plants lacking these two subunits (Ruban et al., 2003). Lhcb4 was found to be essential for function and structural organization of PSII supercomplexes, as no large supercomplexes could be found in the mutant plants (Yakushevska et al., 2003; de Bianchi et al., 2011). Lack of this subunit also affects binding of S trimer and negatively influences non-photochemical quenching capacity (de Bianchi et al., 2011). A crystal structure of the Lhcb4 was solved recently (Pan et al., 2011). Minor antenna proteins also associate with major antennas into larger functional units, as it was shown on a pentameric complex composed of Lhcb4, Lhcb6 and the M trimer (Betterle et al., 2009). This unit disconnects from PSII upon illumination and re-associates with PSII during dark recovery, which was shown to be important for establishment of non-photochemical quenching.

Moreover, as we have recently demonstrated (chapter 4.2), Lhcb6 and Lhcb3 antennas are surprisingly not present in *Pinaceae* and *Gnetales*, subgroups of higher plants. Lhcb6 was considered to be plant specific subunit, which has, together with Lhcb3, evolved during transition of plants from water to land habitat. Their lack in *Pinaceae* and *Gnetales* modifies the PSII supercomplex in such a way that it resembles PSII from evolutionary older organisms and breaks the current dogma that these two subunits are essential for all land plants (for structural details and functional implications, see chapter 4.2).

The last group of plant LHCII is represented by Lhcb7 and Lhcb8, the most recently discovered subunits. Lhcb7 is structurally similar to Lhcb5 and origin of Lhcb8 is in

reclassification of Lhcb4.3, one of isoforms of CP29 (Klimmek et al., 2006). Both of them are rarely expressed, i.e. they are present in substoichiometric amount and their function remains unclear (Ballottari et al., 2012).

LHC-like proteins represent a special example of LHC proteins, from whom PsbS is worth of special interest. This is a four helix, pigment-less subunit, which plays a key role in process of non-photochemical quenching (Li et al., 2000). Recent data indicate that it associates with LHCII trimers and PSII core proteins (Gerotto et al., 2015; Correa-Galvis et al., 2016), nevertheless it is probably not a specific part of the PSII-LHCII supercomplex (Caffarri et al., 2009). It also participates on PSII-LHCII structural reorganization upon high light condition (Betterle et al., 2009; Kereiche et al., 2010; Ruban et al., 2012) and impairs formation of PSII semi crystalline arrays (Kereiche et al., 2010). The basic properties of plant PSII light harvesting proteins are summarized in Table 4.

Table 4. Subunits of plant LHCII with bound cofactors (if known exactly).

Subunit name	Mass (kDa)	Bound cofactors
Lhcb1	28	8 chl *a*, 6 chl *b*, 4 carotenoids
Lhcb2	29	
Lhcb3	29	
Lhcb4 (CP29)	31	9 chl *a*, 3 chl *b*, 1 chl *a*/*b*, 3 carotenoids
Lhcb5 (CP26)	30	8 chl *a*, 4 chl *b*, 1 chl *a*/*b*, 3 carotenoids
Lhcb6 (CP24)	28	-
Lhcb7	40	-
Lhcb8	30	-

Structural characterization of the plant PSII-LHCII supercomplex

In the last decades, a lot of effort has been put into solving a high resolution structure of the plant PSII-LHCII supercomplex. Attempts to solve a high resolution structure of a plant PSII-LHCII supercomplex using X-ray crystallography most likely failed due to the impossibility to purify the supercomplex in a homogeneous and stable form. Therefore, most

of the X-ray crystallography work has been performed on cyanobacterial PSII core complexes due to their greater stability (Zouni et al., 2001; Guskov et al., 2009; Umena et al., 2011). Due to the above-mentioned limitation, our knowledge about the architecture of the plant PSII-LHCII supercomplex comes from single particle electron microscopy studies combined with image analysis.

The first structural characterization of plant PSII with associated LHCII was obtained using mildly solubilized spinach PSII enriched membranes (Boekema et al., 1995). As the outcome, the C_2S_2 supercomplex at 25 Å resolution was obtained. Revealed structure provided the first details about organization of LHCII around PSII core complex. However, as the isolating procedures and instrumental facilities gradually improved, it was possible to achieve higher resolution of larger PSII-LHCII supercomplexes, as it is evidenced by spinach C_2S_2M and $C_2S_2M_2$ supercomplexes obtained at 16 Å resolution (Boekema et al., 1999b; Boekema et al., 1999a). A next significant step forward was achieved in 2009, when a $C_2S_2M_2$ supercomplex at 12 Å resolution was obtained from mildly solubilized *Arabidopsis thaliana* thylakoid membranes (Caffarri et al., 2009). Obtaining of PSII supercomplex structure at such high resolution enabled sufficiently precise fitting of X-ray structures of individual PSII moieties (core complex and trimeric and monomeric LHCII) into the electron microscopy projection map. The structural model further allowed characterization of mutual interactions among PSII subunits and energy transfer routes (Kouril et al., 2012). Structure of such PSII supercomplex is presented in Figure 4.

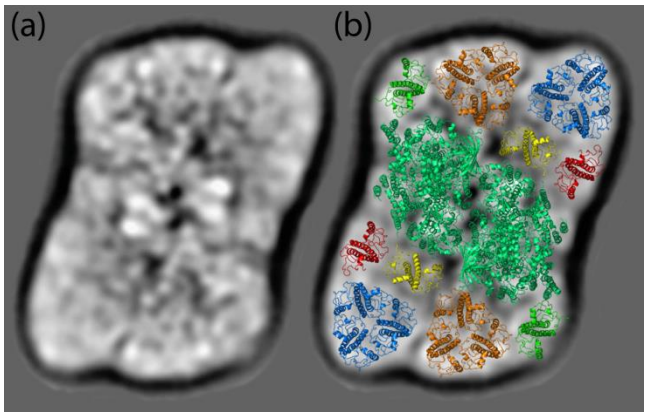

Figure 4. Structure of *Arabidopsis thaliana* $C_2S_2M_2$ supercomplex. (a) electron microscopy map of supercomplex obtained at 12 Å resolution. (b) fitting of X-ray structures into the supercomplex as proposed by Caffarri et al., (2009). Pale green: core complex; blue: M trimer; orange: S trimer; red: Lhcb6; green: Lhcb5; yellow: Lhcb4. Adapted from Caffarri et al. (2009).

Recently, a breakthrough was achieved, when the 3D structure of the C_2S_2 supercomplex was obtained using cryo electron microscopy at 3.2 Å resolution (Wei et al., 2016). This study improved the current knowledge about the organization of the whole supercomplex, as precise localization of PsbO-Q subunits constituting the oxygen evolving complex was presented. A detailed insight into energy transfer pathways between antennas and core complex was also brought, as the exact positions of individual Lhcb proteins were located. The structure of this PSII C_2S_2 supercomplex is presented in the Figure 5.

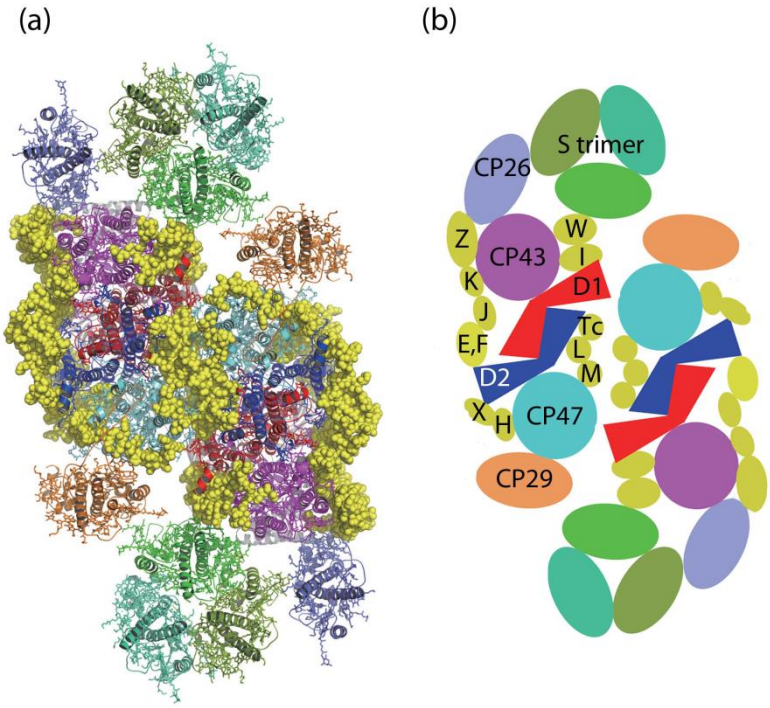

Figure 5. Cryo electron microscopy structure of spinach C_2S_2 supercomplex obtained at 2.8 Å resolution. (a) crystal structure of C_2S_2 supercomplex, (b) schematic subunit depiction. Adapted from Wei et al. (2016).

Larger assemblies of Photosystem II

Photosystem II also tends to form larger assemblies in the grana membrane, which are, in contrast to PSI, formed exclusively between each other. Thus, the following paragraphs will briefly summarize current knowledge about formation of such associations, namely two-dimensional crystals and PSII megacomplexes.

Two-dimensional crystals of Photosystem II

The first evidence of regular arrangements of PSII supercomplexes into semi-crystalline arrays was given several decades ago by freeze fracture analysis of thylakoid membranes (Garber and Steponkus, 1976; Simpson, 1978). Nevertheless, due to the limited resolving possibilities, no structural details could be concluded. The first reasonable results were obtained several years later after electron microscopy investigation of mildly solubilized spinach thylakoid membranes by α-dodecyl maltoside (Boekema et al., 2000). In

these membranes, regular arrangements of PSII supercomplexes into long rows were observed. After a detailed analysis, several types of crystal lattices were discovered. They were composed of either C_2S_2M or C_2S_2 supercomplexes. Later, another type of crystal lattice was found in *Arabidopsis thaliana*, which was formed by $C_2S_2M_2$ supercomplex (Yakushevska et al., 2001a). It was also shown that occurrence and lattice properties of the PSII semi-crystalline arrays are dependent on growth conditions. In plants grown under high light conditions, the amount of semi-crystalline arrays was significantly reduced compared to normal and low light (Kouril et al., 2013). Moreover, there was a relative increase in semi-crystalline arrays formed by C_2S_2 supercomplexes in high light variant compared to crystals formed by $C_2S_2M_2$ in the other light variants, probably as the consequence of light induced disassembly of larger complexes. The formation of semi-crystalline arrays is also initiated by the adaptation of plants to low temperature (Garber and Steponkus, 1976) or by different conditions (e.g. high sugar concentration in the storage medium) used to store the isolated thylakoid membranes or chloroplasts (Semenova, 1995).

The function of the PSII semi-crystalline arrays is still a matter of debates and several possibilities were proposed. It was suggested that these ordered arrays may serve to enhance diffusion of plastoquinone to cytochrome b_6f complex in the crowded membrane (Kirchhoff et al., 2007) and regular arrangements of PSII may also participate on grana formation via mutual interactions of LHCII in the adjacent membrane layers (Yakushevska et al., 2001a; Daum et al., 2010; Kirchhoff et al., 2013; Tietz et al., 2015). It was also shown that formation of the semi-crystalline arrays is dependent on PsbS (Kereiche et al., 2010). In plants with normal or decreased level of PsbS, the formation of semi-crystalline arrays was unaffected, while no arrays were detected in the plants overproducing the PsbS. Thus, it was suggested that formation of these semi-crystalline arrays is also related to non-photochemical quenching, since PsbS is involved in regulation of non-photochemical quenching process (Niyogi et al., 2005).

Megacomplexes of Photosystem II

PSII megacomplexes represent a lateral and specific association of two PSII-LHCII supercomplexes. They were, for the first time, detected in chromatographically purified spinach thylakoid membranes mildly solubilized by α-dodecyl maltoside. The analysis of electron micrographs of that sample revealed three different in parallel arranged PSII megacomplexes (Boekema et al., 1999b; Boekema et al., 1999a) and later, another type of the PSII megacomplex was discovered in *Arabidopsis thaliana* (Yakushevska et al., 2001b). Later, the PSII megacomplexes were detected also in other studies (e.g. Caffarri et al., 2009; Jarvi et al., 2011), but they were not subjected to any structural characterization. The origin and a biological relevance of PSII megacomplexes were obscured since they were considered as building blocks or just fragments of two-dimensional crystals.

In our work (chapter 4.3), we performed a thorough structural analysis of PSII megacomplexes from mildly solubilized *Arabidopsis thaliana* thylakoid membranes. Our results indicate similar arrangements of PSII as published previously (Boekema et al., 1999b; Boekema et al., 1999a; Yakushevska et al., 2001b), when we detected PSII megacomplexes arranged in parallel. However, we also detected several novel types of megacomplexes formed by two PSII supercomplexes interacting in a non-parallel manner. Importantly, we also brought evidence of native origin of both parallel and non-parallel megacomplexes as they were successfully detected at the level of native grana membranes. We also proposed their function in a tuning of utilization of absorbed light energy, however, this has to be elucidated in more detail in further studies.

Experimental techniques

Electron microscopy represents a powerful tool for structural characterization of protein complexes, as it was demonstrated on several PSI and PSII supercomplexes and megacomplexes described in the previous chapter. To facilitate the electron microscopy analysis of protein complexes, a proper separation method is also desirable to purify the complex in a high quantity, purity and a native form. Nowadays, there are generally two native separation methods widely used. The first method represents an ultracentrifugation in sucrose gradient. This technique has been successfully used several times for a separation of large PSII-LHCII supercomplexes (e.g. Caffarri et al., 2009; Wei et al., 2016). However, this technique is vastly time consuming (a run usually takes about 16 h) and demanding for a very expensive equipment. On the other hand, native electrophoresis, which represents the second separation technique, brings several benefits compared to ultracentrifugation. It remarkably shortens the time needed for separation (it takes about 2 h) and uses relatively inexpensive equipment. The following paragraph will briefly introduce the issue of native polyacrylamide gel electrophoresis, namely the so-called clear native polyacrylamide gel electrophoresis (CN-PAGE), a separation technique successfully utilized in all our studies (chapters 4.1, 4.2, 4.3). It is followed by an insight into the basic principles of transmission electron microscopy and image analysis.

CN-PAGE

Clear-native polyacrylamide gel electrophoresis represents a special type of electrophoresis nowadays conveniently used for separation of large and fragile protein complexes in native state.

It was used for the first time in early nineties for separation of labile mitochondrial complexes and it is principally based on an older technique known as blue-native PAGE (BN-PAGE) (Schagger et al., 1994). Nevertheless, the original setup of CN-PAGE had limited resolving possibilities and till these days, it had to undergo several improvement steps.

Originally, the only difference between CN-PAGE and BN-PAGE lied in the complete absence of anionic dye Coomassie brilliant blue (CBB) in the case of CN-PAGE (Schagger et

al., 1994). Since the principle of BN-PAGE is based on the ability of this dye to adsorb to the protein complexes which sets them negative charge necessary for their movement in the electric field (Schagger and Vonjagow, 1991), a usage of CN-PAGE was limited due to the CBB absence to separation of complexes with certain isoelectric point (pI) only. All native electrophoretic applications apply exclusively neutral pH, which means that only acidic proteins with pI lower than the pH of electrophoretic system could be separated (because only those proteins have negative charge). The other "disadvantage" of original CN-PAGE setup was in a significantly prolonged separation and weak resolution of separated protein complexes (Schagger et al., 1994; Wittig and Schagger, 2005). On the other hand, the separation in absence of CBB provided several very important advantages. This dye significantly hampered estimation of catalytic activity of separated protein complexes and interfered with detection of fluorescently labelled proteins, which was conveniently overcome in the case of CN-PAGE. Moreover, there were some indications that CBB might disturb very weak protein-protein interactions and thus, CN-PAGE was considered to be the mildest electrophoretic technique (Wittig and Schagger, 2005).

Therefore, there was an effort to combine advantages of both electrophoretic techniques. This resulted in the high resolution CN-PAGE, an improved method combining the resolving efficiency of BN-PAGE with an exceptional mildness of CN-PAGE (Wittig et al., 2007). This was achieved by a mild, anionic detergent sodium deoxycholate present in a cathode buffer. This detergent incorporates into detergent micelles of solubilized protein complexes and sets them a negative charge, which is essential for their effective separation in the electric field. Moreover, to our best knowledge there is no evidence regarding any negative impact of this detergent on protein-protein interaction.

The separation of protein complexes by native electrophoresis is usually performed using linear gradient polyacrylamide resolving gel. Obviously, gradient gel is used, when a mixture of proteins with broad range of molecular masses is separated. This is typically the case of photosynthetic membrane-bound complexes, which can have a form of large megacomplexes as well as small complexes. When the size of gel pores in the gradient gel meats with the size of a separated protein complex, the complex significantly decreases its

speed of movement in the gel and focuses in a sharp band. Thus, usage of the gradient gel is a beneficial way, how to separate individual proteins of different size from each other. The proper gradient constitution has to be also considered prior every experiment to achieve sufficient separation of complexes of interest. It is practically impossible to clearly resolve all individual protein complexes from a heterogeneous mixture and the gel density should be always adequate to molecular mass of complex of interest. The rule of thumb is: the larger complexes are to be resolved, the less concentrated gel has to be used (and vice versa). Consequently, a proper separation of larger complexes is at the expense of the smaller ones.

Prior the separation of protein complexes by native electrophoresis, biological membranes have to be solubilized in order to extract the protein complexes from the lipid layer. For this purpose, detergents efficiently relieving lipid-lipid and lipid-protein interactions and maintaining even the weakest protein-protein interactions should be used. Nowadays, there are plenty of detergents suitable for extraction of protein complexes from biological membranes (Crepin et al., 2016). Nevertheless, as our long-term experience showed, dodecyl-maltosides (DDM) are the most suitable ones. Dodecyl-maltosides belong to the group of alkyl-glucosides, non-ionic detergents, which combine in their molecules a long hydrophobic alkyl chain with a large hydrophilic head group. In the case of DDM, the alkyl chain is formed by a non-branched twelve-carbon chain and the head group is composed of a maltose molecule. Based on the position of alkyl chain on the maltose head, α- and β- anomers can be distinguished. In the case of α-DDM, the side chain is connected to the head in the axial position, while β-DDM is connected in equatorial position (Seddon et al., 2004). Even though both these detergents share their basic chemical characteristics, their physical properties differ significantly. The best example of different physical properties is the different solubilizing power of both detergents, as evidenced e.g. by Pagliano et al., (2012) and Barera et al., (2012) and also by our results (see Experimental approach chapter). To achieve the optimal yield and resolution of complex of interest, proper detergent (α- or β-DDM in our case) and its concentration have to be determined. For this purpose, a constant amount of membranes is usually treated with different detergents at increasing concentration. This is so-called detergent concentration line, which provides an outline of sample response. Using this approach, the suitable detergent and its concentration can be

determined to obtain specific complexes. As the results presented in the Experimental approach chapter imply, both DDM's are useful in dependence on solubilized plant material and stability of studied protein complex.

Single particle electron microscopy

Single particle electron microscopy is a powerful technique used for both 2D and 3D structural characterization of protein complexes. It is highly suitable for protein assemblies, whose physical properties make difficult their structural characterization by other structural method like X-ray crystallography. Certainly, single particle electron microscopy provides several advantages compared to X-ray crystallography: there is no need to grow crystals, the biological sample does not need to be purified into homogeneity and high protein concentration and it is highly suitable for a study of large and often transient and unstable supercomplexes and megacomplexes. It combines transmission electron microscopy and image analysis (reviewed e.g. in Boekema et al., 2009).

Transmission electron microscopy is an advanced technique, employing its high magnification capacity for visualization of small details, even within individual molecules. In principle, it is, to some extent, similar to a commonly known optical microscopy. However, it uses electrons instead of visible light. The limitation of optical microscopy lies right in the use of visible light (about 380-760 nm), since wavelength of photons is one of the resolution (and magnification) limiting factors. Wavelength of electron is dependent on voltage used for electron acceleration inside the electron microscope column and it can be up to 2.5 pm (if 200 kV acceleration voltage is used). This means that electron microscope may offer several orders of magnitude higher resolution than optical microscope. On the other hand, there are also several instrumental factors like aberration of lenses, which limit the final resolution of electron microscope.

The general setup of transmission electron microscopy is the following: a path of electrons, which are emitted from an electron gun, is controlled and aligned by a set of lenses to form coherent and maximally monochromatic electron beam. These electrons then interact with a specimen, what affects their directions (i.e. the electrons are scattered by

interaction with the specimen). The scattered electrons, which carry now information about the specimen, further pass through the objective lens and through a set of projector lenses, where magnification occurs. Then they interact with a detector, which transforms the carried information into an image.

In the electron microscopy, contrast of the image is one of the crucial factors, which has a great impact of the final results. A general origin of the contrast is in scattering of electrons on the specimen level and the scattering is directly proportional to the atomic number of elements, which form the specimen. Since the biological specimens are formed mostly of biomacromolecules composed of light elements (C, H, O, N), the scattering and resulting contrast is insufficient. A more sufficient contrast can be obtained by a negative staining (Brenner and Horne, 1959). In the negative staining, the biomacromolecules are embedded in heavy metal salt, whose heavy atoms strongly interact with electrons. The heavy metal salt surrounds the space around biomacromolecules and fills their cavities, but the hydrophobic protein interior remains untouched. This causes that the biomacromolecules project out from the background with a good contrast. Nevertheless, negative staining brings an inconvenience, as the complexes in the specimen may become deformed during the staining procedure. This undesirable deformation of complexes is avoided in cryo electron microscopy (Adrian et al., 1984), which represents an alternative for negative staining technique. In this technique, a liquid specimen containing biomacromolecules is rapidly frozen on the electron microscopy grid. Using this method, the biomacromolecules are embedded in a thin layer of amorphous ice and better reflect the genuine cellular aqueous situation of studied complexes. Since the contrast is caused preferentially by the difference between densities of ice and biomacromolecules, the contrast is much weaker compared to the negative staining. Due to this fact, it is uneasy to distinguish between complexes of interest and contaminants or breakdown products. Thus, the cryo electron microscopy is rather suitable for large and symmetric macromolecules, while negative staining is more suitable for smaller and structurally variable macromolecules. In cryo electron microscopy, the complexes are also present in all possible orientations as they are freely distributed in the ice. On the other hand, the complexes are in

negatively stained specimen adhered on the support carbon film and their spatial layout is limited.

The biological samples are also highly sensitive to radiation damage and thus, the intensity of incident electron beam has to be minimized. This results in a low signal-to-noise ratio in the micrograph. To cope with this, image analysis is employed.

Image analysis consists of three basic steps: alignment, classification and averaging. During the alignment step, all the individual projections of complexes (or any inspected particles) obtained by imaging of the specimen are arranged into the same direction. Classification, the second step, efficiently sorts out all different proteins in a heterogeneous dataset into individual classes. This step is able to distinguish even between very fine variances, if performed properly. However, this step is greatly time-consuming and demanding for high computing capacity. The last step, averaging, simply averages individual projections belonging to one class raised from the classification and significantly increases the signal-to-noise ratio. The higher amount of particles is summed, the higher resolution, contrast and structural information is achieved. Nowadays, the image analysis can be performed using various number of specialized software tools, such as XMIPP (Sorzano et al., 2004), RELION (Scheres, 2012), Spider (Frank et al., 1996), EMAN (Ludtke et al., 1999) or IMAGIC (vanHeel et al., 1996).

The final projection map of a protein complex can be fitted with the X-ray structures of its individual subunits (if accessible). This fitting significantly helps to understand the overall structure and organization of studied complex, interactions between subunits and it is also helpful for understanding of complex function.

2. Summary

This thesis is aimed on the structural characterization of various plant photosynthetic complexes using a combination of CN-PAGE and single particle electron microscopy. Single particle electron microscopy is a powerful structural technique and provides ample structural information about a studied complex. In order to facilitate the structural characterization, optimization of a specimen preparation for electron microscopy is a very important step. The optimization is a complex process and comprises of several steps, as described in details in the chapter 3. Experimental approach. First of all, a proper plant material has to be selected. Then, conditions of a protein separation using CN-PAGE, including selection of a proper detergent and its concentration, are optimized. Final step involves extraction of separated protein complexes from the CN-PAGE gel and a preparation of specimen for electron microscopy. Once the workflow is optimized, it can be successfully applied in a structural study. The aim of my thesis was a structural characterization of three large protein assemblies involved in photosynthesis like the PSI-NDH supercomplex from barley, the PSII-LHCII supercomplex from Norway spruce and the PSII megacomplex from *Arabidopsis thaliana*.

The first paper (chapter 4.1) deals with the structural characterization of the PSI-NDH supercomplex isolated from barley (*Hordeum vulgare*). The structural analysis revealed that one NDH complex binds up to two PSI supercomplexes, which are to NDH bound at asymmetric positions. Moreover, positions of rare Lhca5 and Lhca6 antennas stabilizing the whole supercomplex were indicated. As we discovered both supercomplexes with one and two PSI bound to NDH, it implies that gradual formation and dissociation of the PSI-NDH supercomplex may function as a tuning of cyclic electron flow around PSI.

The second paper (chapter 4.2) describes the structural characterization of the PSII supercomplex isolated from Norway spruce (*Picea abies*). Spruce belongs to the group of gymnospermous plants (family *Pinaceae*) and we provided the first structural analysis of PSII supercomplex isolated from this plant group. Moreover, using an extensive genomic analysis we also discovered that the group of land plants including families *Pinaceae* and also

Gnetales lack genes for Lhcb3 and Lhcb6 subunits, which has a noticeable impact on the structural organization of PSII supercomplexes. These two subunits have evolved during transition of plants from water to land and were considered to be characteristic for all land plants. Their absence in these plant groups breaks the current evolutionary dogma and modifies PSII supercomplex in such a way that it resembles PSII from evolutionary older organism, alga *Chlamydomonas reinhardtii*.

The third paper (chapter 4.3) structurally characterizes PSII megacomplexes isolated from *Arabidopsis thaliana*. These megacomplexes are formed of two PSII supercomplexes, which mutually interact in parallel and in non-parallel. The structural characterization of megacomplexes interacting in non-parallel was performed for the first time. The presence of both groups of megacomplexes was also detected on the level of native grana thylakoid membrane, which is an evidence of their nativity and thus a physiological significance.

3. Experimental approach

Methods

Plant material

Arabidopsis thaliana plants were grown for 8 weeks in soil in a growth chamber at 21°C with a photoperiod of 8h light and 16h dark at 100 µmol of photons.m^{-2}.s^{-1} of photosynthetically active radiation.

Barley (*Hordeum vulgare*) plants were grown for 8 days in perlite in a growth chamber at 25°C with a photoperiod of 16h light and 8h dark at 100 µmol of photons.m^{-2}.s^{-1} of photosynthetically active radiation.

Spruce (*Picea abies*) plants were grown for 18 days in perlite in a growth chamber at 21°C with a photoperiod of 16h light and 8h dark at 100 µmol of photons.m^{-2}.s^{-1} of photosynthetically active radiation.

Isolation and solubilization of thylakoid and PSII enriched membranes

Thylakoid membranes from *Arabidopsis thaliana* and barley were isolated according to (Dau et al., 1995)and PSII enriched membranes from spruce were isolated according to (Caffarri et al., 2009).

In all the cases, a constant amount of membranes (corresponding to 10 µg of chlorophylls) was treated with a certain amount of detergent. The detergent amount is defined as the mass ratio of detergent to chlorophylls (DDM/chl). Prior the electrophoretic separation, the mixture of membranes with detergent was supplemented with sample buffer to the final volume of 30 µl (20% glycerol, 50 mM HEPES, 400 mM sucrose, 15 mM NaCl, 5 mM $MgCl_2$, pH 7.2) and centrifuged (10 minutes, 20000g) to remove nonsolubilized material.

CN-PAGE

In all our experiments, CN-PAGE (Wittig et al., 2007) as the separation technique was used. Because we aimed on complexes of high molecular weight, we modified the gel concentration in order to resolve the large complexes at the expense of the smaller ones. We used 4-8% gradient resolving gel with 4% stacking gel. The electrophoretic separation was performed using the Bio-Rad Mini-PROTEAN Tetra Cell system.

Gel imaging

After electrophoresis, the gels were scanned using a gel scanner Amersham Imager 600RGB. To visualise all the bands in the gel, an ordinary image upon white light illumination in transmission mode was acquired. To distinguish between PSI and PSII complexes, a fluorescent image was acquired. The fluorescence quantum yield of PSI is very low at room temperature compared to the high quantum yield of fluorescence of PSII, which unambiguously discriminates both types of photosystems. Excitation was performed at 460 nm, detection of fluorescence was performed using a band-pass filter (690-720 nm).

Electron microscopy and image analysis

Electron microscopy was performed using several electron microscopy configurations: 1) using Philips CM120 electron microscope equipped with a LaB6 filament operating at 120 kV. Images were recorded with a Gatan 4000 SP 4K slow-scan CCD camera at 130000x magnification with a pixel size of 0.23 nm at the specimen level after binning the images to 2048 x 2048 pixels, 2) Tecnai G2 20 Twin electron microscope equipped with a LaB6 cathode, operated at 200 kV. Images were recorded with an UltraScan 4000UHS CCD camera at 130000x magnification with a pixel size of 0.224 nm at the specimen level after binning the images to 2048 x 2048 pixels.

Image analysis was performed using GRIP (GRoningen Image Processing), XMIPP (Sorzano et al., 2004) and RELION (Scheres, 2012) software including multireference and nonreference alignments, multivariate statistical analysis and classification.

Optimization of separation method for structural characterization of photosynthetic supercomplexes and megacomplexes

Plant PSI and PSII are large, multisubunit photosynthetic pigment-protein supercomplexes performing light-driven reactions. Extensive information regarding their structure is available (in detail reviewed e.g. in Busch and Hippler, 2011; Shen, 2015). Moreover, both PSI and PSII supercomplexes tend to form larger associations with other protein complexes and also with each other (summarized in chapter 1). Although these large associations perform physiologically important functions, information regarding their structural organization is still rather limited. Thus, we focused our attention to reveal structures of some of them.

Isolation of the PSI-NDH supercomplex

Selection of plant material and optimization of solubilization

Although there was ample functional and biochemical evidences for the existence of the PSI-NDH supercomplex (Peng et al., 2008; Peng et al., 2009; Peng and Shikanai, 2011), the information regarding its structural organization was missing.

The PSI-NDH supercomplex was originally isolated from *Arabidopsis thaliana* thylakoid membranes solubilized by β-DDM using BN-PAGE (Peng et al., 2008). Thus, we decided to structurally characterize the PSI-NDH supercomplex from the same plant material. Moreover, as we expected that this supercomplex might be too fragile, we tested, in addition to β-DDM, a detergent α-DDM as well for its milder solubilizing action. To optimize yield of the PSI-NDH supercomplex using CN-PAGE separation, we treated thylakoid membranes with gradually increased amounts of individual detergents (Figures 6 and 7).

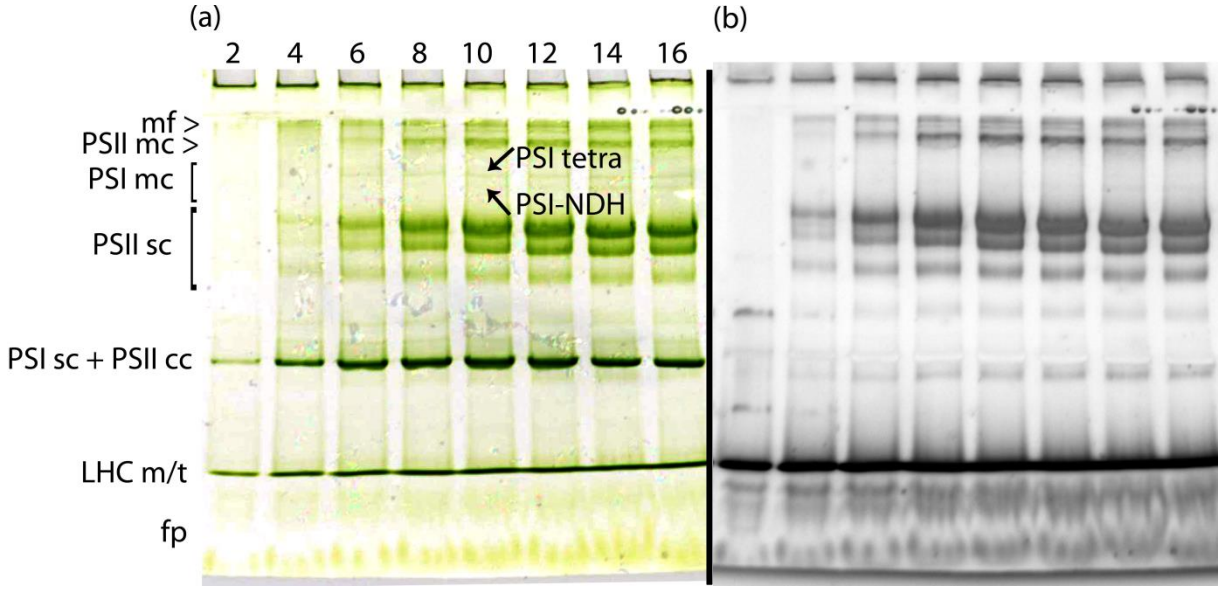

Figure 6. Electrophoretic separation of *Arabidopsis thaliana* thylakoid membranes solubilized by increasing amount of α-DDM. (a) colour image of the gel, (b) room temperature fluorescence of supercomplexes from the same gel. 2-16: DDM/chl ratio; mf: membrane fragments; PSII mc: megacomplexes of PSII; PSI mc: megacomplexes of PSI; PSI tetra: tetramers of PSI; PSII sc: supercomplexes of PSII; PSI sc: supercomplex of PSI; PSII cc: core complex of PSII; LHCm/t: LHC monomers and trimers; fp: free pigments. Designation of individual bands is substantiated in the text.

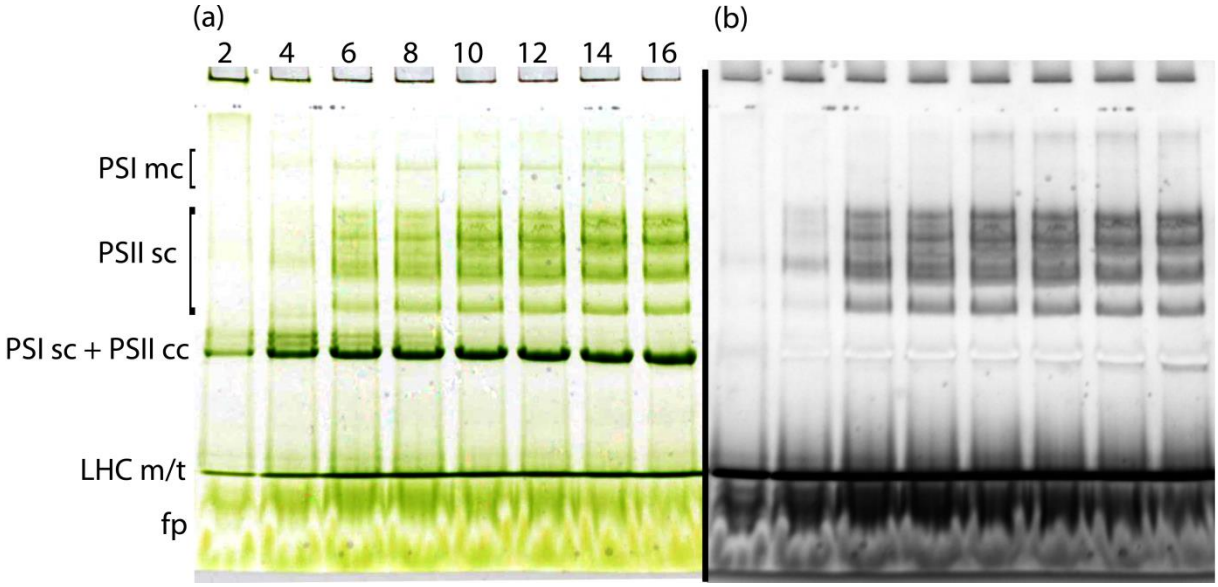

Figure 7. Electrophoretic separation of *Arabidopsis thaliana* thylakoid membranes solubilized by increasing amount of β-DDM. (a) colour image of the gel, (b) room temperature fluorescence of supercomplexes from the same gel. 2-16: DDM/chl ratio; PSI mc: megacomplexes of PSI; PSII sc: supercomplexes of PSII; PSI sc: supercomplex of PSI; PSII cc: core complex of PSII; LHCm/t: LHC monomers and trimers; fp: free pigments. Designation of individual bands is substantiated in the text.

As we aimed preferentially on the PSI-NDH supercomplex, we expected comparable results as originally published by Peng et al., (2008). In that study, a combination of BN-PAGE separation with a western-blotting analysis revealed two high molecular weight bands containing PSI and NDH subunits just above bands with PSII supercomplexes. Thus, in our case, it was necessary to unambiguously distinguish between the PSI-containing bands and the PSII-containing bands in both the CN-PAGE gels (in Figures 6 and 7). This was achieved by the fluorescence imaging of both the gels (details are in the part Methods). Using this method, bands containing the PSI supercomplex can be identified due to a lack of room temperature fluorescence. Thus, the fluorescence imaging unambiguously revealed the position of the PSI supercomplex. Further, it became clear that the group of bands above the PSI supercomplex contain PSII, as they were highly fluorescent. By comparing of our results with other papers dealing with the electrophoretic separation of pigment-protein complexes from thylakoid membranes (Jarvi et al., 2011; Kouril et al., 2016; Pavlovic et al., 2016), we took the liberty to assign the group of PSII-containing bands in the middle of both gels

(Figures 6 and 7) as the PSII supercomplexes. Just above the PSII supercomplexes, the fluorescence imaging of both the gels (Figures 6 and 7) revealed the presence of faint high molecular weight PSI-containing bands most likely corresponding to the bands detected by Peng et al., (2008). In the sample solubilized by α-DDM (Figure 6), two high molecular weight PSI-containing bands were observed. In the case of the sample solubilized with β-DDM, only one high molecular weight PSI-containing band was detected (Figure 7). Nevertheless, densities of all these high molecular weight PSI-containing bands seemed to be insufficient for structural characterization of the PSI-NDH supercomplex. Therefore, we decided to test another plant species in order to determine whether it is possible to obtain these high molecular weight PSI-containing bands with a higher yield. For this purpose, barley plants (*Hordeum vulgare*) were tested. Thylakoid membranes from barley were subjected to the same solubilizing conditions as thylakoid membranes from *Arabidopsis thaliana* (i.e. membranes were solubilized by both α- or β-DDM) and results of their electrophoretic separation are shown in the Figures 8 and 9.

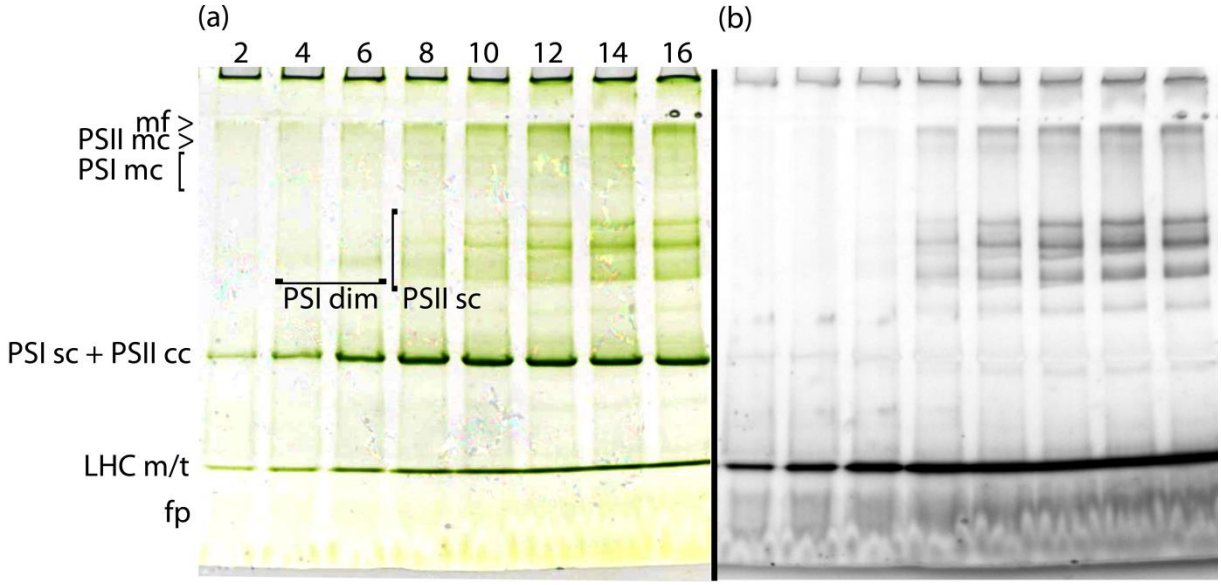

Figure 8. Electrophoretic separation of barley thylakoid membranes solubilized by increasing amount of α-DDM. (a) colour image of the gel, (b) room temperature fluorescence of supercomplexes from the same gel. 2-16: DDM/chl ratio; mf: membrane fragments; PSII mc: megacomplexes of PSII; PSI mc: megacomplexes of PSI; PSI dim: dimers of PSI; PSII sc: supercomplexes of PSII; PSI sc: supercomplex of PSI; PSII cc: core complex of PSII; LHCm/t: LHC monomers and trimers; fp: free pigments. Designation of individual bands is substantiated in the text.

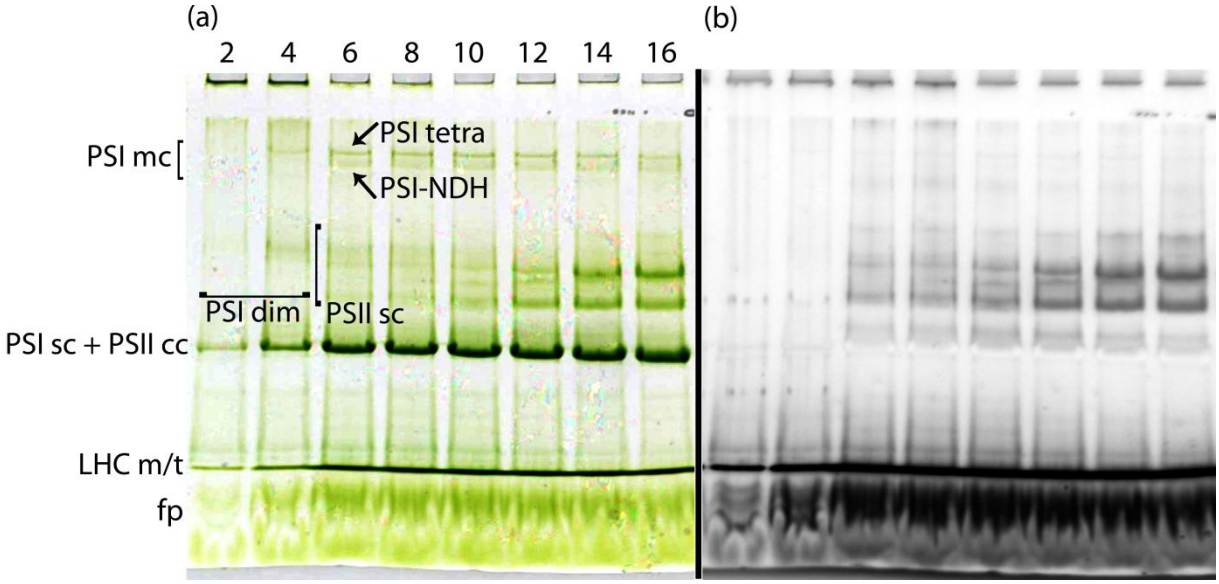

Figure 9. Electrophoretic separation of barley thylakoid membranes solubilized by increasing amount of β-DDM. (a) colour image of the gel, (b) room temperature fluorescence of supercomplexes from the same gel. 2-16: DDM/chl ratio; PSI mc: megacomplexes of PSI; PSI tetra: tetramers of PSI; PSI dim: dimers of PSI; PSII sc: supercomplexes of PSII; PSI sc: supercomplex of PSI; PSII cc: core complex of PSII; LHCm/t: LHC monomers and trimers; fp: free pigments. Designation of individual bands is substantiated in the text.

In the terms of high molecular weight PSI-containing bands, the electrophoretic separation of barley thylakoid membranes provided opposite results compared to membranes isolated from *Arabidopsis thaliana*: whereas barley sample solubilized by β-DDM contained two such bands (Figure 9), barely one band could be detected in barley sample solubilized by α-DDM (Figure 8). However, for the reason that the two high molecular weight PSI-containing bands in the barley sample solubilized by β-DDM (Figure 9) were much denser then the corresponding bands in the *Arabidopsis thaliana* sample (Figure 7), the thylakoid membranes isolated from barley and solubilized by β-DDM were selected for the structural characterization of the PSI-NDH supercomplex.

When the proper plant material providing sufficiently dense high molecular weight PSI-containing bands was selected, suitable amount of detergent (DDM/chl ratio) had to be chosen. After considering the impact of detergent on the densities of bands in the detergent concentration line (Figure 9, values 2-16), the ratio eight was selected as the most proper. At

this ratio, densities of both high molecular weight PSI-containing bands seemed to be equally dense.

After brief electron microscopy screening of both the high molecular weight PSI-containing bands, we discovered that PSI-NDH supercomplex is present in the lower one. Structural characterization of the PSI-NDH supercomplex is described in the chapter 4.1.

On the other hand, electron microscopy inspection of the upper band revealed that the band did not contain PSI-NDH supercomplex, as it was indicated in the paper by Peng et al. (2008). Instead, the band was composed of tetrameric PSI megacomplexes. Figure 10 represents preliminary structural characterization of such tetrameric PSI supercomplexes (unpublished data). However, as it was published already (Kouril et al., 2005a), native plant PSI is present in monomeric form and these PSI tetramers likely represent artificial aggregates.

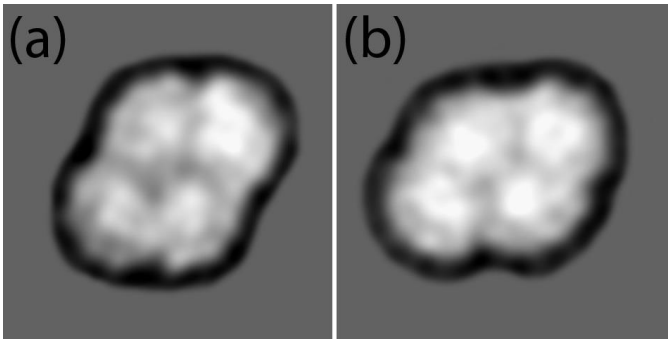

Figure 10. Tetrameric PSI supercomplexes. (a, b) structures represent two types of tetrameric PSI associations discovered in a CN-PAGE gel (Fig. 9).

Moreover, at low detergent concentrations, faint PSI-containing bands appeared in the middle of both CN-PAGE gels with barley sample (Figures 8 and 9). To reveal their composition, complexes from these bands were subjected to electron microscopic analysis. Unfortunately, no reasonable results indicating bands composition were obtained due to very low protein concentration in these bands. However, by considering of the relative

molecular weight of complexes present in mentioned bands and that fluorescence imaging clearly showed the presence of PSI, these bands were preliminarily assigned as dimers of PSI.

It is also worth of interest that the complexes from thylakoid membranes solubilized by α-DDM showed higher level of intactness compared to β-DDM solubilized ones. This is evidenced mainly by higher densities of bands with larger PSII supercomplexes in the samples solubilized by α-DDM (Figures 7 and 9) compared to samples solubilized by β-DDM (Figures 6 and 8). This is in agreement with previously published papers (Barera et al., 2012; Pagliano et al., 2012), which were also dealing with separation of photosynthetic complexes solubilized by α- and β-DDM. These papers show that α-DDM preserves the complexes more intact due to its milder solubilizing properties. The milder solubilizing action of α-DDM is also clearly evident from less dense bands with LHC and free pigments and from higher amount of non-solubilized material stuck in the wells in both samples solubilized by α-DDM.

Despite the original work, dealing with the isolation of the PSI-NDH supercomplex, used *Arabidopsis thaliana* thylakoid membranes (Peng et al., 2008), we found that barley thylakoid membranes are a better option as the PSI-NDH supercomplex was yielded in higher quantity in the barley sample. This implies that optimization of separation technique is an important step preceding structural analysis.

Isolation of PSII megacomplexes from *Arabidopsis thaliana*

In the CN-PAGE gels with *Arabidopsis thaliana* and barley thylakoid membranes solubilized by α-DDM (Figures 6 and 8), two high molecular weight bands appeared just on the top of resolving gels. The fluorescence imaging of the gels showed that both the bands contain PSII. To exclude the possibility that these PSII-containing bands represent fragments of insufficiently solubilized membranes, a brief electron microscopy inspection of complexes present in these bands was performed. The analysis showed that the uppermost band was composed of unspecific aggregates and membrane fragments (data not shown), which were likely formed as a solubilizing artefact or due to insufficient solubilization. On the other hand, the lower band contained a large amount of different megacomplexes, from whose PSII megacomplexes formed of two $C_2S_2M_2$ supercomplexes were vastly prevailing. As these

high molecular weight PSII megacomplex bands were not present in gels with samples solubilized with β-DDM (Figures 7 and 9), it highlights the milder solubilizing action of α-DDM. Details of structural characterization of PSII megacomplexes with proof of their intactness are summarized in the chapter 4.3.

Optimization of separation conditions for a structural characterization of spruce PSII supercomplex

It is known that land plants are generally divided into two major groups: gymnospermous and angiospermous plants. The photosynthetic apparatus of angiospermous plants is well explored, as it is evidenced by dozens of studies performed on *Arabidopsis thaliana*, pea, barley and many other representatives of this group (e.g. Boekema et al., 2001; Caffarri et al., 2009; Jarvi et al., 2011). On the other hand, structural information regarding photosynthetic complexes from gymnospermous plants was completely missing. Thus, we decided to perform structural characterization of the PSII supercomplex in Norway spruce (*Picea abies*), which represents the most abundant and economically the most significant member of gymnosperms. As we aimed on the structural characterization of the PSII supercomplex, we selected PSII enriched membranes isolated from young spruce seedlings. PSII enriched membranes were selected in order to increase the yield of the PSII supercomplexes. Optimization of solubilization conditions was performed in the similar way as in the case of *Arabidopsis thaliana* and barley. Results of electrophoretic separation of spruce PSII enriched membranes solubilized by α- or β-DDM are shown in Figure 11.

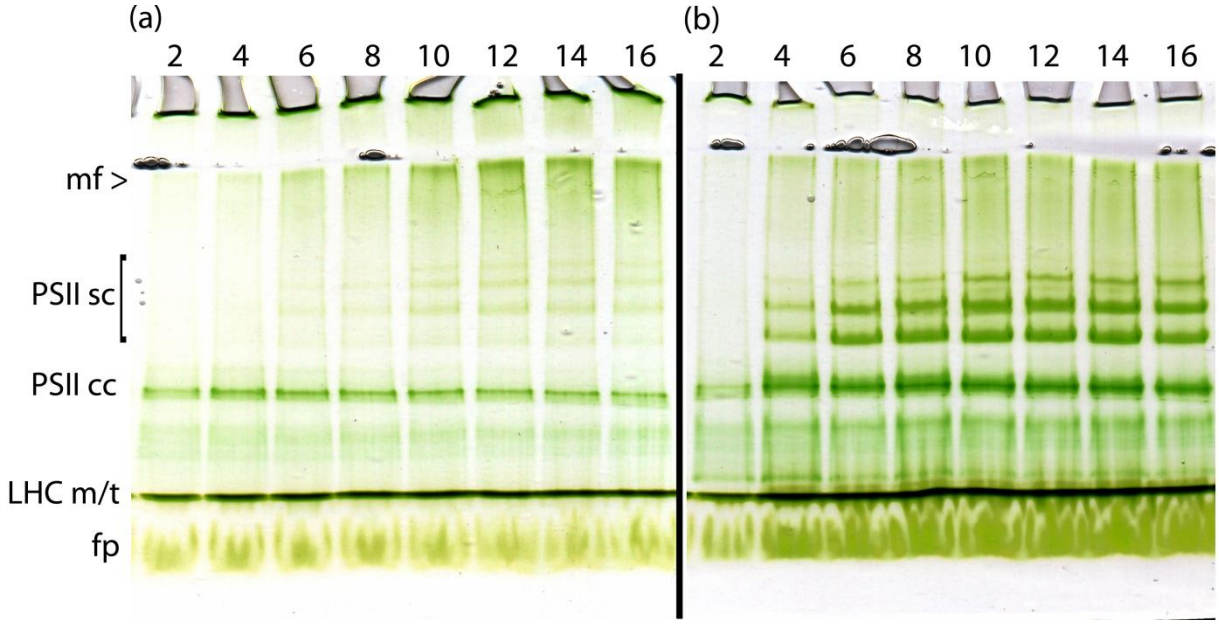

Figure 11. Electrophoretic separation of spruce PSII enriched membranes solubilized by increasing amount of α- or β-DDM. (a) colour image of gel with sample solubilized by α-DDM (b) colour image of gel with sample solubilized by β-DDM. 2-16: DDM/chl ratio; mf: membrane fragments; PSII sc: supercomplexes of PSII; PSII cc: core complex of PSII; LHCm/t: LHCII monomers and trimers; fp: free pigments.

All the bands present in CN-PAGE gel (Figure 11) were composed of different forms of PSII and their assignment was performed in analogy with previous experiments (Figures 6-9). Figure 11 shows that solubilization of membranes by β-DDM provides more dense bands. Thus, for the structural characterization of the PSII supercomplex, solubilization was performed at β-DDM/chl ratio 12. At this ratio, the uppermost PSII supercomplex band subjected to structural analysis seemed to be the densest. The results of structural analysis showed that the architecture of spruce PSII is changed as a consequence of missing Lhcb6 subunit. Thus, a genomic analysis in order to investigate gymnospermous plants' light harvesting proteins was performed. Results imply that spruce is evolutionary deflected from other land plants, as it is lacking Lhcb6 and also Lhcb3 proteins. Details regarding structural characterization of PSII supercomplexes and genomic analysis are summarized in the chapter 4.2.

It is also interesting that the solubilization with β-DDM provided much denser bands with PSII supercomplexes, than solubilization with α-DDM (Figure 11). This is in contrary with membranes from *Arabidopsis thaliana* and barley (Figures 6-9) and refers to possible different lipid composition of spruce thylakoid membranes. Results presented on Figure 11 also clearly show that there were no PSII megacomplexes detected in the CN-PAGE gels with spruce sample. This can be caused by the missing minor antenna Lhcb6 in the spruce PSII (summarized in the chapter 4.2), as it is involved in the PSII megacomplexes formation (summarized in the chapter 4.3).

Specimen preparation

Once the bands with complexes of interest were obtained in sufficient density, a way how to get the complexes out of the gel on the electron microscopy support grid had to be found. There are several methods available.

At first, a method enabling direct transfer of separated protein complexes from a native gel on the grid was recently described (Knispel et al., 2012). Using this method, the grid is placed directly onto a gel band and protein complexes spontaneously adhere on the grid surface. Nevertheless, we did not obtain any satisfying results using this method. We can speculate that protein complex properties (a size and shape) can make the method less suitable for photosynthetic membrane proteins.

The other option is a pipetting of solution containing the protein complexes on the grid – thus the complexes had to be extracted from the gel into solution. Generally, there were two possibilities how to extract protein complexes from the gel into solution: electro elution and spontaneous elution. Electro elution represents a technique allowing fast and quantitative extraction of protein complexes from the gel. During this procedure, the eluted complexes ale electrically forced from a gel and retained on a hydrophobic membrane, where they concentrate. Nevertheless, as the photosynthetic complexes are largely hydrophobic, they frequently irreversibly aggregate on the hydrophobic membrane. Thus, their structural characterization is strongly hampered and this extraction technique seems to be useless for purposes of structural characterization of hydrophobic photosynthetic

complexes. Moreover, the electro elution requires specific and costly equipment. On the other hand, spontaneous elution of protein complexes represents an easy method without any demands for special equipment. It is based on a free diffusion of protein complexes from a cut gel stripe into an elution buffer. When a spontaneous elution is performed, a band (or bands) containing the complexes is excised from the gel. Then the gel stripe is chopped into smaller pieces to enhance the diffusion by increasing its surface and immersed into elution buffer in a micro tube. Volume of the elution buffer should be adjusted to the apparent concentration (density) of complexes in the gel stripe and should be as low as possible. On the other hand, the pieces of the gel have to be always fully immersed in the buffer. As it is described in the methodical part of the chapter 4.1, 30 µl of elution buffer was usually sufficient per one cut gel stripe.

Based on our experience, the spontaneous elution should be performed in dark and cold conditions to minimize a risk of a disintegration of protein complexes. It is usually finished within two hours. A longer time had no significant effect on a higher concentration of protein complexes in the eluate. The density of a gel band subjected to elution was found to be the most critical aspect necessary for reaching sufficient protein concentration in the eluate.

Figure 12 illustrates how the different gel band densities influence the amount of protein complexes present in the specimen.

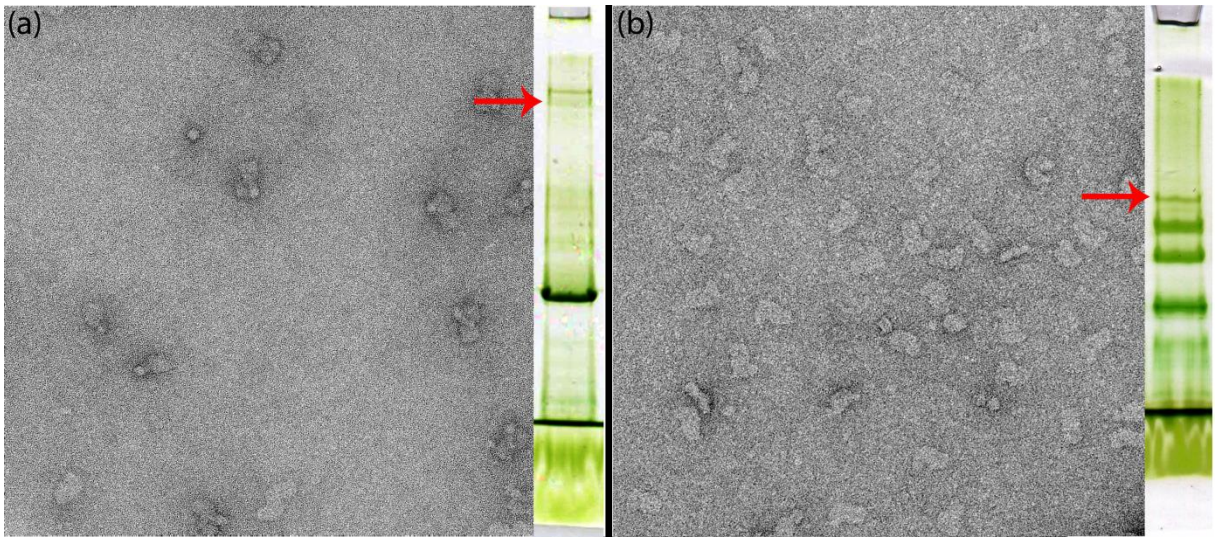

Figure 12. Impact of band density on the amount of protein complexes present in the specimen. (a) left: electron micrograph with the PSI-NDH supercomplexes, right: electrophoretic separation of barley thylakoid membranes as presented in Fig. 9 with marked band used for specimen preparation, (b) left: electron micrograph with the spruce PSII supercomplexes, right: electrophoretic separation of spruce PSII enriched membranes as presented in Fig. 10 with marked band used for specimen preparation. Both excised bands were subjected to the same eluting conditions as described in chapter 4.1.

When the concentration of eluted proteins is too low, the solution can be further concentrated using special centrifugal columns, which are specifically meant for concentrating of protein solutions. These columns contain a hydrophobic membrane with a defined pore size, which retains large protein molecules and releases small solvent and buffer molecules during centrifugation. However, as in the case of electro elution, the photosynthetic complexes largely aggregate on the membrane. This fact emphasizes the importance of optimization of separation conditions to gain dense bands as much as possible.

When the complexes were extracted from the gel into the solution, the specimen was prepared by pipetting the eluate on the glow-discharged carbon coated copper grid and negatively stained with 2% uranyl acetate.

Single particle Image analysis

Single particle image analysis is a step following the specimen imaging. It aligns projections of the protein complexes present in electron micrographs and sorts them out according to their size and shape. As the specimen is usually prepared from one gel band, a homogenous sample of complexes is expected. The CN-PAGE used in our experiments was optimized for separation of large complexes and usually provides very good resolving ability. On the other hand, the specimen can be also very heterogeneous, as complexes of similar molecular weight are difficult to be well separated from each other If this is the case, the imperfectly resolved complexes can be additionally "separated" during image analysis. As an example, Figure 13 represents a result of such image analysis, i.e. its classification part, performed on a data set of PSII megacomplexes from *Arabidopsis thaliana.*

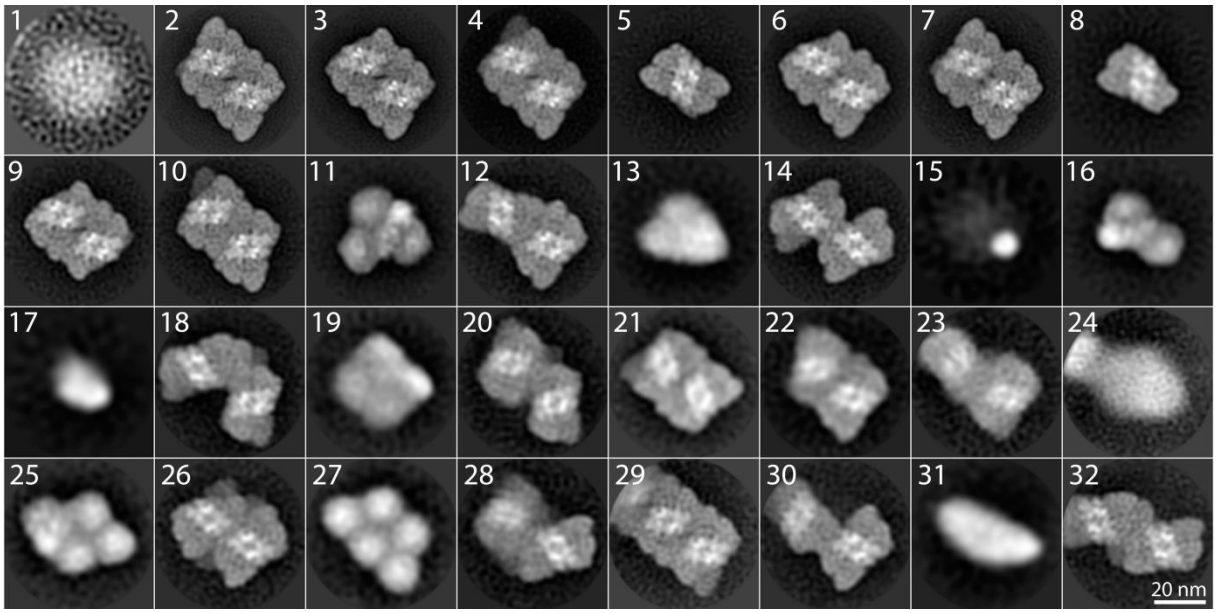

Figure 13. Classification of megacomplexes from specimen obtained from the uppermost *Arabidopsis thaliana* band (Fig. 6). The numbered boxes represent individual classes of different megacomplexes. The classes 2-4, 6, 7, 9, 10, 12, 14, 18, 20-23, 26, 28-30 and 32 represent PSII megacomplexes; classes 5 and 8 represent PSII supercomplexes; classes 11, 16 and 25 represent PSI-NDH supercomplexes; class 27 represents oligomers of PSI and classes 1, 13, 15, 17, 19, 24 and 31 represent impurities or unspecific proteins.

The results presented in Figure 13 show that one band contained large amount of different megacomplexes, which could not be resolved during electrophoretic separation because of their similar molecular weight. The results presented in Figure 13 also imply that theoretically, the separation of solubilized complexes has not indispensably preceded their structural characterization as the image analysis can efficiently sort out different complexes. Nevertheless, it is important to realize that image analysis is greatly time-consuming and the time necessary for its execution significantly rises with increasing number of individual particles. Further, if the separation is not performed, it is necessary to acquire a large amount of micrographs to work with sufficiently large dataset. Thus, as the structural characterization is usually aimed to one complex, it is very convenient to work with a homogenous specimen. Therefore, the optimization of the purification step in order to gain maximally homogenous specimen should be always performed.

4. Conclusions

This thesis is focused on structural characterization of plant photosynthetic supercomplexes and megacomplexes by a combination of CN-PAGE and single particle electron microscopy. Combination of these two techniques represents a powerful method for structural studies of various complexes and using this approach, the structural characterizations of the PSI-NDH supercomplex isolated from barley, PSII megacomplexes isolated from *Arabidopsis thaliana* and PSII supercomplex isolated from Norway spruce were performed. These structural studies were published in two co-author and one first-author publications, which are attached to this thesis. The main conclusions are the following:

- PSI-NDH supercomplex represents an association between PSI and NDH and we provided the very first structural evidence of its formation (chapter 4.1). We propose that the gradual formation and dissociation of the PSI-NDH supercomplex is involved in tuning of cyclic electron flow around PSI.
- The structure of spruce PSII supercomplex represents the first structure of a photosynthetic complex isolated from gymnospermous plants (chapter 4.2). Moreover, we discovered that spruce (and also other members of *Pinaceae* and *Gnetales* families) are evolutionary deflected from other land plants, which has the impact in structure of their PSII supercomplexes.
- PSII megacomplexes represent a lateral association between two PSII supercomplexes (chapter 4.3). We provided an evidence of their native origin, as they were also discovered in the level of native membrane. This is also an evidence of their physiological significance, which remains an object of further research.

5. References

Adrian, M., Dubochet, J., Lepault, J., and McDowall, A.W. (1984). CRYO-ELECTRON MICROSCOPY OF VIRUSES. Nature **308,** 32-36.

Alboresi, A., Caffarri, S., Nogue, F., Bassi, R., and Morosinotto, T. (2008). In Silico and Biochemical Analysis of Physcomitrella patens Photosynthetic Antenna: Identification of Subunits which Evolved upon Land Adaptation. Plos One **3**.

Allen, J.F. (1992). PROTEIN-PHOSPHORYLATION IN REGULATION OF PHOTOSYNTHESIS. Biochimica Et Biophysica Acta **1098,** 275-335.

Amunts, A., and Nelson, N. (2008). Functional organization of a plant photosystem I: Evolution of a highly efficient photochemical machine. Plant Physiology and Biochemistry **46,** 228-237.

Amunts, A., Drory, O., and Nelson, N. (2007). The structure of a plant photosystem I supercomplex at 3.4 angstrom resolution. Nature **447,** 58-63.

Amunts, A., Toporik, H., Borovikova, A., and Nelson, N. (2010). Structure Determination and Improved Model of Plant Photosystem I. Journal of Biological Chemistry **285,** 3478-3486.

Ballottari, M., Girardon, J., Dall'Osto, L., and Bassi, R. (2012). Evolution and functional properties of Photosystem II light harvesting complexes in eukaryotes. Biochimica Et Biophysica Acta-Bioenergetics **1817,** 143-157.

Baradaran, R., Berrisford, J.M., Minhas, G.S., and Sazanov, L.A. (2013). Crystal structure of the entire respiratory complex I. Nature **494,** 443-448.

Barera, S., Pagliano, C., Pape, T., Saracco, G., and Barber, J. (2012). Characterization of PSII-LHCII supercomplexes isolated from pea thylakoid membrane by one-step treatment with alpha- and beta-dodecyl-D-maltoside. Philosophical Transactions of the Royal Society B-Biological Sciences **367,** 3389-3399.

Bassi, R., Rigoni, F., Barbato, R., and Giacometti, G.M. (1988). LIGHT-HARVESTING CHLOROPHYLL-A/B-PROTEINS (LHCII) POPULATIONS IN PHOSPHORYLATED MEMBRANES. Biochimica Et Biophysica Acta **936,** 29-38.

Bellafiore, S., Barneche, F., Peltier, G., and Rochaix, J.D. (2005). State transitions and light adaptation require chloroplast thylakoid protein kinase STN7. Nature **433,** 892-895.

Ben-Shem, A., Frolow, F., and Nelson, N. (2003). Crystal structure of plant photosystem I. Nature **426,** 630-635.

Bennett, J. (1977). PHOSPHORYLATION OF CHLOROPLAST MEMBRANE POLYPEPTIDES. Nature **269,** 344-346.

Bennett, J., Steinback, K.E., and Arntzen, C.J. (1980). CHLOROPLAST PHOSPHOPROTEINS - REGULATION OF EXCITATION-ENERGY TRANSFER BY PHOSPHORYLATION OF THYLAKOID MEMBRANE POLYPEPTIDES. Proceedings of the National Academy of Sciences of the United States of America-Biological Sciences **77,** 5253-5257.

Betterle, N., Ballottari, M., Zorzan, S., de Bianchi, S., Cazzaniga, S., Dall'Osto, L., Morosinotto, T., and Bassi, R. (2009). Light-induced Dissociation of an Antenna Hetero-oligomer Is Needed for Non-photochemical Quenching Induction. Journal of Biological Chemistry **284,** 15255-15266.

Boekema, E.J., Folea, M., and Kouril, R. (2009). Single particle electron microscopy. Photosynthesis Research **102,** 189-196.

Boekema, E.J., van Roon, H., van Breemen, J.F.L., and Dekker, J.P. (1999a). Supramolecular organization of photosystem II and its light-harvesting antenna in partially solubilized photosystem II membranes. European Journal of Biochemistry **266,** 444-452.

Boekema, E.J., van Breemen, J.F.L., van Roon, H., and Dekker, J.P. (2000). Arrangement of photosystem II supercomplexes in crystalline macrodomains within the thylakoid membrane of green plant chloroplasts. Journal of Molecular Biology **301,** 1123-1133.

Boekema, E.J., van Roon, H., Calkoen, F., Bassi, R., and Dekker, J.P. (1999b). Multiple types of association of photosystem II and its light-harvesting antenna in partially solubilized photosystem II membranes. Biochemistry **38,** 2233-2239.

Boekema, E.J., Dekker, J.P., Vanheel, M.G., Rogner, M., Saenger, W., Witt, I., and Witt, H.T. (1987). EVIDENCE FOR A TRIMERIC ORGANIZATION OF THE PHOTOSYSTEM-I COMPLEX FROM THE THERMOPHILIC CYANOBACTERIUM SYNECHOCOCCUS SP. Febs Letters **217,** 283-286.

Boekema, E.J., Jensen, P.E., Schlodder, E., van Breemen, J.F.L., van Roon, H., Scheller, H.V., and Dekker, J.P. (2001). Green plant photosystem I binds light-harvesting complex I on one side of the complex. Biochemistry **40,** 1029-1036.

Boekema, E.J., Hankamer, B., Bald, D., Kruip, J., Nield, J., Boonstra, A.F., Barber, J., and Rogner, M. (1995). SUPRAMOLECULAR STRUCTURE OF THE PHOTOSYSTEM-II COMPLEX FROM GREEN PLANTS AND CYANOBACTERIA. Proceedings of the National Academy of Sciences of the United States of America **92,** 175-179.

Bonardi, V., Pesaresi, P., Becker, T., Schleiff, E., Wagner, R., Pfannschmidt, T., Jahns, P., and Leister, D. (2005). Photosystem II core phosphorylation and photosynthetic acclimation require two different protein kinases. Nature **437,** 1179-1182.

Bonavent.C, and Myers, J. (1969). FLUORESCENCE AND OXYGEN EVOLUTION FROM CHLORELLA PYRENOIDOSA. Biochimica Et Biophysica Acta **189,** 366-+.

Brenner, S., and Horne, R.W. (1959). A NEGATIVE STAINING METHOD FOR HIGH RESOLUTION ELECTRON MICROSCOPY OF VIRUSES. Biochimica Et Biophysica Acta **34,** 103-110.

Busch, A., and Hippler, M. (2011). The structure and function of eukaryotic photosystem I. Biochimica Et Biophysica Acta-Bioenergetics **1807,** 864-877.

Caffarri, S., Kouril, R., Kereiche, S., Boekema, E.J., and Croce, R. (2009). Functional architecture of higher plant photosystem II supercomplexes. Embo Journal **28,** 3052-3063.

Chitnis, V.P., and Chitnis, P.R. (1993). PSAL SUBUNIT IS REQUIRED FOR THE FORMATION OF PHOTOSYSTEM-I TRIMERS IN THE CYANOBACTERIUM SYNECHOCYSTIS SP PCC-6803. Febs Letters **336,** 330-334.

Correa-Galvis, V., Poschmann, G., Melzer, M., Stuhler, K., and Jahns, P. (2016). PsbS interactions involved in the activation of energy dissipation in Arabidopsis. Nature Plants **2**.

Crepin, A., Santabarbara, S., and Caffarri, S. (2016). Biochemical and Spectroscopic Characterization of Highly Stable Photosystem II Supercomplexes from Arabidopsis. (J Biol Chem), pp. 19157-19171.

Dainese, P., and Bassi, R. (1991). SUBUNIT STOICHIOMETRY OF THE CHLOROPLAST PHOTOSYSTEM-II ANTENNA SYSTEM AND AGGREGATION STATE OF THE COMPONENT CHLOROPHYLL-A/B BINDING-PROTEINS. Journal of Biological Chemistry **266,** 8136-8142.

Dau, H., Andrews, J.C., Roelofs, T.A., Latimer, M.J., Liang, W.C., Yachandra, V.K., Sauer, K., and Klein, M.P. (1995). STRUCTURAL CONSEQUENCES OF AMMONIA BINDING TO THE MANGANESE CENTER OF THE PHOTOSYNTHETIC OXYGEN-EVOLVING COMPLEX - AN X-RAY-ABSORPTION SPECTROSCOPY STUDY OF ISOTROPIC AND ORIENTED PHOTOSYSTEM-II PARTICLES. Biochemistry **34,** 5274-5287.

Daum, B., Nicastro, D., Il, J.A., McIntosh, J.R., and Kuhlbrandt, W. (2010). Arrangement of Photosystem II and ATP Synthase in Chloroplast Membranes of Spinach and Pea. Plant Cell **22,** 1299-1312.

de Bianchi, S., Dall'Osto, L., Tognon, G., Morosinotto, T., and Bassi, R. (2008). Minor antenna proteins CP24 and CP26 affect the interactions between photosystem II Subunits and the electron transport rate in grana membranes of Arabidopsis. Plant Cell **20,** 1012-1028.

de Bianchi, S., Betterle, N., Kouril, R., Cazzaniga, S., Boekema, E., Bassi, R., and Dall'Osto, L. (2011). Arabidopsis Mutants Deleted in the Light-Harvesting Protein Lhcb4 Have a Disrupted Photosystem II Macrostructure and Are Defective in Photoprotection. Plant Cell **23,** 2659-2679.

Dekker, J.P., and Boekema, E.J. (2005). Supramolecular organization of thylakoid membrane proteins in green plants. Biochimica Et Biophysica Acta-Bioenergetics **1706,** 12-39.

Efremov, R.G., Baradaran, R., and Sazanov, L.A. (2010). The architecture of respiratory complex I. Nature **465,** 441-U461.

Farah, J., Rappaport, F., Choquet, Y., Joliot, P., and Rochaix, J.D. (1995). ISOLATION OF A PSAF-DEFICIENT MUTANT OF CHLAMYDOMONAS-REINHARDTII - EFFICIENT INTERACTION OF PLASTOCYANIN WITH THE PHOTOSYSTEM-I REACTION-CENTER IS MEDIATED BY THE PSAF SUBUNIT. Embo Journal **14,** 4976-4984.

Fischer, N., Boudreau, E., Hippler, M., Drepper, F., Haehnel, W., and Rochaix, J.D. (1999). A large fraction of PsaF is nonfunctional in photosystem I complexes lacking the PsaJ subunit. Biochemistry **38,** 5546-5552.

Forsberg, J., and Allen, J.F. (2001). Protein tyrosine phosphorylation in the transition to light state 2 of chloroplast thylakoids. Photosynthesis Research **68,** 71-79.

Frank, J., Radermacher, M., Penczek, P., Zhu, J., Li, Y.H., Ladjadj, M., and Leith, A. (1996). SPIDER and WEB: Processing and visualization of images in 3D electron microscopy and related fields. Journal of Structural Biology **116,** 190-199.

Galka, P., Santabarbara, S., Thi, T.H.K., Degand, H., Morsomme, P., Jennings, R.C., Boekema, E.J., and Caffarri, S. (2012). Functional Analyses of the Plant Photosystem I-Light-Harvesting Complex II Supercomplex Reveal That Light-Harvesting Complex II Loosely Bound to Photosystem II Is a Very Efficient Antenna for Photosystem I in State II. Plant Cell **24,** 2963-2978.

Garber, M.P., and Steponkus, P.L. (1976). ALTERATIONS IN CHLOROPLAST THYLAKOIDS DURING COLD-ACCLIMATION. Plant Physiology **57,** 681-686.

Gerotto, C., Franchin, C., Arrigoni, G., and Morosinotto, T. (2015). In Vivo Identification of Photosystem II Light Harvesting Complexes Interacting with PHOTOSYSTEM II SUBUNIT S. Plant Physiology **168,** 1747-U1105.

Gobets, B., and van Grondelle, R. (2001). Energy transfer and trapping in photosystem I. Biochimica Et Biophysica Acta-Bioenergetics **1507,** 80-99.

Guskov, A., Kern, J., Gabdulkhakov, A., Broser, M., Zouni, A., and Saenger, W. (2009). Cyanobacterial photosystem II at 2.9-angstrom resolution and the role of quinones, lipids, channels and chloride. Nature Structural & Molecular Biology **16,** 334-342.

Haldrup, A., Naver, H., and Scheller, H.V. (1999). The interaction between plastocyanin and photosystem I is inefficient in transgenic Arabidopsis plants lacking the PSI-N subunit of photosystem I. Plant Journal **17,** 689-698.

Haldrup, A., Simpson, D.J., and Scheller, H.V. (2000). Down-regulation of the PSI-F subunit of photosystem I (PSI) in Arabidopsis thaliana - The PSI-F subunit is essential for photoautotrophic growth and contributes to antenna function. Journal of Biological Chemistry **275,** 31211-31218.

Hayashida, N., Matsubayashi, T., Shinozaki, K., Sugiura, M., Inoue, K., and Hiyama, T. (1987). THE GENE FOR THE 9 KD POLYPEPTIDE, A POSSIBLE APOPROTEIN FOR THE IRON-SULFUR CENTER-A AND CENTER-B OF THE PHOTOSYSTEM-I COMPLEX, IN TOBACCO CHLOROPLAST DNA. Current Genetics **12,** 247-250.

Hoj, P.B., Svendsen, I., Scheller, H.V., and Moller, B.L. (1987). IDENTIFICATION OF A CHLOROPLAST-ENCODED 9-KDA POLYPEPTIDE AS A 2 4FE-4S PROTEIN CARRYING CENTER-A AND CENTER-B OF PHOTOSYSTEM-I. Journal of Biological Chemistry **262,** 12676-12684.

Hu, P., Lv, J., Fu, P.C., and Mi, H.L. (2013). Enzymatic characterization of an active NDH complex from Thermosynechococcus elongatus. Febs Letters **587,** 2340-2345.

Iwai, M., Takizawa, K., Tokutsu, R., Okamuro, A., Takahashi, Y., and Minagawa, J. (2010). Isolation of the elusive supercomplex that drives cyclic electron flow in photosynthesis. Nature **464,** 1210-U1134.

Jansson, S. (1994). THE LIGHT-HARVESTING CHLOROPHYLL A/B BINDING-PROTEINS. Biochimica Et Biophysica Acta-Bioenergetics **1184,** 1-19.

Jansson, S. (1999). A guide to the Lhc genes and their relatives in Arabidopsis. Trends in Plant Science **4,** 236-240.

Jansson, S., Andersen, B., and Scheller, H.V. (1996). Nearest-neighbor analysis of higher-plant photosystem I holocomplex. Plant Physiology **112,** 409-420.

Jarvi, S., Suorsa, M., Paakkarinen, V., and Aro, E.M. (2011). Optimized native gel systems for separation of thylakoid protein complexes: novel super- and mega-complexes. Biochemical Journal **439,** 207-214.

Jensen, P.E., Haldrup, A., Zhang, S.P., and Scheller, H.V. (2004). The PSI-O subunit of plant photosystem I is involved in balancing the excitation pressure between the two photosystems. Journal of Biological Chemistry **279,** 24212-24217.

Jensen, P.E., Bassi, R., Boekema, E.J., Dekker, J.P., Jansson, S., Leister, D., Robinson, C., and Scheller, H.V. (2007). Structure, function and regulation of plant photosystem I. Biochimica Et Biophysica Acta-Bioenergetics **1767,** 335-352.

Jordan, P., Fromme, P., Witt, H.T., Klukas, O., Saenger, W., and Krauss, N. (2001). Three-dimensional structure of cyanobacterial photosystem I at 2.5 angstrom resolution. Nature **411,** 909-917.

Kereiche, S., Kiss, A.Z., Kouril, R., Boekema, E.J., and Horton, P. (2010). The PsbS protein controls the macro-organisation of photosystem II complexes in the grana membranes of higher plant chloroplasts. Febs Letters **584,** 759-764.

Kirchhoff, H., Sharpe, R.M., Herbstova, M., Yarbrough, R., and Edwards, G.E. (2013). Differential Mobility of Pigment-Protein Complexes in Granal and Agranal Thylakoid Membranes of C-3 and C-4 Plants. Plant Physiology **161,** 497-507.

Kirchhoff, H., Haase, W., Wegner, S., Danielsson, R., Ackermann, R., and Albertsson, P.-A. (2007). Low-light-induced formation of semicrystalline photosystem II arrays in higher plant chloroplast. Biochemistry **46,** 11169-11176.

Klimmek, F., Sjodin, A., Noutsos, C., Leister, D., and Jansson, S. (2006). Abundantly and rarely expressed Lhc protein genes exhibit distinct regulation patterns in plants. Plant Physiology **140,** 793-804.

Knispel, R.W., Kofler, C., Boicu, M., Baumeister, W., and Nickell, S. (2012). Blotting protein complexes from native gels to electron microscopy grids. Nature Methods **9,** 182-184.

Kouril, R., Dekker, J.P., and Boekema, E.J. (2012). Supramolecular organization of photosystem II in green plants. Biochimica Et Biophysica Acta-Bioenergetics **1817,** 2-12.

Kouril, R., van Oosterwijk, N., Yakushevska, A.E., and Boekema, E.J. (2005a). Photosystem I: a search for green plant trimers. Photochemical & Photobiological Sciences **4,** 1091-1094.

Kouril, R., Wientjes, E., Bultema, J.B., Croce, R., and Boekema, E.J. (2013). High-light vs. low-light: Effect of light acclimation on photosystem II composition and organization in Arabidopsis thaliana. Biochimica Et Biophysica Acta-Bioenergetics **1827,** 411-419.

Kouril, R., Nosek, L., Bartos, J., Boekema, E.J., and Ilik, P. (2016). Evolutionary loss of light-harvesting proteins Lhcb6 and Lhcb3 in major land plant groups - break-up of current dogma. New Phytologist **210,** 808-814.

Kouril, R., Zygadlo, A., Arteni, A.A., de Wit, C.D., Dekker, J.P., Jensen, P.E., Scheller, H.V., and Boekema, E.J. (2005b). Structural characterization of a complex of photosystem I and light-harvesting complex II of Arabidopsis thaliana. Biochemistry **44,** 10935-10940.

Kouril, R., Strouhal, O., Nosek, L., Lenobel, R., Chamrad, I., Boekema, E.J., Sebela, M., and Ilik, P. (2014). Structural characterization of a plant photosystem I and NAD(P)H dehydrogenase supercomplex. Plant Journal **77,** 568-576.

Kovacs, L., Damkjaer, J., Kereiche, S., Ilioaia, C., Ruban, A.V., Boekema, E.J., Jansson, S., and Horton, P. (2006). Lack of the light-harvesting complex CP24 affects the structure and function of the grana membranes of higher plant chloroplasts. Plant Cell **18,** 3106-3120.

Li, X.P., Bjorkman, O., Shih, C., Grossman, A.R., Rosenquist, M., Jansson, S., and Niyogi, K.K. (2000). A pigment-binding protein essential for regulation of photosynthetic light harvesting. Nature **403,** 391-395.

Lichtenthaler, H.K. (1987). CHLOROPHYLLS AND CAROTENOIDS - PIGMENTS OF PHOTOSYNTHETIC BIOMEMBRANES. Methods in Enzymology **148,** 350-382.

Liu, Z.F., Yan, H.C., Wang, K.B., Kuang, T.Y., Zhang, J.P., Gui, L.L., An, X.M., and Chang, W.R. (2004). Crystal structure of spinach major light-harvesting complex at 2.72 angstrom resolution. Nature **428,** 287-292.

Ludtke, S.J., Baldwin, P.R., and Chiu, W. (1999). EMAN: Semiautomated software for high-resolution single-particle reconstructions. Journal of Structural Biology **128,** 82-97.

Lunde, C., Jensen, P.E., Haldrup, A., Knoetzel, J., and Scheller, H.V. (2000). The PSI-H subunit of photosystem I is essential for state transitions in plant photosynthesis. Nature **408,** 613-615.

Mazor, Y., Borovikova, A., and Nelson, N. (2015). The structure of plant photosystem I super-complex at 2.8 angstrom resolution. Elife **4**.

Morosinotto, T., Breton, J., Bassi, R., and Croce, R. (2003). The nature of a chlorophyll ligand in Lhca proteins determines the far red fluorescence emission typical of photosystem I. Journal of Biological Chemistry **278,** 49223-49229.

Murata, N. (1969). CONTROL OF EXCITATION TRANSFER IN PHOTOSYNTHESIS .I. LIGHT-INDUCED CHANGE OF CHLOROPHYLL A FLUORESCENCE IN PORPHYRIDIUM CRUENTUM. Biochimica Et Biophysica Acta **172,** 242-&.

Nelson, N. (2009). Plant Photosystem I - The Most Efficient Nano-Photochemical Machine. Journal of Nanoscience and Nanotechnology **9,** 1709-1713.

Nelson, N., and Ben-Shem, A. (2004). The complex architecture of oxygenic photosynthesis. Nature Reviews Molecular Cell Biology **5,** 971-982.

Nelson, N., and Ben-Shem, A. (2005). The structure of photosystem I and evolution of photosynthesis. Bioessays **27,** 914-922.

Nelson, N., and Yocum, C.F. (2006). Structure and function of photosystems I and II. Annual Review of Plant Biology **57,** 521-565.

Niyogi, K.K. (2000). Safety valves for photosynthesis. Current Opinion in Plant Biology **3,** 455-460.

Niyogi, K.K., Li, X.P., Rosenberg, V., and Jung, H.S. (2005). Is PsbS the site of non-photochemical quenching in photosynthesis? Journal of Experimental Botany **56,** 375-382.

Ohyama, K., Fukuzawa, H., Kohchi, T., Shirai, H., Sano, T., Sano, S., Umesono, K., Shiki, Y., Takeuchi, M., Chang, Z., Aota, S., Inokuchi, H., and Ozeki, H. (1986). CHLOROPLAST GENE ORGANIZATION DEDUCED FROM COMPLETE SEQUENCE OF LIVERWORT MARCHANTIA-POLYMORPHA CHLOROPLAST DNA. Nature **322,** 572-574.

Oostergetel, G.T., Keegstra, W., and Brisson, A. (1998). Automation of specimen selection and data acquisition for protein electron crystallography. Ultramicroscopy **74,** 47-59.

Pagliano, C., Barera, S., Chimirri, F., Saracco, G., and Barber, J. (2012). Comparison of the alpha and beta isomeric forms of the detergent n-dodecyl-D-maltoside for solubilizing photosynthetic complexes from pea thylakoid membranes. Biochimica Et Biophysica Acta-Bioenergetics **1817,** 1506-1515.

Pan, X.W., Li, M., Wan, T., Wang, L.F., Jia, C.J., Hou, Z.Q., Zhao, X.L., Zhang, J.P., and Chang, W.R. (2011). Structural insights into energy regulation of light-harvesting complex CP29 from spinach. Nature Structural & Molecular Biology **18,** 309-U394.

Pavlovic, A., Stolarik, T., Nosek, L., Kouril, R., and Ilik, P. (2016). Light-induced gradual activation of photosystem II in dark-grown Norway spruce seedlings. Biochimica Et Biophysica Acta-Bioenergetics **1857,** 799-809.

Peng, L.W., and Shikanai, T. (2011). Supercomplex Formation with Photosystem I Is Required for the Stabilization of the Chloroplast NADH Dehydrogenase-Like Complex in Arabidopsis. Plant Physiology **155,** 1629-1639.

Peng, L.W., Shimizu, H., and Shikanai, T. (2008). The Chloroplast NAD(P)H Dehydrogenase Complex Interacts with Photosystem I in Arabidopsis. Journal of Biological Chemistry **283,** 34873-34879.

Peng, L.W., Yamamoto, H., and Shikanai, T. (2011). Structure and biogenesis of the chloroplast NAD(P)H dehydrogenase complex. Biochimica Et Biophysica Acta-Bioenergetics **1807,** 945-953.

Peng, L.W., Fukao, Y., Fujiwara, M., Takami, T., and Shikanai, T. (2009). Efficient Operation of NAD(P)H Dehydrogenase Requires Supercomplex Formation with Photosystem I via Minor LHCI in Arabidopsis. Plant Cell **21,** 3623-3640.

Peter, G.F., and Thornber, J.P. (1991). BIOCHEMICAL-COMPOSITION AND ORGANIZATION OF HIGHER-PLANT PHOTOSYSTEM-II LIGHT-HARVESTING PIGMENT-PROTEINS. Journal of Biological Chemistry **266,** 16745-16754.

Ruban, A.V. (2016). Nonphotochemical Chlorophyll Fluorescence Quenching: Mechanism and Effectiveness in Protecting Plants from Photodamage. Plant Physiology **170,** 1903-1916.

Ruban, A.V., Johnson, M.P., and Duffy, C.D.P. (2012). The photoprotective molecular switch in the photosystem II antenna. Biochimica Et Biophysica Acta-Bioenergetics **1817,** 167-181.

Ruban, A.V., Wentworth, M., Yakushevska, A.E., Andersson, J., Lee, P.J., Keegstra, W., Dekker, J.P., Boekema, E.J., Jansson, S., and Horton, P. (2003). Plants lacking the main light-harvesting complex retain photosystem II macro-organization. Nature **421,** 648-652.

Schagger, H., and Vonjagow, G. (1991). BLUE NATIVE ELECTROPHORESIS FOR ISOLATION OF MEMBRANE-PROTEIN COMPLEXES IN ENZYMATICALLY ACTIVE FORM. Analytical Biochemistry **199,** 223-231.

Schagger, H., Cramer, W.A., and Vonjagow, G. (1994). ANALYSIS OF MOLECULAR MASSES AND OLIGOMERIC STATES OF PROTEIN COMPLEXES BY BLUE NATIVE ELECTROPHORESIS AND ISOLATION OF MEMBRANE-PROTEIN COMPLEXES BY 2-DIMENSIONAL NATIVE ELECTROPHORESIS. Analytical Biochemistry **217,** 220-230.

Scheres, S.H.W. (2012). RELION: Implementation of a Bayesian approach to cryo-EM structure determination. Journal of Structural Biology **180,** 519-530.

Seddon, A.M., Curnow, P., and Booth, P.J. (2004). Membrane proteins, lipids and detergents: not just a soap opera. Biochimica Et Biophysica Acta-Biomembranes **1666,** 105-117.

Semenova, G.A. (1995). PARTICLE REGULARITY ON THYLAKOID FRACTURE FACES IS INFLUENCED BY STORAGE-CONDITIONS. Canadian Journal of Botany-Revue Canadienne De Botanique **73,** 1676-1682.

Shen, J.R. (2015). The Structure of Photosystem II and the Mechanism of Water Oxidation in Photosynthesis. Annual Review of Plant Biology, Vol 66 **66,** 23-48.

Shi, L.X., and Schroder, W.P. (2004). The low molecular mass subunits of the photosynthetic supracomplex, photosystem II. Biochimica Et Biophysica Acta-Bioenergetics **1608,** 75-96.

Shikanai, T. (2007). Regulation of photosynthesis via PSI cyclic electron transport. Photosynthesis Research **91,** 246-246.

Shikanai, T. (2016). Chloroplast NDH: A different enzyme with a structure similar to that of respiratory NADH dehydrogenase. Biochimica Et Biophysica Acta-Bioenergetics **1857,** 1015-1022.

Shinozaki, K., Ohme, M., Tanaka, M., Wakasugi, T., Hayashida, N., Matsubayashi, T., Zaita, N., Chunwongse, J., Obokata, J., Yamaguchishinozaki, K., Ohto, C., Torazawa, K., Meng, B.Y., Sugita, M., Deno, H., Kamogashira, T., Yamada, K., Kusuda, J., Takaiwa, F., Kato, A., Tohdoh, N., Shimada, H., and Sugiura, M. (1986). THE COMPLETE NUCLEOTIDE-SEQUENCE OF THE TOBACCO CHLOROPLAST GENOME - ITS GENE ORGANIZATION AND EXPRESSION. Embo Journal **5,** 2043-2049.

Simpson, D.J. (1978). FREEZE-FRACTURE STUDIES ON BARLEY PLASTID MEMBRANES .2. WILD-TYPE CHLOROPLAST. Carlsberg Research Communications **43,** 365-389.

Sorzano, C.O.S., Marabini, R., Velazquez-Muriel, J., Bilbao-Castro, J.R., Scheres, S.H.W., Carazo, J.M., and Pascual-Montano, A. (2004). XMIPP: a new generation of an open-source image processing package for electron microscopy. Journal of Structural Biology **148,** 194-204.

Standfuss, R., van Scheltinga, A.C.T., Lamborghini, M., and Kuhlbrandt, W. (2005). Mechanisms of photoprotection and nonphotochemical quenching in pea light-harvesting complex at 2.5A resolution. Embo Journal **24,** 919-928.

Tietz, S., Puthiyaveetil, S., Enlow, H.M., Yarbrough, R., Wood, M., Semchonok, D.A., Lowry, T., Li, Z., Jahns, P., Boekema, E.J., Lenhert, S., Niyogi, K.K., and Kirchhoff, H. (2015). Functional Implications of Photosystem II Crystal Formation in Photosynthetic Membranes. Journal of Biological Chemistry **290,** 14091-14106.

Umena, Y., Kawakami, K., Shen, J.R., and Kamiya, N. (2011). Crystal structure of oxygen-evolving photosystem II at a resolution of 1.9 angstrom. Nature **473,** 55-U65.

van Oort, B., Alberts, M., de Bianchi, S., Dall'Osto, L., Bassi, R., Trinkunas, G., Croce, R., and van Amerongen, H. (2010). Effect of Antenna-Depletion in Photosystern II on Excitation Energy Transfer in Arabidopsis thaliana. Biophysical Journal **98,** 922-931.

vanHeel, M., Harauz, G., Orlova, E.V., Schmidt, R., and Schatz, M. (1996). A new generation of the IMAGIC image processing system. Journal of Structural Biology **116,** 17-24.

Varotto, C., Pesaresi, P., Jahns, P., Lessnick, A., Tizzano, M., Schiavon, F., Salamini, F., and Leister, D. (2002). Single and double knockouts of the genes for photosystem I subunits G, K, and H of Arabidopsis. Effects on photosystem I composition, photosynthetic electron flow, and state transitions. Plant Physiology **129,** 616-624.

Wei, X.P., Su, X.D., Cao, P., Liu, X.Y., Chang, W.R., Li, M., Zhang, X.Z., and Liu, Z.F. (2016). Structure of spinach photosystem II-LHCII supercomplex at 3.2 angstrom resolution. Nature **534,** 69-+.

Wientjes, E., Oostergetel, G.T., Jansson, S., Boekema, E.J., and Croce, R. (2009). The Role of Lhca Complexes in the Supramolecular Organization of Higher Plant Photosystem I. Journal of Biological Chemistry **284,** 7803-7810.

Wientjes, E., Drop, B., Kouril, R., Boekema, E.J., and Croce, R. (2013). During State 1 to State 2 Transition in Arabidopsis thaliana, the Photosystem II Supercomplex Gets Phosphorylated but Does Not Disassemble. Journal of Biological Chemistry **288,** 32821-32826.

Wittig, I., and Schagger, H. (2005). Advantages and limitations of clear-native PAGE. Proteomics **5,** 4338-4346.

Wittig, I., Karas, M., and Schaegger, H. (2007). High resolution clear native electrophoresis for In-gel functional assays and fluorescence studies of membrane protein complexes. Molecular & Cellular Proteomics **6,** 1215-1225.

Wollman, F.A. (2001). State transitions reveal the dynamics and flexibility of the photosynthetic apparatus. Embo Journal **20,** 3623-3630.

Yakushevska, A.E., Jensen, P.E., Keegstra, W., van Roon, H., Scheller, H.V., Boekema, E.J., and Dekker, J.P. (2001a). Supermolecular organization of photosystem II and its associated light-harvesting antenna in Arabidopsis thaliana. European Journal of Biochemistry **268,** 6020-6028.

Yakushevska, A.E., Keegstra, W., Boekema, E.J., Dekker, J.P., Andersson, J., Jansson, S., Ruban, A.V., and Horton, P. (2003). The structure of photosystem II in Arabidopsis: Localization of the CP26 and CP29 antenna complexes. Biochemistry **42,** 608-613.

Yakushevska, A.E., Ruban, A.V., Jensen, P.E., Keegstra, W., van Roon, H., Niyogi, K.K., Scheller, H.V., Horton, P., Dekker, J.P., and Boekema, E.J. (2001b). Supermolecular organization of photosystem II and its associated light-harvesting antenna in the wild-type and npq4 mutant of Arabidopsis thaliana. Photosynthesis Research **69,** 52-52.

Yamamoto, H., Peng, L.W., Fukao, Y., and Shikanai, T. (2011). An Src Homology 3 Domain-Like Fold Protein Forms a Ferredoxin Binding Site for the Chloroplast NADH Dehydrogenase-Like Complex in Arabidopsis. Plant Cell **23,** 1480-1493.

Yamori, W., Shikanai, T., and Makino, A. (2015). Photosystem I cyclic electron flow via chloroplast NADH dehydrogenase-like complex performs a physiological role for photosynthesis at low light. Scientific Reports **5**.

Zhang, S.P., and Scheller, H.V. (2004). Light-harvesting complex II binds to several small Subunits of photosystem I. Journal of Biological Chemistry **279,** 3180-3187.

Zouni, A., Witt, H.T., Kern, J., Fromme, P., Krauss, N., Saenger, W., and Orth, P. (2001). Crystal structure of photosystem II from Synechococcus elongatus at 3.8 angstrom resolution. Nature **409,** 739-743.